frontiers | Research Topics

Epidemic status and prevention of swine infectious diseases

Edited by
Zhou Mo, Lian-Feng Li and Keisuke Suganuma

Published in
Frontiers in Veterinary Science

ISSN 1664-8714
ISBN 978-2-83251-960-8
DOI 10.3389/978-2-83251-960-8

About Frontiers

Frontiers is more than just an open access publisher of scholarly articles: it is a pioneering approach to the world of academia, radically improving the way scholarly research is managed. The grand vision of Frontiers is a world where all people have an equal opportunity to seek, share and generate knowledge. Frontiers provides immediate and permanent online open access to all its publications, but this alone is not enough to realize our grand goals.

Frontiers journal series

The Frontiers journal series is a multi-tier and interdisciplinary set of open-access, online journals, promising a paradigm shift from the current review, selection and dissemination processes in academic publishing. All Frontiers journals are driven by researchers for researchers; therefore, they constitute a service to the scholarly community. At the same time, the *Frontiers journal series* operates on a revolutionary invention, the tiered publishing system, initially addressing specific communities of scholars, and gradually climbing up to broader public understanding, thus serving the interests of the lay society, too.

Dedication to quality

Each Frontiers article is a landmark of the highest quality, thanks to genuinely collaborative interactions between authors and review editors, who include some of the world's best academicians. Research must be certified by peers before entering a stream of knowledge that may eventually reach the public - and shape society; therefore, Frontiers only applies the most rigorous and unbiased reviews. Frontiers revolutionizes research publishing by freely delivering the most outstanding research, evaluated with no bias from both the academic and social point of view. By applying the most advanced information technologies, Frontiers is catapulting scholarly publishing into a new generation.

What are Frontiers Research Topics?

Frontiers Research Topics are very popular trademarks of the *Frontiers journals series*: they are collections of at least ten articles, all centered on a particular subject. With their unique mix of varied contributions from Original Research to Review Articles, Frontiers Research Topics unify the most influential researchers, the latest key findings and historical advances in a hot research area.

Find out more on how to host your own Frontiers Research Topic or contribute to one as an author by contacting the Frontiers editorial office: frontiersin.org/about/contact

Epidemic status and prevention of swine infectious diseases

Topic editors

Zhou Mo — Provincial Key Laboratory of Veterinary Bio-pharmaceutical High tech Research, Jiangsu Agri-animal Husbandry Vocational College, China

Lian-Feng Li — Harbin Veterinary Research Institute, Chinese Academy of Agricultural Sciences, China

Keisuke Suganuma — Obihiro University of Agriculture and Veterinary Medicine, Japan

Citation

Mo, Z., Li, L.-F., Suganuma, K., eds. (2023). *Epidemic status and prevention of swine infectious diseases*. Lausanne: Frontiers Media SA.

doi: 10.3389/978-2-83251-960-8

The authors declare that the research was conducted in the absence of any commercial or financial relationships that could be construed as a potential conflict of interest

Table of contents

frontiers | Frontiers in Veterinary Science

TYPE Editorial
PUBLISHED 06 March 2023
DOI 10.3389/fvets.2023.1169644

OPEN ACCESS

EDITED AND REVIEWED BY
Michael Kogut,
Agricultural Research Service (USDA),
United States

*CORRESPONDENCE
Mo Zhou
✉ zhoumo_wk@hotmail.com

SPECIALTY SECTION
This article was submitted to Veterinary Infectious Diseases, a section of the journal Frontiers in Veterinary Science

RECEIVED 19 February 2023
ACCEPTED 20 February 2023
PUBLISHED 06 March 2023

CITATION
Zhou M, Li L and Suganuma K (2023) Editorial: Epidemic status and prevention of swine infectious diseases. *Front. Vet. Sci.* 10:1169644. doi: 10.3389/fvets.2023.1169644

Editorial: Epidemic status and prevention of swine infectious diseases

Mo Zhou[1]*, Lianfeng Li[2] and Keisuke Suganuma[3]

[1]Jiangsu Key Laboratory for High-Tech Research and Development of Veterinary Biopharmaceuticals, Engineering Technology Research Center for Modern Animal Science and Novel Veterinary Pharmaceutic Development, Jiangsu Agri-Animal Husbandry Vocational College, Taizhou, China, [2]Harbin Veterinary Research Institute, Chinese Academy of Agricultural Sciences, Harbin, China, [3]National Research Center for Protozoan Diseases, Obihiro University of Agriculture and Veterinary Medicine, Obihiro, Japan

KEYWORDS

epidemic status, prevention, diagnosis, swine, infectious diseases

Editorial on the Research Topic
Epidemic status and prevention of swine infectious diseases

Swine infectious disease is an essential factor affecting the stable development of the swine industry and has caused severe economic losses to the breeding industry. The rapid expansion of the swine breeding scale has provided certain primary conditions for the high incidence and spread of swine infectious diseases, which have a severe impact on the development of the swine breeding industry. Therefore, it is necessary to pay special attention to swine infectious diseases, fully understand their epidemic characteristics, formulate scientific and reasonable prevention and control countermeasures, and form scientific and effective prevention and control of swine infectious diseases.

The objective of this Research Topic was to bring attention to the swine infectious disease and gather different contributions highlighting essential aspects of contagious swine disease, including the epidemic status, the diagnostic method and the vaccine development.

Pseudorabies virus (PRV) causes reproductive problems in sows and boars and a high mortality rate in piglets, which results in huge economic losses for the swine industry (1). Currently, the widespread porcine PRV belongs to genotype II, and the protection of the traditional vaccine against genotype I PRV has declined. And new mutated strains can cause human infection (2). Zhang et al. investigated the prevalence of the PRV in the Hebei Province of China between 2017 and 2018. Serum samples collected showed a 46.27% positive rate for PRV gE antibodies. A total of 11 PRV variants have been isolated, and all are highly homologous, clustered in a similar group as HSD-1/2019, which causes acute encephalitis in humans.

Porcine circovirus type 2 and type 3 (PCV2 and PCV3) are two critical viral pathogens in the swine industry that have a significant economic impact in the world (3, 4). Nan et al. investigated the prevalence and genetic diversity of PCV2 in the northern Guangdong Province of China. 51.38% (297/573) of samples tested positive for PCV2. Study strains belonged to three genotypes of PCV2: PCV2a, PCV2b, and PCV2d. In addition, Yang et al. investigated the prevalence and genetic diversity of PCV3 and PCV2 in the southwest region of China between 2020 and 2022. 26.46% of the samples were positive for PCV2 and 33.46% for PCV3. Coinfection rates were 5.75% in 2020 and 10.45% in 2022. PCV2d is the predominant PCV2 genotype and the PCV3 isolates with high nucleotide homology and three mutations in antibody recognition domains. Their genotyping, immunogenicity, and immune evasion will be further studied under the help of these studies.

Porcine reproductive and respiratory syndrome virus (PRRSV) causes significant financial losses to the swine industry. Base on ORF5, type 2 PRRSV strains can be classified into NADC30-like, QYYZ-like, VR2332-like, and JXA1-like strains (5, 6). An analysis of genetic variation was conducted by Li P. et al. on the isolated PRRSV ORF5 gene. NADC30-like PRRSV strains are still dominant in Shandong Province, while NADC34-like are starting to become more prevalent. Xu et al. obtained 24 QYYZ-like PRRSV isolates from central and southern provinces of China. Therefore, QYYZ-like strains were commonplace in central and south China and played a role in the PRRSV epidemic by providing recombinant fragments. In addition, a genome-wide analysis of four PRRSV isolates from a single farm in China was conducted by Liu et al. Two isolates had 150-aa deletions identical to the live attenuated virus vaccine strain, and the pathogenicity of these isolates was different. PRRSV genomes have evolved through recombination between field strains and vaccine strains.

The swine enteric coronavirus (SeCoV) severely threatens public health and global security and causes significant losses for the global swine industry. A total of four SeCoV viruses are known to cause swine acute diarrhea syndrome: transmissible gastroenteritis virus (TGEV), porcine epidemic diarrhea virus (PEDV), porcine delta coronavirus (PDCoV), and swine acute diarrhea syndrome coronavirus (7, 8). Li M. et al. gave a comprehensive overview of the effects of CoV on apoptosis, autophagy, and innate immunity have been studied, providing insight into the pathogenic mechanism of the virus. Autophagy is an intrinsic defense mechanism that mediates the autophagic elimination of viral components, but viruses have evolved various strategies to escape or subvert the antiviral effects of autophagy. The study of SeCoV and its interaction with the host is crucial for understanding the pathogenic mechanism of the virus and developing effective treatments and preventions. Furthermore, several areas of Shandong Province were investigated for PEDV infection by Shen et al. Positive rates of 37.5% were found for PEDV, and significant variations were found in the structure domain region of the S gene. The study provides valuable information on the molecular epidemiology of PEDV and helps prevent and control the disease.

The African swine fever virus (ASFV) has spread rapidly in China, resulting in significant economic losses (9). The simultaneous presence of ASFV genotypes I and II in China made field identification more challenging since both genotypes are capable of causing chronic infection and morbidity in pigs. In response to this, Cao et al. developed a duplex fluorescent quantitative PCR assay to distinguish ASFV genotypes I and II based on the B646L sequences. The assay has high specificity and is highly reproducible, and it is an essential tool for detecting ASFV differentially.

Haemophilus parasuis (HPS) is one of the major infectious diseases affecting the swine industry globally and causes significant economic losses. Vaccination is the primary method of preventing HPS infections (10, 11). Based on pan-genomic analysis of 121 strains and reverse vaccine design, Pang et al. developed a multiepitope vaccine against HPS. Based on pre-predicted epitopes in the outer membrane proteins of the HPS core genome, the vaccine construct showed high immunogenicity and high Toll-like receptor 2 binding affinity. According to *in silico* immune simulations, the vaccine elicited an effective immune response. Mouse polyclonal antibodies produced from the vaccine protein bind different serotypes and non-typable HPS *in vitro*. Multiepitope vaccines are promising candidates for HPS pan-prophylaxis.

These studies in this research reported the epidemic status of the PRV, PCV, PRRSV, and PEDV and the genetic basis of these pathogens. Furthermore, this Research Topic also reported the development of the novel diagnostic methods and vaccines against ASFV and HPS. This Research Topic will help us to control swine infectious diseases effectively.

Author contributions

All authors listed have made a substantial, direct, and intellectual contribution to the work and approved it for publication.

Acknowledgments

We thank the authors and reviewers and the Division of Swine Infectious Disease Prevention and Control in Jiangsu Agri-Animal Husbandry Vocational College that contributed to this Research Topic. We also thank the support from the project of Jiangsu Agri-Animal Husbandry Vocational College (NSF2022CB04 and NSF2022CB25), the key project of Jiangsu Province's Key Research and Development Plan (modern Agriculture) (BE2020407), the Natural Science Research Project of Higher Education of Jiangsu Province (2020220375), and the Qing Lan Project of Jiangsu Province.

Conflict of interest

The authors declare that the research was conducted in the absence of any commercial or financial relationships that could be construed as a potential conflict of interest.

Publisher's note

References

1. Zheng HH, Jin Y, Hou CY, Li XS, Zhao L, Wang ZY, et al. Seroprevalence Investigation and genetic analysis of pseudorabies virus within pig populations in Henan province of China during 2018-2019. *Infect Genet Evol.* (2021) 92:104835. doi: 10.1016/j.meegid.2021.104835

2. Wang D, Tao X, Fei M, Chen J, Guo W, Li P, et al. Human encephalitis caused by pseudorabies virus infection: A case report. *J Neurovirol.* (2020) 26:442–8. doi: 10.1007/s13365-019-00822-2

3. Wang Y, Noll L, Lu N, Porter E, Stoy C, Zheng W, et al. Genetic diversity and prevalence of porcine circovirus type 3 (PCV3) and type 2 (PCV2) in the Midwest of the USA during 2016-2018. *Transbound Emerg Dis.* (2020) 67:1284–94. doi: 10.1111/tbed.13467

4. Saporiti V, Huerta E, Correa-Fiz F, Grosse Liesner B, Duran O, Segalés J, et al. Detection and genotyping of Porcine circovirus 2 (PCV-2) and detection of Porcine circovirus 3 (PCV-3) in sera from fattening pigs of different European countries. *Transbound Emerg Dis.* (2020) 67:2521–31. doi: 10.1111/tbed.13596

5. Wang J, Lin S, Quan D, Wang H, Huang J, Wang Y, et al. Full genomic analysis of new variants of porcine reproductive and respiratory syndrome virus revealed multiple recombination events between different lineages and sublineages. *Front Vet Sci.* (2020) 7:603. doi: 10.3389/fvets.2020.00603

6. Sun YK, Li Q, Yu ZQ, Han XL, Wei YF, Ji CH, et al. Emergence of novel recombination lineage 3 of porcine reproductive and respiratory syndrome viruses in Southern China. *Transbound Emerg Dis.* (2019) 66:578–87. doi: 10.1111/tbed.13067

7. Sun P, Jin J, Wang L, Wang J, Zhou H, Zhang Q, et al. Porcine epidemic diarrhea virus infections induce autophagy in vero cells *via* ros-dependent endoplasmic reticulum stress through Perk and Ire1 Pathways. *Vet Microbiol.* (2021) 253:108959. doi: 10.1016/j.vetmic.2020.108959

8. Park JY, Ryu J, Hong EJ, Shin HJ. Porcine epidemic diarrhea virus infection induces autophagosome formation but inhibits autolysosome formation during replication. *Viruses.* (2022) 14:1050. doi: 10.3390/v14051050

9. Sun E, Huang L, Zhang X, Zhang J, Shen D, Zhang Z, et al. Genotype I African swine fever viruses emerged in domestic pigs in China and caused chronic infection. *Emerg Microbes Infect.* (2021) 10:2183–93. doi: 10.1080/22221751.2021.1999779

10. Jalal K, Khan K, Ahmad D, Hayat A, Basharat Z, Abbas MN, et al. Pan-genome reverse vaccinology approach for the design of multi-epitope vaccine construct against *Escherichia albertii*. *Int J Mol Sci.* (2021) 2:12814. doi: 10.3390/ijms222312814

11. D'Mello A, Ahearn CP, Murphy TF, Tettelin H. ReVac: A reverse vaccinology computational pipeline for prioritization of prokaryotic protein vaccine candidates. *BMC Genomics.* (2019) 20:981. doi: 10.1186/s12864-019-6195-y

frontiers | Frontiers in Veterinary Science

ORIGINAL RESEARCH
published: 24 June 2022
doi: 10.3389/fvets.2022.930871

Epidemiological Investigation of Porcine Pseudorabies Virus in Hebei Province, China, 2017–2018

Cheng Zhang[1,2†], Huan Cui[2,3†], Wuchao Zhang[1†], Lijia Meng[1†], Ligong Chen[1], Zhongyi Wang[4], Kui Zhao[3], Zhaoliang Chen[1], Sina Qiao[1], Juxiang Liu[1], Zhendong Guo[2*] and Shishan Dong[1*]*

[1] College of Veterinary Medicine, Hebei Agricultural University, Baoding, China, [2] Changchun Veterinary Research Institute, Chinese Academy of Agriculture Sciences, Changchun, China, [3] College of Animal Medicine, Jilin University, Changchun, China, [4] Beijing Institute of Biotechnology, Beijing, China

OPEN ACCESS

Edited by:
Lian-Feng Li,
Harbin Veterinary Research Institute (CAAS), China

Reviewed by:
Wu Hongxia,
Harbin Veterinary Research Institute (CAAS), China
Yingying Fu,
Academy of Military Science of the Chinese People's Liberation Army, China

***Correspondence:**
Juxiang Liu
ljx0315@126.com
Zhendong Guo
guozd@foxmail.com
Shishan Dong
dongshishan@163.com

[†] These authors have contributed equally to this work

Specialty section:
This article was submitted to Veterinary Infectious Diseases, a section of the journal Frontiers in Veterinary Science

Received: 28 April 2022
Accepted: 01 June 2022
Published: 24 June 2022

Citation:
Zhang C, Cui H, Zhang W, Meng L, Chen L, Wang Z, Zhao K, Chen Z, Qiao S, Liu J, Guo Z and Dong S (2022) Epidemiological Investigation of Porcine Pseudorabies Virus in Hebei Province, China, 2017–2018. Front. Vet. Sci. 9:930871. doi: 10.3389/fvets.2022.930871

Pseudorabies (PR) is a serious disease affecting the pig industry in China, and it is very important to understand the epidemiology of pseudorabies virus (PRV). In the present study, 693 clinical samples were collected from Bartha-K61 vaccinated pigs with symptoms of suspected PRV infection between January 2017 and December 2018. All cases were referred for full clinical autopsy with detailed examination of histopathological examination, virus isolation and genetic evolution analysis of the PRV glycoprotein E (*gE*) gene. In addition, PRV *gE* antibodies in 3,449 serum samples were detected by the enzyme-linked immunosorbent assay (ELISA). The clinical data revealed that abortion and stillbirth are the most frequent appearances in pregnant sows of those cases. Histopathological examination exhibited a variety of pathological lesions, such as lobar pneumonia, hepatitis, lymphadenitis, nephritis, and typical nonsuppurative encephalitis. A total of 248 cases tested positive for the PRV gE gene. 11 PRV variants were isolated and confirmed by *gE* gene sequencing and phylogenetic analysis. These strains had 97.1%-100.0% nucleotide homology with the PRV reference strains. Notably, the isolated strains were highly homologous and clustered in the same branch as HSD-1/2019, which caused human acute encephalitis. Serological tests showed that the positive rate of PRV *gE* antibody in the 3449 serum samples collected from the Hebei Province was 46.27%. In conclusion, PRV variant strains Are high prevalence in the Hebei Province, which not only causes huge economic losses to the breeding industry but also potentially poses a threat to public health.

Keywords: pseudorabies virus, epidemiological analysis, virus isolation, phylogenetic analysis, serological investigation

INTRODUCTION

Pseudorabies (PR) is an acute infectious disease caused by pseudorabies virus (PRV) in many domestic animals and wild animals (1). It has a wide range of hosts and can infect mammals such as deer, bears, wolves, birds and humans (2, 3). Pigs are considered as the main and intermediate host of the PRV (4). The PRV mainly damages the reproductive system, respiratory system and nervous

system of pigs in different ages. PRV is characterized by reproductive dysfunction of pregnant sows, neurological symptoms and high mortality of suckling piglets, and it is one of the important diseases harmful to the healthy development of the pig industry (1, 5–7).

The glycoprotein E (*gE*) gene is the main virulence gene of PRV, and the protein encoded by the *gE* gene plays an important role in mediating the fusion of virus entry, the release of virus particles, and the neurotrophic activity of viruses (8). PRV with *gE* gene deletion maintained immunogenicity but significantly reduced virulence (9). Before 2011, PR was largely controlled by the widespread application of the *gE* deletion vaccine in China (10). However, since 2012, there have been increasing reports of PR occurring in pigs vaccinated with the Bartha-K61 vaccine due to the emergence of variant strains of PRV (11–13). According to previous reports, the widely used PRV Bartha-K61 strain was shown to be incapable of providing complete protection against this new PRV variant (14). Despite great efforts to eradicate PRV in China, PR remains a serious threat to the Chinese pig industry (10, 15). During 2012–2021, the emergence of mutant PRV strains was reported in most provinces of China, resulting in the death of many pigs and huge economic losses (16). Since 2017, China has reported at least 14 cases of human infection with PRV, and a study in the cerebrospinal fluid of patients with an isolated first anthropogenic PRV strain HSD-1/2019 (17–23).

As an important area for pig breeding in China, Hebei Province has not been reported on the epidemiology of PRV before our study, so the investigation of the epidemiology of PRV in Hebei Province is of great significance. In this study, a total of 693 suspected clinical cases of PRV infection and 3,449 pig serum samples were collected from Hebei Province during the 24-month period from January 2017 to December 2018. Pathological examination, histological observation, virus isolation and identification, genetic evolution analysis and antibody level analysis were carried out. We found that the PRV variant strain is still prevalent in Hebei and poses a threat to the pig industry and public health.

MATERIALS AND METHODS

Clinical Cases and Sample Collection

A total of 693 clinical cases of suspected PRV infection in 299 pig farms were collected during 2017–2018, which covered almost all cities of Hebei Province (**Table 1**). All pigs in this study had been inoculated with live PRV vaccine (Bartha-K61 strain). All examination and sample collection of the pigs were conducted in a biosafety laboratory. Corresponding tissue samples comprising brain, lung, liver, lymph node and kidney were collected from each pig. Samples were split into two groups, one of which was used to detect pathogens by polymerase chain reaction (PCR) or reverse transcription-polymerase chain reaction (RT–PCR), and another spot sample was fixed with 10% neutral formalin and used for hematoxylin-eosin (HE) staining and immunohistochemical (IHC) staining.

Histopathologic Examination

Histopathological testing was performed using samples that were positive for PRV by PCR. The samples fixed in 10% neutral formalin were embedded in paraffin, and the tissue samples were cut into 4 mm thick sections. Hematoxylin and Eosin Staining Kit (C0105M, Beyotime, China) was used for HE staining and two-step anti-mouse IgG-HRP immunohistochemistry Kit (SV0001, BOSTER, China) was used for IHC staining. HE and IHC staining was performed following the manufacturer's instructions. The primary antibody used in IHC staining was mouse anti-PRV-gE mAb (LD-DW-Z0022, LV DU, China), diluted 1:1000.

Virus Detection

DNA and RNA were extracted from collected tissue samples using the EasyPure® Viral DNA/RNA Kit (ER201-01, TRANS, China) according to the manufacturer's instructions. RNA was converted into cDNA by the PrimeScript™ RT Reagent Kit with gDNA Eraser (Takara, Dalian, China). Tissue samples were analyzed for the presence of porcine circovirus type 2 (PCV2), porcine circovirus type 3 (PCV3), classical swine fever virus (CSFV), porcine reproductive and respiratory syndrome virus (PRRSV), or porcine epidemic diarrhea virus (PEDV) by PCR or RT–PCR as previously reported (24). The primers used in this study are listed in **Supplementary Table 1**.

Isolation and Identification of Virus

All PRV positive samples were homogenized in Dulbecco's modified Eagle's medium (DMEM) (Gibco, Grand Island, NY, USA). The sample was then centrifuged at 8,000 × g for 15 min at 4°C, and the supernatants were filtered through 0.22 μm membrane filters (Millipore, Billerica, MA, USA). The monolayer porcine kidney cell line PK-15 (CCL-33, ATCC, USA) was incubated with filtered supernatant for 1.5 h. DMEM was supplemented with 10% fetal bovine serum (Gibco, Grand Island, NY, USA), 100 μg/mL streptomycin, and 100 U/mL penicillin. The inoculated PK-15 cells were placed in a 5% CO_2 incubator at 37°C. Cells were observed daily for cytopathic effect (CPE). When the CPE reached 80%, the cells were harvested, frozen and thawed three times. The virus was further purified by plaque assay, and the isolated virus was identified by RT–PCR or PCR.

Sequence and Genetic Evolution Analysis

The extracted PRV DNA was amplified by PCR according to previous studies to obtain the full length of the *gE* gene (25). The full-length *gE* gene primers are shown in **Supplementary Table 1**. Sequencing was performed by Comate Biotech Company (Jilin, China). The sequences obtained were submitted to the GenBank database (**Supplementary Table 2**). Reference sequences of *gE* genes were downloaded from NCBI GenBank (**Supplementary Table 2**), and the downloaded sequences were aligned and compared with the strains in this study using Cluster W. Phylogenetic analysis was performed using MEGA7.0.21 software (Sinauer Associates, Inc., Sunderland, MA, USA) based on the maximum likelihood (ML) with a bootstrap value of 1,000.

TABLE 1 | Information on the clinical cases in this study.

Origin city	Numbers	Clinical symptoms				
		High temperature	Abortion	Stillbirth	Neurological disorders	Respiratory problems
Shijiazhuang	167	14	40	52	35	26
Baoding	104	10	20	25	26	23
Xingtai	78	5	19	24	20	10
Hengshui	37	0	12	19	0	6
Langfang	59	9	16	25	3	6
Zhangjiakou	74	3	20	35	16	0
Cangzhou	96	0	30	27	21	18
Tangshan	52	6	5	24	8	9
Handan	26	4	15	7	0	0
Total numbers	693	51	177	238	129	98

Serologic Assays

A total of 3,449 serum samples were collected from 2017 to 2018, covering almost all of Hebei Province, and the collection locations, growth stages and scales of farms of serum samples were recorded in detail (**Tables 3**, **4**). Commercial ELISA kits (IDEXX Laboratories, Westbrook, ME, USA) were used to detect PRV *gE* antibody levels in serum samples to distinguish vaccine strains from wild-type virulent PRV strains, according to the manufacturer's instructions.

RESULTS

Clinical Symptoms

The body temperature of the PRV-infected sows reached 40–41°C, accompanied by phenomena such as giving birth to weak pigs (**Figure 1A**). The newborn piglets were weak in their capacity to suck the breast. Soon after, empty chewing and molars were seen, leading to a large amount of foam liquid flowing from the corner of the mouth (**Figure 1B**). Flush conjunctiva, turbid cornea, eyelid edema, eye fixation and glazed eyes were observed. Later, dyskinesia of the posterior limbs and a shaking body were found (**Figure 1C**). Abortion was also a common symptom (**Figure 1D**). Hemorrhagic spots were observed on the renal cortex (**Figure 1E**). Cerebral hemorrhage and congested meninges were visible (**Figure 1F**). The congested lung was swollen with focal white necrosis, and severe pulmonary hemorrhage was also observed (**Figure 1G**). Multiple small focal areas of necrosis were observed in the liver (**Figure 1H**). According to **Table 1**, abortion and stillbirth occur most frequently in the clinical manifestations of pigs suspected of PRV infection. Neurological disorders and respiratory problems were moderate, and high temperature was the least common.

Observation of Histopathological Changes

The results of pathological observations are shown in **Figure 2**. The brain had multiple symptoms, including focal hemorrhage, focal vacuolation of brain parenchyma, a large amount of lymphocyte infiltration, degeneration, necrosis and neuronophagia of neurocytes, hematoxylin and congestion and formation of perivascular cuffing, forming typical nonsuppurative encephalitis. For the lung, capillaries in the alveolar walls were congested, and alveolar walls were thickened. A large number of erythrocytes, necrotic and exfoliated epithelial cells, lymphocytes and incarnadine inflammatory protein and tissue liquid were observed in the alveolar space. The smooth muscle layer of the vascular walls was necrotic, thickened and congested. Partial epithelial cells of the bronchial mucosa were necrotic and had a great number of inflammatory cells, which were mainly lymphocytes as well as exfoliated epithelial cells. Loosening and edema were obvious in the mesenchyme surrounding the bronchiole, and there was a bulk of lymphocytes and erythrocytes within. Obvious lobar pneumonia was formed. The liver had multiple symptoms, including hepatic sinus expansion and congestion, hepatic steatosis and necrosis, and a large amount of lymphocyte infiltration in the hepatic lobule indicated degenerative hepatitis. The lymph nodes had multiple symptoms including congestion and hemorrhage of lymph nodes, decreased lymphoid follicles and necrotic and disintegrated lymphocytes. Degenerated necrosis and hemorrhage of the vascular wall were observed. The tonsilla had multiple symptoms including congestion and hemorrhage, degeneration and necrosis of epithelial cells. Necrosis of lymphocytes in lymphoid nodules. The kidney had multiple symptoms including congestion and hemorrhage, degeneration and necrosis of renal tubular epithelial cells. A large amount of incarnadine protein and exfoliated epithelial cells were observed in the cavity.

The IHC results are shown in **Figure 3**. Virus-positive particles were widely found in the brain, and they mainly appeared in the cytoplasm and axon of neurons (**Figures 3A–D**). The cortical area of the lymph node contains many positive particles, indicating the presence of PRV in the cortical area, and the virus-positive particles mainly exist in lymphocytes and macrophages (**Figures 3E,F**).

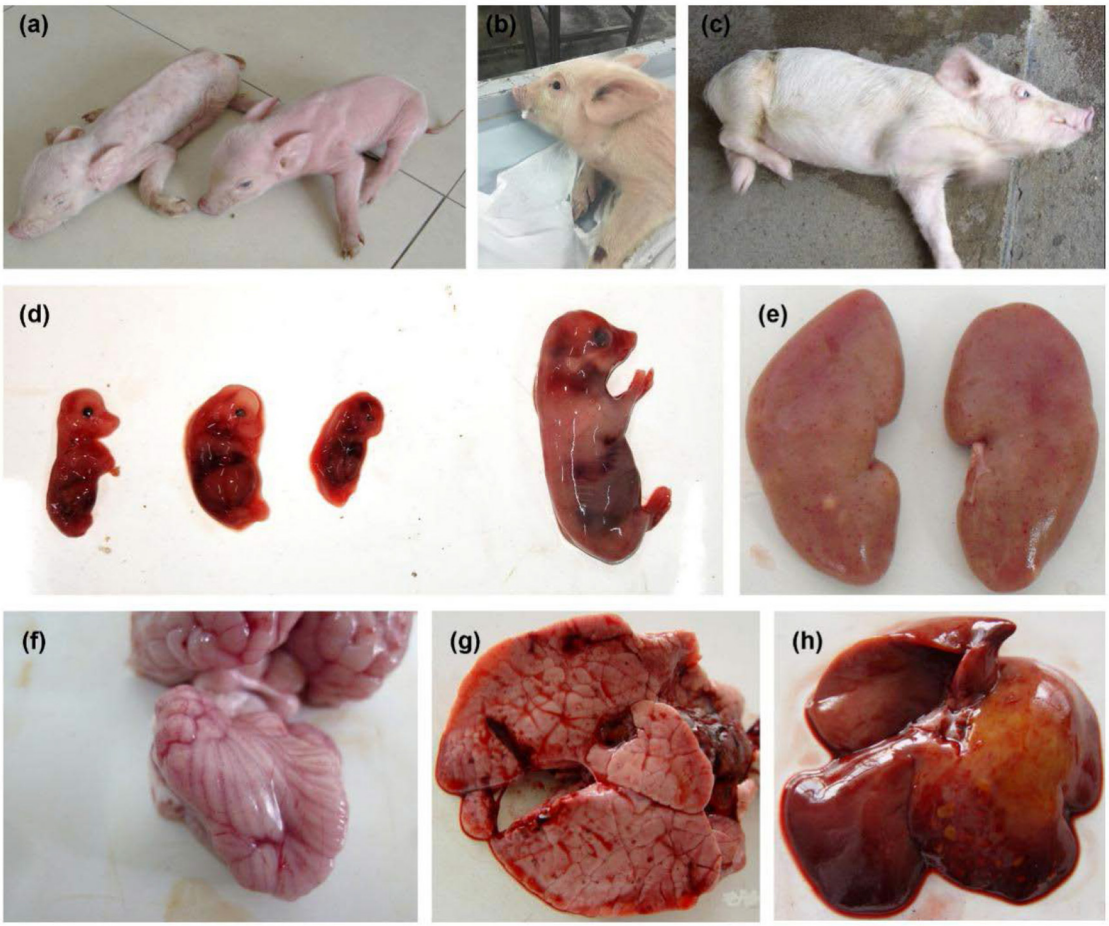

FIGURE 1 | Clinical symptoms observed in pseudorabies virus-infected pigs. **(A)** Giving birth to weak piggies. **(B)** Foaming at the mouth. **(C)** Severe neurological disorders. **(D)** Aborted fetus. **(E)** Hemorrhagic spot on the renal cortex. **(F)** Cerebral hemorrhage and congested meninges. **(G)** Pulmonary hemorrhage. **(H)** Liver with multiple small focal areas of necrosis.

gE Genes Positive Rate

During the 24 months from January 2017 to December 2018, 693 suspected PRV infection cases from Hebei Province were collected. Among the suspected PRV infection cases, the *gE* gene was detected in 248 (35.78%) of 693 suspected cases of PRV infection, in which PCV2, PCV3, PRRSV and CSFV were negative.

Evolutionary Genetic Analysis

11 strains with different gE gene sequences were obtained after 248 PRV-gE gene repeats were deleted. Analysis of the 11 sequences showed that the nucleotide homology and amino acid homology were 97.1–100.0% and 95.0–100.0%, respectively, with the reference strain (**Table 2**), which were highly homologous with HSD-1/2019 causing human acute encephalitis. Compared with the reference strains, the changes in gE genes in this study are shown in **Figure 4,** which are highly consistent with the epidemic strains and human infection strains in recent years. Phylogenetic analysis of the gE gene showed that PRV isolates from China were located on a separate phylogenetic clade from isolates from other countries (**Figure 5**). In this branch, the gE genes of the 11 strains in this study were adjacent to PRV variants TJ, HLJ8 and HB1201, and closely related to HSD-1/2019. The gE genes of the 11 strains in this study were far different from those of Fa, Ea and SC. These results indicate a close phylogenetic relationship between the isolates in this study and PRV variants in China, including HSD-1/2019, which causes human acute encephalitis.

Serological Investigation of Serum Samples

A total of 3449 serum samples were collected from January 2017 to December 2018 in Hebei Province, of which 1596 were positive for gE-specific antibodies, and the overall seropositivity rate (SRP) for the study was 46.27%. **Tables 3**, **4** show the SPR of different regions, production stages and breeding scales. According to the data in **Table 4**, Shijiazhuang city has the highest SPR (59.6%), and Baoding city has the lowest SPR (30.8%).

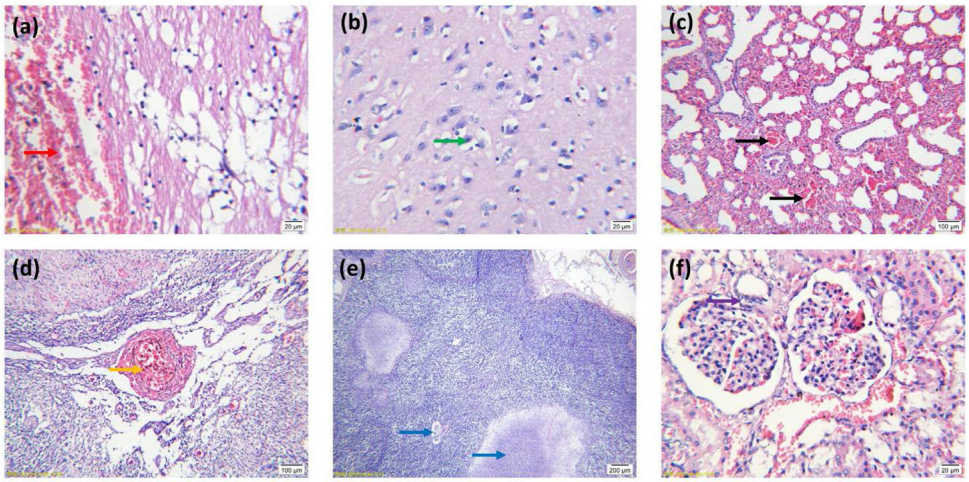

FIGURE 2 | Histopathological features of tissues stained with hematoxylin and eosin. **(A)** Focal hemorrhage of the brain (arrow red). **(B)** Necrosis and neuronophagia of neurocytes (arrow green). **(C)** Lung congestion (arrow black). **(D)** Congestion and hemorrhage of lymph nodes (arrow orange). **(E)** Necrosis of lymphoid follicles (arrow blue). **(F)** Degeneration and necrosis of renal tubular epithelial cells (arrow purple). **(A,B,F)** Images were obtained at 100× magnification; **(C,D)** Images were obtained at 20× magnification; **(E)** Images were obtained at 10× magnification.

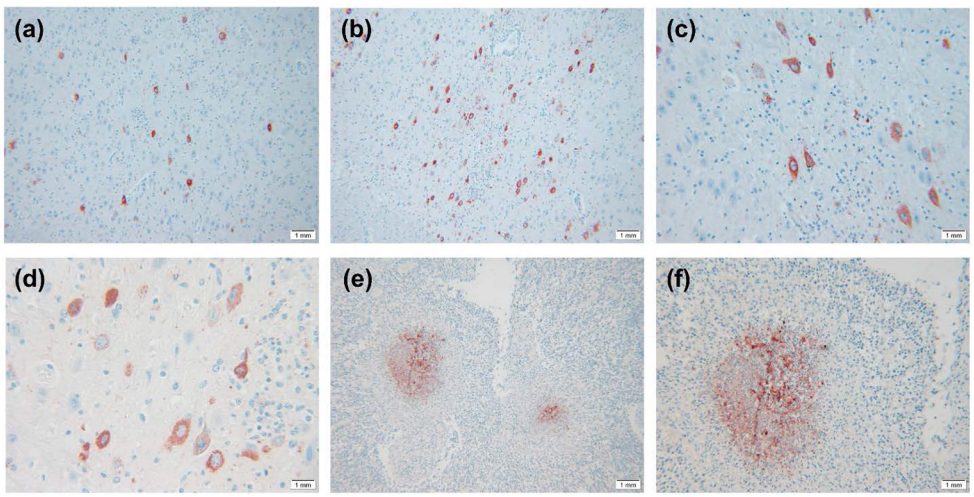

FIGURE 3 | IHC results of PRV-infected pig tissue. **(A–D)** Virus-positive particles were widely found in the brain, and virus-positive particles mainly appeared in the cytoplasm and axons of neurons in the brain. **(E,F)** There were a large number of virus-positive particles in the cortex of lymph nodes, and the virus-positive particles mainly existed in lymphocytes and macrophages. Images were obtained at 400× magnification.

The SPR of other cities ordered from high to low is Tangshan city (56.9%), Zhangjiakou city (53.3%), Langfang city (52.9%), Handan city (51.7%), Hengshui city (49.1%), Cangzhou city (38.3%), and Xingtai city (37.1%). Meanwhile, the data in **Table 3** also show the SPR of different stages, and the SPR of growing finishing pigs was the highest (59.7%). They were followed by nursery pigs (54.9%), suckling piglets (48.8%), multiparous sows (46.8%), boars (24.5%) and gilts (19.7%). As shown in **Table 4**, the SPR of pig farms with basal sows≥3,000 pigs is the lowest (27.4%), and the SPR of basal sows of 200–500 pigs is the highest (55.7%). The SPR of pig farms with 500–1,000 basal sows was 51.6% and that of pig farms with 1000–3000 basal sows was 48.7%.

DISCUSSION

PR has become a recognized infectious disease, which causes huge economic losses to the breeding industry and poses a threat to public health security. Since 2017, China has reported at least 14 cases of human infection with PRV. Considering these cases of human PRV infection and the close relationship between pigs and humans, a large ammount of clinical cases and serum samples

TABLE 2 | Nucleotide and amino acid identities for glycoprotein E (*gE*) gene between 11 gE genes and that of 19 representative PRV isolates (%).

Identities	Nia-1	NS374	CL-15	75V19	00V72	Becker	NiA3	Hercules	Kolchis	Kaplan	ADV32751-Italy2014
Origin	Ireland	Belgium	Argentina	Belgium	Belgium	USA	Spain	Greece	Greece	Hungary	Italy
Isolate time	1962	1971	1971	1975	2000	2003	2008	2010	2010	2011	2014
Accession no.	FJ605136	FJ605135	JF460026	FJ605133	FJ605132	AY368490	EU502923	KT983810	KT983811	JF797218	KU198433
Nt	97.2-97.4	97.6-97.7	97.7-97.9	97.5-97.6	97.1-97.2	97.9-98.0	97.7-97.8	97.6-97.8	97.6-97.8	97.7-97.8	97.9-98.0
AA	95.3-95.5	95.5-95.7	95.8-96.0	96.5-96.7	95.0-95.2	95.8-96.0	95.7-95.8	96.0-96.2	96.0-96.2	96.0-96.2	95.8-96.0

Identities	SC	Ea	Fa	HB1201	HLJ8	TJ	HuBXY/2018	hSD-1/2019
Origin	China	China	China	China	China	China	China	China
Isolate time	1986	1999	2012	2012	2013	2014	2018	2019
Accession no.	KM676290	AF171937	KM189913	KU057086	KT824771	KJ789182	MT468549	MT468550
Nt	99.6-99.7	99.6-99.7	99.6-99.7	99.6-99.9	99.9-100.0	99.8-99.9	99.9-99.9	99.9-99.9
AA	99.1-99.3	99.1-99.3	99.1-99.3	99.8-100.0	99.8-100.0	99.5-99.7	99.8-100.0	99.8-100.0

Nt, nucleotide; AA, amino acid.

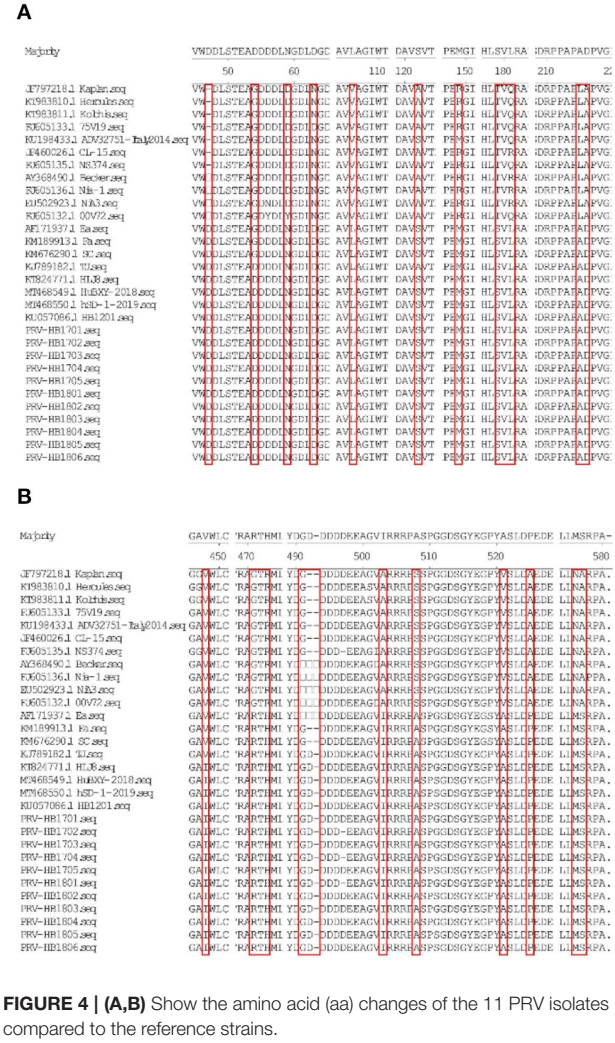

FIGURE 4 | (A,B) Show the amino acid (aa) changes of the 11 PRV isolates compared to the reference strains.

were collected from 2017 to 2018 in Hebei Province, China for the study.

It has been reported that pigs infected with the PRV variant strain showed severe clinical symptoms such as high fever, tonsil bleeding, lung swelling and necrosis (26). Among the pigs suspected of PRV infection, abortion and stillbirth have the most occurrence (27), which is consistent with the cases in our study. HE staining analysis showed typical pathological changes in the brain and lungs of PRV-infected pigs, including nonsuppurative encephalitis and lobular pneumonia, and immunohistochemical staining showed multiple positive staining signals in the brain, indicating that PRV had strong neurotropic characteristics. At the same time, lymph node hyperemia, hemorrhage, lymphatic follicle reduction, lymphocyte necrosis, disintegration and other pathological changes were also observed. There were many positive particles in the cortical region of lymph nodes, indicating the presence of PRV in the cortical region.

From 2011 to 2021, the positive rate of PRV *gE* gene nucleic acid in pigs in China was 11.5% (16), and the prevalence of PRV was closely related to region (25). In this study, from January 2017 to December 2018, we collected a total of 693 suspected cases of PR infection in Hebei Province, China, of which 248 (35.78%) were PRV *gE* gene positive. The results of our study are much higher than those of previous studies, which may be related to sample collection methods and geographical locations. Compared with other studies, the increase in the PRV *gE* gene-positive rate was closely related to the relatively backward breeding production level and lax production management in Hebei Province. The high positive rate of the *gE* gene in Hebei Province once again highlights the importance of continuous monitoring of PRV. In clinical cases, PRV is commonly coinfected with other viruses, such as PRRSV, CFSV, PCV2, PCV3, etc. (28). In this study, mixed infection of a variety of viruses also appeared, indicating that other diseases are prevalent in Hebei, which requires further research.

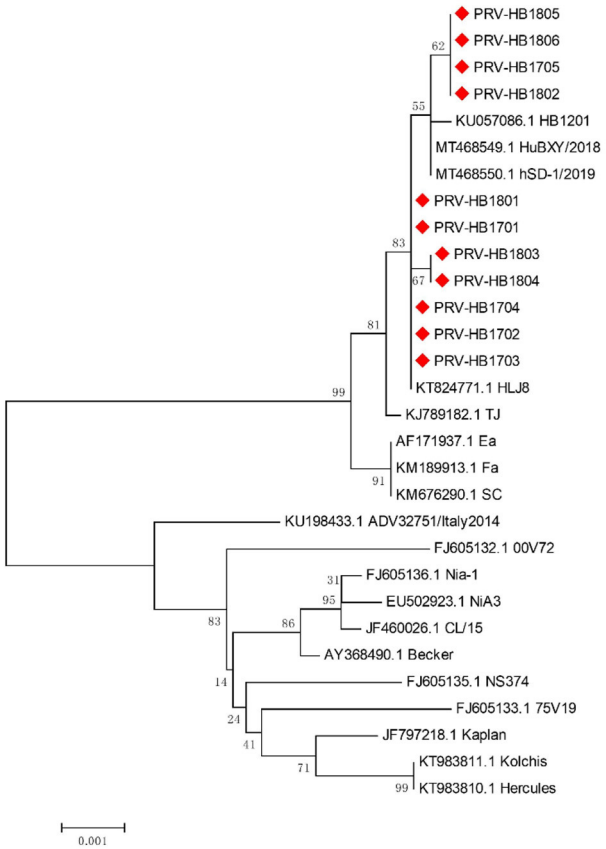

FIGURE 5 | Phylogenetic analysis and comparison based on pseudorabies virus (PRV) glycoprotein E (*gE*) nucleotide sequences. Red diamonds, 11 PRV isolates from Hebei Province collected from 2017 to 2018.

The *gE* gene of 11 PRV strains isolated in this study had high homology with PRV variant strains, including the human PRV strain HSD-1/2019. The PRV *gE* gene is closely associated with virulence (15). Alignment of amino acid sequences revealed that the same amino acid mutations as previously reported were found in *gE* compared to the reference strain (27). Mutations in the *gE* gene may affect the virulence of isolates, which requires further study. The *gE* genes of the 11 strains in this study were in the same clade as the PRV variants TJ, HLJ8 and HB1201 and were closely related to HSD-1/2019. Traditional PRV vaccines cannot provide sufficient cross-protection against PRV variant isolates (15). In fact, since 2012, PRV variant strains have been widely spread in China, and there have been increasing reports of human infection with PRV, so more attention should be given to PRV (16).

A recent study collected data from 2011 to 2020 and found that the seroprevalence of PRV *gE* in China was 29.87% (76,553/256,326) (16). The seroprevalence of PRV *gE* varies in different regions of China. In Henan Province, 30.14% (1,419/4,708) of the samples collected in 2018–2019 were

TABLE 4 | Serum sample information from farms of different sizes.

Number of basal sows	Serum numbers	Positive number	SPR (%)	Sample percentage
200–500	978	545	55.7%	28.4%
500–1,000	892	460	51.6%	25.9%
1,000–3,000	743	362	48.7%	21.5%
≥3,000	836	229	27.4%	24.2%

TABLE 3 | Information on the serum samples from 2017 to 2018.

Origin city	Serum numbers	Positive number	SPR (%)	Herds					
				Boars	Gilts	Multiparous sows	Suckling piglets	Nursery pigs	Growing-finishing pigs
Shijiazhuang	990	590	59.6	37	68	494	110	192	89
Baoding	1,097	338	30.8	24	54	707	102	142	68
Xingtai	213	79	37.1	11	27	54	54	46	21
Hengshui	57	28	49.1	10	10	17	3	13	4
Langfang	87	46	52.9	18	21	13	5	17	13
Zhangjiakou	629	335	53.3	20	45	357	80	47	80
Cangzhou	149	57	38.3	13	26	27	27	48	8
Tangshan	109	62	56.9	18	23	13	27	14	14
Handan	118	61	51.7	4	10	46	20	22	16
Total number	3,449	-	-	155	284	1,728	428	541	313
Positive number	1,596	-	-	38	56	809	209	297	187
SPR (%)	46.27	-	-	24.5	19.7	46.8	48.8	54.9	59.7

gE seropositive (10), while in Heilongjiang Province, 16.3% (3,067/18,815) were *gE* seropositive from 2013 to 2018 (29). The positive rate of *gE* in Shandong Province from 2013 to 2016 was 57.8% (2,909/5,033) (27). In this study, the positive rate of *gE* antibody in serum samples was 46.27%, similar to that in Shandong Province but different from that in other provinces. The positive rate of serum *gE* was different among different cities in Hebei Province, but it remained at a high level in general. The reason for this situation may be that some pig farms did not test in advance when they introduced (or retained) breeding pigs, leading to the introduction of positive and toxic backup breeding pigs. Meanwhile, due to unreasonable immunization procedures, some pig farms were infected with wild viruses after the introduction of negative backup breeding pigs, leading to positive antibodies. In this situation, new strains of infection appeared. The decreased immune effect of the previous vaccine may have caused the increase in the positive rate in Hebei Province. Our data also showed that the growing-finishing pigs had the highest SPR, followed by the nursery pigs, suckling piglets, multiparous sows, boars and gilts. We found that with the increase in the weeks of age of commercial pigs, the positive rate showed an increasing trend, which also reflected the gradual increase in infection risk. The *gE* seropositivity of multiparous sows was 46.8% (809/1728), which is consistent with previous studies indicating that multiparous sows are at high risk of PRV infection (27). Piglets infected with PRV through vertical transmission can cause persistent and recurrent infection in pig herds. By comparing four farms of different sizes, it was found that the larger the breeding scale was, the lower the *gE* positive rate was. Large-scale pig farms in Hebei Province generally adopt a three-point or multipoint breeding mode (a pig farm is divided into different areas according to the function of different piggery, the different areas are relatively closed, and different week-old pigs are transported to the specified piggery by field transport vehicles). These two models reduce the chance of return from high-risk herds to breeding herds, which helps control the disease. In addition, large-scale pig farms pay more attention to biosafety, reducing the risk of infection. All the data showed that the seropositive rate of PRV variant strains was still high in Hebei Province, China, which posed a challenge to pig breeding in Hebei Province, China.

In this study, systematic investigation including clinical autopsy, histological examination, virus isolation, sequencing and phylogenetic analysis, and serological investigation showed that the PRV variant strain was still prevalent in Hebei Province, China, and the protective effect of current vaccines against the new strain was poor. With the widespread epidemic of PRV strains in pigs in Hebei Province, China, it can be predicted that this disease will still be one of the most important diseases affecting the healthy development of the pig industry in Hebei Province in the future. Our study did not last longer due to the impact of the African swine fever outbreak. In view of the increasing reports of PRV infection in humans after 2017. Future study should be carried out from the following aspects: Strengthen the feeding management of pigs by improving hardware and feeding nutritious feeds to avoid the prevalence of related "endogenous" diseases on farms. Establish high-level biosafety system and strengthen the biosafety awareness of farm staff to avoid the recurrence of PRV infection in human, and control the invasion of "exogenous diseases in pig farms" caused by seed introduction, traffic flow, human flow and logistics, etc. Define the idea of prevention and control of diseases in pig farms, make suitable immunization and health program to build up a protective shield for pig farms, and implement it firmly through production management. Regularly monitor the immunization and prevention and control of pig herd to minimize the danger of diseases. The prevention and control of PR should still focus on purifying pig farms. In conclusion, this study is helpful to analyze the epidemiological situation of PRV in Hebei Province and provide basic data for the prevention and control of PRV.

DATA AVAILABILITY STATEMENT

The datasets presented in this study can be found in online repositories. The names of the repository/repositories and accession number(s) can be found in the article/**Supplementary Material**.

ETHICS STATEMENT

The animal study was reviewed and approved by Animal Ethics Committee of Hebei Agricultural University.

AUTHOR CONTRIBUTIONS

JL, SD, and ZG designed the project. CZ, HC, and WZ performed the experiments. LC, ZC, KZ, SQ, ZW, and LM analyzed the data. CZ, ZG, and HC drafted the manuscript. JL and SD critically revised the manuscript. All authors contributed to the article and approved the submitted version.

FUNDING

This study was supported by the Key Research Projects in Hebei Province (20326622D and 18227517D) and Hebei Industrial Technology System (HBCT2018150210).

SUPPLEMENTARY MATERIAL

The Supplementary Material for this article can be found online at: https://www.frontiersin.org/articles/10.3389/fvets.2022.930871/full#supplementary-material

REFERENCES

1. Pomeranz LE, Reynolds AE, Hengartner CJ. Molecular biology of pseudorabies virus: impact on neurovirology and veterinary medicine. *Microbiol Mol Biol Rev.* (2005) 69:462–500. doi: 10.1128/MMBR.69.3.462-500.2005
2. Klupp BG, Lomniczi B, Visser N, Fuchs W, Mettenleiter TC. Mutations affecting the UL21 gene contribute to avirulence of pseudorabies virus vaccine strain Bartha. *Virology.* (1995) 212:466–73. doi: 10.1006/viro.1995.1504
3. Fan S, Yuan H, Liu L, Li H, Wang S, Zhao W, et al. Pseudorabies virus encephalitis in humans: a case series study. *J Neurovirol.* (2020) 26:556–64. doi: 10.1007/s13365-020-00855-y
4. Marcaccini A, López Peña M, Quiroga MI, Bermúdez R, Nieto JM, Alemañ N. Pseudorabies virus infection in mink: a host-specific pathogenesis. *Vet Immunol Immunopathol.* (2008) 124:264–73. doi: 10.1016/j.vetimm.2008.03.013
5. Mettenleiter TC. Immunobiology of pseudorabies (Aujeszky's disease). *Vet Immunol Immunopathol.* (1996) 54:221–9. doi: 10.1016/S0165-2427(96)05695-4
6. Ekstrand MI, Enquist LW, Pomeranz LE. The alpha-herpesviruses: molecular pathfinders in nervous system circuits. *Trends Mol Med.* (2008) 14:134–40. doi: 10.1016/j.molmed.2007.12.008
7. Cramer SD, Campbell GA, Njaa BL, Morgan SE, Smith SK 2nd, McLin WR, et al. Pseudorabies virus infection in Oklahoma hunting dogs. *J Vet Diagn Invest.* (2011) 23:915–23. doi: 10.1177/1040638711416628
8. Prieto J, Martín Hernández AM, Tabarés E. Loss of pseudorabies virus thymidine kinase activity due to a single base mutation and amino acid substitution. *J Gen Virol.* (1991) 72 (Pt 6):1435–9. doi: 10.1099/0022-1317-72-6-1435
9. Mulder WA, Jacobs L, Priem J, Kok GL, Wagenaar F, Kimman TG, et al. Glycoprotein gE-negative pseudorabies virus has a reduced capability to infect second- and third-order neurons of the olfactory and trigeminal routes in the porcine central nervous system. *J Gen Virol.* (1994) 75 (Pt 11):3095–106. doi: 10.1099/0022-1317-75-11-3095
10. Zheng HH, Jin Y, Hou CY, Li XS, Zhao L, Wang ZY, et al. Seroprevalence investigation and genetic analysis of pseudorabies virus within pig populations in Henan province of China during 2018-2019. *Infect Genet Evol.* (2021) 92:104835. doi: 10.1016/j.meegid.2021.104835
11. Luo Y, Li N, Cong X, Wang CH, Du M, Li L, et al. Pathogenicity and genomic characterization of a pseudorabies virus variant isolated from Bartha-K61-vaccinated swine population in China. *Vet Microbiol.* (2014) 174:107–15. doi: 10.1016/j.vetmic.2014.09.003
12. Gu Z, Dong J, Wang J, Hou C, Sun H, Yang W, et al. A novel inactivated gE/gI deleted pseudorabies virus (PRV) vaccine completely protects pigs from an emerged variant PRV challenge. *Virus Res.* (2015) 195:57–63. doi: 10.1016/j.virusres.2014.09.003
13. Hu D, Zhang Z, Lv L, Xiao Y, Qu Y, Ma H, et al. Outbreak of variant pseudorabies virus in Bartha-K61-vaccinated piglets in central Shandong Province, China. *J Vet Diagn Invest.* (2015) 27:600–5. doi: 10.1177/1040638715593599
14. An TQ, Peng JM, Tian ZJ, Zhao HY, Li N, Liu YM, et al. Pseudorabies virus variant in Bartha-K61-vaccinated pigs, China, 2012. *Emerg Infect Dis.* (2013) 19:1749–55. doi: 10.3201/eid1911.130177
15. Yu X, Zhou Z, Hu D, Zhang Q, Han T, Li X, et al. Pathogenic pseudorabies virus, China, 2012. *Emerg Infect Dis.* (2014) 20:102–4. doi: 10.3201/eid2001.130531
16. Tan L, Yao J, Yang Y, Luo W, Yuan X, Yang L, et al. Current status and challenge of pseudorabies virus infection in China. *Virol Sin.* (2021) 36:588–607. doi: 10.1007/s12250-020-00340-0
17. Ai JW, Weng SS, Cheng Q, Cui P, Li YJ, Wu HL, et al. Human endophthalmitis caused by pseudorabies virus infection, China, 2017. *Emerg Infect Dis.* (2018) 24:1087–90. doi: 10.3201/eid2406.171612
18. Zhao WL, Wu YH, Li HF, Li SY, Fan SY, Wu HL, et al. Clinical experience and next-generation sequencing analysis of encephalitis caused by pseudorabies virus. *Zhonghua Yi Xue Za Zhi.* (2018) 98:1152–7. doi: 10.3760/cma.j.issn.0376-2491.2018.15.006
19. Yang H, Han H, Wang H, Cui Y, Liu H, Ding S. A case of human viral encephalitis caused by pseudorabies virus infection in China. *Front Neurol.* (2019) 10:534. doi: 10.3389/fneur.2019.00534
20. Yang X, Guan H, Li C, Li Y, Wang S, Zhao X, et al. Characteristics of human encephalitis caused by pseudorabies virus: a case series study. *Int J Infect Dis.* (2019) 87:92–9. doi: 10.1016/j.ijid.2019.08.007
21. Zheng L, Liu X, Yuan D, Li R, Lu J, Li X, et al. Dynamic cerebrospinal fluid analyses of severe pseudorabies encephalitis. *Transbound Emerg Dis.* (2019) 66:2562–5. doi: 10.1111/tbed.13297
22. Wang D, Tao X, Fei M, Chen J, Guo W, Li P, et al. Human encephalitis caused by pseudorabies virus infection: a case report. *J Neurovirol.* (2020) 26:442–8. doi: 10.1007/s13365-019-00822-2
23. Liu Q, Wang X, Xie C, Ding S, Yang H, Guo S, et al. A novel human acute encephalitis caused by pseudorabies virus variant strain. *Clin Infect Dis.* (2021) 73:e3690–700. doi: 10.1093/cid/ciaa987
24. Tan L, Li Y, He J, Hu Y, Cai X, Liu W, et al. Epidemic and genetic characterization of porcine epidemic diarrhea virus strains circulating in the regions around Hunan, China, during 2017-2018. *Arch Virol.* (2020) 165:877–89. doi: 10.1007/s00705-020-04532-7
25. Sun Y, Liang W, Liu Q, Zhao T, Zhu H, Hua L, et al. Epidemiological and genetic characteristics of swine pseudorabies virus in mainland China between 2012 and 2017. *PeerJ.* (2018) 6:e5785. doi: 10.7717/peerj.5785
26. Ren Q, Ren H, Gu J, Wang J, Jiang L, Gao S. The epidemiological analysis of pseudorabies virus and pathogenicity of the variant strain in Shandong Province. *Front Vet Sci.* (2022) 9:806824. doi: 10.3389/fvets.2022.806824
27. Gu J, Hu D, Peng T, Wang Y, Ma Z, Liu Z, et al. Epidemiological investigation of pseudorabies in Shandong Province from 2013 to 2016. *Transbound Emerg Dis.* (2018) 65:890–8. doi: 10.1111/tbed.12827
28. Ma Z, Liu M, Liu Z, Meng F, Wang H, Cao L, et al. Epidemiological investigation of porcine circovirus type 2 and its coinfection rate in Shandong province in China from 2015 to 2018. *BMC Vet Res.* (2021) 17:17. doi: 10.1186/s12917-020-02718-4
29. Zhou H, Pan Y, Liu M, Han Z. Prevalence of porcine pseudorabies virus and its coinfection rate in Heilongjiang Province in China from 2013 to 2018. *Viral Immunol.* (2020) 33:550–4. doi: 10.1089/vim.2020.0025

Conflict of Interest: The authors declare that the research was conducted in the absence of any commercial or financial relationships that could be construed as a potential conflict of interest.

frontiers | Frontiers in Veterinary Science

ORIGINAL RESEARCH
published: 24 June 2022
doi: 10.3389/fvets.2022.933896

Evolutionary Analysis of Four Recombinant Viruses of the Porcine Reproductive and Respiratory Syndrome Virus From a Pig Farm in China

Jiankui Liu[1,2,3]*, *Liling Lai*[1], *Ye Xu*[1,3], *Yuan Yang*[1], *Jiarui Li*[1], *Chen Liu*[1,3], *Cuiqin Hunag*[1,2,3] *and Chunhua Wei*[1,2,3]*

[1] College of Life Sciences, Longyan University, Longyan, China, [2] Engineering Research Center for the Prevention and Control of Animal Original Zoonosis, Fujian Province University, College of Life Science, Longyan University, Longyan, China, [3] College of Animal Science, Fujian Agriculture and Forestry University, Fuzhou, China

OPEN ACCESS

Edited by:
Keisuke Suganuma,
Obihiro University of Agriculture and Veterinary Medicine, Japan

Reviewed by:
Fei Gao,
Shanghai Veterinary Research Institute (CAAS), China
Gaurav Kumar Sharma,
Indian Veterinary Research Institute (IVRI), India

***Correspondence:**
Jiankui Liu
liujiankui99@126.com
Chunhua Wei
weichunhua02@163.com

Specialty section:
This article was submitted to Veterinary Infectious Diseases, a section of the journal Frontiers in Veterinary Science

Received: 01 May 2022
Accepted: 30 May 2022
Published: 24 June 2022

Citation:
Liu J, Lai L, Xu Y, Yang Y, Li J, Liu C, Hunag C and Wei C (2022) Evolutionary Analysis of Four Recombinant Viruses of the Porcine Reproductive and Respiratory Syndrome Virus From a Pig Farm in China. Front. Vet. Sci. 9:933896. doi: 10.3389/fvets.2022.933896

The porcine reproductive and respiratory syndrome virus (PRRSV) is one of the most important pathogens causing substantial economic losses to the Chinese swine industry. In this study, we analyzed the complete genome sequences of four PRRSV isolates (PRRSV2/CN/SS0/2020, PRRSV2/CN/SS1/2021, PRRSV2/CN/L3/2021, and PRRSV2/CN/L4/2020) isolated from a single pig farm from 2020 to 2021. The genomes of the four isolates were 14,962–15,023 nt long, excluding the poly (A) tails. Comparative analysis of the genome sequences showed that the four isolates shared 93.2–98.1% homology and they had no close PRRSV relatives registered in the GenBank (<92%). Furthermore, PRRSV2/CN/SS0/2020 and PRRSV2/CN/SS1/2021 had characteristic 150-aa deletions (aa481+aa537-566 +aa628–747) that were identical to the live attenuated virus vaccine strain TJM-F92 (derived from the HP-PRRSV TJ). Further analysis of the full-length sequences suggests that the four isolates were natural recombinant strains between lineages 1 (NADC30-like), 3 (QYYZ-like), and 8.7 (JXA1-like). Animal experiments revealed discrepancies in virulence between PRRSV2/CN/SS0/2020 and PRRSV2/CN/L3/2021. The strain with high homology to HP-PRRSV demonstrates higher pathogenicity for pigs than the other isolate with low homology to HP-PRRSV. Taken together, our findings suggest that PRRSVs have undergone genome evolution by recombination among field strains/MLV-like strains of different lineages.

Keywords: porcine reproductive and respiratory syndrome virus (PRRSV), genome characterization, evolution, recombination, pathogenicity

INTRODUCTION

The porcine reproductive and respiratory syndrome (PRRS) is caused by the porcine reproductive and respiratory syndrome virus (PRRSV). It was first reported in 1987 and has spread rapidly since to become a worldwide menace (1, 2). The PRRSV genome is an ∼15 kb-long positive single-stranded RNA virus that has been classified under the *Nidovirales* order and *Arteriviridae* family

(https://talk.ictvonline.org/taxonomy). The viral RNA contains at least ten open overlapping reading frames (ORFs): ORF1a, ORF1b, ORF2a, ORF2b, ORF3, ORF4, ORF5a, and ORF5–ORF7 (3–6). Among these ORFs, ORF1a and ORF1b comprise almost three-quarters of the viral genome and encode at least 16 nonstructural proteins (such as nsp1α, nsp1β, nsp2-6, nsp2TF, nsp2N, nsp7α, nsp7β, and nsp8–12), whereas other ORFs located at the 3' terminus code for eight structural proteins: GP2, E, GP3, GP4, GP5a, GP5, M, and N, respectively (3, 5, 7, 8).

All PRRSV strains isolated to date have been classified into two major genotypes, namely, the European (type 1) and North American (type 2) genotypes, with type 2 PRRSV being predominant in China since its initial report there in 1996 (9, 10). PRRS is considered one of the most important infectious diseases in Chinese swineherds as it causes severe economic losses in the swine industry every year. Currently, the Chinese type 2 PRRSV strains can be classified into different lineages, including lineage 1 (NADC30-like), 3 (QYYZ-like), 5 (VR2332-like), and 8 (JXA1-like and CH-1a-like) based on phylogenetic analysis of ORF5 sequences (11, 12). The diversity of the Chinese type 2 PRRSV has been increasing due to recombination events among the different PRRSV lineages since the emergence of NADC30-like PRRSVs in China in 2012 (12–23). In the present study, we identify four recombinant PRRSV strains circulating in a swine farm in Fujian province, China. Phylogenetic and molecular evolutionary analyses indicated that these strains evolved from natural recombination among the NADC30-, QYYZ-, and JXA1-like variants. To further understand the four strains, we genetically characterized the complete genomes of the viruses.

MATERIALS AND METHODS

Sample Collection and Viral Isolation

From 2020 to 2021, a severe reproductive and respiratory disease was observed in pigs from four independent pens in a swine farm in Fujian province, China. This farm created a PRRS-positive stable herd by inoculating 0.05 dose/pig of MLV TJM-F92 vaccine (derived from the HP-PRRSV TJ) from 2018. The affected pigs from the two pens exhibited high fever (40.3–41.8°C), severe respiratory syndrome, and high morbidity (30%) and mortality (20%), whereas those from the other two pens exhibited fever, severe respiratory syndrome and reproductive problems, and especially high abortion rate (10%) was observed in the sows. PRRSV was detected using an RT-PCR kit (Beijing Anheal Laboratories Co., Ltd., Beijing, China) according to the manufacturer's instructions. PRRSV was positive when the CT value was ≤30. MARC-145^{CD163} cell lines (a stable cell line highly expressing porcine CD163) were used for PRRSV isolation from the positive samples (12). The tissues (lung, lymph nodes, and serum samples) were homogenized with DMEM containing antibiotics and antimycotics to obtain a 50% (w/v) suspension. After freeze-thawing thrice, the samples were centrifuged at 10,000 × g for 10 min and the supernatants were sieved through a 0.22-μm filter. MARC-145^{CD163} cells were mixed with 100 μL of supernatant and incubated at 37 °C with 5% CO_2 for 3–5 days. PRRSVs were passaged three times in MARC-145^{CD163} cells for subsequent analysis after being plaque-purified three times.

RNA Isolation and RT-PCR

RNA was extracted from the positive tissues (lungs, serum, and lymph nodes) and the virus using a Viral RNA Mini Kit (TIANGEN, Beijing, China) according to the manufacturer's instructions. cDNA was generated using the HiScript® III 1st Strand cDNA Synthesis Kit (Vazyme Biotech Co., Ltd, Nanjing, China) following the supplier's instructions. The full-length viral genomes were amplified using six viral-specific primers (**Supplementary Table 1**). Subsequently, we confirmed the complete genome using other PCR primers as described previously (24, 25). The purified PCR products were cloned into the pEASY®-Blunt Simple Cloning Vector (TransGen Biotech, Beijing, China). To determine a consensus sequence of each fragment, at least three recombinant clones were sent to the Ruibo Life Technologies Corporation (Beijing, China) for sequencing by using the Sanger approach in both directions for each fragment.

Complete Genomic Sequence and Recombination Analysis

Forty-four representative PRRSV strains available in GenBank, including the type 1 and type 2 strains, were used for the comparative sequence analysis in this study (**Table 1**). Multiple sequence alignments and genome analyses were performed using the MEGA 7.0 software and the DNAStar 7.0 package. Phylogenetic trees were constructed using the neighbor-joining method in MEGA 7.0 and bootstrap confidence values from 1,000 replicates.

Potential recombination within the whole genome sequences was determined using seven methods (RDP, BootScan, GENECONV, Chimera, Maxchi, SiScan, and 3Seq) *via* the recombination detection program 4.10 (RDP 4.10) (26). A recombination event was identified when at least five of the seven methods reported recombination signals in RDP 4.10 with the highest acceptable p of 0.05 (27). The possible recombination event was further confirmed using the SIMPLOT software (version 3.5.1) with a 200-bp window width and a 20-bp step size (28).

Challenge Experiment

To evaluate the pathogenicity of the recombinant strains, two strains PRRSV2/CN/SS0/2020 (98.3% homology with JXA1) and PRRSV2/CN/L3/2021 (86.3% homology with JXA1) were selected for animal experiments. Fifteen 4-week-old pigs confirmed to be free of PRRSV and PCV2 were randomly divided into 3 groups (5 pigs/group). The pigs in group 1 were intranasally administered with 2 mL of PRRSV2/CN/SS0/2020 containing 2×10^5 TCID50 and those in group 2 were intranasally administered with 2 mL of PRRSV2/CN/SS0/2020 containing 2×10^5 TCID50. The pigs in the negative control group were inoculated with 2 mL of Dulbecco's Modified Eagle Medium (DMEM). Rectal temperature was recorded daily from 0 to 14 days post-challenge (dpc). Serum was collected at 0, 4, 7, 11, and 14 dpc to detect PRRSV-specific antibodies using PRRSV

TABLE 1 | Representative PRRSV strains used in this study.

No.	Name	GenBank accession no.	Origin	No.	Name	GenBank accession no.	Origin
1	JXwn06	EF641008	China	23	FJZ03	KP860909	China
2	TJ	EU860248	China	24	MN184A	DQ176019	U.S.A
3	JXA1	EF112445	China	25	MN184B	DQ176020	U.S.A
4	HUN4	EF635006	China	26	HENNAN-XINX	KF611905	China
5	JXA1 P80	FJ548855		27	MN184C	EF488739	U.S.A
6	MLV-like TJbd14-1	KP742986	China	28	FJY04	KP860910	China
7	CH-1a	AY032626	China	29	FJYR	KT804696	China
8	CH-1R	EU807840	China	30	FJM4	KY412888	China
9	HB-1(sh)/2002	AY150312	China	31	JX143	EU708726	China
10	HB-2(sh)/2002	AY262352	China	32	HLJA1	KT351739	China
11	VR-2332	U87392	China	33	NT1	KP179402	China
12	NT1	KP179402	China	34	FJZH	KP998478	China
13	PA8	AF176348	Canada	35	FJSD	KP998474	China
14	BJ-4	AF331831	China	36	1105-GD-GL	KR612137	China
15	RespPRRS MLV	AF066183	U.S.A	37	110102-GD-ST	KR018789	China
16	GD-KP	KU978619	China	38	YJ1-10	KC282627	China
17	GM2	JN662424	China	39	140116-GD-YWC	KR018799	China
18	FJFS	KP998476	China	40	140520-GD-SXB	KR018784	China
19	QYYZ	JQ308798	China	41	GDsg	KX621003	China
20	NADC30	JN654459	U.S.A	42	GXBS06-2012	KC617956	China
21	FJY04	KP860910	China	43	LV	M96262	Netherlands
22	CHsx1401	KP861625	China	44	MLV TJM F-92		China

using ELISA kit (IDEXX Laboratories Inc., Westbrook, ME, USA). Viral load in the sera of each group was detected by an IFA-microtitration infectivity assay as previously described (29). All animals were euthanized at 14 dpc for necropsy. In addition, lung tissues of pigs were collected at necropsy and fixed in 10% neutral-buffered formalin and routinely processed for histological examination. The procedures of animal handling and experimentation performed in this study were approved by the Longyan University Animal Ethics Committee (Permit number: permit no.LY20210010X).

Data Analysis

Statistical analysis in this study was performed using a one- or two-way ANOVA analysis of variance in GraphPad Prism software (version 6.0), and the results were considered statistically significant when $p < 0.05$.

RESULTS

Complete Genome Sequence Analysis of PRRSV

Four strains of PRRSV were isolated using MARC-145^{CD163} cells and designated as PRRSV2/CN/SS0/2020 (Accession number: ON365556), PRRSV2/CN/SS1/2021 (Accession number: ON093974), PRRSV2/CN/L3/2021 (Accession number: OL416130), and PRRSV2/CN/L4/2020 (Accession number: OL422822). Typical PRRSV CPE characterized by cell fusion and shedding was observed in MARC-145CD^{163} cells (**Supplementary Figure 1**). The genomes of the four isolates were 14,962–15,023 nt in length, excluding the poly (A) tails at the 3' end. Comparative analyses of genome sequences showed that the four isolates shared 93.2–98.1% homology and had a 83.7–86.8% identity with VR2332-like PRRSVs (VR-2332, RespPRRSV MLV, and BJ-4), 86.1–91.5% with JXA1-like PRRSVs (JXA1, HuN4, and TJd14-1), 81.9–86.6% with NADC30-like PRRSVs (NADC30, FJZ03, and Chsx1401), 82.9–86.5% with QYYZ-like PRRSVs (QYYZ, GM2, and FJFS), and only 59.2–59.8% with LV (**Supplementary Table 2**).

To evaluate the genomic characteristics of the four PRRSV isolates, each region of the genomes of the four strains was further compared with four viruses from different lineages, including NADC30-like strains, QYYZ-like strains, VR2332-like strains (VR-2332 and BJ-4), JXA1-like strains, and the LV (the prototype of type 1 PRRSV) strain (Table 2). The 5'-UTR of the four PRRSV isolates was 188–191 nt long and they had an identity of 87.3–91.5% with NADC30-like strains, 93.7–95.7% with QYYZ-like strains, 89.4–91.0% with VR2332-like strains, 97.4–98.4% with JXA1-like strains, and 61.5–62.2% with LV. The 3'-UTR of the four PRRSVs was found to be ∼145–154 nt long, excluding the poly (A) tail, and their sequence was 86.1–89.9% homologous with that of the NADC30-like strains, 89.4–92.1% with that of the QYYZ-like strains, 90.7–91.4% with that of the VR2332-like strains, 85.3–88.7% with that of the JXA1-like strains, and 74.3–75.2% with that of LV (**Table 2**).

TABLE 2 | Sequence distance of four isolates in this study with reference strains.

	VR2332	BJ-4	JXA1	HuN4	TJbd14-1	NADC30	CHsx1401	FJZ03	QYYZ	FJFS	GM2	LV
	% identity toPRRSV2/CN/SS1/2021 /% identity toPRRSV2/CN/L3/2021/% identity to PRRSV2/CN/L4/2020/ PRRSV2/CN/SS0/2020											
Nucleotides												
5' UTR	89.4/91.0/ 90.4/90.5	89.4/91.0/ 90.4/90.5	97.4/98.4/ 97.9/98.4	97.4/98.4/ 97.9/98.4	97.4/97.9/ 97.9/98.4	89.9/91.5/ 91.0/91.0	87.3/ 88.8/88.3/88.4	88.9/90.4/ 89.9/89.9	93.7/94.1/ 94.7/94.7	95.2/94.1/ 95.7/95.2	93.7/94.1/ 94.7/94.7	62.0/62.0/ 61.5/61.7
ORF1a	53.2/82.7/ 82.5/84.7	83.1/82.4/ 82.3/84.5	89.6/84.7/ 84.6/92.2	89.6/84.7/ 84.6/92.3	89.6/84.9/ 84.9/92.4	83.2/ 86.6/86.7/82.5	82.1/85.1/ 85.2/81.5	82.1/85.9/ 86.0/81.8	81.2/80.0/ 79.9/82.4	81.9/80.8/ 80.8/83.3	80.9/79.8/ 79.7/82.0	55.1/55.1/ 55.1/55.1
ORF1b	88.4/88.4/ 88.5/88.5	88.5/88.5/ 88.5/88.6	92.9/93.0/ 93.2/93.1	92.8/92.9/ 93.1/93.1	92.7/92.7/ 93.0/93.0	86.3/86.3/ 86.4/86.4	85.7/85.7/ 85.8/85.8	85.9/85.9/ 86.0/86.0	88.1/88.2/ 88.4/88.2	87.6/87.7/ 87.7/87.8	83.3/83.3/ 83.4/88.3	63.2/63.2/ 63.2/63.1
ORF2-7	87.8/88.0/ 88.8/88.3	87.6/87.8/ 88.6/88.1	86.6/86.6/ 87.3/87.1	86.9/86.9/ 87.5/87.4	86.7/86.7/ 87.4/87.2	85.7/85.4/ 86.4/85.6	85.4/85.1/ 86.1/85.3	85.2/84.9/ 85.6/85.1	89.6/89.5/ 90.1/90.0	90.0/89.9/ 90.7/90.3	89.2/89.1/ 89.7/89.6	65.2/65.2/ 65.3/65.2
3' UTR	90.7/90.7/ 91.4/92.7	90.7/90.7/ 91.4/92.7	87.3/85.3/ 86.0/88.7	87.3/85.3/ 86.0/88.7	87.3/85.3/ 86.0/88.7	88.7/87.4/ 89.4/89.4	87.4/86.1/ 88.1/88.1	89.2/86.5/ 86.5/89.9	90.7/92.1/ 90.7/92.1	89.4/90.7/ 89.4/90.7	89.4/90.7/ 89.4/90.7	75.2/75.2/ 74.3/74.3
aa												
NSP1α	95.2/96.4/ 95.8/97.0	95.2/96.4/ 95.8/97.0	94.6/95.8/ 95.2/97.6	94.6/95.8/ 95.2/97.6	94.6/95.8/ 95.2/97.6	95.2/96.4/ 95.8/95.8	92.8/94.8/ 93.4/95.8	92.8/93.4/ 92.8/94.0	96.4/97.1/ 96.4/97.6	92.8/93.4/ 92.8/95.2	96.4/97.0/ 96.4/83.2	65.1/65.1/ 64.5/65.7
NSP1β	81.6/82.5/ 82.5/82.5	81.1/82.0/ 82.0/82.0	93.5/94.0/ 94.0/94.5	94.0/94.5/ 94.5/94.9	93.1/93.5/ 93.5/94.0	74.2/74.2/ 75.6/74.7	72.4/72.4/ 73.7/72.8	74.2/73.7/ 75.1/74.2	82.5/83.4/ 83.4/83.4	88.9/89.4/ 89.4/89.9	82.9/83.4/ 83.4/83.9	41.3/41.8/ 41.8/41.8
NSP2	71.0/69.4/ 69.2/74.1	70.4/68.9/ 68.7/73.5	85.3/68.2/ 67.8/91.6	85.2/67.6/ 67.4/91.6	86.9/65.6/ 65.5/93.8	70.6/82.9/ 83.6/68.7	68.7/80.1/ 80.4/67.3	70.1/82.1/ 82.9/68.0	69.0/63.8/ 63.4/72.0	70.6/66.5/ 66.7/74.2	68.4/63.8/ 63.4/71.4	28.9/32.0/ 32.2/27.9
NSP3	91.5/91.7/ 91.5/92.8	91.5/91.7/ 91.5/92.8	92.4/91.3/ 91.5/94.4	92.6/91.5/ 91.7/94.4	92.6/91.7/ 91.9/95.1	90.1/90.6/ 90.4/89.7	93.9/96.0/ 95.3/92.4	94.4/95.1/ 94.4/93.3	82.2/82.7/ 82.4/88.1	82.2/82.7/ 82.4/88.1	82.2/82.7/ 82.4/88.1	58.2/58.2/ 58.0/58.7
NSP4	94.6/94.6/ 94.6/94.6	94.6/94.6/ 94.6/94.6	96.6/96.6/ 96.6/96.6	96.6/96.6/ 96.6/96.6	96.1/96.1/ 96.1/96.1	96.1/96.1/ 96.1/96.1	93.1/93.1/ 93.1/93.1	92.6/92.6/ 92.6/92.6	93.1/93.1/ 93.1/93.1	92.6/92.6/ 92.6/92.6	93.6/93.6/ 93.6/93.6	62.1/62.1/ 62.1/62.1
NSP5	88.8/88.2/ 88.8/88.8	89.4/88.8/ 89.4/89.4	91.2/91.8/ 91.8/91.2	91.2/91.8/ 91.8/91.2	91.2/91.8/ 91.8/91.2	91.2/91.8/ 91.8/91.2	88.8/89.4/ 90.0/88.8	90.6/90.6/ 91.2/90.6	88.2/88.2/ 88.8/88.2	87.6/87.6/ 88.2/87.6	87.6/87.6/ 88.2/87.6	71.2/71.8/ 72.4/71.2
NSP6	87.5/87.5/ 87.5/87.5	87.5/87.5/ 87.5/87.5	93.8/93.8/ 93.8/93.8	93.8/93.8/ 93.8/93.8	93.8/93.8/ 93.8/93.8	87.5/87.5/ 87.5/87.5	81.2/81.2 /81.2/81.2	87.5/87.5/ 87.5/87.5	93.8/93.8/ 93.8/93.8	93.8/93.8/ 93.8/93.8	93.8/93.8/ 93.8/93.8	75.0/75.0/ 75.0/75.0
NSP7	88.0/87.3/ 87.3/88.4	86.9/86.9/ 86.1/87.3	92.3/93.1/ 92.3/92.7	92.3/93.1/ 92.3/92.7	92.3/93.1/ 92.3/92.7	84.2/84.6/ 83.8/84.6	83.0/83.4/ 82.6/83.4	83.4/83.8/ 83.0/83.8	88.8/89.6/ 88.8/89.2	89.2/90.0/ 89.2/89.6	88.0/88.0/ 87.3/88.4	47.8/48.2/ 47.8/48.2
NSP8	95.6/97.8/ 97.8/95.6	95.6/97.8/ 97.8/95.6	95.6/97.8/ 97.8/95.6	95.6/97.8/ 97.8/95.6	95.6/97.8/ 97.8/95.6	91.1/93.3/ 93.3/91.1	88.9/91.1/ 91.1/88.9	91.1/93.3/ 93.3/91.1	95.6/97.8/ 97.8/95.6	91.1/93.3/ 93.3/91.1	95.6/97.8/ 97.8/95.6	65.9/68.2/ 68.2/65.9
NSP9	96.9/97.2/ 97.2/97.0	96.6/96.9/ 96.9/96.7	98.1/98.4/ 98.4/98.3	98.0/98.3/ 98.3/98.1	98.1/98.4/ 98.4/98.3	96.6/96.9/ 96.9/96.7	95.6/95.9/ 95.9/95.8	96.0/96.3/ 96.3/96.1	96.4/96.7/ 96.7/96.6	95.2/95.2/ 95.3	96.4/96.7/ 96.6	74.8/74.6/ 74.6/74.6
NSP10	95.5/95.5/ 95.5/95.5	95.5/95.5/ 95.5/95.5	98.2/98.2/ 98.2/98.2	98.9/98.9/ 98.9/98.9	98.0/98.0/ 98.0/98.0	95.0/95.0/ 95.0/95.0	94.8/94.8/ 94.8/94.8	94.6/94.6/ 94.6/94.6	97.3/97.3/ 97.3/97.3	93.7/93.7/ 93.7/93.7	95.7/95.7/ 95.7/95.7	64.9/64.9/ 64.9/64.9
NSP11	92.8/92.8/ 92.8/92.8	93.7/93.7/ 93.7/93.7	96.9/96.9/ 96.9/96.9	96.9/96.9/ 96.9/96.9	96.9/96.9/ 96.9/96.9	95.5/95.5/ 95.5/95.5	93.3/93.3/ 93.3/93.3	94.2/94.2/ 94.2/94.2	93.3/93.3/ 93.3/93.3	92.8/92.8/ 92.8/92.8	93.7/93.7/ 93.7/93.7	76.6/76.6/ 76.6/76.6
NSP12	92.2/91.5/ 92.2/92.2	92.2/91.5/ 92.2/92.2	95.4/94.8/ 95.4/95.4	95.4/94.8/ 95.4/95.4	95.4/94.8/ 95.4/95.4	92.2/91.5/ 92.2/92.2	91.5/90.8/ 91.5/91.5	93.5/92.8/ 93.5/93.5	92.8/92.2/ 92.8/92.8	93.5/94.1/ 93.5/93.5	93.5/92.8/ 93.5/93.5	46.3/46.3/ 46.3/46.3
ORF2a/GP2	91.0/90.2/ 91.0/91.4	90.2/89.5/ 90.2/90.6	87.9/87.9/ 88.7/88.3	87.5/87.5/ 88.3/87.9	88.3/88.3/ 89.1/88.7	89.5/87.5/ 88.3/88.7	91.8/89.8/ 90.6/91.0	88.7/87.5/ 87.5/87.9	93.0/93.0/ 93.8/93.4	89.5/89.5/ 90.2/89.8	92.6/92.6/ 93.4/93.0	61.4/61.8/ 62.2/61.8

(Continued)

TABLE 2 | Continued

	VR2332	BJ-4	JXA1	HuN4	TJbd14-1	NADC30	CHsx1401	FJZ03	QYYZ	FJFS	GM2	LV
	% identity toPRRSV2/CN/SS1/2021 /% identity toPRRSV2/CN/L3/2021/% identity to PRRSV2/CN/L4/2020/ PRRSV2/CN/SS0/2020											
ORF2b/E	91.8/93.2/ 93.2/91.8	90.4/91.8/ 91.8/90.4	91.8/90.4/ 90.4/91.8	91.9/90.4/ 90.4/91.9	91.8/90.4/ 90.4/91.8	91.8/90.4/ 90.4/91.8	89.0/87.7/ 87.7/89.0	91.8/90.4/ 90.4/91.8	94.5/93.2/ 93.2/94.5	82.2/80.8/ 80.8/82.2	94.5/93.2/ 93.2/94.5	71.8/71.4/ 71.4/71.8
ORF3/GP3	86.6/87.4/ 86.6/87.0	87.0/87.8/ 87.0/87.4	84.6/85.0/ 84.3/85.0	85.0/85.4/ 84.6/85.4	84.6/85.0/ 84.3/85.0	84.3/84.3/ 83.5/83.5	84.6/84.6/ 83.9/83.9	81.9/82.3/ 81.1/81.5	88.2/88.2/ 87.4/87.8	90.2/90.2/ 89.4/89.8	87.4/87.0/ 86.6/87.4	56.5/57.3/ 56.1/56.5
ORF4/GP4	89.3/89.9/ 90.4/89.3	89.3/89.9/ 90.4/89.3	87.1/87.6/ 88.2/87.1	89.3/89.9/ 90.4/89.3	89.3/89.9/ 90.4/89.3	87.1/87.6/ 88.2/87.1	86.0/86.5/ 87.1/86.0	86.0/86.5/ 87.1/86.0	87.6/88.2/ 88.8/87.6	90.4/90.4/ 91.0/90.4	87.1/87.6/ 88.2/87.1	69.7/70.2/ 69.7/69.7
ORF5/GP5	81.0/81.5/ 81.0/82.5	80.5/81.0/ 80.5/82.0	82.5/83.1/ 81.5/83.5	82.5/83.0/ 81.5/83.5	82.5/83.0/ 81.5/83.5	84.0/84.5/ 83.0/85.0	83.5/83.5/ 84.0/84.5	82.5/82.5/ 82.0/83.5	91.5/92.0/ 92.0/93.0	91.0/91.5/ 91.5/92.5	90.0/90.5/ 90.5/91.5	58.2/57.1/ 57.1/58.7
ORF5a	78.3/78.3/ 78.3/78.3	78.3/78.3/ 78.3/78.3	71.7/71.7/ 71.7/71.7	71.7/71.7/ 71.7/71.7	71.7/71.7/ 71.7/71.7	76.1/76.1/ 76.1/76.1	76.1/76.1/ 76.1/76.1	78.3/78.3/ 78.3/78.3	89.1/89.1/ 89.1/89.1	89.1/89.1/ 89.1/89.1	91.3/91.3/ 91.3/91.3	46.5/46.5/ 46.5/46.5
ORF6/M	94.3/94.3/ 94.8/94.3	94.3/94.3/ 94.8/94.3	93.1/93.1/ 94.3/93.1	93.1/93.1/ 94.3/93.1	93.1/93.1/ 94.3/93.1	93.1/93.1/ 93.7/93.1	93.1/93.1/ 94.8/93.1	93.7/93.7/ 94.3/93.7	95.4/95.4/ 97.1/95.4	96.0/96.0/ 97.1/96.0	95.4/95.4/ 96.6/95.4	78.0/78.0/ 78.0/78.0
ORF7/N	92.7/91.1/ 91.1/91.9	92.7/91.1/ 91.1/91.9	92.7/91.1/ 91.1/91.9	92.7/91.1/ 91.1/91.9	91.9/90.2/ 90.2/91.1	89.4/88.6/ 92.7/90.2	84.6/83.7/ 87.8/85.4	88.6/87.8/ 91.9/89.4	90.2/88.6/ 91.7/92.7	90.3/88.6/ 93.5/90.2	86.2/84.6/ 87.8/88.6	62.0/60.8/ 63.3/61.7

aa, Amino acids.

ORF1a and ORF1b encode the non-structural proteins (Nsp) of PRRSV. A nucleotide sequence comparison of ORF1 showed that in the four strains, ORF1b was relatively conserved as compared to ORF1a. Of all the Nsp sequences, the most variable ones were from Nsp1β and Nsp2 within ORF1a, which had 72.4–94.9% and 63.4–86.9% amino acid identity with the reference strains, respectively (**Table 2**).

Open reading frames 2a to 7 encode the PRRSV structural proteins. Nucleotide sequence comparison of this region showed that the four strains shared 95.2–99.1% nucleotide identity, 84.9–86.4% identity with NADC30-like strains, 89.1–90.7% identity with QYYZ-like strains, 87.6–88.8% identity with VR2332-like strains, and 86.6–87.5% identity with JXA1-like strains. In contrast, these ORF regions only shared 65.2–65.3% identity with LV.

Phylogenetic Analysis of PRRSV

Four respective phylogenetic trees were constructed based on the full-length genome sequences, Nsp2, ORF2-7, and ORF5 nucleotide sequences of the four PRRSV isolates and 27 representative strains of type 2 PRRSV.

Interestingly, the tree based on the full-length genome sequences showed that the four PRRSVs formed a separate branch that was in the middle of lineages 3 and 8.7, which are represented by QYYZ and JXA1, respectively (**Figure 1A**). The tree based on the ORF2-7 or ORF5 sequences indicates that the four strains were grouped in lineage 3, together with the QYYZ-like strains (**Figures 1C,D**). The tree constructed based on Nsp2 indicates that PRRSV2/CN/L3/2021 and PRRSV2/CN/L4/2020 were clustered into lineage 1, together with the NADC30-like strains, and PRRSV2/CN/SS0/2020 was clustered into lineage 8.7, together with the JXA1-like strains; however, PRRSV2/CN/SS1/2021 was in a separate branch (**Figure 1B**).

Amino Acid Analysis of NSP2 and ORF5

The Nsp2-coding region is recognized as one of the most variable proteins with different deletions and insertions. Therefore, Nsp2 is often used to analyze the genetic variations and molecular epidemiology of PRRSV. As shown in **Figure 2**, two isolates, namely PRRSV2/CN/L3/2021 and PRRSV2/CN/L4/2020, had a unique discontinuous deletion of 131-aa in the Nsp2-coding region, which was identical to that of the NADC30 and NADC30-like strains. Meanwhile, PRRSV2/CN/L4/2020 had an additional 1-aa deletion at the 15th aa. Interestingly, both PRRSV2/CN/L3/2021 and PRRSV2/CN/L4/2020 had two additional 2-aa insertions at amino acid positions 224–225 (**Figure 2A**). Notably, PRRSV2/CN/SS0/2020 and PRRSV2/CN/SS1/2021 had characteristic 150-aa deletions (aa481+aa537-566+aa628–747) that were identical to those of the live attenuated virus vaccine strain TJM-F92 (derived from the HP-PRRSV TJ) (30) and TJbd14–1 (13), which is an MLV-like strain that evolved from the HP-PRRSV vaccine virus TJM-F92 (**Figure 2B**). Notably, comparative sequence analysis showed that PRRSV2/CN/SS0/2020 and PRRSV2/CN/SS1/2021 exhibited the highest nucleotide similarity (89.5–95.3%) and amino acid similarity (87.0–94.0%) with TJbd14-1 and TJM-F92.

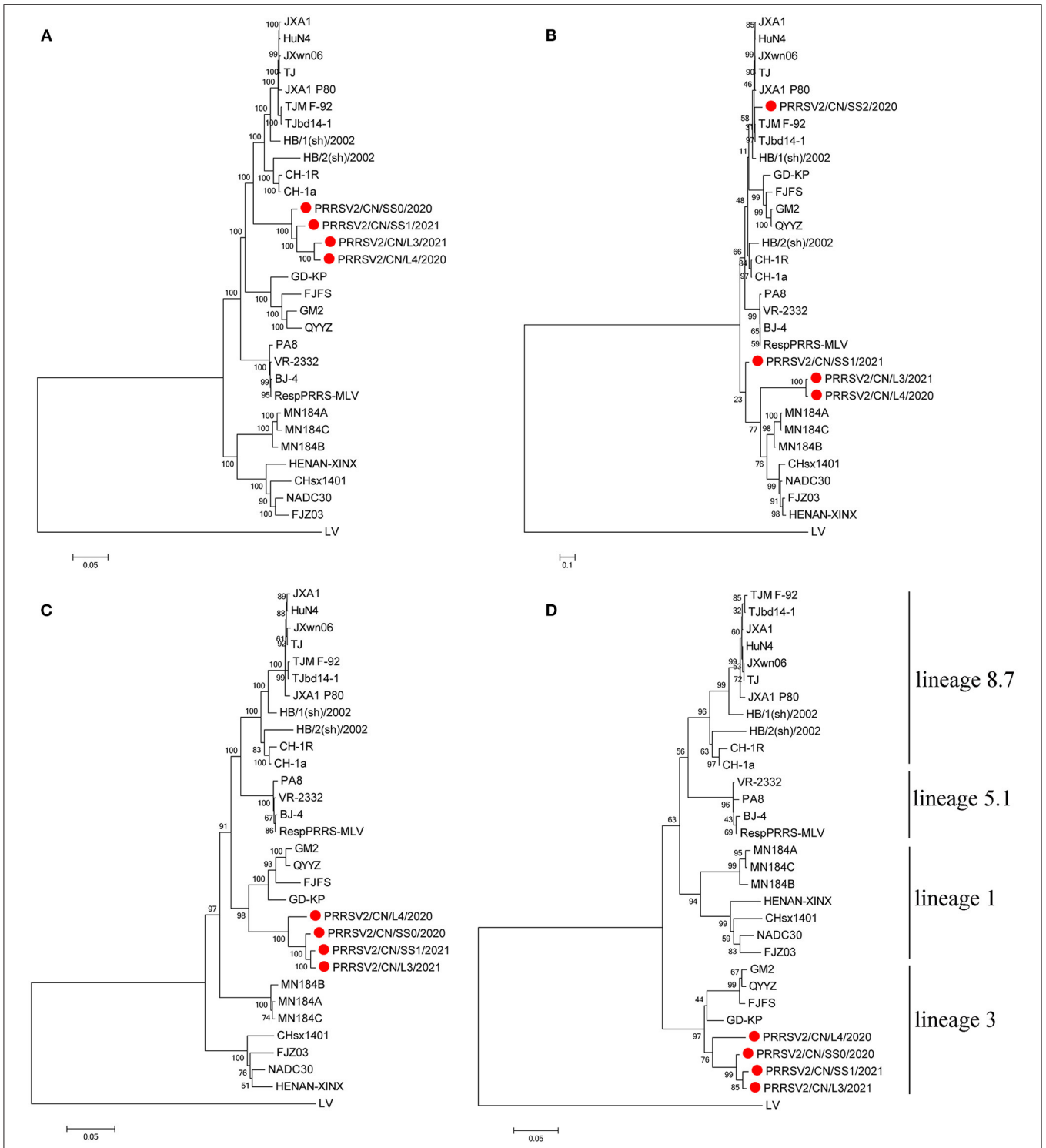

FIGURE 1 | Phylogenetic tree based on the full length **(A)**, Nsp2 **(B)**, ORF2-7 **(C)**, and ORF5 **(D)** of the four PRRSV strains from this study and reference strains. The four PRRSV strains isolated in this study are labeled with a red circle. The reliability of the tree was evaluated by bootstrapping using Mega 7.0 with 1000 replicates.

The GP5 protein encoded by ORF5 is the most variable structural protein of the virus. At least six antigenic regions (ARs) were reported within GP5 (AR1-15, AR27-35, AR37-51, AR149-156, AR166-181, and AR192-200) (31, 32). Three ARs (AR27-35,

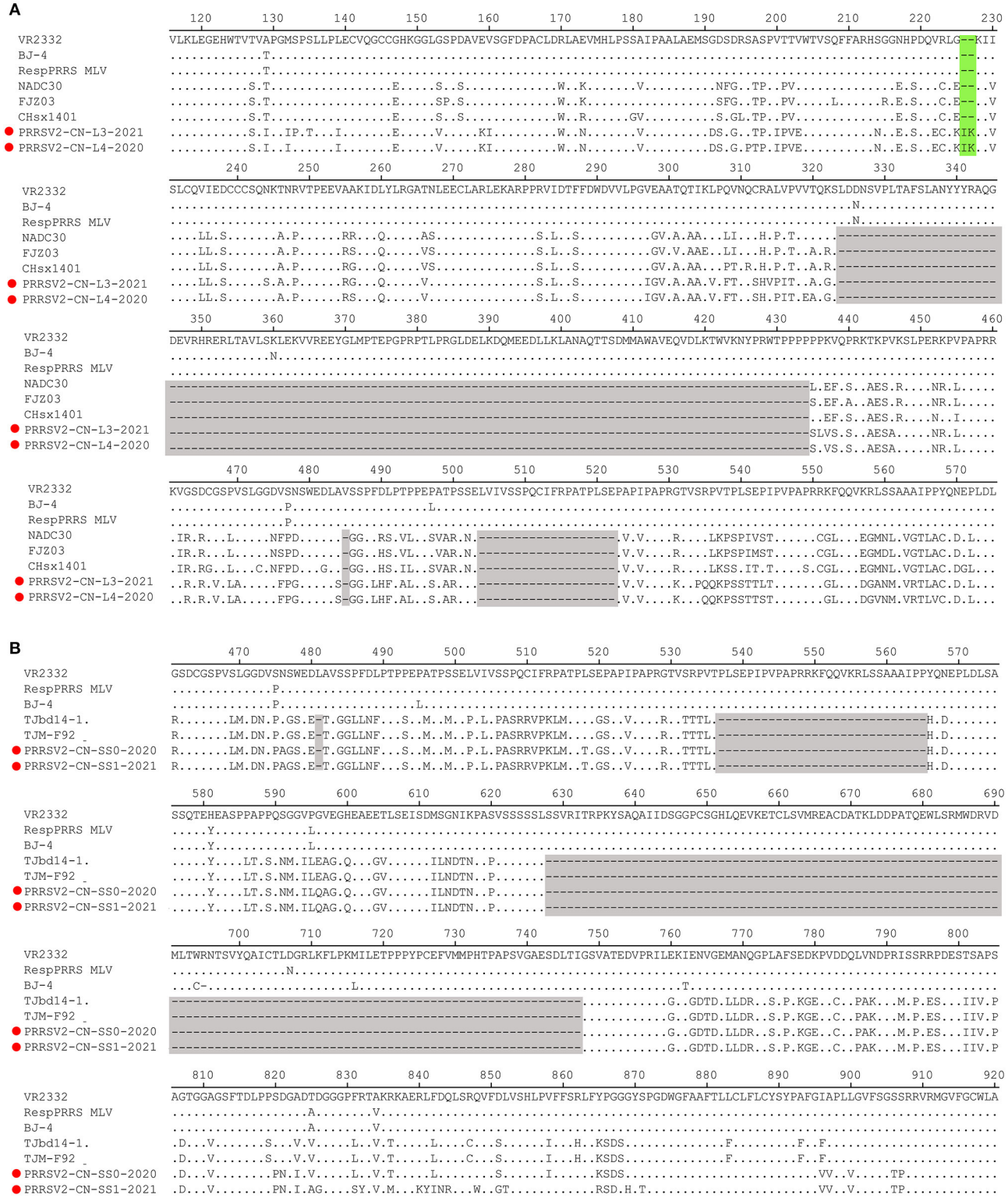

FIGURE 2 | Amino acids alignment for Nsp2 of the four PRRSV isolates with representative strains. **(A)** The 131-aa discontinuous deletions (aa324–434, aa485, and aa504–522) highlighted in gray boxes show the deletion signature of PRRSV2/CN/L3/2021, PRRSV2/CN/L4/2021, and NADC30-like strains. Additional 2-aa insertion in PRRSV2/CN/L3/2021 and PRRSV2/CN/L4/2021 is marked in the green box. **(B)** The 150-aa discontinuous deletions (aa481+aa537-566+aa628–747) highlighted in gray boxes show the deletion signature of PRRSV2/CN/SS0/2020, PRRSV2/CN/SS1/2021, and MLV TJM-F92 strain.

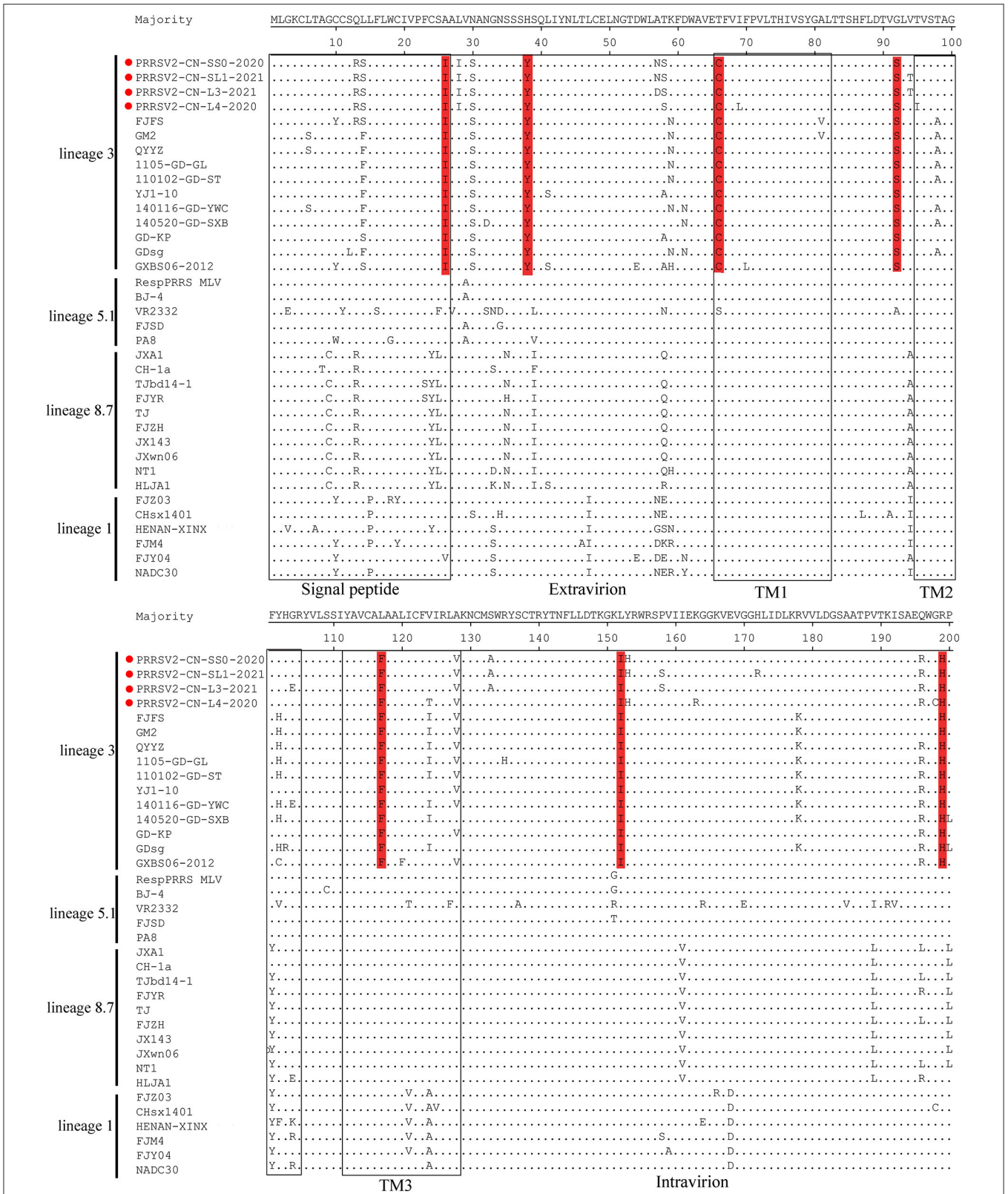

FIGURE 3 | Analysis and comparison of amino acid mutations in GP5 compared to reference viruses. The signal peptide and transmembrane (TM) domains in GP5 are highlighted by rectangles. Important amino acid changes between four strains (red cicrlce) and QYYZ-like PRRSVs in GP5 are indicated in red.

AR37-51, and AR192-200) at the N-terminus of the four strains were the most similar to the QYYZ-like strains but differed from the JXA1-like, VR-2332-like, and NADC30-like strains. Additionally, seven unique amino acids distributed in GP5 were only identified in QYYZ-like strains and the four strains (I^{26}, Y^{38}, C^{66}, S^{92}, F^{117}, I^{152}, and H^{199}) (**Figure 3**). Studies have shown that the 13th and 151st amino acids of GP5 are related to the virulence of the virus (33). In the present study, four strains had both $R^{13}Q$ and $R^{151}G$ mutation as compared with the VR2332 strain.

Recombination Analysis

The recombination analysis using the RDP version 4.10 software revealed that the four isolates are the result of recombination between JXA1-like, QYYZ-like, and NADC30-like strains circulating in China (**Table 3**, **Figure 4**, **Supplementary Figure 2**). Additionally, the putative recombinant events and statistically incongruent phylogenetic trees were further confirmed using SimPlot v3.5.1 and statistically incongruent phylogenetic trees (**Figure 4**, **Supplementary Figure 2**). From the similarity plot, the breakpoints of recombination events of four strains are mainly located in nsp1, nsp2, nsp3, nsp11, and nsp12 (**Figure 4**, **Supplementary Figure 2**).

PRRSV2/CN/SS0/2020 and PRRSV2/CN/L3/2021 Exhibited Pathogenicity for Pigs

Pigs infected with PRRSV2/CN/SS0/2020 exhibited obvious clinical signs, including respiratory distress, anorexia, and coughing from 3 dpc. The body temperatures of PRRSV2/CN/SS0/2020-inoculated group began to reach above 40°C at 3–14 dpc, with a peak (>41 °C) at 8–9 dpc. In contrast, the pigs infected with PRRSV2/CN/L3/2021 had less fever and less severe clinical signs (**Figure 5A**). Control pigs showed normal rectal temperature and behavior throughout the experiment. One of five PRRSV2/CN/SS0/2020-infected pigs died at 10 dpc, whereas no mortality was observed in PRRSV2/CN/L3/2021-infected group and negative control group. In addition, pigs in PRRSV2/CN/SS0/2020-infected group had significantly more severe interstitial pneumonia than did pigs inoculated with PRRSV2/CN/L3/2021 (**Figure 5B**), which indicates that PRRSV2/CN/SS0/2020 is a highly virulent PRRSV isolate for pigs.

The PRRSV was isolated from the serum of pigs challenged with the two strains at 4 dpc. The mean virus titers of PRRSV2/CN/SS0/2020 or PRRSV2/CN/L3/2021 reached peak levels at 7 dpc ($10^{6.2}$ TCID50/mL and $10^{5.0}$ TCID50/mL, respectively) and high viremia persisted until 14 dpc in every PRRSV-infected group (**Figure 5C**). Furthermore, the mean virus loads for PRRSV2/CN/SS0/2020-infected group were significantly higher than those of the PRRSV2/CN/L3/2021-infected group at 7 and 11 dpc ($p < 0.05$). Meanwhile, no PRRSV was detected in the control group throughout the experiment. The specific antibodies of PRRSV N protein in the sera of pigs were detected by a commercial ELISA kit. All pigs in the PRRSV2/CN/SS0/2020-infected group became

TABLE 3 | Information of recombination events of four isolates.

Isolate	Breakpoint position in alignment		Major parent	Minor parent	*P*-value						
	Beginning	Ending			RDP	GENECONV	Bootscan	MaxChi	Chimera	SiScan	3Seq
PRRSV/CN/SS0/2020	526	698	HuN4	NADC30	2.707×10^{-7}	–	4.288×10^{-8}	2.716×10^{-3}	5.675×10^{-4}	–	8.854×10^{-5}
	3,826	5,391	HuN4	NADC30	1.752×10^{-4}	–	1.565×10^{-15}	2.205×10^{-6}	1.317×10^{-8}	2.367×10^{-17}	7.579×10^{-12}
	11,788	15,411	HuN4	QYYZ	9.132×10^{-24}	–	1.827×10^{-21}	1.520×10^{-28}	1.373×10^{-9}	6.812×10^{-8}	7.327×10^{-14}
PRRSV/CN/SS1/2021	476	722	HuN4	NADC30	1.111×10^{-10}	–	5.944×10^{-11}	5.360×10^{-5}	4.379×10^{-7}	-	1.188×10^{-9}
	1,837	2,211	HuN4	NADC30	1.071×10^{-19}	–	4.382×10^{-19}	3.864×10^{-15}	3.221×10^{-12}	1.002×10^{-10}	3.730×10^{-14}
	3,790	5,231	HuN4	NADC30	1.335×10^{-42}	–	7.166×10^{-39}	3.607×10^{-24}	6.873×10^{-24}	1.923×10^{-24}	3.730×10^{-14}
	13,227	15,411	HuN4	FJFS	3.905×10^{-25}	–	1.803×10^{-23}	5.300×10^{-19}	8.432×10^{-22}	1.320×10^{-12}	1.865×10^{-14}
PRRSV/CN/L3/2021	480	686	JXA1	NADC30	6.014×10^{-12}	–	3.383×10^{-12}	2.429×10^{-06}	1.528×10^{-07}	–	7.946×10^{-11}
	1,845	5,390	JXA1	FJFS	2.715×10^{-99}	1.571×10^{-51}	2.248×10^{-75}	4.195×10^{-41}	1.632×10^{-24}	2.000×10^{-54}	1.332×10^{-14}
	11,600	15,411	JXA1	NADC30	6.795×10^{-21}	–	1.840×10^{-19}	1.185×10^{-18}	7.242×10^{-22}	3.896×10^{-13}	9.858×10^{-13}
PRRSV2/CN/L4/2020	1,897	5,388	JXA1	NADC30	1.284×10^{-94}	5.386×10^{-53}	2.066×10^{-88}	1.009×10^{-41}	2.533×10^{-47}	3.794×10^{-48}	3.454×10^{-14}
	11,401	15,411	JXA1	QYYZ	6.892×10^{-21}	3.818×10^{-04}	1.029×10^{-14}	2.023×10^{-06}	1.956×10^{-09}	1.320×10^{-13}	4.884×10^{-14}

Breakpoint position inPRRSV genome with reference to the VR-2332 strain.

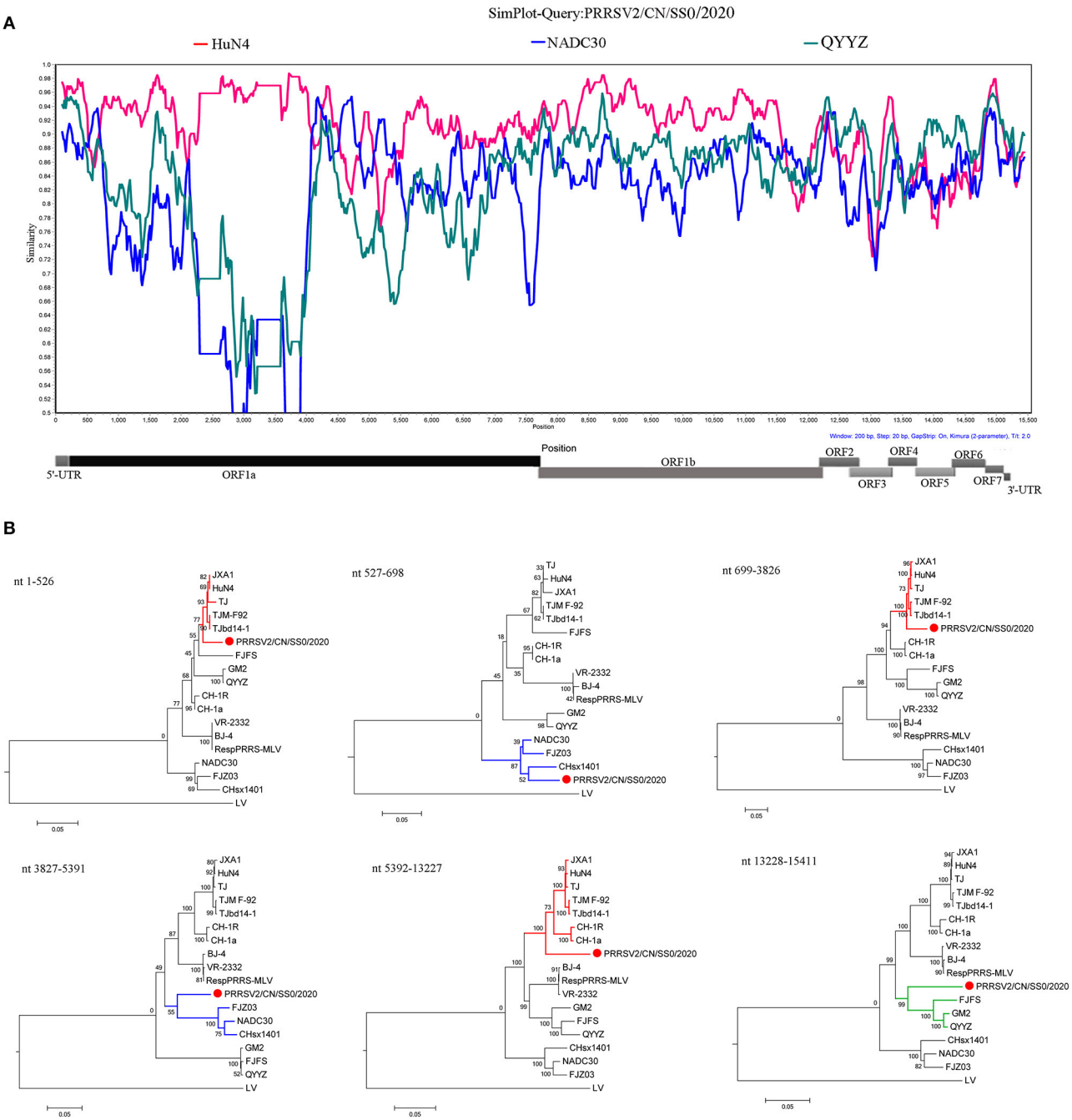

FIGURE 4 | Similarity plot analysis **(A)** and phylogenetic trees analysis based on different regions **(B)** of PRRSV2/CN/SS0/2020. For similarity plot analysis, the y-axis indicates the percentage identity between the parental sequences and the query sequence. The complete genome RRSV2/CN/SS0/2020 was chosen as the query sequence, respectively.

seroconverted at 7 dpc, whereas PRRSV2/CN/L3/2021-infected were seroconverted at 11 dpc (**Figure 5D**). In contrast, PRRSV-specific antibodies were not detected in the control group throughout the experiment.

DISCUSSION

Porcine reproductive and respiratory syndrome virus is one of the most important pathogens causing substantial economic

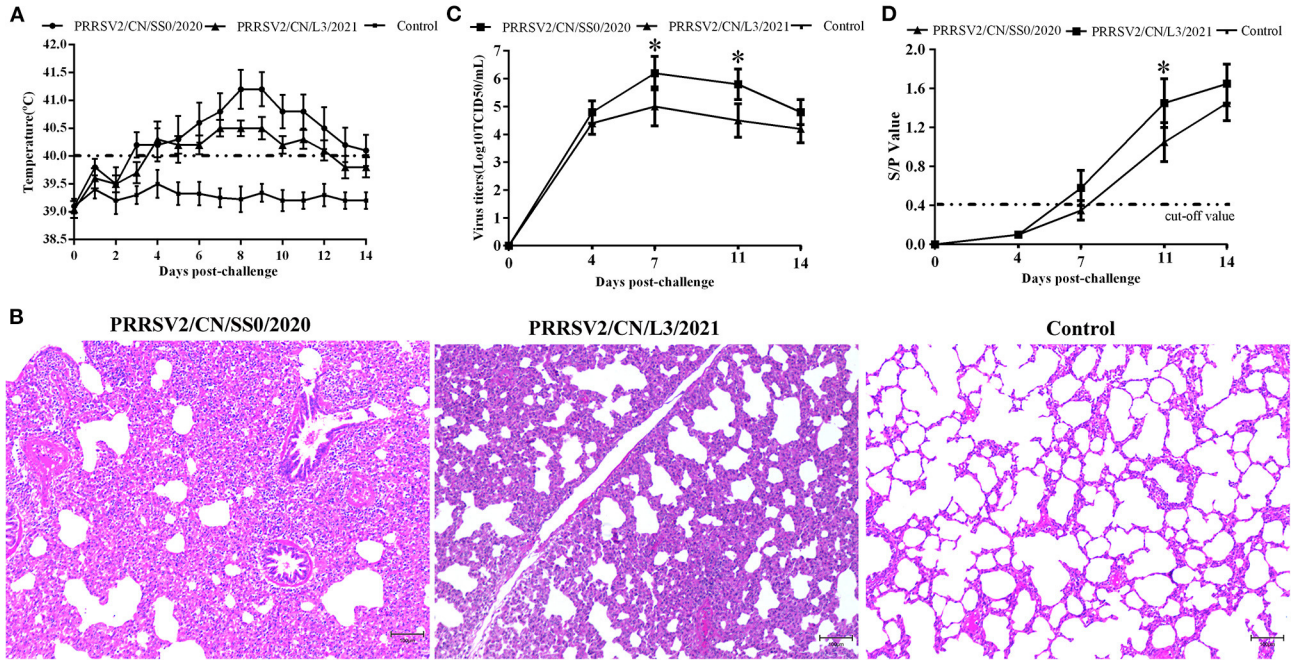

FIGURE 5 | The rectal temperature, microscopic lung lesions, viremia, and antibody levels of pigs during the challenge experiment. **(A)** Rectal temperatures of pigs inoculated with PRRSV2/CN/SS0/2020, PRRSV2/CN/L3/2021, and DMEM. The clinical fever cut-off value was set at 40 °C. **(B)** Microscopic lung lesions of the inoculated pigs. **(C)** Dynamics of viral loads of the inoculated pigs during the experiment. **(D)** PRRSV-specific antibodies response in serum of challenged pigs. The cut-off value for seroconversion was set at a sample-to-positive (s/p) ratio of 0.4. Data are expressed as mean ± standard deviation (S.D). Asterisk indicates significant differences between the PRRSV2/CN/SS0/2020- and PRRSV2/CN/L3/2021-infected groups (*$p < 0.05$).

losses to the Chinese swine industry. According to the global PRRSV classification system, four different lineages of PRRSV (lineages 1, 3, 5, and 8) co-existed in Chinese swine herds, and two of them (lineages 1 and 8) are currently the predominant strains circulating in China. With the emergence of NADC30-like PRRSVs in China since 2012, recombinant strains have been frequently observed in the field. Notably, multiple studies have shown that PRRSV variants evolved from recombination events between lineage 1 and one or two other lineages (12–23). In this study, four PRRSV strains (PRRSV2/CN/SS0/2020, PRRSV2/CN/SS1/2021, PRRSV2/CN/L3/2021, and PRRSV2/CN/L4/2020) were also identified as recombinant viruses from three lineages of type 2 PRRSV (NADC30-like, QYYZ-like, and JXA1-like viruses). Importantly, the four strains in this study had a low whole-genome nucleotide similarity with other PRRSV sequences in GenBank (< 92%), which raised the concern of the introduction of new viruses into other large-scale pig farms. Therefore, to further our knowledge about these recombinant PRRSV strains, we characterized them genetically and phylogenetically to obtain insights that link genotypic with phenotypic data.

The natural genomic recombination between different lineages of PRRSV has been shown to play an important role in the generation of novel strains (34–36). Several studies have shown that the patterns of recombination of PRRSV in the field are becoming increasingly complex; for instance, 14LY01-FJ, 14LY02-FJ, 15LY01-FJ, 15LY02-FJ, JL580, GXNN1839, GXYL1403, HeN1401, HeN1601, FJ1402, FJXS15, SC-d, and TJnh1501 have evolved from the recombination between two lineages (17, 18, 20, 22, 36–39), whereas SD17–38, PRRSV2/CN/N9185/2018, PRRSV2/CN/X4833/2018, SDhz1512, and SCcd16 were natural recombinant viruses among three lineages (12, 14, 16, 23). More surprisingly, FJLIUY-2017 was derived from recombinant strains of four lineages (15). Notably, the diversity of recombinant PRRSV strains poses a major obstacle to the effective control of viral transmission (38, 40). In the present study, a comparison of whole-genome sequences and recombination analysis revealed that the four recombinant isolates (PRRSV2/CN/L3/2021, PRRSV2/CN/L4/2020, PRRSV2/CN/SS02020, and PRRSV2/CN/SS1/2021) were also natural recombinant viruses among the three lineages (lineage 1, 3, and 8.7). However, full-length sequencing of the virus showed that the entire genome of the four strains had low identity with the PRRSV strains available in GenBank, suggesting that PRRSVs have undergone evolution *via* natural recombination in recent years. Previous studies showed that Nsp1, Nsp2, Nsp3, Nsp9, Nsp11, and ORF2 are the hot spots for PRRSV RNA recombination (12, 13, 15, 17, 22, 23, 25, 36). In the present study, breakpoints of the four recombinant strains were also mainly located in Nsp1, Nsp2, Nsp3, and Nsp11, indicating that PRRSV gains genetic diversity by increasing recombination events at specific regions.

Nsp2 and ORF5 are the most variable proteins in the viral genome and are usually used as target genes for the molecular epidemiological surveillance of PRRSV (27). Compared with VR2332, the Nsp2 gene of PRRSV contains different patterns of amino acid insertions and deletions. For example, an outbreak in China with highly pathogenic PRRSVs (HP-PRRSV, JXA1-like) in 2006 had a unique 30-aa deletion in the Nsp2 region, whereas a unique 131-aa (111aa+1aa+19aa) deletion pattern in Nsp2 is the footprint of NADC30 and NADC30-like strains (11, 41). In the present study, the Nsp2 gene of the two strains (PRRSV2/CN/L3/2021 and PRRSV2/CN/L4/2020) had the 131-aa deletion, which is identical to NADC30-like strains, suggesting that these two strains may belong to lineage 1. Additionally, 2-aa insertions were also found in PRRSV2/CN/L3/2021 and PRRSV2/CN/L4/2020. Previous studies showed that MLV TJM-F92 has a unique 150-aa deletion (aa481+aa537-566+aa628–747) signature in its Nsp2-coding region (30). Interestingly, two strains identified in our study (PRRSV2/CN/SS0/2020 and PRRSV2/CN/SS1/2021) had characteristic 150-aa deletions that were identical to TJbd14-1 (an MLV-like strain that evolved from TJM-F92) and TJM-F92, suggesting that the PRRSV genome may have evolved more compactly by eliminating dispensable genomic regions (42). Furthermore, the phylogenetic analysis based on the ORF5 gene demonstrated that the four strains belonged to the QYYZ-like virus. In addition, the GP5 antigenic regions in the four strains were similar to those of the related lineage 3 representative strains but different from other lineage representative strains. The discordance between Nsp2 patterns and ORF5 lineages resulted from the recombination of PRRSVs. In other words, there is limited understanding of the recombinant PRRSV genomic data, especially if quantifying PRRSV diversity has only focused on ORF5 and Nsp2 analysis. In addition, the 137th aa of the GP5 protein is assumed to differentiate the attenuated vaccine strain (A^{137}) and the wild strain (S^{137}). Residue S^{137} was present in all four strains, suggesting that the four strains may be wild viruses (43). Additionally, a retrospective survey found that a massive vaccination with HP-PRRSV live attenuated vaccine (TJM-F92) was effective in preventing and controlling PRRS in this farm since 2018. Thus, we propose that PRRSV2/CN/SS0/2020 and PRRSV2/CN/SS1/2021 may have evolved from recombination among MLV TJM-F92 and NADC30-like or other PRRSV strains. Whether this strain directly evolved from MLV TJM-F92 needs to be further investigated.

Viremia and severity of fever are closely related to PRRSV virulence (44). In the present study, PRRSV2/CN/SS0/2020-infected pigs had higher viremia than PRRSV2/CN/L3/2021 from 4 dpc to 14 dpc, suggesting that PRRSV2/CN/SS0/2020 has higher virulence for pigs. In addition, pigs inoculated with the PRRSV2/CN/SS0/2020 strain had persistently higher fever (>40°C for 12 days) and interstitial pneumonia compared to the PRRSV2/CN/L3/2021-infected group. Notably, one pig in the PRRSV2/CN/SS0/2020 group died within 2 weeks, whereas the pigs in the PRRSV2/CN/L3/2021 survived throughout the experiment. These data showed that PRRSV2/CN/SS0/2020 demonstrates higher pathogenicity than PRRSV2/CN/L3/2021. This finding is consistent with previous results that recombinant PRRSV strains derived from field PRRSV strains and vaccine-like strains could result in higher pathogenicity for pigs, such as FJXS15 and TJnh150 (13, 18).

In conclusion, we determined the complete genome sequences of four recombinant PRRSV isolates (PRRSV2/CN/SS0/2020, PRRSV2/CN/SS1/2021, PRRSV2/CN/L3/2021, and PRRSV2/CN/L4/2020). Four isolates were natural recombinant among three lineages (lineage 1, 3, and 8) and have the absence of close relatives to PRRSV sequence in GenBank (<92%). PRRSV2/CN/SS0/2020 exhibits higher pathogenicity than PRRSV2/CN/L3/2021. Our findings suggest that PRRSVs have undergone genome evolution by recombination among field strains/MLV-like strains of different lineages.

DATA AVAILABILITY STATEMENT

The datasets presented in this study can be found in online repositories. The names of the repository/repositories and accession number(s) can be found in the article/**Supplementary Material**.

AUTHOR CONTRIBUTIONS

JLiu and CW performed the experiments. YX, CL, and YY conceived and designed the experiments. LL, CH, and JLi performed the data analyses. JLiu completed the writing of the manuscript. All authors contributed to the article and approved the submitted version.

FUNDING

This study was supported by Leading Project Foundation of Science Department of Fujian Province (2021N0032), Research Foundation of Engineering Research Center for the Prevention and Control of Animal Original Zoonosis, Fujian Province University, (Grant No. 2021ZN002), Qimai Foundation of Shanghang District of Longyan City, Fujian Province (2020SHQM07) and Longyan University Young Talents Program.

SUPPLEMENTARY MATERIAL

The Supplementary Material for this article can be found online at: https://www.frontiersin.org/articles/10.3389/fvets.2022.933896/full#supplementary-material

REFERENCES

1. Benfield DA, Nelson E, Collins JE, Harris L, Goyal SM, Robison D, et al. Characterization of Swine Infertility and Respiratory Syndrome (SIRS) virus (isolate ATCC VR-2332). *J Vet Diagn Invest.* (1992) 4:127–33. doi: 10.1177/104063879200400202
2. Wensvoort G, Terpstra D, Pol JM, ter Laak EA, Bloemraad M, de Kluyver EP, et al. Mystery swine disease in the Netherlands: the isolation of Lelystad virus. *Vet Q.* (1991) 13:121–30. doi: 10.1080/01652176.1991.9694296
3. Firth AE, Zevenhoven-Dobbe JC, Wills NM, Go YY, Balasuriya UB, Atkins JF, et al. Discovery of a small arterivirus gene that overlaps the GP5 coding sequence and is important for virus production. *J Gen Virol.* (2011) 92:1097–106. doi: 10.1099/vir.0.029264-0
4. Johnson CR, Griggs TF, Gnanandarajah J, Murtaugh MP. Novel structural protein in porcine reproductive and respiratory syndrome virus encoded by an alternative ORF5 present in all arteriviruses. *J Gen Virol.* (2011) 92:1107–16. doi: 10.1099/vir.0.030213-0
5. Lunney JK, Fang Y, Ladinig A, Chen N, Li Y, Rowland B, et al. Porcine reproductive and respiratory syndrome virus (PRRSV): pathogenesis and interaction with the immune system. *Annu Rev Anim Biosci.* (2016) 4:129–54. doi: 10.1146/annurev-animal-022114-111025
6. Muhlenberg JJ. PRRSV, the virus. *Vet Res.* (2000) 31:11–21. doi: 10.1051/vetres:2000103
7. Dokland T. The structural biology of PRRSV. *Virus Res.* (2010) 154:86–97. doi: 10.1016/j.virusres.2010.07.029
8. Wu WH, Fang Y, Rowland RR, Lawson SR, Christopher-Hennings J, Yoon KJ, et al. The 2b protein as a minor structural component of PRRSV. *Virus Res.* (2005) 114:177–81. doi: 10.1016/j.virusres.2005.06.014
9. Nelsen CJ, Murtaugh MP, Faaberg KS. Porcine reproductive and respiratory syndrome virus comparison: divergent evolution on two continents. *J Virol.* (1999) 73:270–80. doi: 10.1128/JVI.73.1.270-280.1999
10. Zhou YJ, Hao XF, Tian ZJ, Tong GZ, Yoo D, An TQ, et al. Highly virulent porcine reproductive and respiratory syndrome virus emerged in China. *Transbound Emerg Dis.* (2008) 55:152–64. doi: 10.1111/j.1865-1682.2008.01020.x
11. Guo Z, Chen XX, Li R, Qiao S, Zhang G. The prevalent status and genetic diversity of porcine reproductive and respiratory syndrome virus in China: a molecular epidemiological perspective. *Virol J.* (2018) 15:2. doi: 10.1186/s12985-017-0910-6
12. Liu J, Xu Y, Lin Z, Fan J, Dai A, Deng X, et al. Epidemiology investigation of PRRSV discharged by faecal and genetic variation of ORF5. *Transbound Emerg Dis.* (2021) 68:2334–44. doi: 10.1111/tbed.13894
13. Bian T, Sun Y, Hao M, Zhou L, Ge X, Guo X, et al. A recombinant type 2 porcine reproductive and respiratory syndrome virus between NADC30-like and a MLV-like: genetic characterization and pathogenicity for piglets. *Infect Genet Evol.* (2017) 54:279–86. doi: 10.1016/j.meegid.2017.07.016
14. Chen N, Ye M, Li S, Huang Y, Zhou R, Yu X, et al. Emergence of a novel highly pathogenic recombinant virus from three lineages of porcine reproductive and respiratory syndrome virus 2 in China 2017. *Transbound Emerg Dis.* (2018) 65:1775–85. doi: 10.1111/tbed.12952
15. Liu J, Wei C, Lin Z, Fan J, Xia W, Dai A, et al. Recombination in lineage 1, 3, 5, and 8 of porcine reproductive and respiratory syndrome viruses in China. *Infect Genet Evol.* (2019) 68:119–26. doi: 10.1016/j.meegid.2018.12.006
16. Liu Y, Li J, Yang J, Zeng H, Guo L, Ren S, et al. Emergence of different recombinant porcine reproductive and respiratory syndrome viruses, China. *Sci Rep.* (2018) 8:4118. doi: 10.1038/s41598-018-22494-4
17. Liu JK, Zhou X, Zhai JQ, Li B, Wei CH, Dai AL, et al. Emergence of a novel highly pathogenic porcine reproductive and respiratory syndrome virus in China. *Transbound Emerg Dis.* (2017) 64:2059–74. doi: 10.1111/tbed.12617
18. Liu J, Zhou X, Zhai J, Wei C, Dai A, Yang X, et al. Recombination in JXA1-R vaccine and NADC30-like strain of porcine reproductive and respiratory syndrome viruses. *Vet Microbiol.* (2017) 204:110–20. doi: 10.1016/j.vetmic.2017.04.017
19. Sun YK, Li Q, Yu ZQ, Han XL, Wei YF, Ji CH, et al. Emergence of novel recombination lineage 3 of porcine reproductive and respiratory syndrome viruses in Southern China. *Transbound Emerg Dis.* (2019) 66:578–87. doi: 10.1111/tbed.13067
20. Wang HM, Liu YG, Tang YD, Liu TX, Zheng LL, Wang TY, et al. A natural recombinant PRRSV between HP-PRRSV JXA1-like and NADC30-like strains. *Transbound Emerg Dis.* (2018) 65:1078–86. doi: 10.1111/tbed.12852
21. Zhang Q, Xu X, You S, Li Y, Wang H, Bai J, et al. Emerging of two new subgenotypes of porcine reproductive and respiratory syndrome viruses in Southeast China. *Microb Pathog.* (2016) 97:27–33. doi: 10.1016/j.micpath.2016.05.011
22. Zhao K, Ye C, Chang XB, Jiang CG, Wang SJ, Cai XH, et al. Importation and recombination are responsible for the latest emergence of highly pathogenic porcine reproductive and respiratory syndrome virus in China. *J Virol.* (2015) 89:10712–6. doi: 10.1128/JVI.01446-15
23. Zhou L, Kang R, Zhang Y, Ding M, Xie B, Tian Y, et al. Whole genome analysis of two novel type 2 porcine reproductive and respiratory syndrome viruses with complex genome recombination between lineage 8, 3, and 1 strains identified in Southwestern China. *Viruses.* (2018) 10:328. doi: 10.3390/v10060328
24. Zhang H, Leng C, Ding Y, Zhai H, Li Z, Xiang L, et al. Characterization of newly emerged NADC30-like strains of porcine reproductive and respiratory syndrome virus in China. *Arch Virol.* (2019) 164:401–11. doi: 10.1007/s00705-018-4080-7
25. Zhou L, Kang R, Ji G, Tian Y, Ge M, Xie B, et al. Molecular characterization and recombination analysis of porcine reproductive and respiratory syndrome virus emerged in Southwestern China during 2012–2016. *Virus Genes.* (2018) 54:98–110. doi: 10.1007/s11262-017-1519-y
26. Martin DP, Lemey P, Lott M, Moulton V, Posada D, Lefeuvre P. RDP3: a flexible and fast computer program for analyzing recombination. *Bioinformatics.* (2010) 26:2462–3. doi: 10.1093/bioinformatics/btq467
27. Yin B, Qi S, Sha W, Qin H, Liu L, Yun J, et al. Molecular characterization of the Nsp2 and ORF5 (ORF5a) Genes of PRRSV strains in nine provinces of China during 2016–2018. *Front Vet Sci.* (2021) 8:605832. doi: 10.3389/fvets.2021.605832
28. Lole KS, Bollinger RC, Paranjape RS, Gafkari D, Kulkarni SS, Novak NG, et al. Full-length human immunodeficiency virus type 1 genomes from subtype C-infected seroconverters in India, with evidence of intersubtype recombination. *J Virol.* (1999) 73:152–60. doi: 10.1128/JVI.73.1.152-160.1999
29. Zhou L, Yang B, Xu L, Jin H, Ge X, Guo X, et al. Efficacy evaluation of three modified-live virus vaccines against a strain of porcine reproductive and respiratory syndrome virus NADC30-like. *Vet Microbiol.* (2017) 207:108–16. doi: 10.1016/j.vetmic.2017.05.031
30. Leng X, Li Z, Xia M, Li X, Wang F, Wang W, et al. Mutations in the genome of the highly pathogenic porcine reproductive and respiratory syndrome virus potentially related to attenuation. *Vet Microbiol.* (2012) 157:50–60. doi: 10.1016/j.vetmic.2011.12.012
31. de Lima M, Pattnaik AK, Flores EF, Osorio FA. Serologic marker candidates identified among B-cell linear epitopes of nsp2 and structural proteins of a North American strain of porcine reproductive and respiratory syndrome virus. *Virology.* (2006) 353:410–21. doi: 10.1016/j.virol.2006.05.036
32. Zhou YJ, Yua H, Tian ZJ, Liu JX, An TQ, Peng JM, et al. Monoclonal antibodies and conserved antigenic epitopes in the C terminus of GP5 protein of the North American type porcine reproductive and respiratory syndrome virus. *Vet Microbiol.* (2009) 138:1–10. doi: 10.1016/j.vetmic.2009.01.041
33. Allende R, Kutish GF, Laegreid W, Lu Z, Lewis TL, Rock DL, et al. Mutations in the genome of porcine reproductive and respiratory syndrome virus responsible for the attenuation phenotype. *Arch Virol.* (2000) 145:1149–61. doi: 10.1007/s007050070115
34. Kappes MA, Faaberg KS. PRRSV structure, replication and recombination: origin of phenotype and genotype diversity. *Virology.* (2015) 479:475–86. doi: 10.1016/j.virol.2015.02.012
35. Shi M, Holmes EC, Brar MS, Leung FC. Recombination is associated with an outbreak of novel highly pathogenic porcine reproductive and respiratory syndrome viruses in China. *J Virol.* (2013) 87:10904–7. doi: 10.1128/JVI.01270-13
36. Zhang Z, Zhou L, Ge X, Guo X, Han J, Yang H. Evolutionary analysis of six isolates of porcine reproductive and respiratory syndrome virus from a single pig farm: MLV-evolved and recombinant viruses. *Infect Genet Evol.* (2018) 66:111–9. doi: 10.1016/j.meegid.2018.09.024
37. Zhang Q, Jiang P, Song Z, Lv L, Li L, Bai J. Pathogenicity and antigenicity of a novel NADC30-like strain of porcine reproductive and

respiratory syndrome virus emerged in China. *Vet Microbiol.* (2016) 197:93–101. doi: 10.1016/j.vetmic.2016.11.010

38. Wang J, Lin S, Quan D, Wang H, Huang J, Wang Y, et al. Full genomic analysis of new variants of porcine reproductive and respiratory syndrome virus revealed multiple recombination events between different lineages and sublineages. *Front Vet Sci.* (2020) 7:603. doi: 10.3389/fvets.2020.00603
39. Sun YF, Zhou L, Bian T, Tian XX, Ren WK, Lu C, et al. Efficacy evaluation of two commercial modified-live virus vaccines against a novel recombinant type 2 porcine reproductive and respiratory syndrome virus. *Vet Microbiol.* (2018) 216:176–82. doi: 10.1016/j.vetmic.2018.02.016
40. Meng XJ. Heterogeneity of porcine reproductive and respiratory syndrome virus: implications for current vaccine efficacy and future vaccine development. *Vet Microbiol.* (2000) 74:309–29. doi: 10.1016/S0378-1135(00)00196-6
41. Zhou L, Wang Z, Ding Y, Ge X, Guo X, Yang H. NADC30-like strain of porcine reproductive and respiratory syndrome virus, China. *Emerg Infect Dis.* (2015) 21:2256–7. doi: 10.3201/eid2112.150360
42. Han J, Wang Y, Faaberg KS. Complete genome analysis of RFLP 184 isolates of porcine reproductive and respiratory syndrome virus. *Virus Res.* (2006) 122:175–82. doi: 10.1016/j.virusres.2006.06.003
43. Wesley RD, Mengeling WL, Lager KM, Clouser DF, Landgraf JG, Frey ML. Differentiation of a porcine reproductive and respiratory syndrome virus vaccine strain from North American field strains by restriction fragment length polymorphism analysis of ORF5. *J Vet Diagn Invest.* (1998) 10:140–4. doi: 10.1177/104063879801000204
44. Stadejek T, Larsen LE, Podgórska K, Bøtner A, Botti S, Dolka I, et al. Pathogenicity of three genetically diverse strains of PRRSV Type 1 in specific pathogen free pigs. *Vet Microbiol.* (2017) 209:13–9. doi: 10.1016/j.vetmic.2017.05.011

Conflict of Interest: The authors declare that the research was conducted in the absence of any commercial or financial relationships that could be construed as a potential conflict of interest.

Publisher's Note: All claims expressed in this article are solely those of the authors and do not necessarily represent those of their affiliated organizations, or those of the publisher, the editors and the reviewers. Any product that may be evaluated in this article, or claim that may be made by its manufacturer, is not guaranteed or endorsed by the publisher.

frontiers | Frontiers in Veterinary Science

ORIGINAL RESEARCH
published: 30 June 2022
doi: 10.3389/fvets.2022.945381

Genome-Wide Characterization of QYYZ-Like PRRSV During 2018–2021

Hu Xu[1†], Lirun Xiang[2†], Yan-Dong Tang[2†], Chao Li[2], Jing Zhao[2], Bangjun Gong[2], Qi Sun[2], Chaoliang Leng[3], Jinmei Peng[2], Qian Wang[2], Guohui Zhou[2], Tongqing An[2], Xuehui Cai[2], Zhi-Jun Tian[2], Hongliang Zhang[2] and Mingxin Song[1]**

[1] College of Veterinary Medicine, Northeast Agricultural University, Harbin, China, [2] State Key Laboratory of Veterinary Biotechnology, Harbin Veterinary Research Institute, Chinese Academy of Agricultural Sciences, Harbin, China, [3] Henan Key Laboratory of Insect Biology in Funiu Mountain, Henan Provincial Engineering Laboratory of Insect Bioreactors, China-UK-NYNU-RRes Joint Laboratory of Insect Biology, Nanyang Normal University, Nanyang, China

In the last decade, the emergence of QYYZ-like porcine reproductive and respiratory syndrome virus (PRRSV) has attracted increasing attention due to the high incidence of PRRSV mutation and recombination. However, the endemic status and genomic characteristics of the QYYZ-like strains are unclear. From 2018 to October 2021, 24 QYYZ-like PRRSV isolates were obtained from 787 PRRSV-positive clinical samples. Only one QYYZ-like positive sample was from a northern province, and the rest were from central and southern provinces. We selected 9 samples for whole-genome sequencing, revealing genome lengths of 15,008–15,316 nt. We retrieved all the available whole-genome sequences of QYYZ-like PRRSVs isolated in China from 2010 to 2021 ($n = 28$) from GenBank and analyzed them together with the new whole-genome sequences ($n = 9$). Phylogenetic tree analysis based on the ORF5 gene showed that all QYYZ-like PRRSV strains belonged to sublineage 3.5 but were clustered into three lineages (sublineage 1.8, sublineage 3.5, and sublineage 8.7) based on whole-genome sequences. Genomic sequence alignment showed that QYYZ-like strains, have characteristic amino acids insertions or deletions in the Nsp2 region (same as NADC30, JXA1 and QYYZ) and that thirteen strains also had additional amino acid deletions, mostly between 468 and 518 aa. Moreover, QYYZ-like strains (sublineage 3.5) have seven identical characteristic amino acid mutations in ORF5. Recombination analysis revealed that almost all QYYZ-like complete genome sequences (36/37) were products of recombination and mainly provided structural protein fragments (GP2-N) for the recombinant strains. Overall, QYYZ-like strains were mainly prevalent in central and southern China from 2018 to 2021, and these strains provided recombinant fragments in the PRRSV epidemic in China.

Keywords: QYYZ-like PRRSV, whole-genome analysis, complex patterns of recombination, recombination hotspots, epidemiological characteristics

OPEN ACCESS

Edited by:
Zhou Mo,
Heilongjiang University, China

Reviewed by:
Jianguo Dong,
Xinyang Agriculture and Forestry University, China
Yifeng Jiang,
Shanghai Veterinary Research Institute (CAAS), China

***Correspondence:**
Mingxin Song
songmx@neau.edu.cn
Hongliang Zhang
zhanghongliang01@caas.cn

†These authors have contributed equally to this work and share first authorship

Specialty section:
This article was submitted to Veterinary Infectious Diseases, a section of the journal Frontiers in Veterinary Science

Received: *17 May 2022*
Accepted: *06 June 2022*
Published: *30 June 2022*

Citation:
Xu H, Xiang L, Tang Y-D, Li C, Zhao J, Gong B, Sun Q, Leng C, Peng J, Wang Q, Zhou G, An T, Cai X, Tian Z-J, Zhang H and Song M (2022) Genome-Wide Characterization of QYYZ-Like PRRSV During 2018–2021. Front. Vet. Sci. 9:945381. doi: 10.3389/fvets.2022.945381

INTRODUCTION

Porcine respiratory and reproductive syndrome (PRRS) is a major disease in the pig industry that causes huge economic losses to the swine industry worldwide (1). The causative agent, porcine reproductive and respiratory syndrome virus (PRRSV), is an enveloped, positive-sense, single-stranded RNA virus belonging to the genus *Betaarterivirus* and family *Arteriviridae* of order

Nidovirales (2). Due to its high degree of genetic diversity, PRRSV has been further divided into two species, PRRSV-1 (formerly known as European genotype 1) and PRRSV-2 (formerly known as North American genotype 2) (3). Since PRRSV was first discovered in China in 1996, the PRRSV-2 strain has been the main circulating strain in China (4).

Phylogenetic analyses of ORF5 of PRRSV-2 strains showed that PRRSV-2 could be divided into nine distinct lineages, with each lineage containing several sublineages (5, 6). Four different PRRSV-2 lineages have become widespread in China, including lineage 8 (JXA1-like/CH-1a-like), lineage 5 (VR-2332-like), lineage 1 (NADC30-like/NADC34-like), and lineage 3 (QYYZ-like) (7). The first PRRSV-2 strain CH-1a of China was isolated in 1996 in lineage 8 (8). HP-PRRSV (JXA1-like) was recognized in 2006 and originated from CH-1a-like strains (9). In 2013, some NADC30-like strains were isolated in China, and they have gradually become the dominant strains in recent years (10). NADC34-like strains were first reported in China in 2017 and became one of the major epidemic strains in 2020 (7, 11). Lineage 3 strains were initially reported in Taiwan and have emerged in Hong Kong (12). The FJ-1 strain was the first lineage 3 PRRSV detected in mainland China in 2005. The representative isolate of lineage 3 was QYYZ, which was identified in 2010 in mainland China and gradually became prevalent in southern China (12, 13). More importantly, lineage 3 viruses with greater virulence have been reported in southern China, and these viruses, recombining with lineage 1 and 8 PRRSV, pose a great threat to the Chinese pig industry (14–17).

Several studies have summarized the origin, classification, epidemic history and population dynamics of QYYZ-like strains based on the ORF5 gene (18, 19). However, the prevalence and genomic characteristics of these strains in recent years remain unclear. In this study, we carried out molecular epidemiological investigations for QYYZ-like PRRSV surveillance from 2018 to 2021. Meanwhile, the genome-wide characteristics of QYYZ-like strains and the role of these strains in the PRRSV epidemic were explored by comparing the latest strains and all reported genome-wide sequences.

MATERIALS AND METHODS

Sample Collection and Genome Sequencing

From 2018 to 2021, we collected 1,803 clinical samples (including lung, lymph node and serum samples) of suspected PRRSV infection from different pig farms in 16 provinces in China (Heilongjiang, Jilin, Liaoning, Shandong, Henan, Guangdong, Guangxi, Zhejiang, Hebei, Hubei, Xinjiang, Inner Mongolia, Tianjin, Sichuan, Jiangxi and Jiangsu). Tissue sample processing, RNA extraction, cDNA preparation, RT–PCR and genome sequencing were performed as described in previous reports (8, 11). The primers used to detect PRRSV and amplify entire gene sequences were reported previously (20).

Sequence Analysis and Phylogenetic Analysis

Sequence analysis was performed with DNASTAR (version 7.1) software. Phylogenetic trees and molecular evolutionary analyses were conducted by MEGA 7 software using the neighbor-joining method with 1,000 bootstrap replications (21). The generated phylogenetic tree was annotated using the online software ITOL (https://itol.embl.de/) (22).

Recombination Analysis

To determine whether recombination screening occurred in the generation of QYYZ-like PRRSV strains, recombination events were considered only when supported by at least four of seven recombination detection algorithms (RDP, GENECONV, BootScan, MaxChi, Chimera, SiScan and 3Seq) in the Recombination Detection Program version 4.8 (RDP v.4.8). Finally, the pictures of recombination events were drawn by SimPlot v3.5.1 within a 500-bp window sliding along the genome alignment (20-bp step size).

RESULTS AND DISCUSSION

From 2018 to 2021, 1,803 clinical samples were collected from 16 provinces of China; 787 (43.64%) tested positive for PRRSV according to RT–PCR. Of the 787 positive samples, 191 were from central or southern provinces (Henan, Guangdong, Guangxi, Zhejiang, Hubei, Sichuan, Jiangsu, and Jiangxi), and the remaining 596 were from northern provinces (Heilongjiang, Jilin, Liaoning, Shandong, Hebei, Xinjiang, Inner Mongolia, and Tianjin) (**Figure 1**). Through ORF5 phylogenetic analysis, 24 samples were confirmed to have QYYZ-like PRRSV. The results showed that QYYZ-like PRRSV did not cause a pandemic in China but persisted during 2018–2021. Interestingly, almost all samples with QYYZ-like PRRSV were from central and southern provinces, including Henan (4), Guangdong (9), Zhejiang (1) and Guangxi (9), and only one QYYZ-like strain came from Heilongjiang Province (**Table 1**). The QYYZ-like strains accounted for approximately 12% (23/191) of the cases in the central and southern provinces (**Figure 1**). Therefore, QYYZ-like PRRSV was mainly prevalent in central and southern China. To further study the complete genome characteristics of QYYZ-like PRRSV in China, we selected 9 strains (HNLCL15-1903, GXXNF10-1803, GXXNF53-1805, GDXNF60-1805, GXXNF74-1806, GXXNF78-1806, GDXNF229-1811, HNTZJ1714-2011, GXTZJ2325-2112) from 24 newly identified QYYZ-like isolates based on large homology differences and different branches of an ORF5 phylogenetic tree for whole-genome sequencing. The genomes of these isolates were 15,008–15,316 nt in length, excluding 3′ poly (A) tails. The significant difference in gene length between the newly QYYZ-like PRRSV strains may be due to the different deletion or insertion patterns in the Nsp2 region.

To evaluate the genomic characteristics of the newly identified QYYZ-like PRRSV strains, the genomes of the novel PRRSV isolates were compared with those of different lineage viruses, including JXA1 (lineage 8), NADC30 (lineage 1) and QYYZ (lineage 3) (**Table 2**). Genome alignment revealed that the

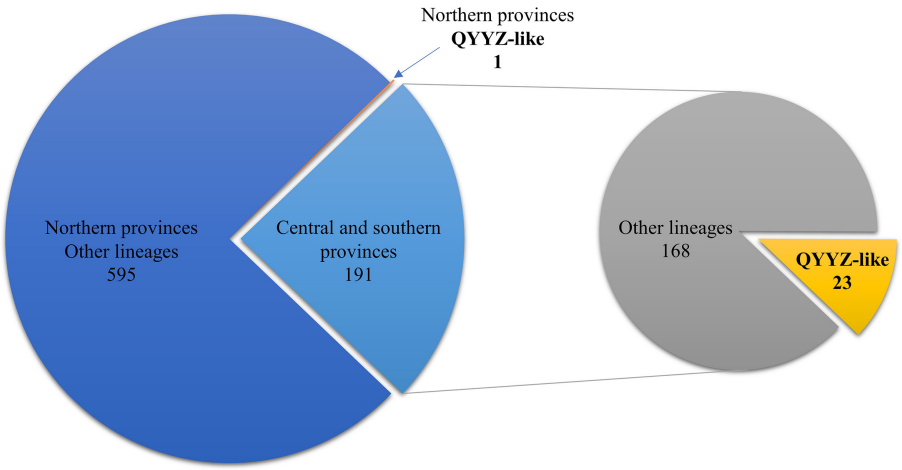

FIGURE 1 | Number of QYYZ-like strains detected in different regions from 2018 to 2021. Among the 596 PRRSV-positive samples from northern provinces, 1 was a QYYZ-like strain. The remaining 191 PRRSV-positive samples were from central and southern provinces, of which 23 were QYYZ-like strains.

TABLE 1 | Information on 24 strains of the newly identified QYYZ-like PRRSV.

No.	Isolates	Accession no.	Time	Isolation source	Province	Gene region
1	GDXNF8-1802	ON462023	2018.02	Lung/lymph nodes	Guangdong	ORF5
2	GXXNF10-1803	ON462046	2018.03	Serum	Guangxi	Whole genome
3	GDXNF17-1804	ON462024	2018.04	Lung/lymph nodes	Guangdong	ORF5
4	GXXNF53-1805	ON462047	2018.05	Lung	Guangxi	Whole genome
5	GDXNF59-1805	ON462025	2018.05	Lung	Guangdong	ORF5
6	GDXNF60-1805	ON462048	2018.05	Lung	Guangdong	Whole genome
7	GXXNF74-1806	ON462049	2018.06	Lung	Guangxi	Whole genome
8	GXXNF75-1806	ON462026	2018.06	Lung	Guangxi	ORF5
9	GXXNF76-1806	ON462027	2018.06	Lung	Guangxi	ORF5
10	GXXNF77-1806	ON462028	2018.06	Lung/lymph nodes	Guangxi	ORF5
11	GXXNF78-1806	ON462050	2018.06	Lung/lymph nodes	Guangxi	Whole genome
12	GXXNF79-1806	ON462029	2018.06	Lung	Guangxi	ORF5
13	GDXNF134-1809	ON462030	2018.09	Lung	Guangdong	ORF5
14	ZJWK211-1809	ON462022	2018.09	Serum	Zhejiang	ORF5
15	GDXNF229-1811	ON462051	2018.11	Lung/lymph nodes	Guangdong	Whole genome
16	HNLCL15-1903	ON462043	2019.03	Serum/lung	Henan	Whole genome
17	HNLCL19-1904	ON462031	2019.04	Serum/lung	Henan	ORF5
18	HNLCL25-1905	ON462032	2019.05	Serum/lung	Henan	ORF5
19	HNLCL43-1906	ON462033	2019.06	Serum/lung	Henan	ORF5
20	GDHSW97-2001	ON462034	2020.01	Lung	Guangdong	ORF5
21	GDHSW100-2001	ON462035	2020.01	Lung	Guangdong	ORF5
22	HLJTZJ1224-2011	ON462036	2020.11	Lung	Heilongjiang	ORF5
23	HNTZJ1714-2011	ON462044	2020.11	Serum	Henan	Whole genome
24	GXTZJ2325-2112	ON462045	2021.12	Lung	Guangxi	Whole genome

ORF5 gene of 24 QYYZ-like PRRSV strains shared 91.2–96.0% nucleotide homology with that of QYYZ, which was higher than the homology shared with that of JXA1 (81.9–85.7%) and NADC30 (82.2–85.2%). The homology among the 24 QYYZ-like strains was 86.4–100% (**Table 2**), and most of the QYYZ-like PRRSV ORF5 genes had low homology. The complete genome results also showed that the 9 newly identified QYYZ-like PRRSV strains shared 84.6–96.1% identity with JXA1, 82.3–90.8% identity with NADC30, and 83.6–93.8% identity with QYYZ (**Table 2**). Among them, the isolates GXXNF53-1805, GDXNF60-1805, GXXNF78-1806 and HNTZJ1714-2011 showed the highest identity (93.2, 95.4, 96.1, and 89.0%) with JXA1;

TABLE 2 | Nucleotide and amino acid sequence similarity between the 24 new QYYZ-like PRRSVs and the reference strain.

Amino acids/nucleotides	JXA1	NADC30	QYYZ	QYYZ-like (newly)
5'UTR	–/96.8–98.9	–/91.0–93.1	–/94.1–95.2	–/94.1–99.5
Nsp1α	94.4–99.4/93.0–98.1	93.9–96.7/85.6–89.4	95.6–97.2/89.6–92.2	92.8–98.9/88.7–96.9
Nsp1β	87.6–95.5/89.3–97.0	73.7–75.8/75.7–80.2	79.7–82.7/81.5–84.3	84.7–95.0/88.3–96.2
Nsp2	70.9–96.3/76.0–97.3	68.6–88.1/73.6–90.4	68.0–87.3/74.7–91.4	67.3–92.9/73.4–94.3
Nsp3	86.1–99.1/81.3–98.1	87.0–96.5/80.6–93.6	87.8–98.3/80.9–94.3	86.1–99.1/80.1–96.1
Nsp4	90.7–100/81.9–98.5	89.2–93.1/81.4–93.8	91.7–97.5/83.5–95.4	90.2–99.0/81.0–97.5
Nsp5	87.6–95.9/80.2–97.1	86.5–96.5/80.2–94.3	87.6–97.1/80.6–95.3	86.5–95.3/78.8–94.1
Nsp6	93.8–100/85.4–100	93.8–100/83.3–97.9	93.8–100/83.3–97.9	93.8–100/81.2–100
Nsp7α	87.2–99.3/81.7–98.2	91.3–94.0/81.0–93.7	86.6–98.0/80.3–94.0	85.9–98.0/79.9–86.2
Nsp7β	71.8–100/77.9–99.1	70.9–90.9/77.6–92.7	75.5–94.5/78.5–94.5	69.1–100/75.8–98.2
Nsp8	93.3–100/88.1–98.5	91.1–95.6/83.0–94.8	93.3–100/88.1–94.1	88.9–100/83.7–97.8
Nsp9	96.6–99.5/85.4–98.9	96.0–98.3/85.3–95.0	95.0–98.1/84.4–92.5	94.9–99.1/84.3–97.5
Nsp10	93.7–99.5/84.5–98.6	94.6–97.7/84.8–95.1	93.0–99.8/84.6–98.1	92.7–99.3/84.1–97.2
Nsp11	92.8–98.2/85.9–95.7	91.9–96.3/84.0–91.2	93.7–97.8/86.1–96.7	91.5–96.9/83.3–96.9
Nsp12	96.1–100/86.4–98.9	92.9–96.1/85.3–90.1	93.5–99.4/85.7–97.4	92.9–99.4/84.0–98.1
ORF2a	86.0–90.3/87.8–92.0	87.2–88.3/84.2–87.4	92.6–96.5/91.7–97.0	88.7–94.6/89.0–94.7
ORF2b	86.5–91.9/91.0–94.6	83.8–91.9/88.7–91.4	91.9–98.6/94.1–96.4	87.8–94.6/90.5–94.6
ORF3	83.5–87.5/84.4–89.5	78.0–95.9/82.6–86.5	85.1–95.3/86.7–95.3	83.1–93.3/86.4–93.3
ORF4	85.5–96.1/84.7–94.4	88.3–91.6/86.0–88.5	87.2–96.1/86.2–95.2	87.2–94.4/84.5–92.7
ORF5	82.1–85.1/83.4–85.4	84.1–87.6/82.8–86.7	92.0–96.5/91.2–96.0	88.6–100/86.4–100
ORF5a	72.5–78.8/81.0–85.9	73.1–80.8/82.4–86.5	84.6–98.1/89.7–98.1	80.4–98.1/85.0–96.2
ORF6	94.3–96.6/89.0–91.2	92.0–95.4/88.2–90.9	96.0–98.9/92.8–97.5	95.4–98.9/90.3–96.4
ORF7	87.9–90.3/85.2–89.2	88.7–99.2/84.7–95.2	90.3–99.2/90.9–96.5	87.1–97.6/84.1–95.2
3'UTR	81.2–88.9	83.6–93.0	90.1–96.0	83.8–94.5
Whole genome	84.6–96.1	82.3–90.8	83.6–93.8	87.3–94.7

The ORF5 homology results were for 24 newly identified PRRSV strains, and the other regional homology results were for 9 whole-genome sequences.

the isolates GXXNF10-1803, GXXNF74-1806, GDXNF229-1811 and GXTZJ2325-2112 displayed the highest identity (87.8, 93.8, 91.0, and 86.3%) with QYYZ; and HNLCL15-1903 shared the highest identity with NADC30, but the homology was only 90.8%, suggesting that the newly identified QYYZ-like PRRSVs may have undergone large variation or recombination.

To establish genetic relationships between Chinese QYYZ-like PRRSV strains and other PRRSV isolates, we constructed phylogenetic trees based on both the ORF5 gene and complete genomic sequence. Phylogenetic analysis based on ORF5 gene sequences demonstrated that all 24 new QYYZ-like PRRSV strains could be classified into sublineage 3.5 (**Figure 2A**). To analyze the genetic diversity of the novel QYYZ-like PRRSV in as much detail as possible, we expanded a data set (n = 470) including all ORF5 sequences of lineage 3 collected from GenBank and submitted before December 2021. As shown in **Figure 2B**, all 24 newly identified QYYZ-like strains in China (deep red labeled) clustered deeply within sublineage 3.5 from mainland China and did not form a separate clade. They are distantly related to sublineages 3.1–3.3 circulating in Taiwan and sublineage 3.4 circulating in Hong Kong (**Figure 2B**). To understand the genome-wide characteristics of QYYZ-like strains in China, we collected the whole-genome sequences of all QYYZ-like strains (ORF5 classified into sublineage 3.5) from GenBank (n = 28) (**Table 3**) and submitted before December 2021 and constructed phylogenetic trees together with the new strains (n = 9). Since the homology of QY2010 (Accession: JQ743666.1) and QYYZ (Accession: JQ308798.1) was up to 100% and the collection time of the two strains was very close, we regarded them as one strain and expressed them as QYYZ (**Table 3**). As shown in **Figure 2C**, 37 isolates were clustered into several branches with viruses belonging to different lineages. A total of 21 strains (GXXNF53-1805, GDXNF60-1805, GXXNF78-1806, HNTZJ1714-2011, etc.) were closely related to JXA1 and Hun4 (HP-PRRSV sublineage 8.7), while ten strains (GXXNF10-1803, GXXNF74-1806, GDXNF229-1811, etc.) were clustered into a separate branch close to QYYZ (sublineage 3.5). Additionally, HNLCL15-1903, GXTZJ2325-2112, SCya18 and FJLIUY-2017 were closer to NADC30 (sublineage 1.8). There was a large difference between the ORF5 gene-based and whole genome-based phylogenetic analyses. The epidemiology of PRRSV has been investigated largely by sequencing the ORF5 gene and classifying virus lineages based on ORF5 phylogenetic analysis (5, 6, 33). With the increasing number of recombinant strains, it is necessary to sequence the whole genome of key strains in order to classify them.

Nsp2 is the most significant variable region, with remarkable mutations, insertions and deletions, and is recognized as an

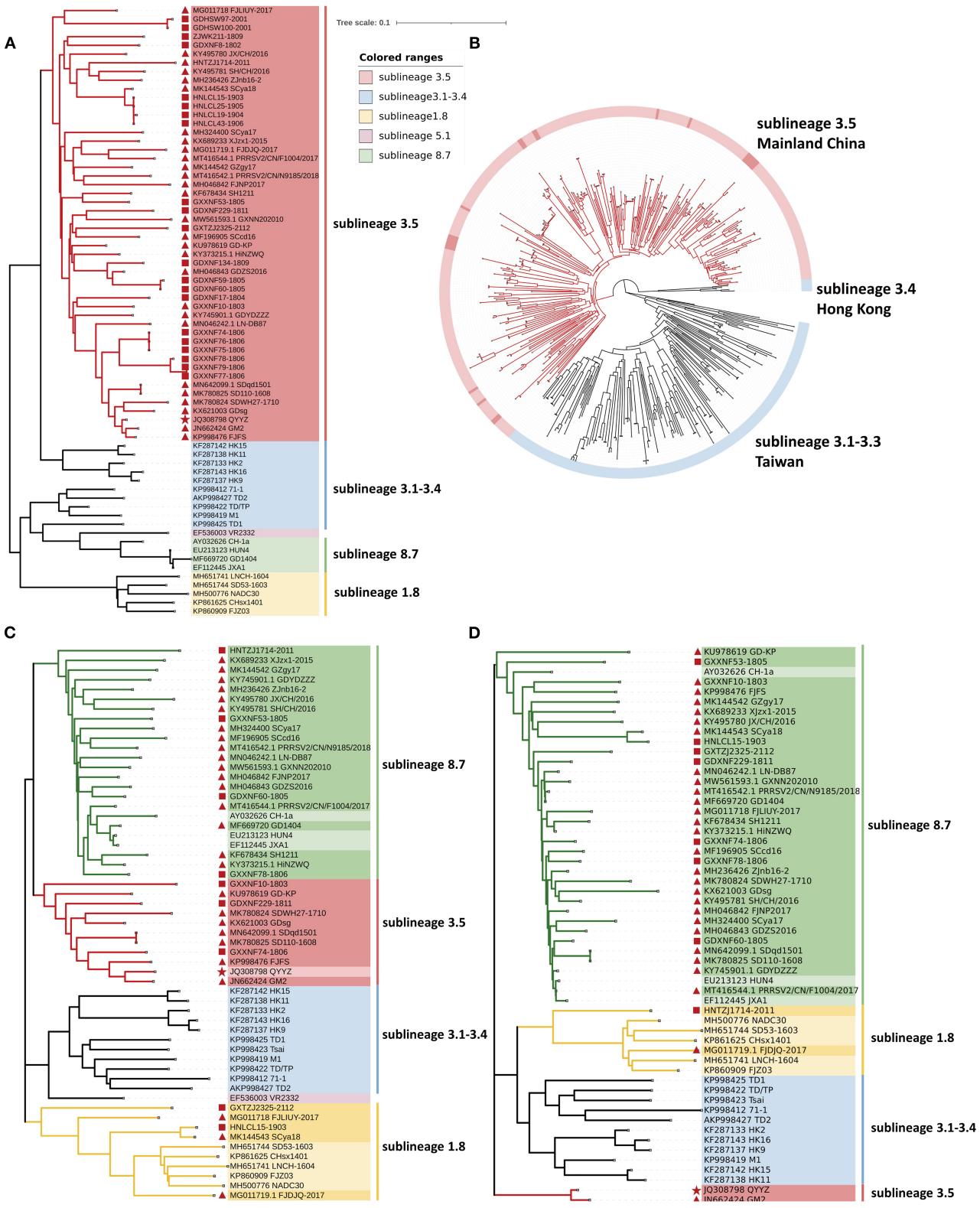

FIGURE 2 | Phylogenetic analysis of QYYZ-like PRRSVs. **(A)** Phylogenetic tree constructed based on the ORF5 gene of novel QYYZ-like PRRSV isolates and reference PRRSV strains from each lineage. **(B)** Phylogenetic tree reconstructed based on the global data set ($n = 470$) of the lineage 3 PRRSV ORF5 genome. **(C)** Phylogenetic tree constructed based on full-length genomes of 37 QYYZ-like PRRSV isolates and reference PRRSV strains from each lineage. **(D)** Phylogenetic tree

(Continued)

FIGURE 2 | constructed based on the Nsp1 gene of 37 QYYZ-like PRRSV isolates and reference PRRSV strains from each lineage. The QYYZ-like prototype strain QYYZ is labeled with a red star (★). Newly obtained sequences in this study are labeled with red squares (■). The QYYZ-like strains with complete genome sequences obtained from GenBank are labeled with red triangles (▲).

TABLE 3 | Information on the whole genomes of all reported QYYZ-like PRRSV strains in China.

Taxa	Isolation date	Recombination with	QYYZ-like regions	Accession no.	References
GXXNF10-1803	2018.03	JXA1	Nsp2-Nsp8, ORF2-7	ON462046	This study
GXXNF53-1805	2018.05	JXA1	ORF2-ORF7	ON462047	This study
GDXNF60-1805	2018.05	JXA1	ORF2-ORF7	ON462048	This study
GXXNF74-1806	2018.06	JXA1	Nsp2-Nsp7, NSP9-ORF7	ON462049	This study
GXXNF78-1806	2018.06	JXA1	ORF2-ORF3, ORF5-ORF7	ON462050	This study
GDXNF229-1811	2018.11	JXA1	Nsp2-Nsp5, Nsp9-ORF7	ON462051	This study
HNLCL15-1903	2019.03	SH/CH/2016+NADC30	Nsp10-ORF6	ON462043	This study
HNTZJ1714-2011	2020.11	JXA1+NADC30	ORF2-ORF7	ON462044	This study
GXTZJ2325-2112	2021.12	JXA1+NADC30	Nsp4-ORF7	ON462045	This study
QYYZ	2010	-	-	JQ308798	(12)
QY2010	2010	-	-	JQ743666	(23)
GM2	2011	VR2332	Nsp1-Nsp8, Nsp11-ORF7	JN662424	(12)
SH1211	2012	JXA1	Nsp12-ORF2, ORF5-ORF6	KF678434	(24)
FJFS	2012	JXA1	Nsp2-ORF7	KP998476	(19)
GD1404	2014	JXA1	ORF4-ORF7	KT961415	(25)
HiNZWQ	2014	JXA1	ORF3-ORF6	KY373215	Not found
XJzx1-2015	2015	CH-1a	ORF5-ORF7	KR080330	(26)
GDsg	2015	JXA1	Nsp2-Nsp9, NSP10-ORF7	KX621003	(27)
SDqd1501	2015	JXA1	Nsp2-Nsp8, Nsp11-ORF7	MN642099	(28)
GD-KP	2015	JXA1+VR2332	Nsp2-Nsp3, Nsp5-NSP7, NSP11-ORF7	KU978619	(19)
SCcd16	2016	NADC30+JXA1	ORF5-ORF7	MF196905	(14)
GDZS2016	2016	JXA1	ORF2-ORF6	MH046843	(13)
ZJnb16-2	2016	JXA1	ORF2-ORF7	MH174986	(15)
SH/CH/2016	2016	JXA1	NSP12-ORF7	KY495781	(29)
JX/CH/2016	2016	JXA1	NSP12-ORF7	KY495780	(30)
SD110-1608	2016	JXA1	Nsp2-Nsp9, Nsp11-ORF7	MK780825	(19)
GDYDZZZ	2016	JXA1	NSP12-ORF7	KY745901	Not found
GZgy17	2017	JXA1	ORF2-ORF6	MK144542	(29)
FJNP2017	2017	JXA1	ORF2-ORF7	MH046842	(13)
SCya17	2017	JXA1+NADC30	ORF3-ORF5	MH324400	(14)
FJLIUY-2017	2017	NADC30+BJ4+JXA1	ORF5-ORF7	MG011718	(16)
SDWH27-1710	2017	JXA1	Nsp2-ORF7	MK780824	(19)
FJDJQ-2017	2017	NADC30	ORF2-ORF7	MG011719	Not found
LN-DB87	2017	JXA1	ORF2-ORF7	MN046242	(31)
PRRSV2/CN/F1004/2017	2017	JXA1	ORF4-ORF7	MT416544	(32)
SCya18	2018	SH/CH/2016 +NADC30	NSP11-ORF6	MK144543	(29)
PRRSV2/CN/N9185/2018	2018	NADC30+JXA1	ORF4-ORF7	MT416542	(32)
GXNN202010	2020	JXA1	ORF2-ORF7	MW561593	Not found

Since the homology of QY2010 and QYYZ was up to 100% and the collection time of the two strains was very close, we regarded them as one strain and expressed them as QYYZ in the paper.

important target gene for analyzing the genetic variation and molecular epidemiology of PRRSV (34). Partial Nsp2 sequence alignment showed that 37 Nsp2 sequences (from complete genome sequences of sublineage 3.5 PRRSVs) were divided into 5 large patterns (**Figure 3A**). Compared to Nsp2 of VR2332, the Nsp2 proteins of pattern A strains had a deletion pattern that was identical to that of JXA1 (1 aa +29 aa). Pattern B strains not only have the same 30-amino acid (aa) deletion in Nsp2 as JXA1 (1 aa +29 aa) but also have a 36-aa insertion at position 817-852, which was the same as QYYZ (**Figure 3A**). Pattern C strains also have the same 36-aa insertion in Nsp2 as QYYZ (**Figure 3A**). Additionally, Pattern

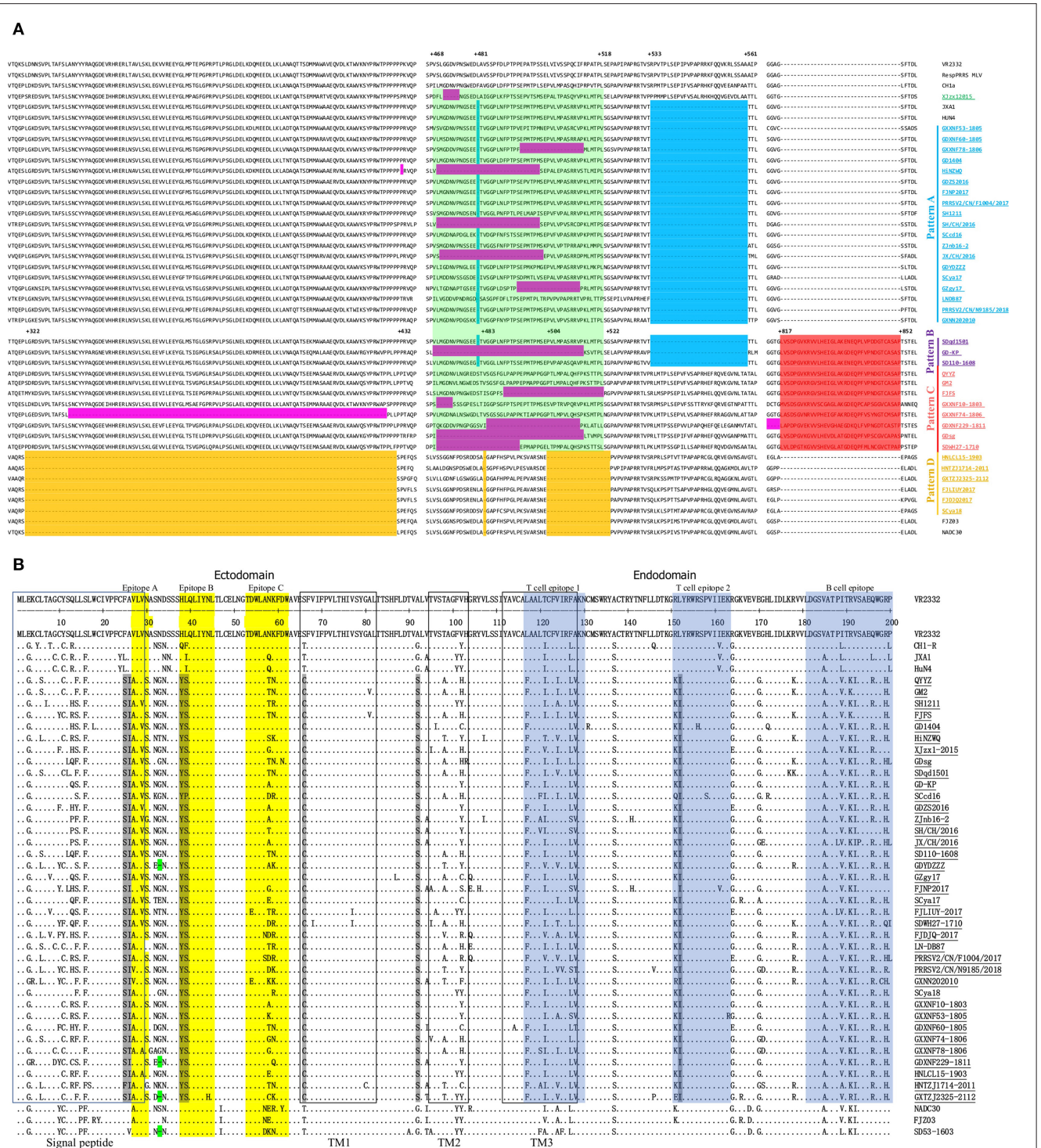

FIGURE 3 | Alignment of the deduced amino acid sequences among QYYZ-like PRRSVs. **(A)** The positions marked in the figure represent positions of the Nsp2 amino acid sequence and refer to the position of VR-2332. Red indicates the QYYZ strain 36-aa characteristic continuous insertion; yellow indicates the NADC30-like PRRSV 131-aa characteristic discontinuous deletion; blue indicates the HP-PRRSV 30-aa characteristic discontinuous deletion; and purple indicates some additional a deletions in QYYZ-like PRRSVs. **(B)** Alignment of the deduced amino acid sequence based on the ORF5 gene. The signal peptide and transmembrane (TM) regions are shown in blue and black boxes, respectively. The linear antigenic epitopes and cellular epitopes are indicated in yellow and blue, respectively. The seven amino acids characteristic of QYYZ-like strains are shown in gray.

D strains contained the discontinuous 131-aa deletion in Nsp2 identical to that in NADC30 (111 + 1 + 19 aa) (**Figure 3A**). In addition, 13 of the 37 Chinese lineage 3 PRRSV strains (XJzx12015, HiNZWQ, GXXNF78-1806, SH/CH/2016, GZgy17, JX/CH/2016, GD-KP, FJFS, GXXNF10-1803, GXXNF74-1806, GDXNF229-1811, GDsg, and SDWH27-1710) also have special amino acid deletions in the Nsp2 region, and they all have different deletion patterns (**Figure 3A**). Interestingly, 12 out of 13 strains with special amino acid deletions showed an amino acid deletion at positions 468-518 (**Figure 3A**). QYYZ-like PRRSV strains appeared to have more amino acid insertions or deletions in the Nsp2 region than other PRRSV strains. They seem to be more prone to amino acid deficiencies at position 468-518 of Nsp2. The Nsp2 hypervariable region (323-521) not only plays an important regulatory role in maintaining the balance of different viral mRNA species but also regulates PRRSV tropism to primary porcine alveolar macrophages (PAMs) (35). Therefore, these amino acid deletions in the Nsp2 region may alter the cellular tropism of the strains.

GP5 is the major envelope protein of PRRSV and is responsible for the lack of immunological cross-protection among different PRRSV strains due to its hypervariability (36–38). Comparison analyses of the amino acid sequence of QYYZ-like GP5 with those of the other representative strains showed that most strains encode 201 aa, but GDXNF229-1811, GDYDZZZ, and GXTZJ2325-2112 have a 1-aa deletion at residue 33 in VR2332, which is identical to the mutation in SD53-1603 (**Figure 3B**). Seven unique amino acid substitutions, namely, $F^{25}\rightarrow S^{25}$, $A^{26}\rightarrow I^{26}$, $H^{38}\rightarrow Y^{38}$, $L^{39}\rightarrow S^{39}$, $T^{66}\rightarrow C^{66}$, $A^{92}\rightarrow S^{92}$, and $L^{152}\rightarrow I^{152}$, compared with the VR2332 strain. These amino acid mutations were identified only in all QYYZ-like strains but no other representative PRRSV strains (**Figure 3B**). Interestingly, although the QYYZ-like strains have low homology among them, they still showed consistent molecular features, which may be used as molecular markers to distinguish QYYZ-like strains from other type 2 PRRSV strains in China. GP5 is an envelope protein essential for viral infection, and at least three B-cell and two T-cell epitopes were identified for GP5 (39, 40). Two characteristic mutations of QYYZ-like strains, at positions 38(Y^{38}) and 39(S^{39}), are in epitope B (37-45 aa), which is a highly conserved peptide sequence that presumably functions as a major target for broadly neutralizing antibodies (37, 41). At the same time, there was one amino acid substitution in T-cell epitope 2 (I^{152}), compared to PRRSV strains in other lineages (42). We then analyzed the functional domains in GP5 of QYYZ-like strains, including the signal peptide and transmembrane (TM) domain (43). Two residues (S^{25} and I^{26}) resided within the signal peptide (aa 1-31). Moreover, there was a unique amino acid mutation at position 66 in the TM region of the QYYZ-like strains, substituting T^{66} to C^{66}. Briefly, we found 7 unique amino acid mutations in the GP5 protein, and some mutation sites were located in cell epitopes, the signal peptide and the TM region. These amino acid substitutions might lead to the failure of receptor recognition and thus result in the failure of vaccines.

Recombination is a pervasive phenomenon among PRRSV isolates, and there are an increasing number of reports about the recombination of QYYZ-like PRRSVs (14, 16, 44). In recent years, many recombinant QYYZ-like PRRSVs have reportedly reemerged with increased pathogenicity (12, 18, 34, 45, 46). To identify possible recombination events of the new QYYZ-like PRRSVs in China, RDP4 and SimPlot software were used to assess possible recombinant events (**Table 4** and **Supplementary Figure 1**). This analysis demonstrated that all nine new QYYZ-like isolates were recombinant viruses. Six recombinant isolates (GXXNF10-1803, GXXNF53-1805, GDXNF60-1805, GXXNF74-1806, GXXNF78-1806, and GDXNF229-1811) emerged from recombination events between HP-PRRSV isolates and QYYZ-like virus; three recombinant isolates (HNLCL15-1903, HNTZJ1714-2011, and GXTZJ2325-2112) were also derived from NADC30-like PRRSV, HP-PRRSV isolates, and QYYZ-like PRRSV (**Table 4** and **Supplementary Figure 1**). These putative recombination events were further supported by statistically incongruent phylogenetic trees (**Supplementary Figure 1**). According to a similarity plot, these nine strains have an extremely complex recombination pattern (**Supplementary Figure 1**). Interestingly, the HNLCL15-1903 strain has almost the same recombination pattern as the previous strain SCya18 (MK144543.1) and high homology (BLAST analysis: 97.99%). SCya18 was isolated in Sichuan Province in 2018 (29), while HNLCL15-1903 was isolated in Henan Province in 2019. The two provinces are not adjacent, and under the background of low homology and complex recombination of QYYZ-like strains, the emergence of two strains with high similarity is noteworthy.

To better explore the recombination characteristics of QYYZ-like strains in China (**Table 3**), we summarized the reported genome-wide recombination of all QYYZ-like strains (ORF5 classified into sublineage 3.5). Interestingly, all 37 QYYZ-like PRRSV strains except for QYYZ (the QYYZ-like original strain) have undergone recombination (**Table 3** and **Supplementary Figure 2B**). The distribution of recombination breakpoints is dispersed and complex, there is no obvious recombination hotspot, and there are relatively many recombination breakpoints located in Nsp12(7), Nsp2(13) and GP2(13) (**Supplementary Figure 2B**). In a previous study in China, it was found that between 2014 and 2018, the high-frequency interlineage (mainly lineage 1 and lineage 8) recombination regions were located in Nsp9 and GP2 to GP3 (20, 31). Obviously, the recombination hot spots of QYYZ-like strains (sublineage 3.5) are not exactly the same as those of lineage 1 and lineage 8 strains. At the same time, it can be clearly seen that QYYZ-like strains mainly provide fragments of structural protein regions (GP2-N) for recombinant strains (**Supplementary Figure 2A**), while in the Nsp1 region of the sequence, only GM2 is provided by the QYYZ strain (**Table 3**). We used the Nsp1 region of QYYZ-like strains to construct a phylogenetic tree for verification (**Figure 2D**). The majority (33/37) of the QYYZ-like strains were grouped into sublineage 8.7 (JXA1-like), and FJLIUY-2017 and HNTZJ1714-2011 were grouped into sublineage 1.8 (NADC30-like). Only GM2 and QYYZ were classified as sublineage 3.5 (QYYZ-like). To obtain better information about the QYYZ-like strains, we suggest that researchers add a pair of primers to sequence the Nsp1

TABLE 4 | Information on recombination events of QYYZ-like PRRSV isolates detected by RDP4 software.

Strains	Breakpoints		Parental sequence		Detection methods (*p*-value)						
	Beginning	Ending	Minor	Major	RDP	GENECONV	BootScan	MaxChi	Chimera	SiScan	3Seq
GXXNF10-1803	1	3,507	JXA1	QYYZ	2.448×10^{-36}	-	1.505×10^{-27}	1.677×10^{-28}	1.081×10^{-23}	9.166×10^{-82}	4.440×10^{-16}
	7,781	12,294	JXA1	QYYZ	2.352×10^{-20}	4.191×10^{-10}	1.829×10^{-19}	8.522×10^{-11}	6.504×10^{-5}	-	4.440×10^{-16}
HNLCL15-1903	1	1,659	SH/CH/2016	NADC30	5.474×10^{-47}	1.583×10^{-16}	6.869×10^{-38}	1.302×10^{-37}	1.196×10^{-17}	-	1.110×10^{-16}
	10,531	14,132	SH/CH/2016	NADC30	4.798×10^{-13}	4.699×10^{-8}	3.515×10^{-13}	2.702×10^{-10}	9.689×10^{-3}	-	1.221×10^{-15}
GXXNF53-1805	12,685	15,314	QYYZ	JXA1	4.068×10^{-37}	-	4.114×10^{-34}	1.467×10^{-13}	3.866×10^{-12}	-	3.330×10^{-15}
GDXNF60-1805	12,541	15,316	QYYZ	JXA1	1.153×10^{-26}	1.115×10^{-14}	5.567×10^{-26}	9.478×10^{-09}	1.709×10^{-09}	-	4.440×10^{-16}
GXXNF74-1806	1	2,339	JXA1	QYYZ	3.589×10^{-85}	5.042×10^{-53}	2.133×10^{-82}	1.171×10^{-31}	7.599×10^{-35}	-	4.440×10^{-16}
	6,924	8,969	JXA1	QYYZ	1.197×10^{-73}	7.929×10^{-30}	3.125×10^{-73}	3.349×10^{-23}	3.736×10^{-25}	-	1.110×10^{-16}
GXXNF78-1806	11,987	12,851	QYYZ	JXA1	2.804×10^{-68}	1.001×10^{-35}	1.478×10^{-67}	2.161×10^{-19}	1.175×10^{-21}	-	4.440×10^{-16}
	13,673	15,266	QYYZ	JXA1	4.474×10^{-83}	6.225×10^{-53}	1.542×10^{-80}	1.379×10^{-28}	6.139×10^{-30}	-	1.099×10^{-14}
GDXNF229-1811	1	2,285	JXA1	QYYZ	5.898×10^{-65}	1.549×10^{-52}	3.919×10^{-70}	8.204×10^{-25}	7.417×10^{-21}	-	3.330×10^{-16}
	6,317	8,812	JXA1	QYYZ	6.152×10^{-86}	2.128×10^{-72}	1.950×10^{-86}	8.256×10^{-27}	2.368×10^{-21}	-	3.330×10^{-16}
HNTZJ1714-2011	488	3,548	NADC30	JXA1	8.808×10^{-125}	2.849×10^{-88}	7.364×10^{-54}	2.100×10^{-50}	8.792×10^{-58}	1.554×10^{-50}	4.440×10^{-15}
	11,668	15,011	QYYZ	JXA1	1.119×10^{-3}	4.470×10^{-19}	1.405×10^{-12}	4.438×10^{-8}	9.950×10^{-6}	8.177×10^{-40}	-
GXTZJ2325-2112	1	2,004	JXA1	QYYZ	1.870×10^{-12}	-	1.777×10^{-13}	1.089×10^{-9}	1.218×10^{-14}	2.968×10^{-11}	
	2,004	5,268	NADC30	QYYZ	2.595×10^{-95}	1.055×10^{-67}	3.404×10^{-92}	7.725×10^{-30}	8.322×10^{-38}	1.696×10^{-51}	1.332×10^{-15}

region of the virus when it is identified as a QYYZ-like strain by ORF5 sequencing.

Now, an overwhelming majority of the PRRSV-2 strains in China can be classified into JXA1-like/CH-1a-like (sublineage 8.7), VR2332-like (sublineage 5.1), NADC30-like/NADC34-like (lineage 1), and QYYZ-like (sublineage 3.5). The CH-1a-like strains first appeared in China and then gradually evolved into JXA1-like (HP-PRRSV) strains (45). The JXA1-like strains are also widespread in Cambodia, Thailand, Vietnam and many other Asian countries (6, 47–49). VR2332-like strains containing the Ingelvac PRRS MLV vaccine sequence are the most widespread, with viruses introduced to more than 10 countries (5). Lineage 1 (NADC30-like and NADC34-like) strains are also globally epidemic and have spread to South America, North America and Asia (7, 33, 50–52). The lineage 3 strains originated in Taiwan. Interestingly, after 20 years of transmission and evolution, these strains are prevalent only in greater China (mainland China, Taiwan, and Hong Kong) (18). Moreover, the QYYZ-like strains (sublineage 3.5) were prevalent only in mainland China. According to the results of this study and previous studies, QYYZ-like strains have been occasionally reported in northern China (19, 26, 28, 53) but are mainly prevalent in southern and central China (12–16, 23–25, 27, 29, 30, 32). Although recombination of PRRSV is very common, many non-recombination strains of JXA1-like (54), VR2332-like (28) and NADC30-like/NADC34-like PRRSV (7, 55) have been reported after long-term evolution in China. All QYYZ-like strains were recombined with other lineages of PRRSV except the prototype strain QYYZ. Thus, we speculated that the non-recombination QYYZ-like strains are no longer circulating and that they played a role as a provider of recombination fragments in the PRRSV epidemic in China.

CONCLUSION

In summary, QYYZ-like PRRSV strains did not have a large-scale epidemic status but persisted in central and southern China during 2018–2021. QYYZ-like strains have low homology and extremely complex amino acid insertion and deletion patterns in the Nsp2 region. However, they have seven identical amino acid mutations in the GP5 protein. These strains all underwent complex recombination except the prototype strain QYYZ and mainly provided structural protein fragments (GP2-N) for the recombinant strains. These results will help us to understand the overall genomic characteristics of QYYZ-like PRRSV, which is useful for the prevention and control of this virus.

DATA AVAILABILITY STATEMENT

The original contributions presented in the study are included in the article/**Supplementary Material**, further inquiries can be directed to the corresponding author/s.

ETHICS STATEMENT

The animal study was reviewed and approved by Sampling procedures were performed in accordance with the guidelines of the Animal Ethics Committee of the School of Harbin Veterinary Research Institute of the Chinese Academy of Agricultural Sciences. The Animal Ethics Committee Approval Number was SYXK(Hei) 2011022.

AUTHOR CONTRIBUTIONS

Conceived and designed the experiments: MS, Y-DT, HZ, and Z-JT. Performed the experiments: HX and LX. Contributed reagents or materials and assisted in some experiments: CLi, JZ, BG, QS, JP, QW, GZ, TA, and XC. Analyzed the data: LX, CLe, and Z-JT. Contributed to the writing of the manuscript: HX, LX, and HZ. All authors contributed to the article and approved the submitted version.

FUNDING

This study was supported by the National Parasitic Resources Center (NPRC-2019-194-30), the National Natural Science Foundation of China (Grant no. 32172890 and 32002315), and the China Postdoctoral Fund (Grant no. 2020M680788).

SUPPLEMENTARY MATERIAL

The Supplementary Material for this article can be found online at: https://www.frontiersin.org/articles/10.3389/fvets.2022.945381/full#supplementary-material

Supplementary Figure 1 | Recombination analysis of GXXNF10-1803, GXXNF53-1805, GDXNF60-1805, GXXNF74-1806, GXXNF78-1806, GDXNF229-1811, HNLCL15-1903, HNTZJ1714-2011, and GXTZJ2325-2112. Phylogenic trees were constructed based on different parent regions. Blue represents HP-PRRSV, yellow represents NADC30-like PRRSV, and red represents QYYZ-like PRRSV.

Supplementary Figure 2 | Summary of recombination breakpoints of all reported QYYZ strains in China. **(A)** The number of recombinant fragments provided by QYYZ in each region of 37 recombinant strains. The ORF5 of all 37 recombinant strains was provided by the QYYZ strain, while the Nsp1 region was provided by the QYYZ strain in only two strains. **(B)** Recombination breakpoints identified across the full-length genome. The putative recombinants are listed in the key, with the red triangles matching each corresponding breakpoint. Most breakpoints were localized in Nsp2 and GP2, and the backgrounds of the two regions are highlighted in green.

REFERENCES

1. Nathues H, Alarcon P, Rushton J, Jolie R, Fiebig K, Jimenez M, et al. Cost of porcine reproductive and respiratory syndrome virus at individual farm level - An economic disease model. *Prev Vet Med.* (2017) 142:16–29. doi: 10.1016/j.prevetmed.2017.04.006
2. Adams MJ, Lefkowitz EJ, King AMQ, Harrach B, Harrison RL, Knowles NJ, et al. Changes to taxonomy and the international code of virus classification and nomenclature ratified by the international committee on taxonomy of viruses. *Arch Virol.* (2017) 162:2505–38. doi: 10.1007/s00705-017-3358-5
3. Kuhn JH, Lauck M, Bailey AL, Shchetinin AM, Vishnevskaya TV, Bao Y, et al. Reorganization and expansion of the nidoviral family Arteriviridae. *Arch Virol.* (2016) 161:755–68. doi: 10.1007/s00705-015-2672-z
4. An TQ, Zhou YJ, Liu GQ, Tian ZJ, Li J, Qiu HJ, et al. Genetic diversity and phylogenetic analysis of glycoprotein 5 of PRRSV isolates in mainland China from 1996 to 2006: coexistence of two NA-subgenotypes with great diversity. *Vet Microbiol.* (2007) 123:43–52. doi: 10.1016/j.vetmic.2007.02.025
5. Shi M, Lam TT, Hon CC, Hui RK, Faaberg KS, Wennblom T, et al. Molecular epidemiology of PRRSV: a phylogenetic perspective. *Virus Res.* (2010) 154:7–17. doi: 10.1016/j.virusres.2010.08.014
6. Shi M, Lam TT, Hon CC, Murtaugh MP, Davies PR, Hui RK, et al. Phylogeny-based evolutionary, demographical, and geographical dissection of North American type 2 porcine reproductive and respiratory syndrome viruses. *J Virol.* (2010) 84:8700–11. doi: 10.1128/JVI.02551-09
7. Xu H, Li C, Li W, Zhao J, Gong B, Sun Q, et al. Novel characteristics of Chinese NADC34-like PRRSV during 2020-2021. *Transbound Emerg Dis.* (2022). doi: 10.1111/tbed.14485. [Epub ahead of print].
8. Leng CL, Tian ZJ, Zhang WC, Zhang HL, Zhai HY, An TQ, et al. Characterization of two newly emerged isolates of porcine reproductive and respiratory syndrome virus from Northeast China in 2013. *Vet Microbiol.* (2014) 171:41–52. doi: 10.1016/j.vetmic.2014.03.005
9. An TQ, Tian ZJ, Xiao Y, Li R, Peng JM, Wei TC, et al. Origin of highly pathogenic porcine reproductive and respiratory syndrome virus, China. *Emerg Infect Dis.* (2010) 16:365–7. doi: 10.3201/eid1602.090005
10. Guo Z, Chen XX, Li X, Qiao S, Deng R, Zhang G. Prevalence and genetic characteristics of porcine reproductive and respiratory syndrome virus in central China during 2016-2017: NADC30-like PRRSVs are predominant. *Microb Pathog.* (2019) 135:103657. doi: 10.1016/j.micpath.2019.103657
11. Zhang HL, Zhang WL, Xiang LR, Leng CL, Tian ZJ, Tang YD, et al. Emergence of novel porcine reproductive and respiratory syndrome viruses (ORF5 RFLP 1-7-4 viruses) in China. *Vet Microbiol.* (2018) 222:105–8. doi: 10.1016/j.vetmic.2018.06.017
12. Lu WH, Tun HM, Sun BL, Mo J, Zhou QF, Deng YX, et al. Re-emerging of porcine respiratory and reproductive syndrome virus (lineage 3) and increased pathogenicity after genomic recombination with vaccine variant. *Vet Microbiol.* (2015) 175:332–40. doi: 10.1016/j.vetmic.2014.11.016
13. Sun YK, Li Q, Yu ZQ, Han XL, Wei YF, Ji CH, et al. Emergence of novel recombination lineage 3 of porcine reproductive and respiratory syndrome viruses in Southern China. *Transbound Emerg Dis.* (2019) 66:578–87. doi: 10.1111/tbed.13067
14. Zhou L, Kang R, Zhang Y, Ding M, Xie B, Tian Y, et al. Whole genome analysis of two novel Type 2 porcine reproductive and respiratory syndrome viruses with complex genome recombination between lineage 8, 3, and 1 strains identified in Southwestern China. *Viruses.* (2018) 10:60328. doi: 10.3390/v10060328
15. Han G, Xu H, Wang K, He F. Emergence of Two different recombinant PRRSV strains with low neutralizing antibody susceptibility in China. *Sci Rep.* (2019) 9:2490. doi: 10.1038/s41598-019-39059-8
16. Liu J, Wei C, Lin Z, Fan J, Xia W, Dai A, et al. Recombination in lineage 1, 3, 5 and 8 of porcine reproductive and respiratory syndrome viruses in China. *Infect Genet Evol.* (2019) 68:119–26. doi: 10.1016/j.meegid.2018.12.006
17. Zhao J, Xu L, Xu Z, Deng H, Li F, Sun X, et al. Emergence and spread of NADC34-like PRRSV in Southwest China. *Transbound Emerg Dis.* (2022) 69:254–67. doi: 10.1111/tbed.14463
18. Sun YK, Han XL, Wei YF, Yu ZQ, Ji CH, Li Q, et al. Phylogeography, phylodynamics and the recent outbreak of lineage 3 porcine reproductive and respiratory syndrome viruses in China. *Transbound Emerg Dis.* (2019) 66:2152–62. doi: 10.1111/tbed.13269
19. Zhang WL, Zhang HL, Xu H, Tang YD, Leng CL, Peng JM, et al. Two novel recombinant porcine reproductive and respiratory syndrome viruses belong to sublineage 3.5 originating from sublineage 3.2. *Transbound Emerg Dis.* (2019) 66:2592–600. doi: 10.1111/tbed.13320

20. Zhang H, Leng C, Ding Y, Zhai H, Li Z, Xiang L, et al. Characterization of newly emerged NADC30-like strains of porcine reproductive and respiratory syndrome virus in China. *Arch Virol.* (2019) 164:401–11. doi: 10.1007/s00705-018-4080-7
21. Kumar S, Stecher G, Tamura K. MEGA7: molecular evolutionary genetics analysis version 7.0 for bigger datasets. *Mol Biol Evol.* (2016) 33:1870–4. doi: 10.1093/molbev/msw054
22. Letunic I, Bork P. Interactive tree of life (iTOL) v5: an online tool for phylogenetic tree display and annotation. *Nucleic Acids Res.* (2021) 49:W293–6. doi: 10.1093/nar/gkab301
23. Deng Y, Pan Y, Wang D, Zhou Q, Bi Y, Chen F, et al. Complete genome sequence of porcine reproductive and respiratory syndrome virus strain QY2010 reveals a novel subgroup emerging in China. *J Virol.* (2012) 86:7719–20. doi: 10.1128/JVI.00977-12
24. Fan B, Wang H, Bai J, Zhang L, Jiang P. A novel isolate with deletion in GP3 gene of porcine reproductive and respiratory syndrome virus from mid-eastern China. *Biomed Res Int.* (2014) 2014:306130. doi: 10.1155/2014/306130
25. Zhang Q, Bai J, Hou H, Song Z, Zhao Y, Jiang P. A novel recombinant porcine reproductive and respiratory syndrome virus with significant variation in cell adaption and pathogenicity. *Vet Microbiol.* (2017) 208:150–8. doi: 10.1016/j.vetmic.2017.07.028
26. Zhang X, Li Y, Xiao S, Yang X, Chen X, Wu P, et al. High-frequency mutation and recombination are responsible for the emergence of novel porcine reproductive and respiratory syndrome virus in northwest China. *Arch Virol.* (2019) 164:2725–33. doi: 10.1007/s00705-019-04373-z
27. Dong JG, Yu LY, Wang PP, Zhang LY, Liu YL, Liang PS, et al. A new recombined porcine reproductive and respiratory syndrome virus virulent strain in China. *J Vet Sci.* (2018) 19:89–98. doi: 10.4142/jvs.2018.19.1.89
28. Zhang Z, Qu X, Zhang H, Tang X, Bian T, Sun Y, et al. Evolutionary and recombination analysis of porcine reproductive and respiratory syndrome isolates in China. *Virus Genes.* (2020) 56:354–60. doi: 10.1007/s11262-020-01751-7
29. Zhou L, Kang R, Zhang Y, Yu J, Xie B, Chen C, et al. Emergence of two novel recombinant porcine reproductive and respiratory syndrome viruses 2 (lineage 3) in Southwestern China. *Vet Microbiol.* (2019) 232:30–41. doi: 10.1016/j.vetmic.2019.01.026
30. Zhang F, Song D, Ye Y, Guo N, Zhang M, Li H, et al. Complete genome sequence of a novel subgenotype of porcine reproductive and respiratory syndrome virus strain JX/CH/2016, isolated in Jiangxi, China. *Genome Announc.* (2017) 5:e00980-17. doi: 10.1128/genomeA.00980-17
31. Yu F, Yan Y, Shi M, Liu HZ, Zhang HL, Yang YB, et al. Phylogenetics, genomic recombination, and NSP2 Polymorphic patterns of porcine reproductive and respiratory syndrome virus in China and the United States in 2014-2018. *J Virol.* (2020) 94:19. doi: 10.1128/JVI.01813-19
32. Liu J, Xu Y, Lin Z, Fan J, Dai A, Deng X, et al. Epidemiology investigation of PRRSV discharged by faecal and genetic variation of ORF5. *Transbound Emerg Dis.* (2021) 68:2334–44. doi: 10.1111/tbed.13894
33. Kim SC, Moon SH, Jeong CG, Park GS, Park JY, Jeoung HY, et al. Whole-genome sequencing and genetic characteristics of representative porcine reproductive and respiratory syndrome virus (PRRSV) isolates in Korea. *Virol J.* (2022) 19:66. doi: 10.1186/s12985-022-01790-6
34. Han G, Lei K, Xu H, He F. Genetic characterization of a novel recombinant PRRSV2 from lineage 8, 1 and 3 in China with significant variation in replication efficiency and cytopathic effects. *Transbound Emerg Dis.* (2020) 67:1574–84. doi: 10.1111/tbed.13491
35. Song J, Gao P, Kong C, Zhou L, Ge X, Guo X, et al. The nsp2 hypervariable region of porcine reproductive and respiratory syndrome virus strain JXwn06 is associated with viral cellular tropism to primary porcine alveolar macrophages. *J Virol.* (2019) 93:e01436-19. doi: 10.1128/JVI.01436-19
36. Veit M, Matczuk AK, Sinhadri BC, Krause E, Thaa B. Membrane proteins of arterivirus particles: structure, topology, processing and function. *Virus Res.* (2014) 194:16–36. doi: 10.1016/j.virusres.2014.09.010
37. Popescu LN, Trible BR, Chen N, Rowland RRR. GP5 of porcine reproductive and respiratory syndrome virus (PRRSV) as a target for homologous and broadly neutralizing antibodies. *Vet Microbiol.* (2017) 209:90–96. doi: 10.1016/j.vetmic.2017.04.016
38. Sui X, Guo X, Jia H, Wang X, Lin W, Li M, et al. Genomic sequence and virulence of a novel NADC30-like porcine reproductive and respiratory syndrome virus isolate from the Hebei province of China. *Microb Pathog.* (2018) 125:349–60. doi: 10.1016/j.micpath.2018.08.048
39. de Lima M, Pattnaik AK, Flores EF, Osorio FA. Serologic marker candidates identified among B-cell linear epitopes of Nsp2 and structural proteins of a North American strain of porcine reproductive and respiratory syndrome virus. *Virology.* (2006) 353:410–21. doi: 10.1016/j.virol.2006.05.036
40. Vashisht K, Goldberg TL, Husmann RJ, Schnitzlein W, Zuckermann FA. Identification of immunodominant T-cell epitopes present in glycoprotein 5 of the North American genotype of porcine reproductive and respiratory syndrome virus. *Vaccine.* (2008) 26:4747–53. doi: 10.1016/j.vaccine.2008.06.047
41. Ostrowski M, Galeota JA, Jar AM, Platt KB, Osorio FA, Lopez OJ. Identification of neutralizing and nonneutralizing epitopes in the porcine reproductive and respiratory syndrome virus GP5 ectodomain. *J Virol.* (2002) 76:4241–50. doi: 10.1128/jvi.76.9.4241-4250.2002
42. Zhao K, Ye C, Chang XB, Jiang CG, Wang SJ, Cai XH, et al. Importation and recombination are responsible for the latest emergence of highly pathogenic porcine reproductive and respiratory syndrome virus in China. *J Virol.* (2015) 89:10712–6. doi: 10.1128/JVI.01446-15
43. Zhu Z, Yuan L, Hu D, Lian Z, Yao X, Liu P, et al. Isolation and genomic characterization of a Chinese NADC34-like PRRSV isolated from Jiangsu province. *Transbound Emerg Dis.* (2021) 69:254–267. doi: 10.1111/tbed.14392
44. Kappes MA, Faaberg KS. PRRSV structure, replication and recombination: Origin of phenotype and genotype diversity. *Virology.* (2015) 479–480:475–86. doi: 10.1016/j.virol.2015.02.012
45. Guo Z, Chen XX, Li R, Qiao S, Zhang G. The prevalent status and genetic diversity of porcine reproductive and respiratory syndrome virus in China: a molecular epidemiological perspective. *Virol J.* (2018) 15:2. doi: 10.1186/s12985-017-0910-6
46. Hou FH, Lee WC, Liao JW, Chien MS, Kuo CJ, Chung HP, et al. Evaluation of a type 2 modified live porcine reproductive and respiratory syndrome vaccine against heterologous challenge of a lineage 3 highly virulent isolate in pigs. *PeerJ.* (2020) 8:e8840. doi: 10.7717/peerj.8840
47. Lager KM, Schlink SN, Brockmeier SL, Miller LC, Henningson JN, Kappes MA, et al. Efficacy of Type 2 PRRSV vaccine against Chinese and Vietnamese HP-PRRSV challenge in pigs. *Vaccine.* (2014) 32:6457–62. doi: 10.1016/j.vaccine.2014.09.046
48. Jantafong T, Sangtong P, Saenglub W, Mungkundar C, Romlamduan N, Lekchareonsuk C, et al. Genetic diversity of porcine reproductive and respiratory syndrome virus in Thailand and Southeast Asia from 2008 to 2013. *Vet Microbiol.* (2015) 176:229–38. doi: 10.1016/j.vetmic.2015.01.017
49. Fukunaga W, Hayakawa-Sugaya Y, Koike F, Van Diep N, Kojima I, Yoshida Y, et al. Newly-designed primer pairs for the detection of type 2 porcine reproductive and respiratory syndrome virus genes. *J Virol Methods.* (2021) 291:114071. doi: 10.1016/j.jviromet.2021.114071
50. Ramirez M, Bauermann FV, Navarro D, Rojas M, Manchego A, Nelson EA, et al. Detection of porcine reproductive and respiratory syndrome virus (PRRSV) 1-7-4-type strains in Peru. *Transbound Emerg Dis.* (2019) 66:1107–13. doi: 10.1111/tbed.13134
51. Kim SC, Jeong CG, Park GS, Park JY, Jeoung HY, Shin GE, et al. Temporal lineage dynamics of the ORF5 gene of porcine reproductive and respiratory syndrome virus in Korea in 2014-2019. *Arch Virol.* (2021) 166:2803–15. doi: 10.1007/s00705-021-05169-w
52. Paploski IAD, Pamornchainavakul N, Makau DN, Rovira A, Corzo CA, Schroeder DC, et al. Phylogenetic structure and sequential dominance of sub-lineages of PRRSV type-2 lineage 1 in the United States. *Vaccines.* (2021) 9:9060608. doi: 10.3390/vaccines9060608
53. Sun YF, Liu Y, Yang J, Li WZ, Yu XX, Wang SY, et al. Recombination between NADC34-like and QYYZ-like strain of porcine reproductive and respiratory syndrome virus with high pathogenicity for piglets in China. *Transbound Emerg Dis*. (2022). doi: 10.1111/tbed.14471. [Epub ahead of print].
54. Ding Y, Wubshet AK, Ding X, Zhang Z, Li Q, Dai J, et al. Evaluation of four commercial vaccines for the protection of piglets against the highly pathogenic porcine reproductive and respiratory syndrome virus (hp-PRRSV) QH-08 strain. *Vaccines.* (2021) 9:1020. doi: 10.3390/vaccines9091020
55. Li L, Chen J, Cao Z, Cao Y, Guo Z, Tong W, et al. Recombinant bivalent live vectored vaccine against classical swine fever and HP-PRRS revealed adequate

heterogeneous protection against NADC30-like strain. *Front Microbiol.* (2021) 12:822749. doi: 10.3389/fmicb.2021.822749

Conflict of Interest: The authors declare that the research was conducted in the absence of any commercial or financial relationships that could be construed as a potential conflict of interest.

Publisher's Note: All claims expressed in this article are solely those of the authors and do not necessarily represent those of their affiliated organizations, or those of the publisher, the editors and the reviewers. Any product that may be evaluated in this article, or claim that may be made by its manufacturer, is not guaranteed or endorsed by the publisher.

frontiers | Frontiers in Veterinary Science

TYPE Brief Research Report
PUBLISHED 10 August 2022
DOI 10.3389/fvets.2022.932612

OPEN ACCESS

EDITED BY
Zhou Mo,
Heilongjiang University, China

REVIEWED BY
Fei Gao,
Shanghai Veterinary Research Institute (CAAS), China
Kayode Olayinka Afolabi,
Anchor University Lagos, Nigeria

*CORRESPONDENCE
Zhibang Deng
zbangd@hunau.edu.cn

SPECIALTY SECTION
This article was submitted to Veterinary Infectious Diseases, a section of the journal Frontiers in Veterinary Science

RECEIVED 30 April 2022
ACCEPTED 15 July 2022
PUBLISHED 10 August 2022

CITATION
Nan W, Wu J, Hu H, Peng G, Tan S and Deng Z (2022) Prevalence and genetic diversity of porcine circovirus type 2 in northern Guangdong Province during 2016–2021. *Front. Vet. Sci.* 9:932612. doi: 10.3389/fvets.2022.932612

Prevalence and genetic diversity of porcine circovirus type 2 in northern Guangdong Province during 2016–2021

Wenjin Nan[1,2], Jingbo Wu[2], Honghui Hu[2], Guoliang Peng[2], Simin Tan[1] and Zhibang Deng[1]*

[1]Lab of Animal Disease Prevention & Control and Animal Model, Hunan Provincial Key Laboratory of Protein Engineering in Animal Vaccines, College of Veterinary Medicine, Hunan Agricultural University (HUNAU), Changsha, China, [2]North Guangdong Collaborative Innovation and Development Center of Pig Farming and Disease Control, Shaoguan University, Shaoguan, China

The emergence and widespread of porcine circovirus-associated diseases (PCVADs), mainly caused by porcine circovirus type 2 (PCV2), threatens the Chinese swine industry. In this study, to investigate the recent prevalence of PCV2 in northern Guangdong Province of China, 573 tissue samples from 132 pig farms were collected during 2016–2021 and analyzed *via* PCR. Overall, 51.38% (297/573, 95%CI 47.74–55.92) samples were tested PCV2 positive. The detection rate of PCV2 was significantly lower in samples collected before 2016-2018 than after the outbreak of African Swine Fever (2019-2021), being 59.85% (158/264, 95%CI 53.94–65.76) and 41.47% (141/340, 95%CI 36.43–46.71), respectively. On the other end, the genetic characteristics of 26 PCV2 strains were further analyzed. These PCV2 strains belonged to three genotypes, including PCV2a, PCV2b, and PCV2d. Specifically, the predominant genotype prevalent during two periods (2016–2018 and 2019–2021) wasPCV2b (81.82%, 9/11) and PCV2d (80.0%, 12/15), respectively. The results above illustrated the high prevalence and the genetic evolution feature of PCV2 in Guangdong Province in recent years.

KEYWORDS

porcine circovirus type 2, epidemiology, complete genome, genetic characteristics, Guangdong Province

Introduction

Porcine circoviruses (PCVs) are small, circular, single-stranded DNA viruses belonging to the genus of *Circovirus* of the family *Circoviridae* (1). Currently, four genotypes of PCVs have been identified, termed porcine circovirus type 1 (PCV1), PCV2, PCV3, and PCV4 (2). Since the first identification of PCV2 in Canada in the 1990s, this pathogen has been considered the primary causative agent of porcine circovirus-associated diseases (PCVADs) (3, 4). PCVADs are mainly characterized by postweaning multisystemic wasting syndromes (PMWS), such as respiratory distress in piglets, slow growth in fattening pigs, reproductive failures in sows, etc., which threatens the development of pig industry worldwide (3, 4).

The PCV2 genome is 1,766–1,768 nucleotide (nt) in length, which mainly comprises two open reading frames (ORFs). The ORF1 encodes the replication-related proteins (Rep and Rep'), while the ORF2 encodes the capsid protein (Cap), which induces the neutralization antibodies production and viral entry (3, 5). According to the genomic characteristics of PCV2 strains, they are divided into eight subtypes (PCV2a-PCV2h) (6). PCV2 strains prevalent before 2008 belonged to three genotypes (PCV2a-PCV2c). The PCV2d was identified in 2010, and then prevalent in pig populations worldwide since 2012 (4). In recent years, other novel PCV2 genotypes (PCV2e-PCV2h) have been identified (5). Other than these, owing to the high sequence similarity among different PCV2 genotypes, the novel recombinant strains generated from different PCV2 genotype strains were also documented (7, 8).

A number of studies have investigated the epidemiology and genetic features of PCV2 in certain regions of China (9–11), which confirmed the rapid evolution of PCV2, and the genotype shift from PCV2b to PCV2d in China. The prevalence and genetic characteristics of PCV2 in Guangdong Province have been documented in previous studies (12, 13). However, the corresponding information for recent years is still missing, particularly after the outbreak of African Swine Fever (ASF). In this study, polymerase chain reaction (PCR) was performed to investigate the epidemiological characteristics of PCV2 in Guangdong Province from 2016 to 2021. Moreover, the complete genomes of 26 PCV2 strains from different periods were sequenced and analyzed.

Materials and methods

Sample collection

From April 2016 to September 2021, 573 tissue samples (lung, tonsil, and lymph node) were collected from 132 pig farms across the northern Guangdong Province (Shaoguan, Qingyuan, Heyuan, Zhaoqing, Guangzhou, and Meizhou cities). Most diseased pigs from these farms showed clinical symptoms characterized by PMWS and/or porcine dermatitis and nephropathy syndrome (PDNS) or reproductive failures. Tissue samples with detailed information including collection sites, collection dates, and clinical symptoms were sent to Shaoguan University for further processing.

DNA extraction and PCV2 detection

Viral DNA genomes were extracted from the tissue sample using commercial kits (GDSBio, Guangdong, China) according to the manufacturer's instructions. Subsequently, the presence of PCV2 nucleic acid was detected by PCR with primers (PCV2-ORF2-P1 and PCV2-ORF2-P2) as described previously (14). The PCR products were analyzed in 1% agarose gel electrophoresis, in which the samples with the expected DNA bands, approximately 450 bp, were noted as PCV2-positive samples.

PCV2 complete genome sequencing

According to the collected regions and years of the positive samples, 26 PCV2-positive samples were selected to amplify the complete genome of the virus with three pairs of primers (Table 1). Each PCR reaction (50 μl) contained 25 μl 2×Taq Master mix (Takara Biotechnology, Dalian, China), 12.0 μl of each primer (10 pmol), 3.0 μl DNA template, and 20.0 μl sterilized water. The PCR amplification was performed with the following steps: 95°C for 5 min; 35 cycles of 95°C for 30 s, 55°C for 30 s, and 72°C for 60/90 s; followed by 72°C for 7 min. The PCR products were purified, cloned into the pUCm-T vector, and sequenced by Sangon Biotech Co. Ltd (Shanghai, China). The sequences of these novel PCV2 strains were submitted to the GenBank (ON361010-ON361035).

TABLE 1 Primers used in this study.

Primer name	Sequence (5'—3')	Length	Annealing temperature	Purpose
PCV2–P1–F:	TGTTTTCGAACGCAGTGCC	1045	55.0	Sequencing
PCV–P1–R	CCGTTGTCCCTGAGATCTAGGA			
PCV2–P2–F	GGACCCCAACCCCATAAAA	1254	55.0	Sequencing
PCV2–P2–R	CCCTCACCTATGACCCCTATGT			
PCV2–P3–F	GTACCTTGTTGGAGAGCGGG	1767∼1678	55.0	Sequencing
PCV2–P3–R	TCACAGCAGTAGACAGGTCA			
PCV2–ORF2–P1	CACGGATATTGTAGTCCTGGT	449	52.0	Detection of PCV2 targeting to ORF2 gene
PCV2–ORF2–P2	CGCACCTTCGGATATACTGTG			

If the complete genome of PCV2 was not successfully amplified using the primer PCV2–P3–F/R, two pairs of primers (PCV2–P1–F/R and PCV2–P2–F/R) were employed.

Bioinformatics analyses

The complete genomes of 20 reference PCV2 strains (including PCV2a, PCV2b, PCV2c, PCV2d, PCV2e, and PCV2h) were downloaded from the GenBank database (Supplementary Table S1). The nucleotide sequences and their corresponding amino acid sequences (Cap and Rep) variations of 26 novel PCV2 strains and reference strains were analyzed *via* the Lasergene DNAStar software. Phylogenetic trees were generated based on the complete genome and ORF2 gene sequences using the neighbor-joining method in the MEGA 7.0 software (Kimura 2-parameter model, 1,000 bootstrap replications).

Data analyses

The statistical significance of the detection rates of PCV2 in pigs among different groups was analyzed using the chi-square test in the SPSS 21.0 software (SPSS Inc., Chicago, IL, USA), in which, P-values < 0.05 were taken as statistically significant. Meanwhile, the minimum infection rate (MIR) with 95% CI was determined *via* the SPSS 21.0 software.

Results

The epidemiology of PCV2 in northern Guangdong Province from 2016 to 2021

In this study, a total of 573 tissue samples from 132 pig farms were collected from northern Guangdong Province for the PCV2 nucleic acids test by conventional PCR. The results showed that 98 out of 132 (74.24%) investigated pig farms were tested PCV2-positive. Overall, 297 tissue samples (51.83%, 95%CI 47.74–55.92) were PCV2-positive, with the positive rates of PCV2 in different regions varying from 27.91–64.94% (Table 2). Moreover, The detection rate of PCV2 was significantly lower in samples collected before 2016–2018 than after the outbreak of African Swine Fever (2019–2021), being 59.85% (158/264, 95%CI 53.94–65.76) and 41.47% (141/340, 95%CI 36.43–46.71), respectively (Table 2). Additionally, the positive rate of PCV2 among pigs with PCVADs (58.45%, 95%CI 53.63–63.27) was significantly higher than in pigs without PCVADs (36.26%, 95%CI 29.05–43.47) (Table 2).

Genome sequence analysis

To further investigate the genetic features of recent PCV2 strains prevalent in Guangdong Province, 26 PCV2 strains were randomly selected among PCV2-positive samples from different regions, whose complete genome sequences were amplified, sequenced, and analyzed (Table 3). The complete genomes of all 26 novel PCV2 strains were 1,764–1,767 nt in length. Particularly, the length of the ORF1 gene encoding the Rep and ORF2 gene encoding the Cap was 945 nt and 702–705 nt, respectively. Pairwise-sequence comparisons among 26 novel isolates ranged from 95.9–99.9% (complete genome), 97.0–99.7% (ORF1), and 94.0–100.0% (ORF2) at the nt level, respectively, and 94.6–99.4% (Rep protein) and 98.6–100.0% (Cap protein) at amino acid (aa) level, respectively.

Phylogenetic analysis

Phylogenetic trees were generated according to the complete genome and ORF2 sequences of the 26 PCV2 strains in this study and 20 reference strains from GenBank. The results showed that the 26 Guangdong strains were divided into three sub-genotypes (PCV2a, PCV2b, and PCV2d) (Figures 1A,B), 12 of 26 (46.15%) isolates belonged to the genotype 2b; and half of all

TABLE 2 Prevalence of PCV2 in pigs in northern Guangdong Province, China.

Factor	Category	No. sample	No. positive	Prevalence (%) (95% CI)	*P*–value
Period	2014∼2018	340	141	41.47 (36.43–46.71)	Reference
	2019∼2021	264	158	59.85 (53.94–65.76)	< 0.01
Symptom	PCVADs	402	235	58.45 (53.63–63.27)	< 0.01
	Others	171	62	36.26 (29.05–43.47)	Reference
Region	Shaoguan	186	91	48.92 (41.74–56.10)	< 0.01
	Qingyuan	96	60	62.50 (52.82–72.18)	< 0.01
	Heyuan	119	58	48.74 (39.76–57.72)	< 0.01
	Zhaoqing	77	50	64.94 (54.28–75.60)	< 0.01
	Guangzhou	43	12	27.91 (14.50–41.32)	Reference
	Meizhou	52	26	50.0 (36.41–63.59)	< 0.01
	Total	573	297	51.83 (47.74–55.92)	

TABLE 3 Detail information of PCV2 strains obtained in this study, including strain name, collection year, isolation region, genotype, and GenBank accession numbers.

Strain	Region	Collection year	Genotype	Accession number
GD–HY–2016	Heyuan, Guangdong	2016	PCV2b	ON361010
GD–QY–2016	Qingyuan, Guangdong	2016	PCV2b	ON361011
GD–GZ–2016	Guangzhou, Guangdong	2016	PCV2b	ON361012
GD–ZQ–2016	Zhaoqing, Guangdong	2017	PCV2b	ON361013
GD–SG–2017	Shaoguan, Guangdong	2017	PCV2a	ON361014
GD–ZQ–2017	Zhaoqing, Guangdong	2017	PCV2d	ON361015
GD–QY–2017	Qingyuan, Guangdong	2017	PCV2b	ON361016
GD–HY–2018	Heyuan, Guangdong	2018	PCV2b	ON361017
GD–MZ–2018	Meizhou, Guangdong	2018	PCV2b	ON361018
GD–SG–2019	Shaoguan, Guangdong	2019	PCV2b	ON361019
GD–QY–2019	Qingyuan, Guangdong	2019	PCV2b	ON361020
GD–SG–2020–1	Shaoguan, Guangdong	2020	PCV2b	ON361021
GD–SG–2020–2	Shaoguan, Guangdong	2020	PCV2d	ON361022
GD–HY–2020	Heyuan, Guangdong	2020	PCV2d	ON361023
GD–MZ–2020	Meizhou, Guangdong	2020	PCV2d	ON361024
GD–ZQ–2020–1	Zhaoqing, Guangdong	2020	PCV2d	ON361025
GD–ZQ–2020–2	Zhaoqing, Guangdong	2020	PCV2d	ON361026
GD–GZ–2020	Guangzhou, Guangdong	2020	PCV2d	ON361027
GD–QY–2020	Qingyuan, Guangdong	2020	PCV2d	ON361028
GD–SG–2021–1	Shaoguan, Guangdong	2021	PCV2d	ON361029
GD–SG–2021–2	Shaoguan, Guangdong	2021	PCV2d	ON361030
GD–GZ–2021	Guangzhou, Guangdong	2021	PCV2d	ON361031
GD–HY–2021	Heyuan, Guangdong	2021	PCV2d	ON361032
GD–MZ–2021	Meizhou, Guangdong	2021	PCV2b	ON361033
GD–QY–2021	Qingyuan, Guangdong	2021	PCV2d	ON361034
GD–ZQ–2021	Zhaoqing, Guangdong	2021	PCV2b	ON361035

isolates belonged to the genotype 2d; only one isolate, GD-SG-2017, was clustered with PCV2a strains. Remarkably, the PCV2a isolate (GD-SG-2017) and 9 of 12 PCV2b isolates were collected between 2016 and 2018, whereas 92.31% (12/13) PCV2d strains were isolated during 2019-2021.

Analysis of Cap amino acid sequences

To investigate the sequence characteristics of the Cap aa sequences obtained in this study, the aa sequence alignment was performed between the 26 PCV2 strains and the 20 reference PCV2 strains. The results showed that the lengths of Cap sequences of 26 PCV2 strains were 233 aa (12 PCV2b isolate and GD-GZ-2021) or 234 aa (12 PCV2d isolates and GD-SG-2017). As shown in Supplementary Table S2, a total of 8 and 4 aa substitutions were found in Cap among 12 PCV2b and 13 PCV2d isolates, respectively. To be more specific, these substitutions were located at sites 25 (R→ H), 59 (K→ R), 63 (R→ K),84 (G→ E), 131 (T→ P), 151 (T→ P), 173 (Y→ H), and 190 (T→ A) in the Cap of PCV2b isolates; and 30 (V→ L), 169 (G→ R), 206 (I→ K), and 233 (N→ K) in the Cap of PCV2d isolates, respectively. Remarkably, a series of unique aa substitutions in the Cap, for instance, the substitutions at sites 25, 59, and 63 were found in GD-GZ-2016 isolate; and site 151 in GD-QY-2016 isolate; and 59, 63, 84, 173, and 190 in GD-HY-2018 isolate, respectively.

Discussion

PCV2 has been prevalent in pig populations in China for many years. The disease (PCVAD) caused by PCV2 is considered a major factor threatening the pig industry (11). Vaccine pressure, viral evolution, natural selection, and international pig transportation contribute to the rapid evolution rate of PCV2 (15). In recent years, two genotype shifts of PCV2 have been observed in China. PCV2a was the predominant prevalent genotype before 2003, which has been gradually replaced by PCV2b from 2003 to 2010. Owing to the high prevalence

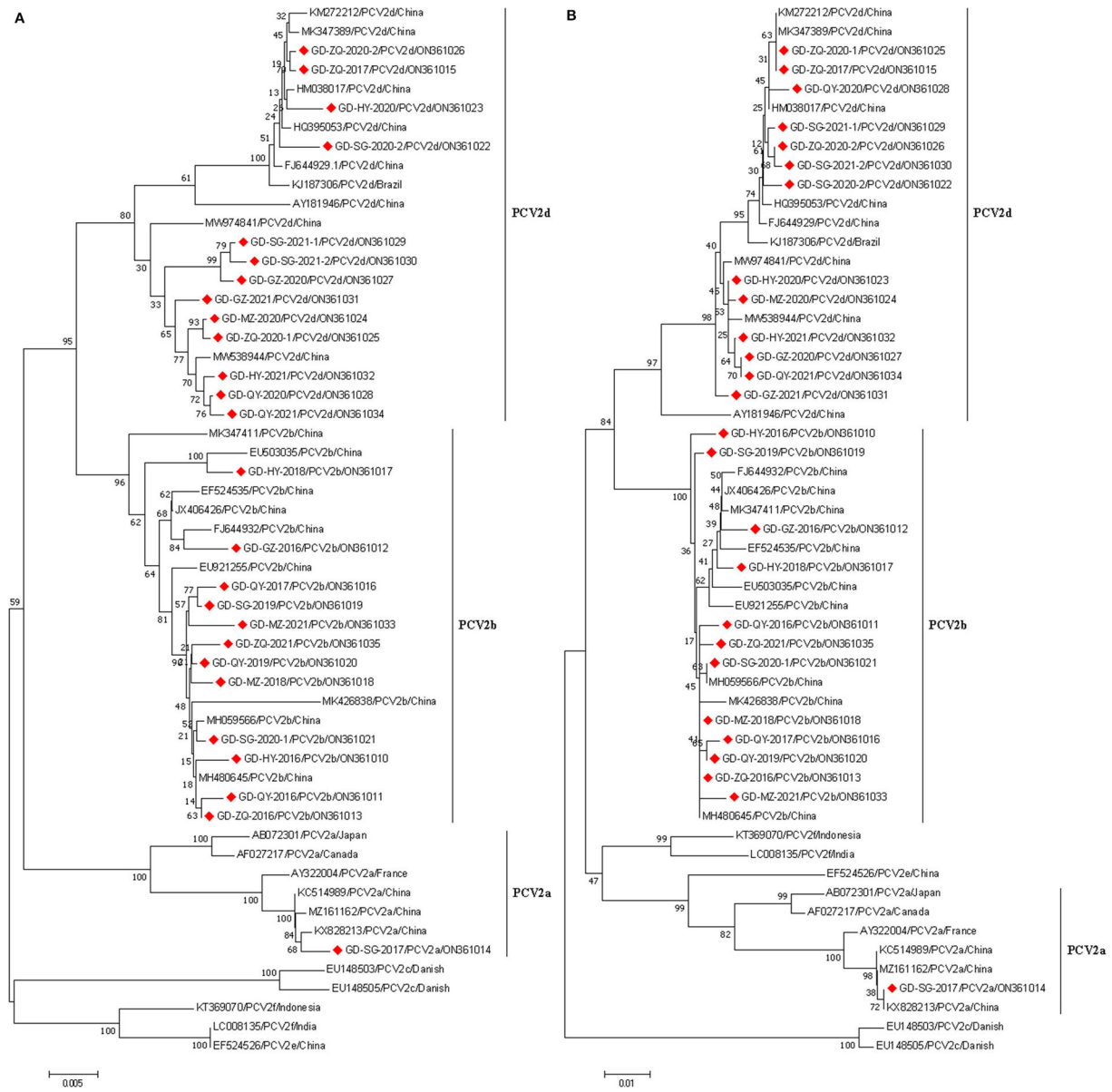

FIGURE 1
Phylogenetic analysis based on the complete genome **(A)** and ORF2 gene **(B)** sequences of 26 PCV2 strains obtained in this study and other reference strains. phylogenetic trees were constructed using the neighbor-joining method with 1,000 bootstrap replicates in MEGA7.0 software. Red squares represented PCV2 isolates obtained in this study.

of PCV2 and the widely applied PCV2 vaccines since 2010, PCV2d is an emerging genotype prevalent in China (4, 16). Moreover, the co-prevalence of multiple PCV2 genotypes was often observed in the same region, even on the same pig farm (4, 7, 14, 17). Thus, an investigation of the prevalence and genetic characteristics of PCV2 will provide scientific evidence for the prevention and control of PCV2.

In this study, 573 samples from pigs were collected to investigate the epidemiological characteristics of PCV2 in the northern Guangdong Province of China. Several features were summarized: 1) high detection rate of PCV2 (51.83%, 297/573) was observed in nearly 75% of the investigated pig farms. The PCV2-positive rate among these samples in northern Guangdong Province was similar to other areas in China, such as Henan (62.4%, 73/117) (18), Shanghai (57.78%, 115/199) (4), and Yunnan (60.93%, 170/279) (11), but higher than that in Shandong Province (36.98%, 490/1325) (19); taken together, these bodies of evidence showed PCV2 high prevalence in China; 2) the positive rate of PCV2 among specimens collected before (2014–2018) was lower than that after (2019–2021) the

outbreak of ASF. Owing to the prevalence of ASF in China (from 2019 to 2021), PCV2-positive pigs were introduced into pig farms to keep the breeding scale. Nevertheless, some pig farmers mainly focused on ASF prevention, but neglected PCV2 prevention, which resulted in the high prevalence of PCV2 from 2019 to 2021 in northern Guangdong province; 3) the PCV2 detection rate among pigs with PCVADs was higher than those without PCVADs. To better prevent the PCV2 spread, the PCV2 positive pigs without PCVADs should not be neglected.

Currently, PCV2 strains have been divided into eight genotypes (PCV2a–h) based on their genomic characteristics, in which, multiple genotypes were prevalent in China (4, 16). More recently, PCV2d has been considered a novel emerging major genotype prevalent in Chinese pig populations (15, 20). Among 26 PCV2 strains obtained in this study, only three genotypes were identified, PCV2a, PCV2b, and PCV2d, the proportions of which were 3.85% (1/26), 46.15% (12/26), and 50.0% (13/26), respectively, suggesting that PCV2b and PCV2d, rather than PCV2a, predominated in these investigated regions. According to the findings from other studies, more than 30% of PCV2 strains prevalent in China before 2018 belonged to the PCV2d genotype (16, 18), particularly, PCV2d has become the major dominant genotype circulating in Shandong Province from 2015 to 2018 (19). However, the results in this study showed that the predominant genotypes of PCV2 during 2014–2018 and 2019–2021 were PCV2b and PCV2d, the proportions of which were 81.82% (9/11) and 80.0% (12/15) in northern Guangdong Province, respectively. Guangdong Province is a major pig breeding area with millions of pigs transferred out, whereas very few pigs were introduced into this province before 2018. These factors resulted in the relatively stable PCV2b genotype in these areas. However, after the outbreak of ASF in China, a large number of pigs were introduced into Guangdong Province, which might lead to the PCV2 genotype shifting from PCV2b to PCV2d.

The PCV2 Cap is the sole structural protein that is responsible for a series of biological processes, such as virus entry into host cells, replication, and activation of host immune responses (21, 22). Therefore, the aa mutations in Cap may determine viral biological characteristics (23). In this study, a series of aa substitutions were found in the Cap protein (Supplementary Table S2), such as the sites of 30 (V→ L) (n = 6), and 59 (K→ R) (n = 2), and 63 (R→ K) (n = 2). It has been confirmed that the aa residues 1–41 of Cap participate in viral nuclear localization (24), while the aa residues 47–63 are crucial for PCV2 epitope recognition (25). Further experiments will be performed to investigate the effects of these aa substitutions on PCV2 infection.

In conclusion, this study revealed the epidemiology and genetic characteristics of PCV2 in recent years in northern Guangdong Province of China and indicated the severe prevalence of PCV2 in these regions. Moreover, this study confirmed the prevalence of multiple PCV2 genotypes in Guangdong Province from 2016 to 2021, while, currently the PCV2d has become the predominant genotype. These findings highlight the importance to investigate the genetic features of currently prevalent PCV2 strains, and to develop novel vaccines to control PCV2d.

Data availability statement

The datasets presented in this study can be found in online repositories. The names of the repository/repositories and accession number(s) can be found in the article/Supplementary material.

Author contributions

Conceptualization: ZD. Methodology: WN, ST, JW, and HH. Software: WN and ST. Formal analysis and investigation: WN, ST, JW, GP, and HH. Resources and original draft writing: WN. Review and revised and funding acquisition: WN and ZD. All authors participated in the article editing and approved the final manuscript.

Funding

This work was supported by Natural Science Foundation of Hunan Province (2021JJ30316) and the Project of Swine Innovation Team in Guangdong Modern Agricultural Research System (2021KJ126).

Conflict of interest

The authors declare that the research was conducted in the absence of any commercial or financial relationships that could be construed as a potential conflict of interest.

Publisher's note

Supplementary material

The Supplementary Material for this article can be found online at: https://www.frontiersin.org/articles/10.3389/fvets.2022.932612/full#supplementary-material

References

1. Tischer I, Gelderblom H, Vettermann W, Koch MAA. Very small porcine virus with circular single-stranded DNA. *Nature.* (1982) 295:64–6. doi: 10.1038/295064a0

2. Ge M, Ren J, Xie YL, Zhao D, Fan FC, Song XQ, et al. Prevalence and genetic analysis of Porcine circovirus 3 in China from 2019 to 2020. *Front Vet Sci.* (2021) 8:773912. doi: 10.3389/fvets.2021.773912

3. Yu WT, Sun YA, He Q, Sun CY, Dong T, Zhang LH, et al. Mitochondrial localization signal of porcine circovirus type 2 capsid protein plays a critical role in Cap-induced apoptosis. *Vet Sci.* (2021) 8:272. doi: 10.3390/vetsci8110272

4. Kang L, Wahaab A, Shi K, Mustafa BE, Zhang Y, Zhang JJ, et al. Molecular epidemic characteristics and genetic evolution of porcine circovirus type 2 (PCV2) in swine herds of Shanghai, China. *Viruses.* (2022) 14:289. doi: 10.3390/v14020289

5. Li N, Liu J, Qi JL, Hao F, Xu L, Guo KK, et al. Genetic diversity and prevalence of porcine circovirus type 2 in China during 2000-2019. *Front Vet Sci.* (2021) 8:788172. doi: 10.3389/fvets.2021.788172

6. Franzo G, Segalés J. Porcine circovirus 2 (PCV-2) genotype update and proposal of a new genotyping methodology. *PLoS ONE.* (2018) 13:e0208585. doi: 10.1371/journal.pone.0208585

7. Qu TL, Li RC, Yan MJ, Luo BY, Yang TT, Yu XL, et al. High prevalence of PCV2d in Hunan Province, China: a retrospective analysis of samples collected from 2006 to 2016. *Arch Virol.* (2018) 163:1897–906. doi: 10.1007/s00705-018-3823-9

8. Wen LB, He KW. Genomic rearrangement and recombination of porcine circovirus type 2 and porcine circovirus-like virus P1 in China. *Front Vet Sci.* (2021) 8:736366. doi: 10.3389/fvets.2021.736366

9. Li LM, Yuan WZ, Guo HY, Ma ZJ, Song QY, Wang XB, et al. Prevalence and genetic variation of porcine circovirus type 2 in Hebei, China from 2004 to 2014. *Gene.* (2016) 586:222–7. doi: 10.1016/j.gene.2016.04.014

10. Xu T, Zhang YH, Tian RB, Hou CY, Li XS, Zheng LL, et al. Prevalence and genetic analysis of porcine circovirus type 2 (PCV2) and type 3 (PCV3) between 2018 and 2020 in central China. *Infect Genet Evol.* (2021) 94:105016. doi: 10.1016/j.meegid.2021.105016

11. Lv NC, Zhu L, Li WG, Li ZL, Qian QS, Zhang TY, et al. Molecular epidemiology and genetic variation analyses of porcine circovirus type 2 isolated from Yunnan Province in China from 2016-2019. *BMC Vet Res.* (2020) 16:96. doi: 10.1186/s12917-020-02304-8

12. Wei CY, Zhang MZ, Chen Y, Xie JX, Huang Z, Zhu WJ, et al. Genetic evolution and phylogenetic analysis of porcine circovirus type 2 infections in southern China from 2011 to 2012. *Infect Genet Evol.* (2013) 17:87–92. doi: 10.1016/j.meegid.2013.03.041

13. Zhai SL, Chen SN, Liu W, Li XP, Deng SF, Wen XH, et al. Molecular detection and genome characterization of porcine circovirus type 2 in rats captured on commercial swine farms. *Arch Virol.* (2016) 161:3237–44. doi: 10.1007/s00705-016-3004-7

14. Hu Y, Zhan Y, Wang DD, Xie XH, Liu TB, Liu W, et al. Evidence of natural co-infection with PCV2b subtypes in vivo. *Arch Virol.* (2017) 162:2015–20. doi: 10.1007/s00705-017-3303-7

15. Xu PL, Zhao Y, Zheng HH, Tian RB, Han HY, Chen HY, et al. Analysis of genetic variation of porcine circovirus type 2 within pig populations in central China. *Arch Virol.* (2019) 164:1445–51. doi: 10.1007/s00705-019-04205-0

16. Wang HJ, Gu JY, Xing G, Qiu XH, An ST, Wang YX, et al. Genetic diversity of porcine circovirus type 2 in China between 1999-2017. *Transbound Emerg Dis.* (2019) 66:599–605. doi: 10.1111/tbed.13040

17. Ouyang T, Zhang XW, Liu XH, Ren LZ. Co-infection of swine with porcine circovirus type 2 and other swine viruses. *Viruses.* (2019) 11:185. doi: 10.3390/v11020185

18. Zheng GM, Lu QX, Wang FY, Xing GX, Feng H, Jin QY, et al. Phylogenetic analysis of porcine circovirus type 2 (PCV2) between 2015 and 2018 in Henan Province, China. *BMC Vet Res.* (2020) 16:6. doi: 10.1186/s12917-019-2193-1

19. Ma ZC, Liu MD, Liu ZH, Meng FL, Wang HY, Cao LL, et al. Epidemiological investigation of porcine circovirus type 2 and its coinfection rate in Shandong Province in China from 2015 to 2018. *BMC Vet Res.* (2021) 17:17. doi: 10.1186/s12917-020-02718-4

20. Hou Z, Wang H, Feng Y, Song M, Li Q, Genetic LJ, et al. Variation and phylogenetic analysis of Porcine circovirus type 2 in China from 2016 to 2018. *Acta Virol.* (2019) 63:459–68. doi: 10.4149/av_2019_413

21. Huang Y, Chen XH, Long YZ, Yang L, Song WB, Liu JJ, et al. Epidemiological analysis from 2018 to 2020 in China and prevention strategy of porcine circovirus type 2. *Front Vet Sci.* (2021) 8:753297. doi: 10.3389/fvets.2021.753297

22. Zhan Y, Yu WT, Cai X, Lei XN, Lei HY, Wang AB, et al. The carboxyl terminus of the porcine circovirus type 2 capsid protein is critical to virus-like particle assembly, cell entry, and propagation. *J Virol.* (2020) 94:e00042–e00020. doi: 10.1128/JVI.00042-20

23. Nawagitgul P, Morozov I, Bolin SR, Harms PA, Sorden SD, Paul PS, et al. Open reading frame 2 of porcine circovirus type 2 encodes a major capsid protein. *J Gen Virol.* (2000) 81:2281–7. doi: 10.1099/0022-1317-81-9-2281

24. Hou Q, Hou SH, Chen Q, Jia H, Xin T, Jiang YT, et al. Nuclear localization signal regulates porcine circovirus type 2 capsid protein nuclear export through phosphorylation. *Virus Res.* (2018) 246:12–22. doi: 10.1016/j.virusres.2017.12.012

25. Lekcharoensuk P, Morozov I, Paul PS, Thangthumniyom N, Wajjawalku W, Meng XJ, et al. Epitope mapping of the major capsid protein of type 2 porcine circovirus (PCV2) by using chimeric PCV1 and PCV2. *J Virol.* (2004) 78:8135–45. doi: 10.1128/JVI.78.15.8135-8145.2004

frontiers | Frontiers in Veterinary Science

TYPE Original Research
PUBLISHED 15 September 2022
DOI 10.3389/fvets.2022.987667

OPEN ACCESS

EDITED BY
Lian-Feng LI,
Harbin Veterinary Research Institute (CAAS), China

REVIEWED BY
Hongliang Zhang,
Harbin Veterinary Research Institute (CAAS), China
Xu Shengkui,
Beijing University of Agriculture, China

*CORRESPONDENCE
Baoquan Li
libq@sdau.edu.cn
Fanliang Meng
18754875921@163.com
Mengda Liu
liumengda@cahec.cn

†These authors have contributed equally to this work

SPECIALTY SECTION
This article was submitted to Veterinary Infectious Diseases, a section of the journal Frontiers in Veterinary Science

RECEIVED 06 July 2022
ACCEPTED 25 August 2022
PUBLISHED 15 September 2022

CITATION
Li P, Shen Y, Wang T, Li J, Li Y, Zhao Y, Liu S, Li B, Liu M and Meng F (2022) Epidemiological survey of PRRS and genetic variation analysis of the ORF5 gene in Shandong Province, 2020–2021. *Front. Vet. Sci.* 9:987667. doi: 10.3389/fvets.2022.987667

Epidemiological survey of PRRS and genetic variation analysis of the ORF5 gene in Shandong Province, 2020–2021

Peixun Li[1†], Yesheng Shen[1†], Tailong Wang[1], Jing Li[1], Yan Li[2], Yiran Zhao[1], Sidang Liu[1], Baoquan Li[1*], Mengda Liu[3*] and Fanliang Meng[1,4*]

[1]College of Animal Medicine, Shandong Agricultural University, Taian, China, [2]College of Veterinary Medicine, Huazhong Agricultural University, Wuhan, China, [3]Division of Zoonoses Surveillance, China Animal Health and Epidemiology Center, Qingdao, China, [4]Huayun (Shandong) Inspection and Quarantine Service Co., Ltd, Taian, China

Since the rise of porcine reproductive and respiratory syndrome virus (PRRSV) in China, mutations have occurred regularly. In particular, the emergence of HP-PRRSV has significantly improved the pathogenicity of PRRSV. It has brought huge economic losses to the Chinese pig farming industry. To understand the current prevalence and evolution of PRRSV in Shandong Province, 1,344 samples suspected of having PRRSV were collected from local hog farms of different sizes. Genetic variation in the isolated PRRSV ORF5 gene was analyzed using the RT-PCR method. The results showed that the detection rate of PRRSV in the collected samples was 25.44%. The predominant strain of PRRSV in Shandong Province is still NADC30-like. However, it cannot be ignored that NADC34-like is also starting to become a prevalent strain. Mutations in ORF5 amino acids 13, 151 and neutralizing epitope (aa36-aa52) in some isolates can cause changes in virulence and ability to escape immunity. This study enriches the epidemiological data on PRRSV in Shandong Province, China. It provides an important reference for the development of new vaccines and for the prevention and control of PRRSV.

KEYWORDS

PRRSV, GP5, epidemiology, genetic evolutionary analysis, prevention and control

Introduction

Porcine reproductive and respiratory syndrome (PRRS) is a highly contagious disease caused by the porcine reproductive and respiratory syndrome virus (PRRSV) (1). It is known as "blue ear disease" because it often leads to bluish purple ears in diseased pigs (2). In affected pigs, the disease primarily causes spontaneous abortion in late pregnancy, as well as stillbirths, mummified fetuses, or weak piglets. It also causes congenital dysplasia in piglets, respiratory distress, interstitial pneumonia and suppressed immune function. Moreover, it is often seen in mixed infections with other pathogens (3–5). PRRSV is currently one of the most serious pathogens posing a threat to global swine production. After beginning in Europe and the Americas in the 1990s, it spread across

the globe (6, 7). The virus was first isolated in China in 1996 (5), and since then PRRSV has become widely prevalent there. A highly pathogenic strain of PRRSV emerged in China in 2006 and became the dominant epidemic strain (8–12). In 2012, in Henan Province, China, Zhou et al. (13) discovered for the first time a NADC30-like highly homologous strain with 131 aa discontinuous deletions in the nsp2 gene. In 2013–2015, NADC30-like strains were reported in many provinces in China (14). The high frequency of NADC30 recombination makes the prevention and control of PRRS extremely difficult (15–17). In 2017, the NADC34 strain was isolated for the first time in China (18). NADC34-like PRRSV is now mildly or moderately pathogenic to piglets (19–21). It primarily affects sows, often leading to severe spontaneous abortions among pregnant sows (19). NADC34-like PRRSV has become widespread in several provinces. The prevalence of NADC34 strains has been observed in 10 provinces and cities, including Heilongjiang, Liaoning, Jilin, Jiangsu, Henan, Hebei and Shandong (22–24). This makes it very necessary to monitor PRRSV and understand its prevalence in Shandong Province.

The genome of PRRSV is approximately 15 kb long, forms a cap structure at the 5′ end during mRNA processing, and has a Poly-A tail structure at the 3′ end (25). The structural proteins of this virus are GP2a, GP3, GP4, GP5, M, E, and N. Among these, GP5 and M proteins are the main envelope proteins of PRRSV (26). GP5 protein is the most variable protein in PRRSV. In addition, GP5 contains glycosylation sites that help recognize cell receptors and neutralize viruses. GP5 is also the main protein that promotes the production of neutralizing antibodies in the body. The rapid mutation and the high recombination frequency of PRRSV stimulate the prevalence of PRRS and exacerbate the difficulty of PRRS prevention and control (27). Therefore, the GP5 protein, as an extremely important PRRSV protein, has become an important indicator in the identification and analysis of PRRSV. To understand the latest epidemiological situation and epidemic strain types of PRRSV in 2020–2021, an experiment was conducted. In this experiment, clinical cases of suspected PRRSV infections were collected from swine farms of varying sizes in Shandong Province. The pathogens were detected by RT-PCR and were sequenced and analyzed for the GP5 protein gene.

Materials and methods

Sample collection

In this study, suspected cases of PRRS were collected from pig farms of different sizes in all cities of Shandong Province in 2020–2021. Blood and nasal cotton swabs were mainly collected from affected pigs, while lymph nodes and lung tissues were collected from dead pigs.

TABLE 1 List of primers used in this study.

Names*	Primer sequence (5′–3′)	Length (bp)
GP5-F	GGGCAACCGTTTTAGCCTGTC	710
GP5-R	GAACGCCAAAAGCACCTTCTG	

*F represents forward PCR primer; R represents reverse PCR primer.

Sample handling

The lymph nodes and pulmonary tissues were collected aseptically excised and crushed in a suspension. The blood was mixed with the corresponding nasal cotton swab. All processed samples were centrifuged, and the supernatant was sucked out to extract the total RNA for the RT-PCR test. Samples containing the low-viral target bands with content were inoculated into Marc-145 cells and PAM cells for blind transmission in three generations. The virus fluid was collected for the RT-PCR test.

Viral RNA extraction

The viral solution was added to the RNA isolater, and the total RNA was extracted according to the instructions of RNA isolater Total RNA Extraction Reagent (Vazyme).

RT-PCR assay

With the use of the HiScript III 1st Strand cDNA Synthesis Kit (Vazyme), the resulting total RNA was reverse transcribed into the cDNA in accordance with the instructions. PCR amplification was performed using the primers in Table 1. The results were observed through agarose gel electrophoresis under a gel system imager.

GP5 gene sequencing and analysis

All samples with positive RT-PCR findings were sequenced for the ORF5 gene. The sequences related to PRRSV Sublineage 1.5, Sublineage 1.8, Lineage 3, Lineage 5, and Lineage 8 were downloaded from the NCBI database as reference strains. These were analyzed using MEGA X and MegAlign.

Recombination analysis

In this study, the full-length genome of SDHY-DZ037 was sequenced for recombination analysis. Alignment was screened using RDP4, implementing the RDP (28), GENECONV (29),

Bootscan (30), Chimaera (31), SiScan (32), MaxChi (33), and 3Seq (34) algorithms. At least four of the above methods can identify a recombination event. In addition, if the breakpoint region of the recombination event is larger than 100 nt, the region can be regarded as a recombination region. To confirm these presumed recombinant events, we generated a series of phylogenetic trees for each sequence region identified during the analysis (35). For each region, evolutionary analysis of maximum likelihood was performed in MEGA X. To visualize the recombinant signal and inferred breakpoint locations, a similarity analysis between the presumptive recombinant sequences and the parental lineages was implemented in SIMPLOT v3.5.1 (36). The window size was set to 200 nt and the step size to 20 nt.

Results

Distribution of sample sources

A total of 1,344 suspected PRRS-positive samples were collected from all cities in Shandong Province in 2020–2021. The number of samples in different regions is shown in Figure 1.

RT-PCR results

Total RNA was extracted from cultured virus fluid and reverse-transcribed into cDNA. PCR was performed using cDNA as the template. The results indicated that the number of PRRSV positive samples was 342, and the detection rate was 25.44%. PCR results from selected PRRSV-positive samples are presented in Figure 2.

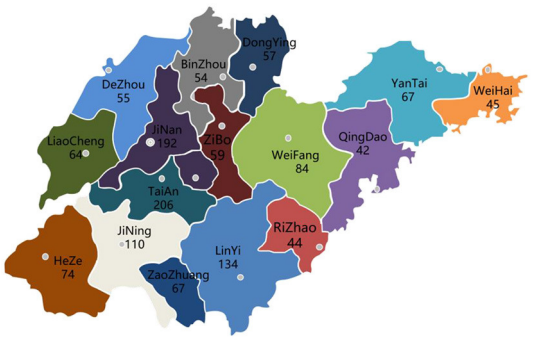

FIGURE 1
Map of sample collection and distribution in Shandong Province from 2020 to 2021 (the number represents the number of samples collected).

Genetic evolutionary analysis of ORF5 gene

In all, 76 strains were sequenced for the PRRSV ORF5 gene (Figure 3). Among them, 49 strains belonged to Sublineage 1.8 in the evolutionary genetic map of the ORF5 gene, representing 64.47% of isolates. Fifteen strains (19.74%) were classified as Sublineage 1.5. One strain (1.32%) was classified as Sublineage 5. Eleven strains (14.47%) were classified as Lineage 8.

Mutation analysis of the deduced amino acid site of ORF5 gene

The MegAlign module of DNASTAR Lasergene software was used to analyze the deduced amino acid mutation sites of 76 ORF5 genes in this study in comparison to some of the reference strains (Figure 4). A few typical mutations have been found. Amino acids 13 and 151 of ORF5-encoding GP5 protein were associated with virulence-related sites of the virus. Virulent strains of R^{13} and R^{151} are those that are often highly virulent (37–39). In this experiment, 13 strains of virus exhibited a $Q^{13} \rightarrow R^{13}$ mutation. Two strains were NADC30-like and the remaining 11 strains were CH-1a and HP-PRRSV-like.

Thirteen strains showed the $K^{151} \rightarrow R^{151}$ mutation, including two strains that were NADC30-like. One strain was NADC34-like and one strain was VR2332-like. The other nine strains were CH-1a and HP-PRRSV-like.

Mutations in the neutralizing epitope region at positions 36–52 of the amino acids encoded by ORF5 may cause the virus to escape the neutralizing effect induced by vaccine immunity. Reduce the protection effectiveness of vaccine immunity. In this study, multiple strains were isolated with mutations in the neutral epitope region. Twenty-three strains showed mutations in the neutral epitope region, of which 9 strains were NADC30-like, 2 strains were NADC34-like, 1 strain was VR2332-like, and the other 11 strains were CH-1a and HP-PRRSV-like.

Amino acid 137 (A^{137}) of GP5 is unique to the VR2332, MLV, and RespPRRS/Repro vaccine strains and is considered to be a discriminating site between wild strains and vaccine strains (38, 40, 41). In this study, three isolates showed mutations from S^{137} to A^{137}. Two of these were NADC34-like and one was VR2332-like.

Recombination analysis

In this study, we found that both SDHY-HZ015 and SDHY-DZ037 showed A^{137}. A^{137} is generally considered a unique locus of the VR2332, MLV, and RespPRRS/Repro vaccine strains. We therefore conducted a genome-wide recombination analysis, using the HiScript III 1st Strand cDNA

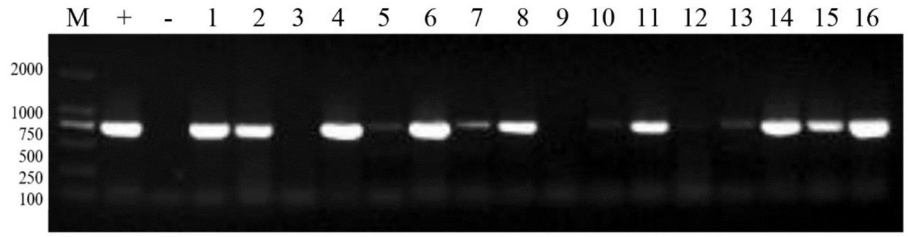

FIGURE 2
PCR results of some PRRSV positive samples. M: 2,000 marker, +: positive control, −: negative control, 1–16: sample numbers.

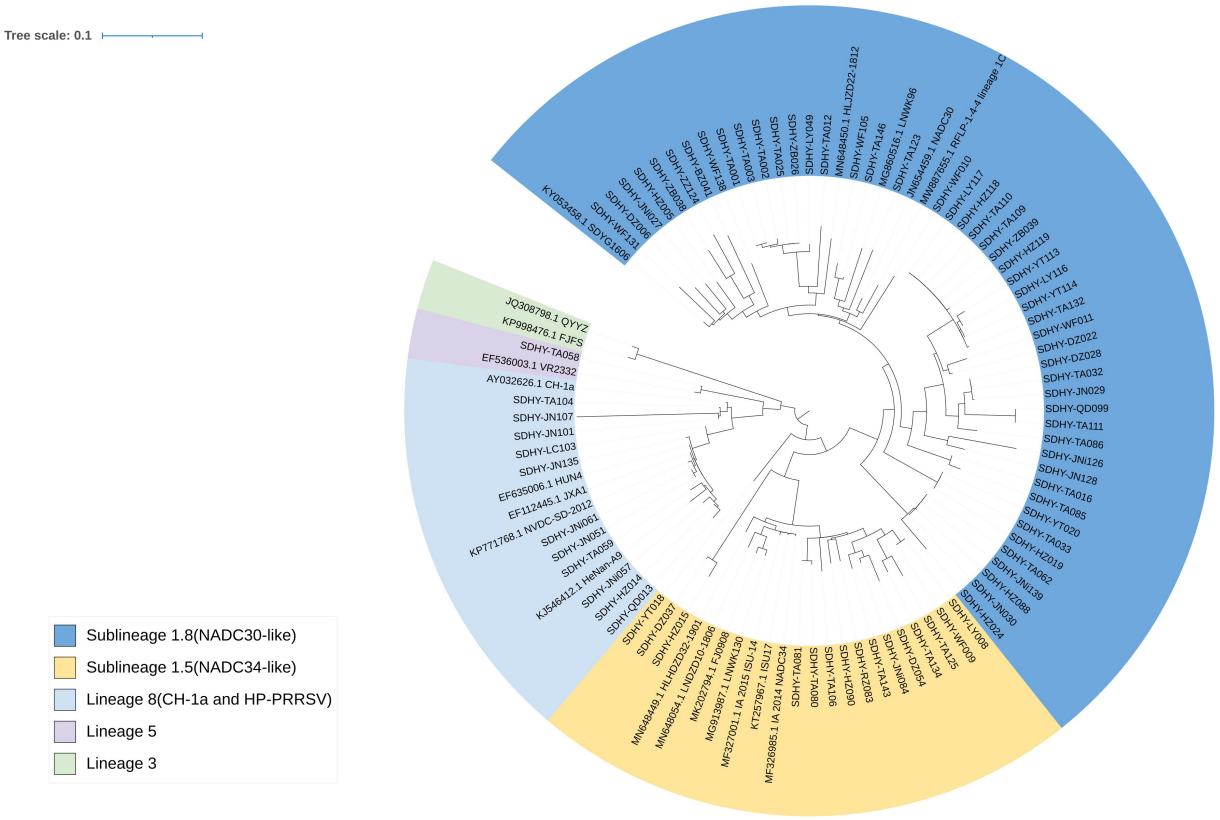

FIGURE 3
Phylogenetic tree based on the PRRSV ORF5 sequence. Evolutionary analysis of maximum likelihood performed in MEGA X. Multiple sequence alignments generated using Clustal W. ITOL was used to modify the genetic evolutionary tree, using different colors to distinguish different lineages and reference strains with GenBank sequence numbers.

Synthesis Kit (Vazyme). The resultant total RNA was reverse transcribed into the cDNA, according to the instructions. PCR amplification was performed using the primers of Supplementary Table 1 (42). The results were observed through agarose gel electrophoresis under a gel system imager. We sent RT-PCR positive products for sequencing (BGI Genomics). Finally, an entire genome of SDHY-DZ037 was successfully isolated. Representative strains of each PRRSV strain were selected as reference. Recombination events and recombination breakpoints were confirmed through RDP4 software. The results are in Supplementary Table 2. Validation and presentation of results was done using SimPlot (Figure 5A). SDHY-DZ037 was a recombinant NADC30-like PRRSV and NADC34-like PRRSV. The primary parent strain was NADC30-like, and the secondary parent strain was NADC34-like. Four recombination events were identified by the RDP4 and SimPlot software. The results showed that: recombination event 1 occurred at nucleic acid 6515-10323 nt (Figure 5D); event 2 occurred at nucleic acid

10916-11773 nt (Figure 5E); event 3 occurred at nucleic acid 12543-12665 nt (Figure 5F); event 4 occurred at nucleic acid 14410-14591 nt (Figure 5G). The area of recombinant gene was shown in the NADC30 (GenBank: JN654459.1) genome (Figure 5B). A phylogenetic analysis was performed on the entire genome and each recombinant region. The genome-wide phylogenetic tree showed that SDHY-DZ037 belonged to Sublineage 1.8 (NADC30-like) (Figure 5C), and all the recombinant regions belonged to Sublineage 1.5 (NADC34-like).

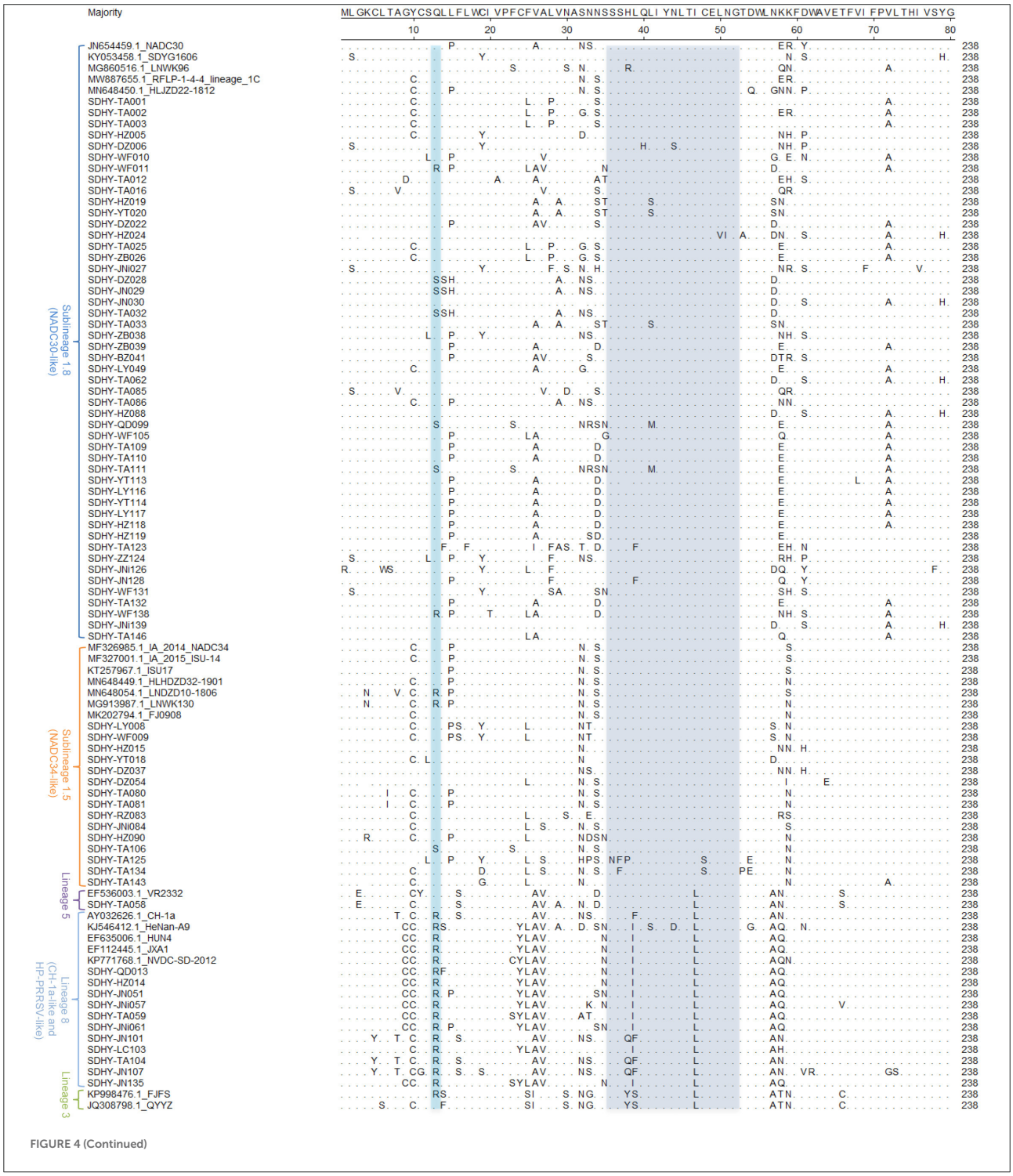

FIGURE 4 (Continued)

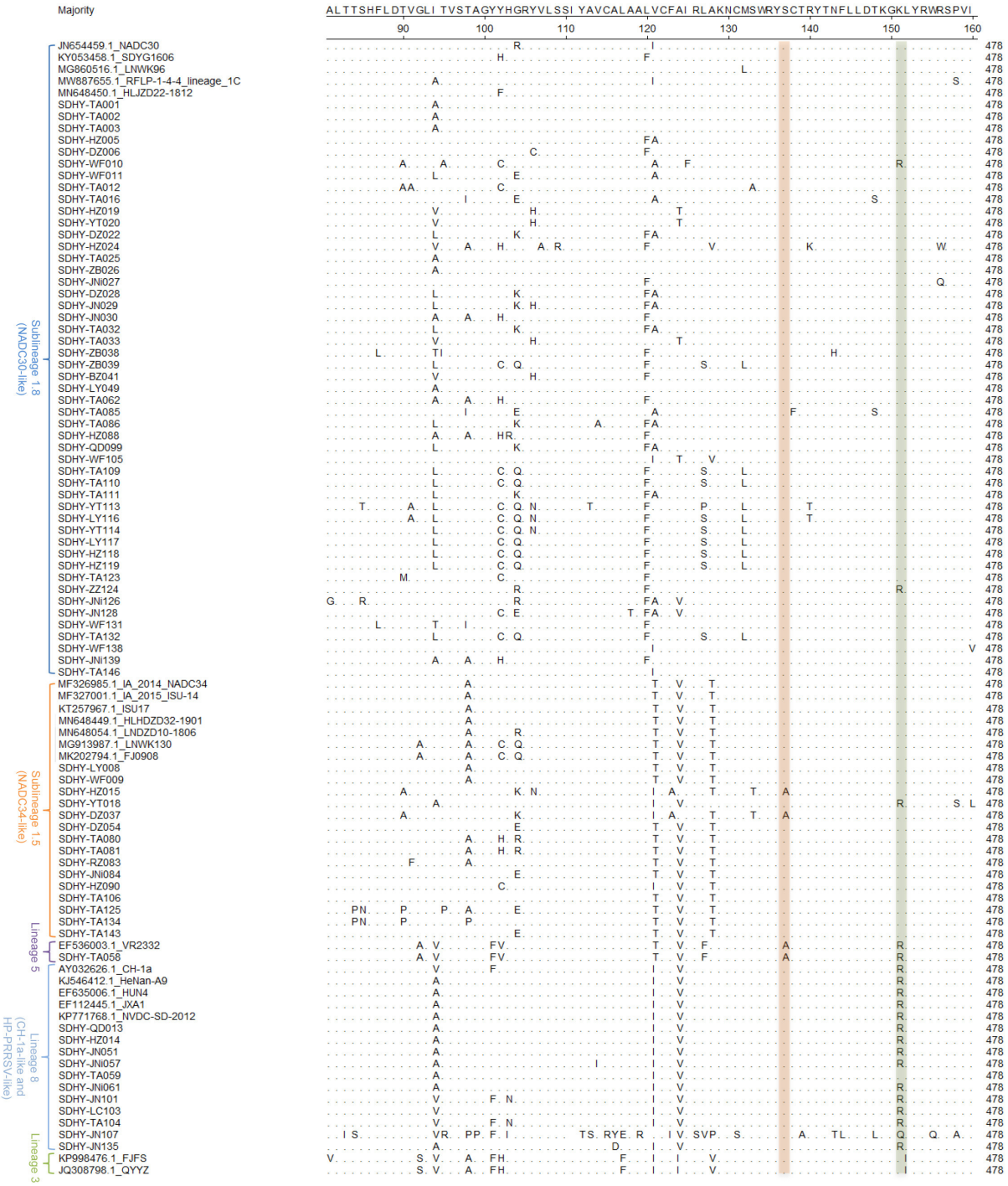

FIGURE 4
Analysis based on the major amino acid mutation sites of the PRRSV ORF5 gene.

Discussion

Since the emergence of PRRSV in China, PRRS has caused serious harm to the country's swine industry. The positive rate of PRRSV in Shandong Province was 9.58% in 2018–2019, and primarily Lineage 1 was predominant (43). To understand the prevalence of PRRSV in Shandong Province in 2020–2021, a total of 1,344 samples (mainly blood and nasal swabs from

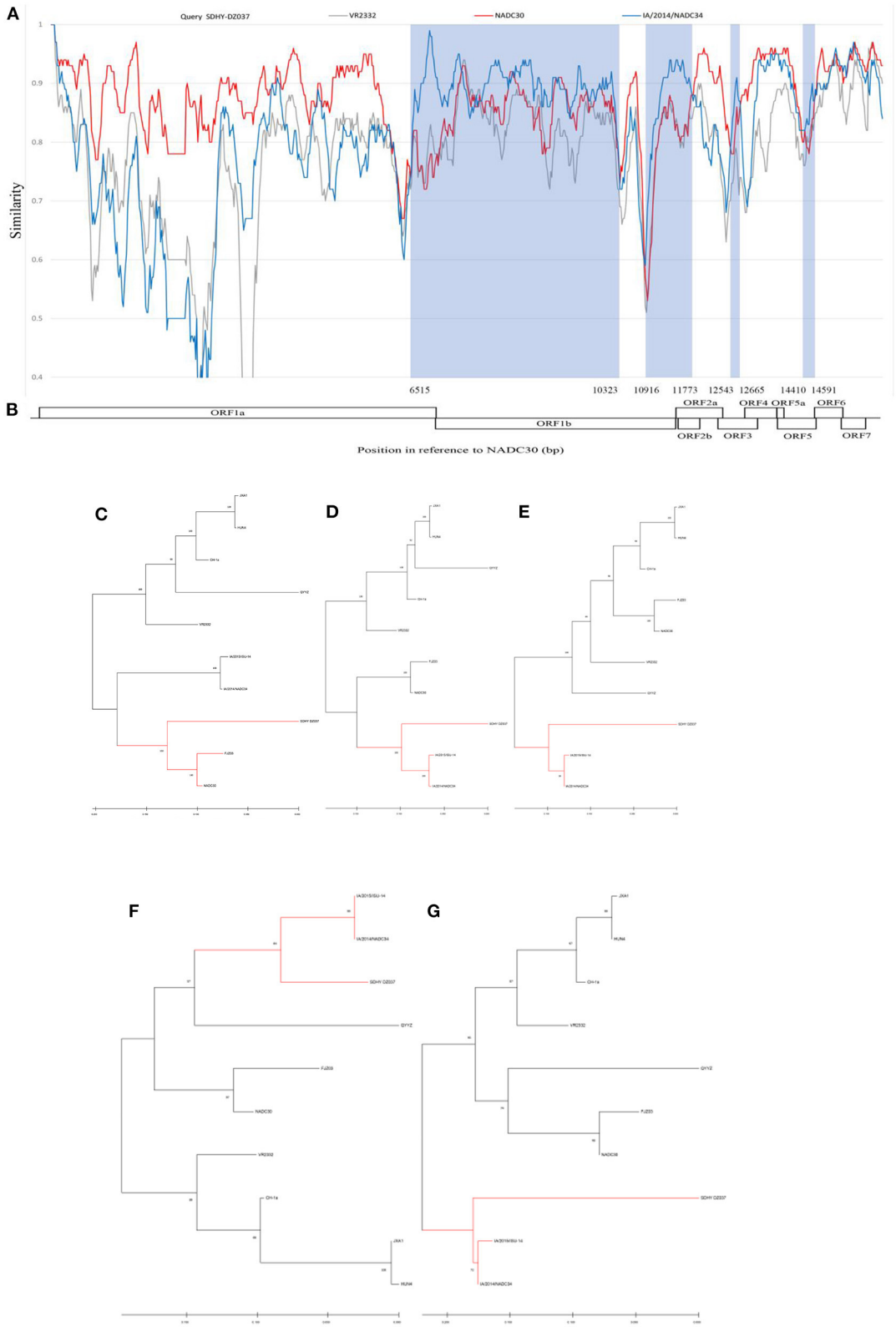

FIGURE 5
In this study, the PRRSV representative strains and SDHY-DZ037 were selected for genome-wide recombination analysis. Similarity maps were generated by the SimPlot v3.5 software **(A)**. The gene region corresponding to the SDHY-DZ037 recombination was shown with NADC30 (GenBank: JN654459.1) **(B)**. Phylogenetic tree based on full-length genome sequence **(C)**. Phylogenetic tree of the nucleotide recombination

(Continued)

FIGURE 5 (Continued)
region at positions 6,515–10,323 **(D)**. Phylogenetic tree of the nucleotide recombination region at positions 10,916–11,773 **(E)**. Phylogenetic tree of the nucleotide recombination region at positions 12,543–12,665 **(F)**. Phylogenetic tree of the nucleotide recombination region at positions 14,410–14,591 **(G)**. Evolutionary analysis of maximum likelihood performed in MEGA X. Multiple sequence alignments generated using Clustal W.

suspected sick pigs) were collected from pig farms of various sizes. The samples came from a wide array of sources, mainly Tai'an and the surrounding cities, and has covered pig farms of different scales in all cities of Shandong Province. A total of 342 samples were positive for PRRSV, giving a positive rate of 25.44%, showing that PRRSV is still one of the main pathogens threatening the swine industry in Shandong. Overall, 76 strains were isolated, of which 49 strains were NADC30-like, accounting for 64.47% of the isolated viruses. Fifteen strains were NADC34-like, representing 19.74% of the isolated viruses; 11 strains were CH-1a and HP-PRRSV-like, accounting for 14.47% of the isolated viruses; and 1 strain was VR2332-like and accounted for 1.32% of the isolated viruses. The NADC30-like strains remain the dominant strains in Shandong. This corresponds to the previous study (43).

The NADC34-like strain was first discovered in Liaoning in 2017 (18). To date, the prevalence of the NADC34-like strain has been reported in at least 10 provinces, including Heilongjiang, Liaoning, Henan, Hebei, Fujian, Jiangsu, Sichuan, Tianjin, and Shandong (24, 44). However, the prevalence of NADC34-like in Shandong Province is still unknown. We conducted an epidemiological survey of PRRSV in Shandong in 2020–2021. The study found that in 2020, NADC30-like strains accounted for 75.00% of PRRSV-positive samples and NADC34-like strains accounted for 15%. In 2021, NADC30-like strains accounted for 52.78% of PRRSV-positive samples and NADC34-like strains accounted for 25%. This indicates that the NADC34 strain is starting to show an epidemic trend in Shandong. One assumes that it could become the dominant strain in the years to come.

Analysis comparing the deduced amino acid loci of the ORF5 gene in the isolated strains and in some reference strains showed that the mutation $Q^{13} \rightarrow R^{13}$ was present in all viruses of Lineage 8, while the mutation $K^{151} \rightarrow R^{151}$ was absent in two viruses at amino acid position 151. SDHY-TA059 still had K at amino acid position 151, and SDHY-JN107 had the mutation $K^{151} \rightarrow Q^{151}$. It appears that some of the strong strains may have lost some of their strong virulence characteristics during the evolutionary process, thereby weakening their virulence (37). Two strains of Sublineage 1.8 showed mutations of $Q^{13} \rightarrow R^{13}$, as opposed to other strains. In addition, two strains of Sublineage 1.8, one strain of Lineage 5, and one strain of Sublineage 1.5 had mutations of $K^{151} \rightarrow R^{151}$. This indicated that certain mutations occur on specific sites during the continuous mutation of viruses. This may make it more virulent than other viruses of the same type. Mutations in the neutralizing epitope region may cause the virus to be insensitive to the neutralizing effect of vaccination and thus avoid it. In this study, 23 isolated strains showed mutations in the neutralizing region of the epitope, accounting for 30.26% of the isolates. These strains may be insensitive to vaccine immunization, which may be an important reason for the poor efficacy of the current PRRSV vaccine.

The $S^{137} \rightarrow A^{137}$ mutation occurred in three of the isolated strains, two of which were NADC34-like and one VR2332-like. It has been reported that amino acid 137 of GP5 was serine for wild strains and alanine for VR2332, MLV, and RespPRRS/Repro vaccine strains (38, 40, 41). Some scholars believe that A^{137} can be used to distinguish Lineage 5 and Lineage 1 (45). Among all the strains isolated in this study, the amino acid 137 of GP5 was mutated to alanine in three strains. The other strains were serine. The three mutated viruses are SDHY-HZ015, SDHY-DZ037, and SDHY-TA058. In this study, a genome-wide recombination of SDHY-DZ037 was analyzed by RDP4 and SimPlot software. The results showed that SDHY-DZ037 was found to be a recombinant strain of NADC30-like and NADC34-like strains but without recombinant VR2332. We speculated that perhaps amino acid position 137 of GP5 had mutated during the PRRSV epidemic. Therefore, perhaps A^{137} was no longer a specific amino acid site within VR2332, MLV, and RespPRRS/Repro vaccine strains, and A^{137} may no longer be suitable for distinguishing Lineage 1 and Lineage 5.

Conclusions

In summary, the NADC30-like strain remained the dominant epidemic strain of PRRSV in Shandong, China, in 2020–2021. It should be noted that NADC34-like strains have also been quite prevalent in this area. Some isolates had mutations in amino acids 13 and 151 of ORF5 and in the region of the neutralizing epitope (aa36–aa52), which may alter the virulence and increase the virus's ability to escape immunity.

Data availability statement

The datasets presented in this study can be found in online repositories. The names of the repository/repositories and accession number(s)can be found below: https://www.ncbi.nlm.nih.gov/genbank/, ON890168-ON890242 and OP168793.

Ethics statement

The animal study was reviewed and approved by the Animal Ethics Committee of Shandong Agricultural University.

Author contributions

Writing–original draft preparation was done by PL and YS. Writing–review and editing was done by BL, ML, and FM. Software was done by PL and YL. Investigation was done by JL, YZ, and TW. Funding acquisition was done by SL. All authors have read and agreed to the published version of the manuscript.

Funding

This study was funded by the Shandong Provincial Agricultural Major Application Technology Innovation Project (Establishment and Demonstration of Healthy Pig Breeding Technology Integration and Product Supply Chain Traceability System).

Conflict of interest

Author FM was employed by Huayun (Shandong) Inspection and Quarantine Service Co., Ltd.

The remaining authors declare that the research was conducted in the absence of any commercial or financial relationships that could be construed as a potential conflict of interest.

Publisher's note

All claims expressed in this article are solely those of the authors and do not necessarily represent those of their affiliated organizations, or those of the publisher, the editors and the reviewers. Any product that may be evaluated in this article, or claim that may be made by its manufacturer, is not guaranteed or endorsed by the publisher.

Supplementary material

The Supplementary Material for this article can be found online at: https://www.frontiersin.org/articles/10.3389/fvets.2022.987667/full#supplementary-material

References

1. Albina E. Epidemiology of porcine reproductive and respiratory syndrome (PRRS): an overview. *Vet Microbiol.* (1997) 55:309–16. doi: 10.1016/S0378-1135(96)01322-3

2. Guo A, Wu G, Gong W, Luo X, Zheng H, Jia H, et al. Outbreaks of highly pathogenic porcine reproductive and respiratory syndrome in Jiangxi province, China. *Ir Vet J.* (2012) 65:1–4. doi: 10.1186/2046-0481-65-14

3. Wang G, Yu Y, Cai X, Zhou EM, Zimmerman JJ. Effects of PRRSV infection on the porcine thymus. *Trends Microbiol.* (2020) 28:212–23. doi: 10.1016/j.tim.2019.10.009

4. Zimmerman JJ, Dee SA, Holtkamp DJ, Murtaugh MP, Stadejek T, Stevenson GW, et al. Porcine reproductive and respiratory syndrome viruses (porcine arteriviruses). In: *Diseases of Swine, 11th edn* (Hoboken, NJ: John Wiley) (2019). p. 685–708.

5. Guo B Q, Chen Z S, Liu W X, Cui Y Z. Isolation and identification of porcine reproductive and respiratory syndrome (PRRS) virus from aborted fetuses suspected of PRRS. *Chin J Anim Poult Infect Dis.* (1996) 2:117–24.

6. Stadejek T, Stankevicius A, Murtaugh MP, Oleksiewicz MB. Molecular evolution of PRRSV in Europe: current state of play. *Vet Microbiol.* (2013) 165:21–8. doi: 10.1016/j.vetmic.2013.02.029

7. Canelli E, Catella A, Borghetti P, Ferrari L, Ogno G, De Angelis E, et al. Phenotypic characterization of a highly pathogenic Italian porcine reproductive and respiratory syndrome virus (PRRSV) type 1 subtype 1 isolate in experimentally infected pigs. *Vet Microbiol.* (2017) 210:124–33. doi: 10.1016/j.vetmic.2017.09.002

8. Guo B, Lager KM, Henningson JN, Miller LC, Schlink SN, Kappes MA, et al. Experimental infection of United States swine with a Chinese highly pathogenic strain of porcine reproductive and respiratory syndrome virus. *Virology.* (2013) 435:372–84. doi: 10.1016/j.virol.2012.09.013

9. Li Y, Wang X, Bo K, Wang X, Tang B, Yang B, et al. Emergence of a highly pathogenic porcine reproductive and respiratory syndrome virus in the Mid-Eastern region of China. *Vet J.* (2007) 174:577–84. doi: 10.1016/j.tvjl.2007.07.032

10. Tian K, Yu X, Zhao T, Feng Y, Cao Z, Wang C, et al. Emergence of fatal PRRSV variants: unparalleled outbreaks of atypical PRRS in China and molecular dissection of the unique hallmark. *PLoS ONE.* (2007) 2:e526. doi: 10.1371/journal.pone.0000526

11. Tong GZ, Zhou YJ, Hao XF, Tian ZJ, An TQ, Qiu HJ. Highly pathogenic porcine reproductive and respiratory syndrome, China. *Emerg Infect Dis.* (2007) 13:1434–6. doi: 10.3201/eid1309.070399

12. Wu J, Li J, Tian F, Ren S, Yu M, Chen J, et al. Genetic variation and pathogenicity of highly virulent porcine reproductive and respiratory syndrome virus emerging in China. *Arch Virol.* (2009) 154:1589–97. doi: 10.1007/s00705-009-0478-6

13. Zhou F, Chang HT, Zhao J, Chen L, Wang XW, Liu HY, et al. Identification and molecular epidemiology of porcine reproductive and respiratory syndrome virus prevailing in Henan province from 2012 to 2013. *Chin J Vet Sci.* (2014) 9:1398–404. doi: 10.16303/j.cnki.1005-4545.2014.09.002

14. Li C, Zhuang J, Wang J, Han L, Sun Z, Xiao Y, et al. Outbreak Investigation of NADC30-Like PRRSV in South-East China. *Transbound Emerg Dis.* (2016) 63:474–9. doi: 10.1111/tbed.12530

15. Zhou L, Wang Z, Ding Y, Ge X, Guo X, Yang H. NADC30-like strain of porcine reproductive and respiratory syndrome virus, China. *Emerg Infect Dis.* (2015) 21:2256–7. doi: 10.3201/eid2112.150360

16. Guo Z, Chen XX Li X, Qiao S, Deng R, Zhang G. Prevalence and genetic characteristics of porcine reproductive and respiratory syndrome virus in central China during 2016-2017: NADC30-like PRRSVs are predominant. *Microb Pathog.* (2019) 135:103657. doi: 10.1016/j.micpath.2019.103657

17. Zhou L, Kang R, Yu J, Xie B, Chen C, Li X, et al. Genetic characterization and pathogenicity of a novel recombined porcine reproductive and respiratory syndrome virus 2 among Nadc30-Like, Jxa1-Like, and Mlv-like strains. *Viruses.* (2018) 10:551. doi: 10.3390/v10100551

18. Zhang HL, Zhang WL, Xiang LR, Leng CL, Tian ZJ, Tang YD, et al. Emergence of novel porcine reproductive and respiratory syndrome viruses (ORF5 RFLP 1-7-4 viruses) in China. *Vet Microbiol.* (2018) 222:105–8. doi: 10.1016/j.vetmic.2018.06.017

19. Song S, Xu H, Zhao J, Leng C, Xiang L, Li C, et al. Pathogenicity of NADC34-like PRRSV HLJDZD32-1901 isolated in China. *Vet Microbiol.* (2020) 246:108727. doi: 10.1016/j.vetmic.2020.108727

20. Xie CZ, Ha Z, Zhang H, Zhang Y, Xie YB, Zhang H, et al. Pathogenicity of porcine reproductive and respiratory syndrome virus (ORF5 RFLP 1-7-4 viruses) in China [published online ahead of print, 2020 Mar 18]. *Transbound Emerg Dis.* (2020) 10.1111/tbed.13549. doi: 10.1111/tbed.13549

21. Li C, Gong B, Sun Q, Xu H, Zhao J, Xiang L, et al. First Detection of NADC34-like PRRSV as a Main Epidemic Strain on a Large Farm in China. *Pathogens.* (2021) 11:32. doi: 10.3390/pathogens11010032

22. Xu H, Li C, Li W, Zhao J, Gong B, Sun Q, et al. Novel characteristics of Chinese NADC34-like PRRSV during 2020-2021 [published online ahead of print, 2022 Feb 19]. *Transbound Emerg Dis.* (2022) 10.1111/tbed.14485. doi: 10.1111/tbed.14485

23. Zhao HZ, Wang FX, Han XY, Guo H, Liu CY, Hou LN, et al. Recent advances in the study of NADC34-like porcine reproductive and respiratory syndrome virus in China. *Front Microbiol.* (2022) 13:950402. doi: 10.3389/fmicb.2022.950402

24. Yuan L, Zhu Z, Fan J, Liu P, Li Y, Li Q, et al. High pathogenicity of a Chinese NADC34-like PRRSV on Pigs [published online ahead of print, 2022 Jun 29]. *Microbiol Spectr.* (2022) e0154122. doi: 10.1128/spectrum.01541-22

25. Snijder EJ, Meulenberg JJ. The molecular biology of arteriviruses. *J Gen Virol.* (1998) 79:961–79. doi: 10.1099/0022-1317-79-5-961

26. Dokland T. The structural biology of PRRSV. *Virus Res.* (2010) 154:86–97. doi: 10.1016/j.virusres.2010.07.029

27. Jiang Y, Li G, Yu L, Li L, Zhang Y, Zhou Y, et al. Genetic diversity of Porcine Reproductive and Respiratory Syndrome Virus (PRRSV) From 1996 to 2017 in China. *Front Microbiol.* (2020) 11:618. doi: 10.3389/fmicb.2020.00618

28. Martin D, Rybicki E. RDP detection of recombination amongst aligned sequences. *Bioinformatics.* (2000) 16:562–3. doi: 10.1093/bioinformatics/16.6.562

29. Padidam M, Sawyer S, Fauquet CM. Possible emergence of new geminiviruses by frequent recombination. *Virology.* (1999) 265:218–25. doi: 10.1006/viro.1999.0056

30. Martin DP, Posada D, Crandall KA, Williamson C, A. modified bootscan algorithm for automated identification of recombinant sequences and recombination breakpoints. *AIDS Res Hum Retroviruses.* (2005) 21:98–102. doi: 10.1089/aid.2005.21.98

31. Posada D, Crandall KA. Evaluation of methods for detecting recombination from DNA sequences: computer simulations. *Proc Natl Acad Sci USA.* (2001) 98:13757–62. doi: 10.1073/pnas.241370698

32. Gibbs MJ, Armstrong JS, Gibbs AJ. Sister-scanning: a Monte Carlo procedure for assessing signals in recombinant sequences. *Bioinformatics.* (2000) 16:573–82. doi: 10.1093/bioinformatics/16.7.573

33. Smith JM. Analyzing the mosaic structure of genes. *J Mol Evol.* (1992) 34:126–9. doi: 10.1007/BF00182389

34. Lam HM, Ratmann O, Boni MF. Improved algorithmic complexity for the 3SEQ recombination detection algorithm. *Mol Biol Evol.* (2018) 35:247–51. doi: 10.1093/molbev/msx263

35. Boni MF, de Jong MD, van Doorn HR, Holmes EC. Guidelines for identifying homologous recombination events in influenza A virus. *PLoS ONE.* (2010) 5:e10434. doi: 10.1371/journal.pone.0010434

36. Lole KS, Bollinger RC, Paranjape RS, Gadkari D, Kulkarni SS, Novak NG, et al. Full-length human immunodeficiency virus type 1 genomes from subtype C-infected seroconverters in India, with evidence of intersubtype recombination. *J Virol.* (1999) 73:152–60. doi: 10.1128/JVI.73.1.152-160.1999

37. Fang K, Liu S, Li X, Chen H, Qian P. Epidemiological and genetic characteristics of porcine reproductive and respiratory syndrome virus in South China between 2017 and 2021. *Front Vet Sci.* (2022) 9:853044. doi: 10.3389/fvets.2022.853044

38. Yin B, Qi S, Sha W, Qin H, Liu L, Yun J, Zhu J, Li G, Sun D. Molecular characterization of the Nsp2 and ORF5 (ORF5a) genes of PRRSV strains in nine provinces of china during 2016-2018. *Front Vet Sci.* (2021) 8:605832. doi: 10.3389/fvets.2021.605832

39. Do DT, Park C, Choi K, Jeong J, Nguyen TT, Le DT, et al. Nucleotide sequence analysis of Vietnamese highly pathogenic porcine reproductive and respiratory syndrome virus from 2013 to 2014 based on the NSP2 and ORF5 coding regions. *Arch Virol.* (2016) 161:669–75. doi: 10.1007/s00705-015-2699-1

40. Wesley RD, Mengeling WL, Lager KM, Clouser DF, Landgraf JG, Frey ML. Differentiation of a porcine reproductive and respiratory syndrome virus vaccine strain from North American field strains by restriction fragment length polymorphism analysis of ORF 5. *J Vet Diagn Invest.* (1998) 10:140–4. doi: 10.1177/104063879801000204

41. Zhou L, Chen S, Zhang J, Zeng J, Guo X, Ge X, et al. Molecular variation analysis of porcine reproductive and respiratory syndrome virus in China. *Virus Res.* (2009) 145:97–105. doi: 10.1016/j.virusres.2009.06.014

42. Zhang HL. *Characteristic Analysis of Various Subgenotype PRRSV and Construction of DIVA Vaccine Strain. (Doctoral Dissertation, Chinese Academy of Agricultural Sciences).* Available online at: https://kns.cnki.net/KCMS/detail/detail.aspx?dbname=CDFDLAST2022&filename=1019108143.nh (accessed August 15, 2019).

43. Xue RX, Sun SF Li YG, Wang ML, Wang GS Li YJ, et al. Diversity of porcine reproductive and respiratory syndrome virus in Shandong, China. *Acta Virol.* (2021) 65:303–6. doi: 10.4149/av_2021_305

44. Sun YF, Liu Y, Yang J, Li WZ, Yu XX, Wang SY, Li LA, Yu H. Recombination between NADC34-like and QYYZ-like strain of porcine reproductive and respiratory syndrome virus with high pathogenicity for piglets in China [published online ahead of print, 2022 Feb 4]. *Transbound Emerg Dis.* (2022) 10.1111/tbed.14471. doi: 10.1111/tbed.14471

45. Kim J, Lee K, Rupasinghe R, Rezaei S, Martínez-López B, Liu X. Applications of machine learning for the classification of porcine reproductive and respiratory syndrome virus sublineages using amino acid scores of ORF5 gene. *Front Vet Sci.* (2021) 8:683134. doi: 10.3389/fvets.2021.683134

frontiers | Frontiers in Veterinary Science

TYPE Original Research
PUBLISHED 23 September 2022
DOI 10.3389/fvets.2022.998874

OPEN ACCESS

EDITED BY
Keisuke Suganuma,
Obihiro University of Agriculture and Veterinary Medicine, Japan

REVIEWED BY
Yimin Wang,
Henan Institute of Science and Technology, China
Muhammad Abid,
The Pirbright Institute, United Kingdom

*CORRESPONDENCE
Shanyuan Zhu
jsnm_zsy@126.com

SPECIALTY SECTION
This article was submitted to Veterinary Infectious Diseases, a section of the journal Frontiers in Veterinary Science

RECEIVED 20 July 2022
ACCEPTED 05 September 2022
PUBLISHED 23 September 2022

CITATION
Cao S, Lu H, Wu Z and Zhu S (2022) A duplex fluorescent quantitative PCR assay to distinguish the genotype I and II strains of African swine fever virus in Chinese epidemic strains.
Front. Vet. Sci. 9:998874.
doi: 10.3389/fvets.2022.998874

A duplex fluorescent quantitative PCR assay to distinguish the genotype I and II strains of African swine fever virus in Chinese epidemic strains

Shinuo Cao, Huipeng Lu, Zhi Wu and Shanyuan Zhu*

Jiangsu Key Laboratory for High-Tech Research and Development of Veterinary Biopharmaceuticals, Jiangsu Agri-animal Husbandry Vocational College, Taizhou, China

African swine fever (ASF) is a highly contagious hemorrhagic disease that affects domestic and wild pigs. A recent study reported that both ASF virus (ASFV) genotypes I and II have invaded farm-raised pigs in China, causing chronic infection and morbidity. To develop a duplex fluorescent quantitative PCR method to distinguish the ASFV genotypes I and II in Chinese epidemic strains, the probes and primers were designed based on the B646L sequences of genotypes I and II listed in the GenBank database. After optimizing the system, a duplex fluorescent quantitative PCR method for simultaneous detection of ASFV genotypes I and II B646L genes was successfully established. This method had no cross-reaction with Porcine circovirus type 2 (PCV2), Pseudorabies virus (PRV), or Porcine Parvovirus (PPV), indicating that it has strong specificity. The sensitivity results indicated that the minimum detection limit of ASFV genotypes I and II B646L was 10 copies/Rxn. The inter- and intra-group coefficients of variation were both <3%, indicating that the method was highly reproducible. Therefore, the established duplex fluorescent quantitative PCR assay is important for the differential detection and epidemiological investigation of ASFV.

KEYWORDS

diagnosis, fluorescent quantitative PCR, TaqMan probe, African swine fever virus genotype I, African swine fever virus genotype II

Introduction

African swine fever (ASF) is a fatal hemorrhagic swine disease that is highly contagious in all ages of pigs with high morbidity and mortality (1, 2). ASF virus (ASFV) is an enveloped, icosahedral, structurally complex, double-stranded DNA virus (3, 4). The disease is listed as a notifiable terrestrial and aquatic animal disease by the World Organization for Animal Health (OIE). The highly virulent ASFV isolates induce a peracute and acute disease characterized by hemorrhages in the skin and internal organs, loss of appetite and high fever. The mortality rate among pigs of all ages can be as high as 100%, and high mortality is an indicator of ASF. A less virulent strain produces mild

clinical signs, such as slight fever, reduced appetite, and depression, that are often mistaken for other conditions in pigs and may lead to an incorrect diagnosis of ASF. Non-hemadsorbing avirulent strains cause subclinical non-hemorrhagic infections and seroconversion, although some animals may develop discrete lesions in the lungs or in the skin near bone-to-skin contact (5). The clinical course of ASF is typically acute or subacute. Subacute or chronic manifestations are more likely when less virulent strains are involved.

Since 1921, African swine fever has been endemic in many countries in Sub-Saharan Africa, particularly in Kenya. Consequently, it threatens food security and the livelihoods of poor and marginalized communities that raise domestic pigs as a means of subsistence (6–8). From Georgia in 2007, ASF spread to the Caucasus region and then to the European continent following its introduction in 2007 (9). A pig farm in Shenyang city in Liaoning Province reported the first ASF outbreak in mainland China in August 2018 (10). The virus has since rapidly spread to 32 provinces, autonomous regions, and municipalities, resulting in heavy losses for the pig industry and other related industries. In addition to the prevalence and direct economic losses from ASF, there have also been significant economic and social impacts, including restrictions on the transportation of pigs and pork products, restrictions on the slaughtering trade, insufficient supply of pork products, rising unemployment, and restrictions on global trade (11). There is no effective vaccine or treatment for controlling the spread of the disease in China at the moment.

According to the 3′-end sequences of the B646L gene that encodes p72, various genotypes of ASFV can be distinguished (12, 13). In Africa, at least 24 genotypes of ASF are naturally circulating. It is believed that all cases of ASFV spreading into Asia and Europe since 2007 are a result of a single epidemic of genotype II (14–16). An acute onset of infection caused by genotype I ASFV was first detected in Portugal outside Africa in 1957 (17). In China, the first ASFV isolates were grouped with genotype II based on sequence analysis (11, 18). China reported the emergence of genotype I ASFV and genotype II less virulent ASFV in 2021. Two strains, ASFV HeN/ZZ-P1/21 and SD/DY-I/21, with no porcine erythrocyte adsorption activity, were isolated from clinically infected pigs from Shandong and Henan farms (19). Genome-wide evolutionary analysis showed that these two strains were highly similar to the low-lethal genotype I strains NH/P68 and OURT88/3 isolated from Portugal in the last century. Both strains were quite different from the virulent genotype I strains L60 and Benin 97 isolated from Europe and Africa. It is generally recognized that ASF is a contagious and lethal disease, but if chronic infections spread, disease control will become more difficult.

Field identification of ASFV has become more challenging due to the emergence of genotype I ASFV in China. Although the fatality rate of this virus is low, it can cause chronic infection and morbidity in pigs. The virus has strong horizontal transmission ability in pigs. We developed a duplex fluorescent quantitative PCR assay for the differential detection of ASFV genotype I and II strains in this study. The method uses two different fluorescence signals derived from two differently labeled probes to differentiate ASFV genotype I and II strains simultaneously. As this assay has a short processing time, is relatively inexpensive and highly accurate. This approach described above should be generalizable and useful for dealing with these issues.

Materials and methods

Primers and probes

Beacon Designer 7.9 software was applied to design gene-specific probes and primers according to the B646L sequence of the P72 protein coding genes of ASFV Pig/HLJ/2018 (MK333180), DB/LN/2018 (MK333181), SD/DY-I/21 (MZ945537), and HeN/ZZ-P1/21 (MZ945536) strains published in GenBank. The primers ASFV-F3 (5′-GGG GAT AAA ATG ACT GGA TA-3′) and ASFV-R3 (5′-CAT CGG TAA GAA TAG GTT TG-3′) can be used for detection of both genotype I and II strains in Chinese epidemic strains. Based on an alignment of all ASFV strains, the primers were designed based on the conserved B646L regions of the genome. Sequence alignment was performed on the National Center for Biotechnology Information (NCBI) website (http://www.ncbi.nlm.nih.gov/BLAST/) (Figure 1). TaqMan probes, FAM-ASFV-T1-3 (FAM-5′-CACCTCCCTGCAGTCCCA-3′-NFQ-MGB) and VIC-ASFV-T2-3 (VIC-5′-CAC TTG GTT GGC CA-3′-NFQ-MGB), were designed to differentiate the genotype I strains from genotype II strains. The primers and probe sequences above were identified as ASFV-specific sequences by BLAST analysis. All probes and primers were synthesized by Tsingke Biotechnology Co., Ltd (Beijing, China).

Viral genomic DNA extraction

Briefly, the genomic DNA was extracted from pseudorabies live vaccine (Bartha-K61 strain), porcine parvovirus disease live vaccine (WH-1), and inactivated porcine circovirus type 2 vaccine (LG) using a viral DNA extraction kit (Omega, Norcross, GA, USA). The DNA was eluted in an equal volume of elution buffer.

Positive standards

The standard plasmids pUC57-ASFV-B646L-T1 and pUC57-ASFV-B646L-T2 were synthesized and sequenced by Tsingke Biotechnology Co., Ltd. Sequencing comparison indicated that the plasmid sequence was completely consistent

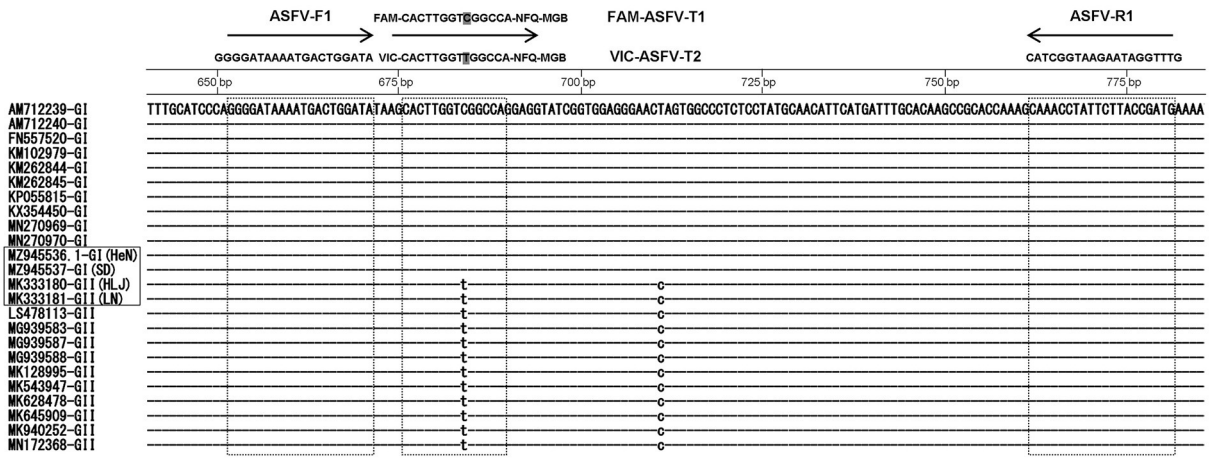

FIGURE 1
Nucleotide sequence alignment of B646L genes of African swine fever virus (ASFV) genotypes I and II with indicated position primers and TaqMan probes: ASFV-F1 primer, ASFV-S1 primer, FAM-ASFV-T1 probe and VIC-ASFV-T2 probe.

TABLE 1 Comparison of the efficiencies of the primer/probe sets of the duplex fluorescence quantitative PCR.

Schemes	ASFV genotype I				ASFV genotype II			
	Probe 1		Probe 2		Probe 1		Probe 2	
	C_T value	Mean value	C_T value	Mean value	C_T value	Mean value	C_T value	Mean value
Set 1	31.004	30.934	-	-	35.519	35.516	31.059	31.187
	30.809		-		35.421		31.534	
	30.989		-		35.607		30.968	
Set 2	30.985	30.961	-	-	44.577	43.548	32.127	32.092
	30.969		-		43.588		32.165	
	30.928		-		42.479		31.985	
Set 3	31.279	31.371	-	-	-	-	31.680	31.652
	31.290		-		-		31.427	
	31.545		-		-		31.850	

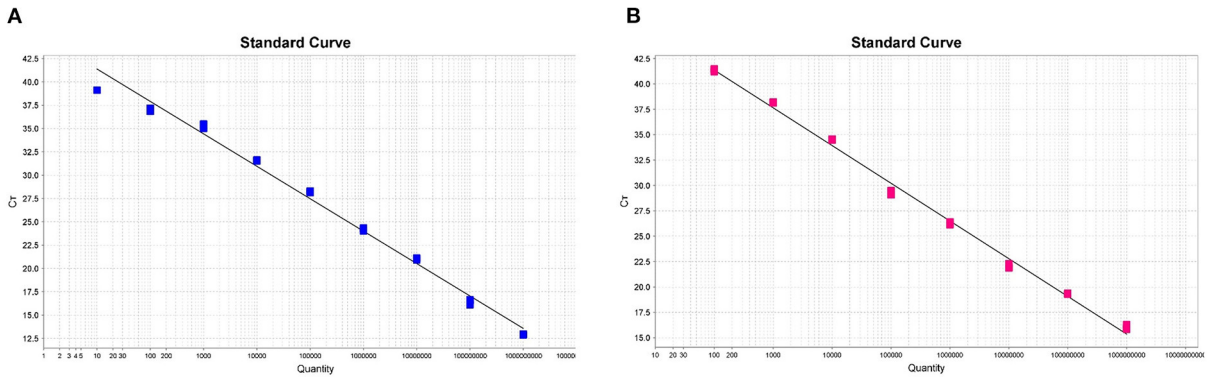

FIGURE 2
The standard curves of the dual fluorescent quantitative PCR for ASFV genotype I **(A)** and II **(B)** in Chinese epidemic strains. Based on the mean of Ct values against log10 of 10-fold serial dilutions of the synthesized plasmids pUC57-ASFV-B646L-T1 and pUC57-ASFV-B646L-T2.

with the B646L gene sequences of Pig/HLJ/2018 (MK333180) and SD/DY-I/21 (MZ945537) published in GenBank. Concentration of each DNA sample was measured using a spectrophotometer (Nanodrop-2000, Thermo Fisher Scientific, Waltham, MA, USA), and the number of copies was calculated. The plasmid was serially diluted 10-fold from 1×10^8 to 1×10^2 copies/Rxn and stored until use at −30 °C.

Specificity of primers

Specificity of primers was detected by common PCR methods, and the prepared primers were used to identify the synthesized plasmid pUC57-ASFV-B646L. The reaction system volume was 20 μL: 0.25 μL LA Taq enzyme, 10 μL 2×GC Buffer, 2 μL dNTP, 0.5 μL upstream and downstream primers, 1 μL plasmid, and ddH_2O added for a total volume of 20 μL. The electrophoresis results were observed and photographed under a UV transilluminator.

Optimization of the duplex fluorescent quantitative PCR

The equal volumes of both FAM-ASFV-T1 and VIC-ASFV-T2 were mixed in the same PCR tube containing pUC57-ASFV-B646L-T1 and pUC57-ASFV-B646L-T2 plasmids. The dual multiplex fluorescent quantitative PCR was performed by QuantStudio™ 3 (Thermo Fisher Scientific, Waltham, MA, USA). A set of primer and probe concentrations was optimized according to the final fluorescent signal values. The dual multiplex fluorescent quantitative PCR was performed as follows: 20 μL reaction mixture contained 0.5 μL of FAM-ASFV-T1 and VIC-ASFV-T2 (10 μM), 1 μL of ASFV-F1 and ASFV-R1 (10 μM), 2 μL of DNA, and 10 μL of Premix Ex Taq Probe qPCR (TaKaRa, Shiga, Japan). Annealing temperatures were set to 58, 59, 60, 61, 62, and 63°C *via* a temperature gradient. In this study, the amplification curve's cycle threshold (CT) value was defined as the number of cycles at which the curve reaches its threshold. Samples were considered positive if the CT value remained above the cutoff.

The sensitivity, specificity and reproducibility of this assay

The following tests were conducted under optimized experimental conditions. This set of primers, probe and the plasmids pUC57-ASFV-B646L-T1, pUC57-ASFV-B646L-T2, or three non-ASFVs (PCV2, PPV, and PRV) were tested by the dual fluorescent quantitative PCR for evaluating the specificity of the assay. In addition, analytical sensitivity of the dual fluorescent quantitative PCR assay was tested using serially diluted positive standards. In addition, the copy number was taken into account when determining sensitivity. The repeatability (intra-assay) and reproducibility (inter-assay) of the dual fluorescent quantitative PCR assay was tested using the positive standards. We performed several batches of these experiments on different days, with three biological replicates per batch.

Comparison of the duplex fluorescent quantitative PCR assay and ASFV UPL PCR

The standard plasmids were used as templates both in the real-time assay as described above and in an ASFV UPL PCR assay developed by Fernández-Pinero et al. (20). Comparing the two methods for detecting ASFV was carried out. Supplementary Table 2 summarizes the original sources and sequences of the primers and probes used in this study.

Results

Screening of primers and probes to distinguish ASFV genotype I and II strains by the duplex fluorescent quantitative PCR for Chinese epidemic strains

Based on FAM fluorescence signal (specific for ASFV genotype I) and VIC (specific for ASFV genotype II strain), three primer/probe sets were screened to distinguish ASFV genotype I and II strain by duplex fluorescent quantitative PCR for Chinese epidemic strains. The results revealed that the primer/probe sets 1 and 2 could not distinguish the ASFV genotype I and genotype II strains, while the primer/probe set 3 could detect and distinguish the two strains simultaneously, and with higher sensitivity (Table 1). Therefore, the primer/probe set 3 was used in subsequent experiments.

The standard curves in the duplex fluorescent quantitative PCR assay

In order to generate the duplex amplification curves and the fluorescent quantitative PCR standard curves, we used successively diluted known copy numbers of pUC57-ASFV-B646L-T1 and pUC57-ASFV-B646L-T2 for fluorescent quantitative PCR reaction under the optimized conditions. As shown in Figures 2A,B, the standard curves were linear in the range of 1×10^9 to 1×10^1 copies for the ASFV genotype I strain and in the range of 1×10^9 to 1×10^2 copies for the genotype II strain. The trendline for the genotype I strain showed a high degree of linearity ($R^2 = 0.989$) (Figure 2A). The standard curve slope was −3.318, and the slope of intercept was 41.132. The regression formula for the standard curve was y =

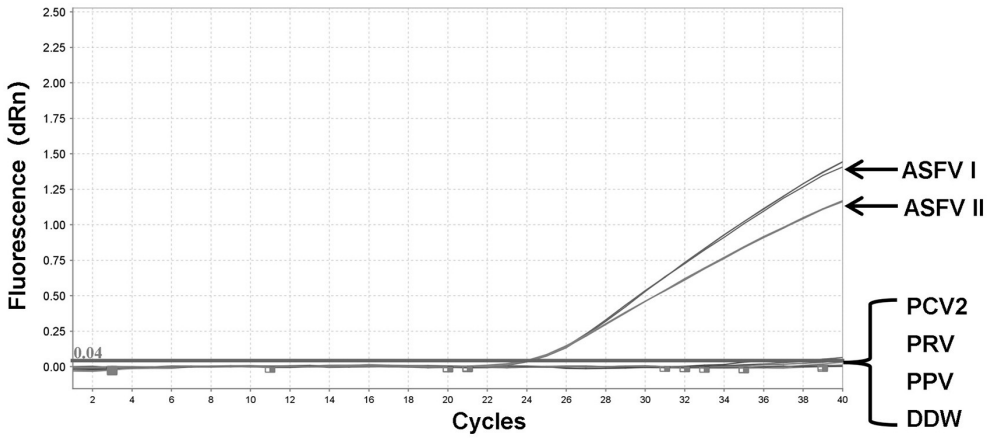

FIGURE 3
Specificity of the dual fluorescent quantitative PCR. No detection signal was obtained for Porcine circovirus type 2 (PCV2), Pseudorabies virus (PRV), or Porcine Parvovirus (PPV).

TABLE 2 Repeatability evaluation of the duplex real-time PCR for intra-assay and inter-assay variation.

Dilution (copies/Rxn)	P72 gene of ASFV genotype I				P72 gene of ASFV genotype II			
	intra-assay variation[a]		inter-assay variation[b]		intra-assay variation[a]		inter-assay variation[b]	
	(C_T)[c]	CV (%)	(C_T) [c]	CV (%)	(C_T) [c]	CV (%)	(C_T) [c]	CV (%)
10^4	31.776 ± 0.080	0.252	32.157 ± 0.378	1.139	29.502 ± 0.210	0.712	28.624 ± 0.218	0.763
10^5	28.736 ± 0.119	0.414	27.705 ± 0.753	2.717	26.150 ± 0.116	0.444	25.041 ± 0.673	2.687
10^6	24.842 ± 0.032	0.129	22.694 ± 0.312	1.375	22.958 ± 0.083	0.362	20.967 ± 0.456	2.175

[a]Intra-assay variation was detemined on three repicates of recombinant plasmid dilutions analyzed in the same PCR run.
[b]Inter-assay variation was calculated on values obtained in three separate PCR runs.
[c]Mean ± standard deviation (SD).
CV coefficient of variation.

$-3.318x + 41.132$. The trendline for genotype II strain showed a high degree of linearity ($R^2 = 0.995$) (Figure 2B). The standard curve slope was −3.713, and the slope of intercept was 48.787. The regression formula for the standard curve was $y = -3.713x + 48.787$. The duplex fluorescent quantitative PCR amplification efficiencies for the two targets were 100.160% (for genotype I) and 95.907% (for genotype II).

Specificity of the duplex fluorescent quantitative PCR assay

To validate the integrity of the extracted DNA, conventional PCRs were performed using the genes of three other porcine DNA viruses (PCV2, PRV, and PPV) (Supplementary Figure 1). The genomic DNA of PCV2, PRV, PPV, pUC57-ASFV-B646L-T1, and pUC57-ASFV-B646L-T2 plasmids was tested by fluorescent quantitative PCR assays. No specific signals were visible on the two channels for several non-ASFV porcine DNA viruses, including PCV2, PRV, and PPV, while the ASFV genotypes I and II could be distinguished correctly (Figure 3).

Sensitivity of the duplex fluorescent quantitative PCR assay

The sensitivity of the assay was evaluated using the standard plasmids ranging from 1×10^9 to 1×10^1 copies/Rxn. In a fluorescent quantitative PCR assay, the 10-fold serial dilutions of the standard plasmids were simultaneously detected. Detection limits of the fluorescent quantitative PCR were 10 copies/Rxn and 100 copies/Rxn for ASFV genotype I and genotype II, respectively.

Reproducibility of the duplex fluorescent quantitative PCR assay

Reproducibility of the assay was determined by examining whether ASFV genotypes I and genotype II could be distinguished between different inter- assay and intra-assay runs. The intra-assay and inter-assay variation of CT values was measured. As shown in Table 2, the developed method

had good repeatability and stability. The intra-assay CV values of the fluorescent quantitative PCR ranged from 0.129 to 0.252% for ASFV genotype I and from 0.362 to 0.712% for ASFV genotype II. For comparison, ASFV UPL PCR was also performed on three concentrations of ASFV genotype I and II P72 positive plasmids used in the validation assay. The findings of this experiment for comparison of the duplex real-time PCR with ASFV UPL PCR are summarized in Supplementary Table 1.

Discussion

Since 2018, the first occurrence of ASF in China and a number of other countries has resulted in tremendous economic losses to the pig and related industries. A rapid and accurate diagnostic method is conducive to the early detection and control of ASFV. Recent studies have demonstrated that genotype I ASFV has invaded Chinese pigs, causing chronic infection and morbidity. Two ASFV isolates, HeN/ZZ-P1/21 and SD/DY-I/21, with no porcine erythrocyte adsorption activity were isolated from clinically infected pigs in Shandong and Henan provinces, respectively. Genome-wide evolutionary analysis showed that these two strains were highly similar to the low-lethal genotype I strains OURT88/3 and NH/P68 isolated from Portugal in the last century. They were quite different from the virulent genotype I strains L60 and Benin 97 isolated from Europe and Africa. Although the fatality rate from the genotype I strain is low, it can cause chronic infection and morbidity in pigs. The virus has strong horizontal transmission ability in pigs. Due to the slow course and various clinical manifestations caused by the infection, this strain results in more hidden prevalence, making early diagnosis difficult and presenting new challenges in the prevention and control of ASF. Therefore, effective countermeasures are needed as soon as possible.

Currently, there is no effective vaccine for ASFV in China, thus, the prevention and control of ASFV rely on monitoring and elimination of the virus. Among various established methods for the detection of ASFV, the HAD test can obtain accurate detection results within 24 h for high-potency ASFV, but it takes at least 6 days to determine a negative result. The test is often negative for low-virulence ASFV, and is thus unsuitable for rapid detection. ASFV antigen detection by ELISA is fast and accurate, but the detection sensitivity is low, because the low virus titer in subacute and chronically infected pigs, and false negative results tend to occur. TaqMan fluorescent quantitative PCR, as a specific, sensitive, and efficient detection method, has the advantage of early detection, thus facilitating early culling and reducing economic losses.

The molecular diagnostic techniques used in the diagnosis of ASF are conventional PCR assay (21) and fluorescent quantitative PCR assays (22), both of which are OIE recommended diagnostic methods. Although these methods have been widely used as two basic techniques to detect ASFV infections in the field, but they are not sensitive enough to observe only trace amounts of ASFV-positive samples. Also, they are not able to distinguish between the ASFV genotype I and II strain infections. In this report, a duplex fluorescent quantitative PCR assay was established based on B646L gene. This method can distinguish the ASFV genotypes I and II. It did not cross-react with PCV2, PRV, or PPV, and the assay had high specificity. The minimum number of tests for this method is 10 copies/Rxn. The TaqMAN-MGB probe based on the ASFV CP530R gene established by Wang Jianhua et al. and the fluorescent quantitative PCR based on ASFV B646L gene established by Zhang Quan et al. could detect at least 61 copies, and results with a minimum of 20 copies were with highly sensitive. The results are similar to those obtained using the K205R gene based on fluorescent quantitative PCR established by Guo Shaoping et al. that has a minimum detection volume of 10 copies and has high sensitivity. The coefficients of variation of repeatability tests between and within groups were all $<0.712\%$. The results showed that the method had good repeatability. Therefore, the TaqMan fluorescent quantitative fluorescence quantitative method based on the ASFV p72 protein coding gene B646L established in this study is a specific, sensitive, and efficient detection method that can be applied in clinical practice.

Conclusion

In summary, a new duplex fluorescent quantitative PCR method using TaqMan probe was developed, allowing simultaneous and differential detection of ASFV genotypes I and II with a rapid, sensitive, specific and reproducible capability. The developed method will contribute to the prevention and control of ASF in China.

Data availability statement

The original contributions presented in the study are included in the article/Supplementary material, further inquiries can be directed to the corresponding author.

Author contributions

SC and SZ conceived and designed the study. SC wrote the manuscript. SZ critically revised the

manuscript. SC, HL, and ZU performed the majority of the experiments. All authors read and approved the final manuscript.

Funding

This work was supported by a grant from the key project of Jiangsu Province's Key Reseach and Development plan (modern Agriculture) (BE2020407), the project of Jiangsu Agri-animal Husbandry Vocational College (NSF2022CB04, NSF2022CB25), and 2020 Taizhou Science and Technology Support Plan (Agriculture) Project (TN202001).

Conflict of interest

The authors declare that the research was conducted in the absence of any commercial or financial relationships that could be construed as a potential conflict of interest.

Publisher's note

All claims expressed in this article are solely those of the authors and do not necessarily represent those of their affiliated organizations, or those of the publisher, the editors and the reviewers. Any product that may be evaluated in this article, or claim that may be made by its manufacturer, is not guaranteed or endorsed by the publisher.

Supplementary material

The Supplementary Material for this article can be found online at: https://www.frontiersin.org/articles/10.3389/fvets.2022.998874/full#supplementary-material

References

1. Wardley RC, de M Andrade C, Black DN, de Castro Portugal FL, Enjuanes L, Hess WR, et al. African swine fever virus brief review. *Arch Virol.* (1983) 76:73–90. doi: 10.1007/BF01311692

2. Karger A, Pérez-Núñez D, Urquiza J, Hinojar P, Alonso C, Freitas FB, et al. An update on African swine fever virology. *Viruses.* (2019) 11:864. doi: 10.3390/v11090864

3. Wang Y, Kang W, Yang W, Zhang J, Li D, Zheng H. Structure of African swine fever virus and associated molecular mechanisms underlying infection and immunosuppression: a review. *Front Immunol.* (2021) 12:715582. doi: 10.3389/fimmu.2021.715582

4. Galindo I, Alonso C. African swine fever virus: a review. *Viruses.* (2017) 9:103. doi: 10.3390/v9050103

5. Blome S, Franzke K, Beer M. African swine fever - a review of current knowledge. *Virus Res.* (2020) 287:198099. doi: 10.1016/j.virusres.2020.198099

6. Wirsching M. Family therapy approach by the pediatric oncology treatment team. *Klin Padiatr.* (1988) 200:279–82. doi: 10.1055/s-2008-1033722

7. Mulumba-Mfumu LK, Saegerman C, Dixon LK, Madimba KC, Kazadi E, Mukalakata NT, et al. African swine fever: update on Eastern, Central and Southern Africa. *Transbound Emerg Dis.* (2019) 66:1462–80. doi: 10.1111/tbed.13187

8. Penrith ML, Bastos AD, Etter E, Beltrán-Alcrudo D. Epidemiology of African swine fever in Africa today: Sylvatic cycle versus socio-economic imperatives. *Transbound Emerg Dis.* (2019) 66:672–86. doi: 10.1111/tbed.13117

9. Costard S, Zagmutt FJ, Porphyre T, Pfeiffer DU. Small-scale pig farmers' behavior, silent release of African swine fever virus and consequences for disease spread. *Sci Rep.* (2015) 5:17074. doi: 10.1038/srep17074

10. Li X, Tian K. African swine fever in China. *Vet Rec.* (2018) 183:300–1. doi: 10.1136/vr.k3774

11. Zhao D, Liu R, Zhang X, Li F, Wang J, Zhang J, et al. Replication and virulence in pigs of the first African swine fever virus isolated in China. *Emerg Microbes Infect.* (2019) 8:438–47. doi: 10.1080/22221751.2019.1590128

12. Qu H, Ge S, Zhang Y, Wu X, Wang Z. A systematic review of genotypes and serogroups of African swine fever virus. *Virus Genes.* (2022) 58:77–87. doi: 10.1007/s11262-021-01879-0

13. Bastos AD, Penrith ML, Crucière C, Edrich JL, Hutchings G, Roger F, et al. Genotyping field strains of African swine fever virus by partial p72 gene characterisation. *Arch Virol.* (2003) 148:693–706. doi: 10.1007/s00705-002-0946-8

14. Gallardo C, Fernández-Pinero J, Pelayo V, Gazaev I, Markowska-Daniel I, Pridotkas G, et al. Genetic variation among African swine fever genotype II viruses, eastern and central Europe. *Emerg Infect Dis.* (2014) 20:1544–7. doi: 10.3201/eid2009.140554

15. Achenbach JE, Gallardo C, Nieto-Pelegrín E, Rivera-Arroyo B, Degefa-Negi T, Arias M, et al. Identification of a new genotype of African swine fever virus in domestic pigs from Ethiopia. *Transbound Emerg Dis.* (2017) 64:1393–404. doi: 10.1111/tbed.12511

16. Quembo CJ, Jori F, Vosloo W, Heath L. Genetic characterization of African swine fever virus isolates from soft ticks at the wildlife/domestic interface in Mozambique and identification of a novel genotype. *Transbound Emerg Dis.* (2018) 65:420–31. doi: 10.1111/tbed.12700

17. Rowlands RJ, Michaud V, Heath L, Hutchings G, Oura C, Vosloo W, et al. African swine fever virus isolate, Georgia, 2007. *Emerg Infect Dis.* (2008) 14:1870–4. doi: 10.3201/eid1412.080591

18. Zhou X, Li N, Luo Y, Liu Y, Miao F, Chen T, et al. Emergence of African swine fever in China, 2018. *Transbound Emerg Dis.* (2018) 65:1482–4. doi: 10.1111/tbed.12989

19. Sun E, Huang L, Zhang X, Zhang J, Shen D, Zhang Z, et al. Genotype I African swine fever viruses emerged in domestic pigs in China and caused chronic infection. *Emerg Microbes Infect.* (2021) 10:2183–93. doi: 10.1080/22221751.2021.1999779

20. Fernández-Pinero J, Gallardo C, Elizalde M, Robles A, Gómez C, Bishop R, et al. Molecular diagnosis of African swine fever by a new real-time PCR using universal probe library. *Transbound Emerg Dis.* (2013) 60:48–58. doi: 10.1111/j.1865-1682.2012.01317.x

21. Agüero M, Fernández J, Romero L, Sánchez Mascaraque C, Arias M, Sánchez-Vizcaíno JM. Highly sensitive PCR assay for routine diagnosis of African swine fever virus in clinical samples. *J Clin Microbiol.* (2003) 41:4431–4. doi: 10.1128/JCM.41.9.4431-4434.2003

22. King DP, Reid SM, Hutchings GH, Grierson SS, Wilkinson PJ, Dixon LK, et al. Development of a TaqMan PCR assay with internal amplification control for the detection of African swine fever virus. *J Virol Methods.* (2003) 107:53–61. doi: 10.1016/S0166-0934(02)00189-1

frontiers | Frontiers in Veterinary Science

TYPE Original Research
PUBLISHED 03 October 2022
DOI 10.3389/fvets.2022.1015717

OPEN ACCESS

EDITED BY
Lian-Feng Li,
Harbin Veterinary Research Institute (CAAS), China

REVIEWED BY
Aibing Wang,
Hunan Agricultural University, China
Yuexiu Zhang,
The Ohio State University, United States

*CORRESPONDENCE
Ning Li
sdtaianlining@126.com
Fanliang Meng
18754875921@163.com
Mengda Liu
liumengda@cahec.cn

†These authors have contributed equally to this work and share first authorship

SPECIALTY SECTION
This article was submitted to Veterinary Infectious Diseases, a section of the journal Frontiers in Veterinary Science

RECEIVED 10 August 2022
ACCEPTED 29 August 2022
PUBLISHED 03 October 2022

CITATION
Shen Y, Yang Y, Zhao J, Geng N, Liu K, Zhao Y, Wang F, Liu S, Li N, Meng F and Liu M (2022) Molecular epidemiological survey of porcine epidemic diarrhea in some areas of Shandong and genetic evolutionary analysis of S gene. *Front. Vet. Sci.* 9:1015717. doi: 10.3389/fvets.2022.1015717

Molecular epidemiological survey of porcine epidemic diarrhea in some areas of Shandong and genetic evolutionary analysis of S gene

Yesheng Shen[1†], Yudong Yang[1†], Jun Zhao[1], Ningwei Geng[1], Kuihao Liu[1], Yiran Zhao[1], Fangkun Wang[1], Sidang Liu[1], Ning Li[1*], Fanliang Meng[1,2*] and Mengda Liu[3*]

[1]School of Animal Science and Technology, Shandong Agricultural University, Tai'an, China, [2]Huayun (Shandong) Inspection and Quarantine Service Co., Tai'an, China, [3]Division of Zoonoses Surveillance, China Animal Health and Epidemiology Center, Qingdao, China

Responsible for the acute infectious disease porcine epidemic diarrhea (PED), PED virus (PEDV) induces severe diarrhea and high mortality in infected piglets and thus severely harms the productivity and economic efficiency of pig farms. In our study, we aimed to investigate and analyze the recent status and incidence pattern of PEDV infection in some areas of Shandong Province, China. We collected 176 clinical samples of PED from pig farms in different regions of Shandong Province during 2019–2021. PEDV, TGEV, and PORV were detected using RT-PCR. The full-length sequences of positive PEDV S genes were amplified, the sequences were analyzed with MEGA X and DNAStar, and a histopathological examination of typical PEDV-positive cases was performed. RT-PCR revealed positivity rates of 37.5% (66/176) for PEDV, 6.82% (12/176) for transmissible gastroenteritis virus, and 3.98% (7/176) for pig rotavirus. The test results for the years 2019, 2020, and 2021 were counted separately, PEDV positivity rates for the years were 34.88% (15/43), 39.33% (35/89), and 36.36% (16/44), respectively. Histopathological examination revealed atrophied, broken, and detached duodenal and jejunal intestinal villi, as typical of PED, and severe congestion of the intestinal submucosa. Moreover, the results of our study clearly indicate that the G2 subtype is prevalent as the dominant strain of PEDV in Shandong Province, where its rates of morbidity and mortality continue to be high. Based on a systematic investigation and analysis of PEDV's molecular epidemiology across Shandong Province, our results enrich current epidemiological data regarding PEDV and provide some scientific basis for preventing and controlling the disease.

KEYWORDS

porcine epidemic diarrhea, epidemiological survey, S gene, genetic evolutionary analysis, prevention and control

Introduction

Porcine epidemic diarrhea (PED) is a common viral disease in raising pigs, one with high morbidity, high mortality, and complex causes that are difficult to control (1–4). Among piglets up to 3 months old, PED is especially problematic, with a prevalence of up to 70%. Nevertheless, epidemiological information on PED in large-scale pig farms in recent years in Shandong Province is currently lacking.

PED virus (PEDV), a member of the genus A coronavirus in the Coronaviridae family, is a linear single-stranded, positive-strand RNA virus ∼28 kb in length (5). In the virus, ORF4, ORF5, and ORF6 encode four structural proteins—the spine (S) protein, the envelope (E) protein, the membrane (M) protein, and the nucleocapsid (N) protein (6, 7)—among which S proteins, due to their high genetic variability, are often used as markers for phylogenetic analysis and epidemiological investigations (8). Based on the genetic characteristics of the PEDV S gene, it is often divided into two subtypes: G1 and G2 (9–11). Between them, the G2 subtype is the more prevalent genotype of PED in China, whereas the more commonly used vaccine strain CV777 is of the G1 subtype (12, 13).

In our study, we collected 176 clinical samples of PED from pig farms in different regions of In Shandong Province, China during 2019–2021 in order to investigate the prevalence of PEDV there. We performed phylogenetic analysis, comparative nucleotide analysis, and comparative analysis of deduced amino acid sequences with the aim of clarifying the epidemiology of PEDV in Shandong Province.

Materials and methods

Sample collection and processing

During 2019–2021, we collected 176 intestinal and fecal samples from pigs with diarrheal symptoms on pig farms in localities throughout Shandong Province (Figure 1). The collected samples were ground into tissue homogenates, transferred into 1.5 ml centrifuge tubes, frozen and thawed 3 times, and stored at −80°C for later use.

RNA extraction and genome amplification

The RNA isolater Total RNA Extraction Reagent R401-01 (Vazyme) was added to the tissue homogenate supernatant, and total RNA was extracted from the intestinal and fecal samples according to the instructions. The primers were synthesized by Sangon; Table 1 shows the sequences of the primers used. Three viruses—PEDV, transmissible gastroenteritis virus (TGEV), and porcine rotavirus (PoRV)—were amplified by RT-PCR using the EasyScript One-Step RT-PCR SuperMix (TransGen Biotech). After 1% agarose gel electrophoresis was performed for 45 min, the results were observed under a gel imaging system. PEDV-positive RNA was reverse-transcribed to cDNA using the ReverTra-Ace First-Strand cDNA Synthesis Kit (Toyobo), after which RT-PCR amplification was performed on PEDV-positive samples using 2 × Phanta Max Master Mix (Vazyme). All steps were performed strictly according to the instructions of the manufacturers.

Sequencing and phylogenetic analysis

PEDV-positive RT-PCR amplification products were sent to Sangon for sequencing. The sequences were compared using MegAlign in DNAStar and analyzed for nucleotide and deduced amino acid homology with a selection of reference strains entered in the NCBI's database (Table 2). MEGA X was used to construct a genetic evolutionary tree based on the PEDV S gene, while Protean in DNAStar was used to analyze the antigenic epitopes of the isolates.

Histopathological observations

The digestive tracts of PEDV-positive pigs were fixed in 10% formalin and removed after 48 h to produce conventional paraffin sections for pathological histological examination using hematoxylin-eosin (HE) staining as a means to observe lesions.

Results

Clinical signs and gross lesions

In practice, severe diarrhea with vomiting (Figure 2A), severe dehydration, and wasting (Figure 2B) can be observed in piglets affected by PED. During autopsies, signs of congestion and hemorrhaging in the intestinal mucosa and mesentery were observed as well (Figure 2C). The walls of the small intestine were thin and transparent, the intestinal lumen was filled with milky or yellow slurry-like contents, and the stomach was clearly dilated and filled with curd-like contents (Figure 2D).

RT-PCR positive rate of PEDV

RT-PCR revealed positivity rates of 37.5% (66/176) for PEDV, 6.82% (12/176) for TGEV, and 3.98% (7/176) for PoRV. Among them, one case of mixed infection of PEDV and TGEV was found, but no case of mixed infection of PEDV and PoRV was found. When the test results for the years 2019, 2020, and 2021 were counted separately, PEDV positivity rates for the

10.3389/fvets.2022.1015717

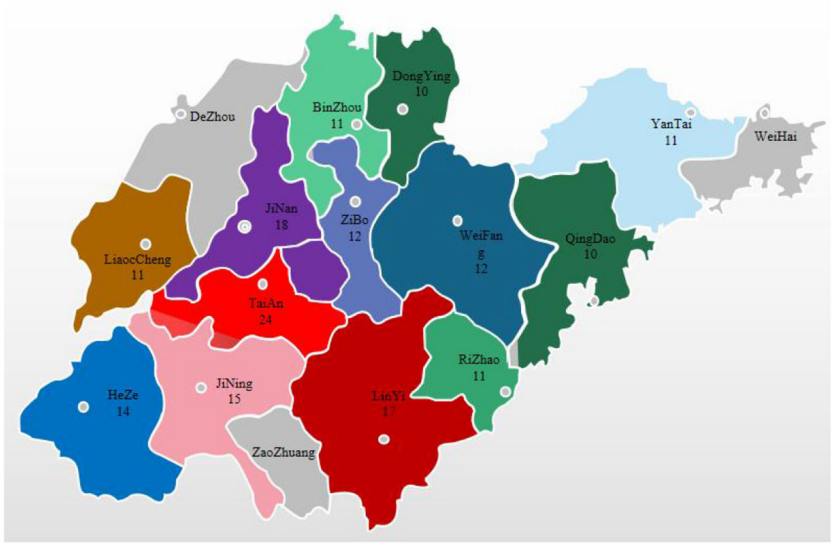

FIGURE 1
Distribution of sample collection by city in Shandong Province, 2019–2021.

TABLE 1 The sequences of primers.

Names	Primers (5′ → 3′)	Annealing temperature/°C	Fragment size/bp
PEDV-F	TGTTGTAGGGGTCCTAGACT	54	792
PEDV-R	GGTGACAAGTGAAGCACAGA		
TGEV-F	ATATGCAGTAGAAGACAAT	44	1,417
TGEV-R	TTAGTTCAAACAAGGAGT		
PoRV-F	GGCTTTAAAAGAGAGAATTTC	48	976
PoRV-R	GGTCACATCATACAGTTCTAAC		
PEDV-S1-F	AGATTGCTCTACCTTATACCTG	49	2,192
PEDV-S1-R	GAAAGAACTAAACCCATTGATA		
PEDV-S2-F	AGCCAACTCAAGTGTTCTCAGG	57	1,691
PEDV-S2-R	AGCCACAGTGTTCAAACCCTT		
PEDV-S3-F	TTAATAAAGTGGTTACTAATGGC	46	1,823
PEDV-S3-R	ATAATAAAGAGCGCATTTTTATA		

F represents forward PCR primer; R represents reverse PCR primer.

years were 34.88% (15/43), 39.33% (35/89), and 36.36% (16/44), respectively (Figure 3).

Results of phylogenetic analysis

Analysis of genetic variation in the S gene of an endemic strain of PEDV

A total of 12 PEDV S gene sequences were obtained after sequencing (Table 3), all of which were subsequently uploaded to the NCBI's database.

A comparative nucleotide analysis of the 12 isolates with the classical vaccine strain CV777 using MegAlign in DNAStar revealed that all isolates had varying degrees of base mutations, deletions, and insertions. In particular, all had three consecutive nt (TTG) insertions at position 164, all had nine consecutive nt (GGGTGTTAA) insertions at position 177, and all had one G insertion at position 206. The SDHY-YT strain had three consecutive nt (ACC) insertions at position 419, whereas the other 11 strains all had AAC insertions. All isolates had an A deletion at position 218 and three consecutive nt (GAA) deletions at positions 480–482 (Figure 4).

A comparison of the deduced amino acid sequences of the 12 isolates with those of CV777 using MegAlign revealed multiple deduced amino acid mutations, deletions, and insertions as well. By contrast, all isolates had four consecutive deduced amino acid

TABLE 2 Reference strain information.

Name	Distracts	GenBank accession no.
83P-5	Japan	AB548618
AD02	Korea	KC879281
BJ-2012-1	China	JX435299
BrI-87	France	Z25483
CH22-JS	China	JQ979290
GHGD-01	China	JN980698
Chinjμ99	Korea	AY167585
CH-S	China	JN547228
CV777-vaccine	China	JN599150
DR13	Korea	DQ862099
HLJ-2012	China	JX512907
IA2	America	KF468754
JS2008	China	KC210146
KH	Japan	AB548622
MN	America	KF468752
NK	Japan	AB548623
N12-GD2017	China	MK533003.1

FIGURE 2
Clinical symptoms and pathological change. **(A)** Diarrhea accompanied by vomiting; **(B)** Dehydration and emaciation; **(C)** Intestinal mucosa and mesenteric hyperemia and bleeding; **(D)** The intestinal wall is clear and filled, and the stomach is dilated.

(QGVN) insertions at positions 59–62, the SDHY-YT strain had a T insertion at position 140, and all other isolates had an N insertion. All 12 isolates additionally had a G deletion at position 160 (Figure 5).

PEDV S gene homology alignment analysis

Analysis using MegAlign in DNAStar revealed that the nucleotide homology among the 12 isolates ranged from 97.2 to 99.9%, while the deduced amino acid homology ranged from 95.9 to 99.7%. Compared with the reference strains, the

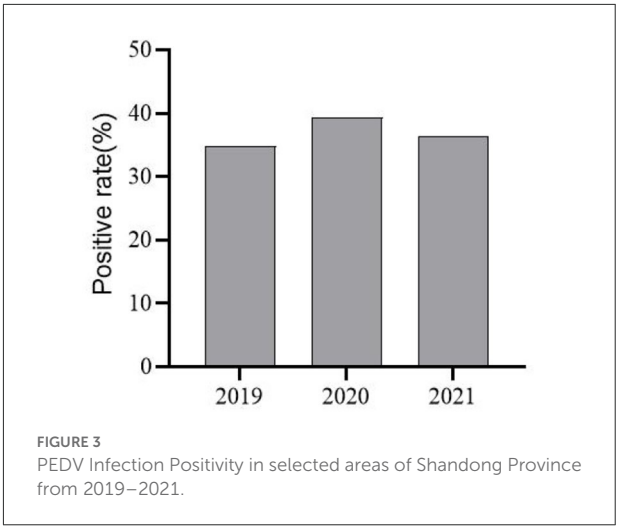

FIGURE 3
PEDV Infection Positivity in selected areas of Shandong Province from 2019–2021.

TABLE 3 Information of PEDV positive materials.

Name	Distracts	Acquisition time	GenBank accession no.
SDHY_DY	Dongying	12-Dec-20	ON988085
SDHY_ZB	Zibo	20-Nov-20	ON988086
SDHY_YT	Yantai	18-Dec-19	ON988087
SDHY_TA03	Tai'an	10-Jan-21	ON988088
SDHY_TA02	Tai'an	7-Dec-20	ON988089
SDHY_TA01	Tai'an	26-Jan-19	ON988090
SDHY_QD	Qingdao	21-Jan-21	ON988091
SDHY_LW	Ji'nan	20-Nov-19	ON988092
SDHY_LC	Liaocheng	2-Mar-21	ON988093
SDHY_JN02	Ji'ning	24-Nov-20	ON988094
SDHY_JN01	Ji'ning	5-Nov-20	ON988095
SDHY_BZ	Binzhou	2-Mar-21	ON988096

nucleotide homology was in the range of 93.0–99.1%, while the deduced amino acid homology was in the range of 90.9–99.4%. Compared with the classical vaccine strain CV777, the nucleotide sequence homology was in the range of 93.1–93.9%, while the deduced amino acid sequence homology was in the range of 91.2–93.0% (Table 4).

Genetic evolutionary analysis of the PEDV S gene

To understand the current genotypes of the dominant strains of PEDV in Shandong Province, we constructed a genetic evolutionary tree (Figure 6) using the neighbor-joining method in MEGA X (14) between the 12 isolates and the reference strains. The results showed that the 12 isolates, all belonging to the G2 genotype, were located in the same branch and in close genetic proximity.

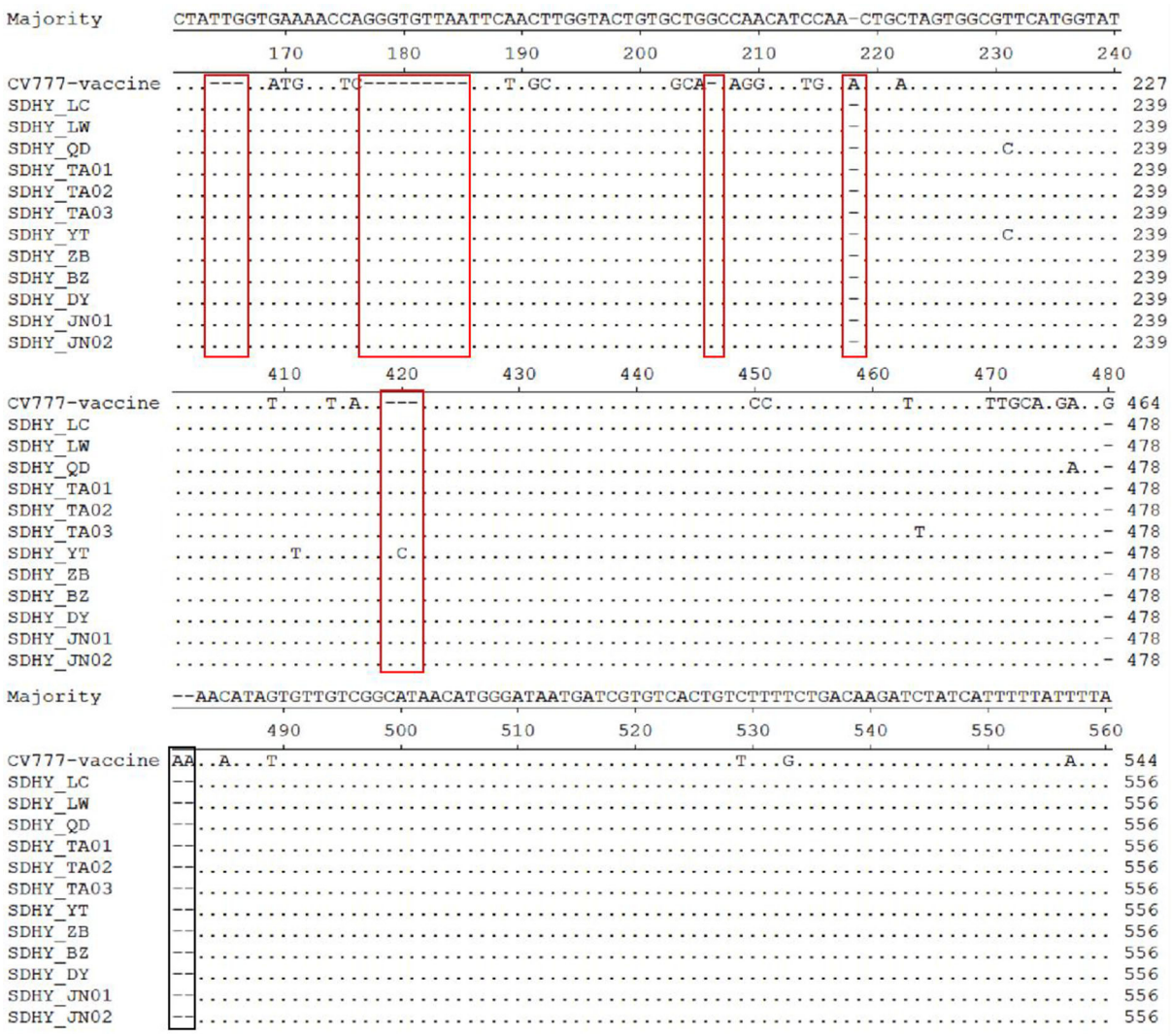

FIGURE 4
Analysis and comparison of nucleotide of the partial S gene.

Predictive analysis results of PEDV S protein antigen index

Next, our antigenic index prediction analysis of the vaccine strain CV777 S protein and the 12 isolated S proteins using the Jameson–Wolf method with Protean in DNAStar revealed that the S protein's overall antigenic index was high, with a significant difference in antigenicity within ~20–280 aa and a less significant difference elsewhere (Figure 7).

Results of histopathological analysis

Histopathological analysis revealed that the duodenal villi had atrophied and detached, and that the submucosa was congested (Figure 8A). The colonic mucosa showed an increased secretion of cupped cells, vacuolation, and the necrosis of epithelial cells (Figure 8B). The jejunal epithelium was necrotic, the submucosa was congested (Figure 8C), the jejunal villi were broken and severely detached (Figure 8D), and the jejunal intestinal canal, filled with necrotic detached epithelial cells, was severely congested and bleeding (Figure 8E). The lamina propria of the gastric mucosa was congested and edematous and showed inflammatory cell infiltration (Figure 8F).

Discussion

Coping with PED continues to be a daunting challenge for pig farming in China (15). Studies have revealed PEDV

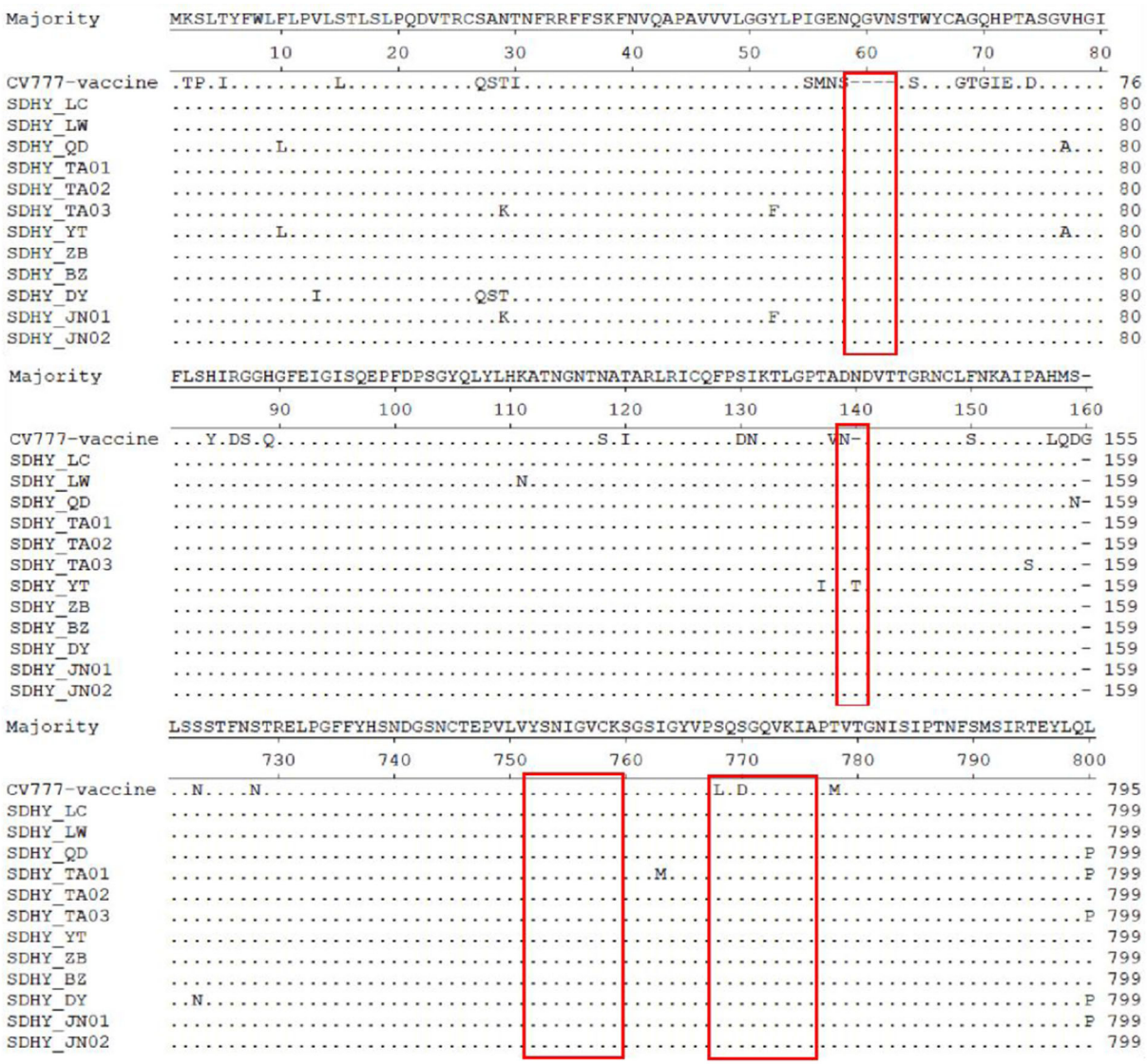

FIGURE 5
Analysis and comparison of amino acid of PEDV S gene.

positivity rates ranging from 30–45%, with slight differences between northern and southern China (16–19). In our study, PEDV positivity was 37.5% (66/176), TGEV positivity was 6.82% (12/176), and PoRV positivity was 3.98% (7/176); however, PEDV was the primary pathogen responsible for diarrhea in the piglets. By year, PEDV positivity in 2019, 2020, and 2021 was respectively 34.88% (15/43), 39.33% (35/89), and 36.36% (16/44). Overall, PED was shown to be moderately to highly prevalent in some areas of Shandong Province, with relatively stable trends in prevalence. By furnishing those findings, our study has filled gaps in epidemiological data concerning PEDV in Shandong Province in recent years.

In past research, the S gene of PEDV, the primary structural protein gene, has shown significant variation. The S gene sequences of the prevalent strains were systematically analyzed to accurately capture current trends in the strains and identify markers of PEDV variation (20). The results showed that all 12 isolates had varying degrees of base mutations, deletions, and insertions in the S gene, with changes occurring primarily in the N-terminal structural domain (NTD) region of S1 (21). Homology analysis of nucleotides and of deduced amino acid sequences showed that although the 12 isolates were closely related to the Chinese isolate N12-GD2017 from 2017, the American isolates MN and IA2 from 2013, and the Chinese strain HLJ-2012 from 2012, they were more closely related to the

10.3389/fvets.2022.1015717

TABLE 4 Homology analysis of nucleotides and deduced amino acids.

Name	Country	Accession number	Isolation of viral nt homology	Isolation of viral aa homology
83P-5	Japan	AB548618	93.3–94.1%	91.9–93.6%
AD02	South Korea	KC879281	95.4–96.3%	94.6–9.65%
BJ-2012-1	China	JX435299	97.1–98.1%	96.8–98.5%
BrI-87	France	Z25483	93.2–94.0%	91.7–93.3%
CH22-JS	China	JQ979290	94.6–95.8%	94.1–95.4%
GHGD-01	China	JN980698	96.7–97.4%	96.4–97.8%
Chinju99	South Korea	AY167585	93.1–93.9%	90.9–92.5%
CH-S	China	JN547228	93.1–93.7%	91.8–93.2%
CV777	China	JN599150	93.1–93.9%	91.2–93.0%
DR13	South Korea	DQ862099	93.2–94.0%	91.9–93.5%
HLJ-2012	China	JX512907	97.5–98.7%	97.7–99.0%
IA2	America	KF468754	97.6–98.9%	96.9–99.1%
JS2008	China	KC210146	93.7–94.2%	91.7–93.5%
KH	Japan	AB548622	93.5–94.2%	92.3–93.7%
MN	America	KF468752	97.6–98.6%	96.8–99.0%
NK	Japan	AB548623	93.9–94.8%	92.6–94.0%
N12-GD2017	China	MK533003.1	98.1–99.1%	97.6–99.4%

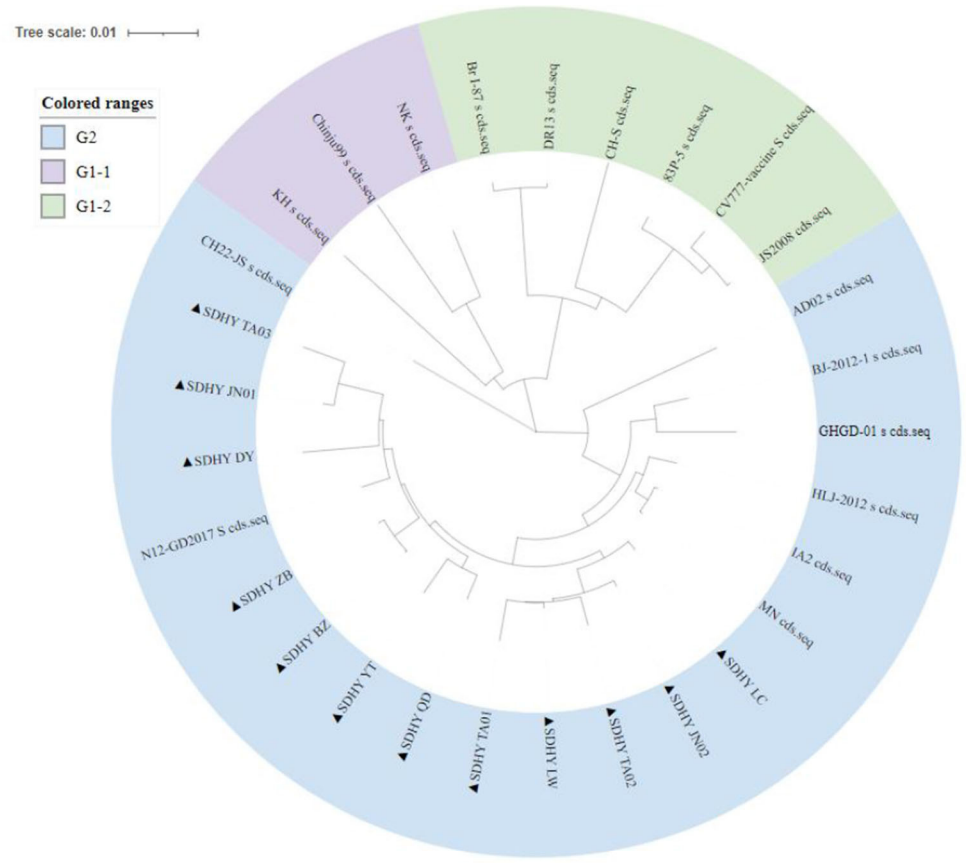

FIGURE 6
A phylogenetic tree based on the nucleotide construction of the PEDV S gene. "Purple" represents G1-1 subtype, "green" represents G1-2 subtype and "blue" represents G2 subtype. "▲" represents the isolates obtained in this study.

classical Chinese vaccine strain CV777, the Japanese strain KH, and the weak Japanese vaccine strain 83P-PEDV. Meanwhile, S1-IDMP were dominated by S1-IDMP S58_S58insQGVN-N135dup-D158_I159del. By contrast, in our study, S1-IDMP were dominated by S1-IDMP S58_S58insQGVN-N135dup-D158_I159del. Taken together, the deduced amino acid sequence mutations in the isolates primarily concentrated in the NTD region of S1. We observed a highly conserved SS2 antigenic epitope sequence (i.e., Y^{748}SNIGVCK) within PEDV; however, two AA substitutions (i.e., 764 at L→ S and 766 at D→ S) occurred at the SS6 antigenic epitope S^{764}QSGQVKI. Antigenic index predictions showed a more pronounced difference in antigenicity at 20 aa to 280 aa, with little difference at the remaining positions, which suggests that PEDV S protein changes primarily concentrated in the S1 gene region. In general, the current epidemic strains of PEDV in Shandong Province have high affinity and more obvious mutations in the S1 gene.

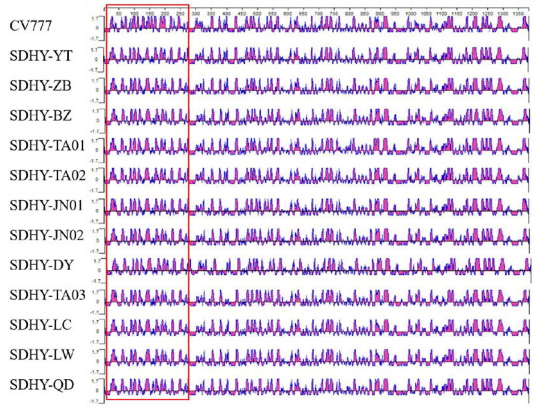

FIGURE 7
PEDV S protein antigen index prediction.

Despite the continued high-intensity vaccination of pigs against PED in Shandong Province, the disease can nevertheless occur after multiple vaccinations. In recent years, the incidence of PED in China has shown that the prevalent strains are the main cause of PED, while the incidence and mortality rates have increased year after year (22). In our study, genetic evolutionary analysis showed that all 12 isolates belong to the G2 subtype. However, most of the PEDV vaccines in Shandong Province currently use the CV777 strain of the G1 subtype as their source strain, which may partly explain the occurrence of PED on pig farms in the province. Therefore, we recommend using the more prevalent strain as the source strain for such vaccines, which may yield a more satisfactory immunization effect.

Conclusion

The results of this study clearly indicate that PEDV is the main pathogen causing diarrheal symptoms in pigs, the G2 subtype is the dominant strain of PEDV in Shandong Province, where its rates of morbidity and mortality continue to be high. At present, the most prevalent strain of PEDV in some areas of the province, however, is only distantly related to the vaccine strain CV777. Using the most prevalent

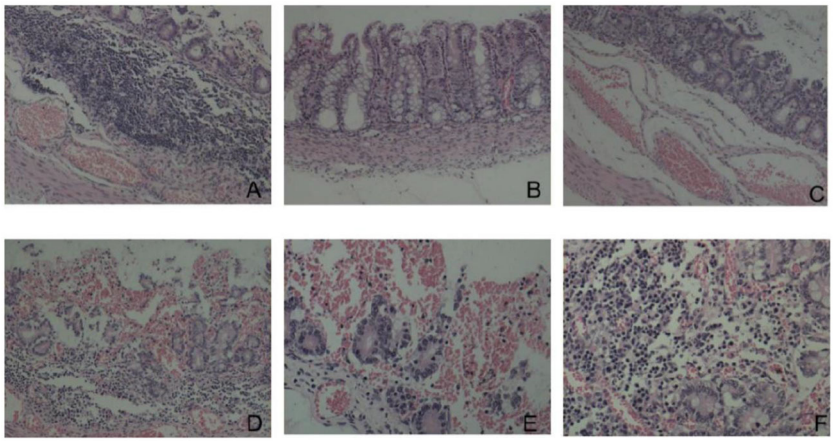

FIGURE 8
Histopathological changes (HE dyeing). **(A)** Duodenal villi had atrophied and detached, submucosa was congested, ×100; **(B)** increased goblet cells and necrosis of epithelial cells, ×200; **(C)** Necrosis of jejunal mucosal epithelial cells and submucosal hyperemia, ×100; **(D)** rupture and shedding of jejunal villi, ×100; **(E)** jejunum full of necrotic and exfoliated epithelial cells, ×100; **(F)** congestion and inflammatory cell infiltration in the lamina propria of gastric mucosa, ×200.

strain for vaccines against PED is therefore recommended. In addition, all 12 PEDV strains S1-IDMP isolated in this study had S58_S58insQGVN-N135dup-D158_I159del-like mutations, which require ongoing attention.

Data availability statement

The sequences of the isolated strains in this study have been uploaded to GenBanK (accession ON890168 to ON988085-ON988096).

Ethics statement

All animal protocols and procedures were performed according to the Chinese Regulations of Laboratory Animals and were approved by the Animal Ethics Committee of Shandong Agricultural University.

Author contributions

YS and YY: writing—original draft preparation. NL, ML, and FM: writing—review and editing. KL and NG: software. YZ, KL, and JZ: investigation. SL: funding acquisition. All authors have read and agreed to the published version of the manuscript.

Funding

This study was funded by the Shandong Provincial Agricultural Major Application Technology Innovation Project (Establishment and Demonstration of Healthy Pig Breeding Technology Integration and Product Supply Chain Traceability System).

Conflict of interest

Author FM was employed by company Huayun (Shandong) Inspection and Quarantine Service Co.

The remaining authors declare that the research was conducted in the absence of any commercial or financial relationships that could be construed as a potential conflict of interest.

Publisher's note

All claims expressed in this article are solely those of the authors and do not necessarily represent those of their affiliated organizations, or those of the publisher, the editors and the reviewers. Any product that may be evaluated in this article, or claim that may be made by its manufacturer, is not guaranteed or endorsed by the publisher.

References

1. Choudhury B, Dastjerdi A, Doyle N, Frossard JP, Steinbach F. From the field to the lab - An European view on the global spread of PEDV. *Virus Res.* (2016) 226:40–9. doi: 10.1016/j.virusres.2016.09.003

2. Li W, Li H, Liu Y, Pan Y, Deng F, Song Y, et al. New variants of porcine epidemic diarrhea virus, China, 2011. *Emerg Infect Dis.* (2012) 18:1350–3. doi: 10.3201/eid1803.120002

3. Shibata I, Tsuda T, Mori M, Ono M, Sueyoshi M, Uruno K. Isolation of porcine epidemic diarrhea virus in porcine cell cultures and experimental infection of pigs of different ages. *Vet Microbiol.* (2000) 72:173–82. doi: 10.1016/S0378-1135(99)00199-6

4. Wang Q, Vlasova AN, Kenney SP, Saif LJ. Emerging and re-emerging coronaviruses in pigs. *Curr Opin Virol.* (2019) 34:39–49. doi: 10.1016/j.coviro.2018.12.001

5. Pensaert MB, de Bouck P. A new coronavirus-like particle associated with diarrhea in swine. *Arch Virol.* (1978) 58:243–7. doi: 10.1007/BF01317606

6. Chen P, Wang K, Hou Y, Li H, Li X, Yu L, et al. Genetic evolution analysis and pathogenicity assessment of porcine epidemic diarrhea virus strains circulating in part of China during 2011-2017. *Infect Genet Evol.* (2019) 69:153–65. doi: 10.1016/j.meegid.2019.01.022

7. Jung K, Saif LJ, Wang Q. Porcine epidemic diarrhea virus (PEDV): an update on etiology, transmission, pathogenesis, and prevention and control. *Virus Res.* (2020) 286:198045. doi: 10.1016/j.virusres.2020.198045

8. Li N, Liu J, Qi J, Hao F, Xu L, Guo K. Genetic diversity and prevalence of porcine circovirus type 2 in China during 2000-2019. *Front Vet Sci.* (2021) 8:788172. doi: 10.3389/fvets.2021.788172

9. Antas M, Olech M, Szczotka-Bochniarz A. Molecular characterization of porcine epidemic diarrhoea virus (PEDV) in Poland reveals the presence of swine enteric coronavirus (SeCoV) sequence in S gene. *PLoS ONE.* (2021) 16:e0258318. doi: 10.1371/journal.pone.0258318

10. Chen J, Liu X, Shi D, Shi H, Zhang X, Li C, et al. Detection and molecular diversity of spike gene of porcine epidemic diarrhea virus in China. *Viruses.* (2013) 5:2601–13. doi: 10.3390/v5102601

11. Dortmans J, Li W, van der Wolf PJ, Buter GJ, Franssen PJM, van Schaik G, et al. Porcine epidemic diarrhea virus (PEDV) introduction into a naive Dutch pig population in 2014. *Vet Microbiol.* (2018) 221:13–8. doi: 10.1016/j.vetmic.2018.05.014

12. Bi J, Zeng S, Xiao S, Chen H, Fang L. Complete genome sequence of porcine epidemic diarrhea virus strain AJ1102 isolated from a suckling piglet with acute diarrhea in China. *J Virol.* (2012) 86:10910–1. doi: 10.1128/JVI.01919-12

13. Shi W, Hao H, Li M, Niu J, Hu Y, Zhao X, et al. Expression and purification of a PEDV-neutralizing antibody and its functional verification. *Viruses.* (2021) 13:472. doi: 10.3390/v13030472

14. Tamura K, Stecher G, Peterson D, Filipski A, Kumar S. MEGA6: molecular evolutionary genetics analysis version 6.0. *Mol Biol Evol.* (2013) 30:2725–9. doi: 10.1093/molbev/mst197

15. Turlewicz-Podbielska H, Pomorska-Mól M. Porcine coronaviruses: overview of the state of the art. *Virol Sin.* (2021) 36:833–51. doi: 10.1007/s12250-021-00364-0

16. Chen X, Zhang XX, Li C, Wang H, Wang H, Meng XZ, et al. Epidemiology of porcine epidemic diarrhea virus among Chinese pig populations: a meta-analysis. *Microb Pathog.* (2019) 129:43–9. doi: 10.1016/j.micpath.2019.01.017

17. Lee DU, Kwon T, Je SH, Yoo SJ, Seo SW, Sunwoo SY, et al. Wild boars harboring porcine epidemic diarrhea virus (PEDV) may play an important role as a PEDV reservoir. *Vet Microbiol.* (2016) 192:90–4. doi: 10.1016/j.vetmic.2016.07.003

18. Mai TN, Yamazaki W, Bui TP, Nguyen VG, Le Huynh TM, Mitoma S, et al. A descriptive survey of porcine epidemic diarrhea in pig populations in northern Vietnam. *Trop Anim Health Prod.* (2020) 52:3781–8. doi: 10.1007/s11250-020-02416-1

19. Reveles-Félix S, Carreón-Nápoles R, Mendoza-Elvira S, Quintero-Ramírez V, García-Sánchez J, Martínez-Bautista R, et al. Emerging strains of porcine epidemic diarrhoea virus (PEDv) in Mexico. *Transbound Emerg Dis.* (2020) 67:1035–41. doi: 10.1111/tbed.13426

20. Su M, Li C, Qi S, Yang D, Jiang N, Yin B, et al. A molecular epidemiological investigation of PEDV in China: characterization of co-infection and genetic diversity of S1-based genes. *Transbound Emerg Dis.* (2020) 67:1129–40. doi: 10.1111/tbed.13439

21. Wang E. *Molecular epidemiological investigation and virus isolation and identification of S1 gene of porcine epidemic diarrhea virus in China from 2015 to 2016* (Master), Heilongjiang Bayi Agricultural University (2018).

22. Gerdts V, Zakhartchouk A. Vaccines for porcine epidemic diarrhea virus and other swine coronaviruses. *Vet Microbiol.* (2017) 206:45–51. doi: 10.1016/j.vetmic.2016.11.029

frontiers | Frontiers in Veterinary Science

TYPE Original Research
PUBLISHED 24 November 2022
DOI 10.3389/fvets.2022.1042792

OPEN ACCESS

EDITED BY
Zhou Mo,
Heilongjiang University, China

REVIEWED BY
Stefan Vilcek,
University of Veterinary Medicine in Kosice, Slovakia
Jean-Pierre Frossard,
Animal and Plant Health Agency (United Kingdom), United Kingdom

*CORRESPONDENCE
Ling Zhu
abtczl72@126.com

†These authors have contributed equally to this work

SPECIALTY SECTION
This article was submitted to Veterinary Infectious Diseases, a section of the journal Frontiers in Veterinary Science

RECEIVED 13 September 2022
ACCEPTED 07 November 2022
PUBLISHED 24 November 2022

CITATION
Yang Y, Xu T, Wen J, Yang L, Lai S, Sun X, Xu Z and Zhu L (2022) Prevalence and phylogenetic analysis of porcine circovirus type 2 (PCV2) and type 3 (PCV3) in the Southwest of China during 2020–2022. *Front. Vet. Sci.* 9:1042792. doi: 10.3389/fvets.2022.1042792

Prevalence and phylogenetic analysis of porcine circovirus type 2 (PCV2) and type 3 (PCV3) in the Southwest of China during 2020–2022

Yanting Yang[1†], Tong Xu[1†], Jianhua Wen[1†], Luyu Yang[1], Siyuan Lai[1], Xiangang Sun[1], Zhiwen Xu[1,2] and Ling Zhu[1,2*]

[1]College of Veterinary Medicine, Sichuan Agricultural University, Chengdu, China, [2]College of Veterinary Medicine Sichuan Key Laboratory of Animal Epidemic Disease and Human Health, Sichuan Agricultural University, Chengdu, China

Introduction: Porcine circovirus type 2 (PCV2) is considered one of the viruses with substantial economic impact on swine industry in the word. Recently, porcine circovirus type 3 (PCV3) has been found to be associated with porcine dermatitis and nephropathy syndrome (PDNS)-like disease. And the two viruses were prone to co-infect clinically.

Methods: To further investigate the prevalence and genetic diversity of the two viruses, 257 pig samples from 23 different pig farms in southwest China with suspected PCVAD at different growth stages were analyzed by real-time PCR between 2020 and 2022 to determine the presence of PCV2 and PCV3.

Results: Results showed high prevalence of PCV2 and PCV3: 26.46% samples were PCV2 positive and 33.46% samples were PCV3 positive. The coinfection rate was doubled from 2020 (5.75%) to 2022 (10.45%). Subsequently, the whole genome sequences of 13 PCV2 and 18 PCV3 strains were obtained in this study. Of these, 1 strain was PCV2a, 5 strains were PCV2b and 7 strains were PCV2d, indicating that PCV2d was the predominant PCV2 genotype prevalent in the Southwest of China.

Discussion: In addition, the phylogenetic analysis of PCV3 showed high nucleotide homology (>98%) between the sequences obtained in this study and reference sequences. And 3 mutations (A24V, R27K and E128D) were found in PCV3 antibody recognition domains, which might be related to the mechanism of viral immune escape. Thus, this study will enhance our understanding of the molecular epidemiology and evolution of PCV2 and PCV3, which are conducive to the further study of the genotyping, immunogenicity and immune evasion of PCVs.

KEYWORDS

prevalence, genotype, phylogenetic analysis, PCV2, PCV3

Introduction

Porcine circoviruses (PCVs) are circular single-stranded DNA virus, belonging to the genus Circovirus of the family Circoviridae, which causes disease in birds, dogs, penguins, foxes, bears and pigs (1). Four types of PCV have been identified, namely PCV1, PCV2, PCV3 and PCV4 (2–5). PCV1 was first detected in 1974 as a cell culture contaminant and was not pathogenic to pigs (6). In 1998, Allan identified a circovirus structurally similar to PCV1, but with <80% homology, and named it PCV2 (3). Unlike PCV1, PCV2 has long been recognized as the major pathogen causing PCVD/PCVAD (Porcine Circovirus Associated Disease), characterized by clinical or subclinical infection with PCV2 in pigs (7). The symptoms include porcine dermatitis and nephropathy syndrome (PDNS), postweaning multisystemic wasting syndrome (PMWS) and porcine respiratory disease complex (PRDC) (8). In 2015, PCV3 was first detected in the U.S and could cause reproductive disorders, skin diseases, and multisystem inflammation in pigs (4, 9). In the last 2 years, a new circovirus was detected, and the affected pigs showed respiratory disorders, intestinal symptoms, and porcine dermatitis nephrotic syndrome (PDNS), named PCV4 (10).

PCV2 is a globally transmitted frequent pathogen and its genome is gradually undergoing genetic mutations. Its viral genome contains 1,766–1,768 nucleotides, with 11 overlapping and mosaic open reading frames. Among them, ORF1 and ORF2 are the two most dominant open reading frames, ORF1 encodes two replication-related proteins, Rep and Rep' (11), ORF2 encodes the viral structural protein (Cap), and the Cap protein is also the only immunogenic protein of PCV2 virus (12). ORF2 is highly variable and commonly used in phylogenetic analyses of PCV2. At present, PCV2 was classified into eight genetic isoforms (PCV2a - PCV2h) (13), and coinfection might occur between the different subtypes, leading to recombination of the ORF1 and ORF2 genes, resulting in new genotypes. Since the discovery of PCV2, there have been two shifts in its prevalent genotype: from PCV2a to PCV2b around 2000; and from PCV2b to PCV2d around 2012 (12).

Since its discovery, PCV3 has been prevalent in several countries including China, Japan, Korea, Sweden, Russia, Thailand, Malaysia and Italy (14, 15). The PCV3 genome contains 1999–2001 nucleotides and is similar to PCV2 in that it also has two major open reading frames, ORF1 and ORF2, encoding the Rep and Cap proteins, respectively, which share only about 40% homology with PCV2 (14). The Cap protein of PCV3 has two amino acid sites that are prone to mutation (A24V and R27K), and PCV3 can be classified into three subtypes PCV3a-3c based on these two mutations (16). The rate of genetic evolution of PCV3 was found to be much lower than that of PCV2, about 10-5 substitutions/locus/year (17).

FIGURE 1
The geographical distribution of 257 samples in Sichuan Province, China. Qionglai, Dayi, Pengzhou, and Jianyang are all parts of Chengdu. The cities with samples collected are marked with green color.

PCV2 and PCV3 are pathogenic to the swine industry which has brought huge economic losses. Co-infections of viruses play a critical role in pathogenicity and clinical symptoms (18). Therefore, monitoring the prevalence and genetic characteristics of both viruses is necessary. Prior to this, there have been partially reports on the prevalence and genetic variation of PCV2 and PCV3 in China (16–21), but the information in the Southwest of China was limited. In this trial, real-time PCR was used to detect the prevalence of PCV2 and PCV3 in the Southwest of China from 2020 to 2022. Based on molecular epidemiology and phylogenetic analysis, this study will deepen our research on the genetic characteristics of PCV2 and PCV3 viruses.

Materials and methods

Sample collection

A total of 257 diagnostic samples from our laboratory were randomly collected from 23 different pig farms in 12 cities in Sichuan province during September 2020 and May 2022 (Figure 1). Of these, 14/23 were vaccinated against PCV2. Different sample types including heart, lung, liver, spleen, kidney, lymph nodes, intestine, nasal swabs and serum were collected. The animals were of different ages. Among diagnostic samples, 72.37% (186/257) were suspected to have respiratory syndrome pathogen, and 27.63% (71/257) were for pathogens of enteric diarrhea. Samples were processed following standard operating procedures.

Detection of PCV2 and PCV3

Total viral DNA was extracted from the collected samples using the FastPure Cell/Tissue DNA Isolation Mini Kit (Cofitt, Hangzhou, China). The DNA samples were detected for PCV2 and PCV3 positivity by a validated TB Green II-based multiplex real-time PCR assay as described previously (22). The results were analyzed with Bio-Rad CFX Manager 4.1.

Detection of other pathogens

In addition to PCV2 and PCV3 detection, according to the different symptoms of the clinical cases from which the samples were derived, porcine epidemic diarrhea virus (PEDV), porcine deltacoronavirus (PDCoV), porcine rotavirus (PoRV), porcine transmissible gastroenteritis virus (TGEV), porcine reproductive and respiratory syndrome virus (PRRSV), swine influenza virus (SIV) and (MHP) were also detected. The assays used were as described previously (23–26).

Whole genome sequencing of PCV2 and PCV3

To obtain full-length sequences of PCV2 and PCV3 for phylogenetic analysis, PCR primers were utilized for whole genome sequencing as previously described (15, 27). Briefly, the 20-μL PCR reaction mixture contained 10 μL of 2 × PrimeSTAR Max Premix (Takara), 2 μL of sample DNA, 0.6 μL of each primer (25 μM), and 6.8 μL of ddH2O. The PCR reaction of PCV2 was executed by 35 cycles of 98°C for 10s, 57°C for 5s, and 72°C for 30s. Amplification conditions of PCV3 were similar to PCV2, excepting that the annealing time was 15s for the PCV3 primer sets.

The purified PCR products cloned into pMD18-T Cloning Vector (Takara, Dalian, China), and propagated in DH5α competent cells (Takara) following the manufacturer's instructions. Each PCR product was cloned three times and independently sequenced by Sangon Biotech Shanghai Co, Ltd. All sequencing reactions were performed in duplicate. The whole genome sequences of PCV2 were obtained in one shot by sequencing. The genomic sequences of PCV3 were assembled from the sequenced overlapping sequences by the EditSeq program of the LaserGene software package (DNASTAR, Inc., Madison, WI).

Sequence analyses

The reference strains and genomic sequences of PCV2 and PCV3 strains obtained in this study were shown in Supplementary Table S1. The complete coding sequence (ORF1 + ORF2) of PCV3 was analyzed. The coding sequence was divided into two sequences: ORF1 (Rep) and ORF2 (Cap), after the non-coding region was deleted. Since ORF2 was in the opposite direction, we reversed it and then spliced ORF1 and ORF2. The PCV3 subtypes were proposed by Li (28). The complete coding sequences of PCV3 and the ORF2 of PCV2 strains were compared using the Clustal W function of the Molecular Evolutionary Genetics Analysis (MEGA) software (version 7.0). Phylogenetic trees were generated by the maximum likelihood (ML) method in MEGA 7.0 with a p-distance model, and a bootstrap of 1000 replicates.

Ethics statement

All samples used in the study were pig samples, did not involve any human samples. Written informed consent was obtained from animal owners for this study. All experimental procedures were reviewed and approved by the Sichuan provincial laboratory management committee [License No: SYXK (chuan) 2019–187].

Results

Prevalence of PCV2 and PCV3 during 2020–2022

Overall prevalence of PCV2 and PCV3

Of the 257 clinical samples detected, the positive rates of PCV2 and PCV3 were 26.46% (68/257) and 33.46% (86/257), respectively, and the coinfection rate of PCV2 and PCV3 was 8.95% (23/257). When the data was analyzed by year, prevalence of PCV3 in samples was 33.33% (26/87) in 2020, 35.92% (35/103) in 2021 and 37.31% (25/67) in 2022, where the prevalence rates were higher for each corresponding year compared to PCV2: 24.14% (21/87) in 2020, 26.13% (27/103) in 2021 and 29.85% (20/67) in 2022. The prevalence of PCV2 and PCV3 has gradually increased in the past 3 years, and the coinfection rate of PCV2 and PCV3 also increased rapidly, from 5.75% (5/87) in 2020, to 9.71% (10/103) in 2021 then to 10.45% (7/67) in 2022 (Table 1).

Geographic distribution of PCV2 and PCV3

The clinical samples in the trial were collected from 12 cities during 2020–2022, which were summarized in Table 2. Both PCV2 and PCV3 were identified from samples of 12 cities. It demonstrated that PCV2 and PCV3 were prevalent in the Southwest of China from 2020 to 2022, and the positive rate of PCV3 was higher than that of PCV2 in any region. Among the 23 pig farms in these 12 cities, 69.57% (16/23) were positive for PCV2 and 47.83% (11/23) were positive for PCV3 and 39.13% (9/23) were diagnosed as coinfection of PCV2 and PCV3.

Prevalence of PCV2 and PCV3 in different sample types

In this study, a total of 9 different types of sample were testing for PCV2 and PCV3, and the positive rates were shown in Table 3. Among them, 42.12% (109/257) were porcine serum, of which 26.61% (29/109) were PCV2 positive and 33.94% (37/109) were PCV3 positive. In the tissue samples, the positive rates of PCV2 and PCV3 were 40% (8/20) and 45% (9/20) in lymph node, 37.84% (14/37) and 48.65% (17/37) in spleen, respectively, which were higher than those in other tissues. Besides, Table 3 illustrated that PCV3 was mostly detected in spleens and PCV2 was more common in lymph node. Meanwhile, the coinfection rates in spleen and lymph node were also higher than those in other sample types.

TABLE 1 The prevalence rates of PCV3 and PCV2 from swine specimens collected in the Southwest of China.

Year	PCV2 positive/total (%)	PCV3 positive/total (%)	Coinfection positive/total (%)
2020	21/87(24.14%)	26/87(33.33%)	5/87(5.75%)
2021	27/103(26.13%)	35/103(35.92%)	10/103(9.71%)
2022	20/67(29.85%)	25/67(37.31%)	7/67(10.45%)
Total	68/257(26.46%)	86/257(33.46%)	23/257(8.95%)

Coinfection with other porcine viruses

In addition to the coinfection of PCV2 and PCV3 mentioned above, we also investigated the coinfection rates of PCVs with other common pathogens in pigs. Of the 56 cases of enterovirus infection including PEDV, PDCoV, PoRV and TGEV, 16. 07% (9/56) were PCV2 positive and 21.43% (12/56) were PCV3 positive. In the 89 respiratory virus infection cases including PRRSV, SIV and MHP, 24.72% (22/89) were PCV2 positive and 34.83% (31/89) were PCV3 positive. These results showed that the coinfection rate with other pathogens of PCV3 is higher than that of PCV2, and the coinfection of PCVs with respiratory pathogens is higher than that of intestinal pathogens, which might be related to the pathogenic mechanism of PCVs.

TABLE 2 The prevalence rates of PCV2 and PCV3 in different cities in the Southwest of China during 2020–2022.

Farms	Cites	PCV2 positive case rate (%)			PCV3 positive case rate (%)		
		2020	2021	2022	2020	2021	2022
Farm 1	Mianyang	1/3 (33.33%)	2/6 (33.33%)	1/4 (25%)	2/3 (66.67%)	2/6 (33.33%)	2/4 (50%)
Farm 2	Mianyang	1/5 (20%)	1/7 (14.29%)	0/3 (0%)	1/5 (20%)	2/7 (28.57%)	1/3 (33.33%)
Farm 3	Mianyang	2/8 (25%)	3/9 (33.33%)	2/7 (28.57%)	3/8 (37.5)	5/9 (55.56%)	3/7 (42.86%)
Farm 4	Mianyang	2/7 (28.57%)	2/6 (33.33%)	1/3 (33.33%)	3/7 (42.86%)	2/6 (33.33%)	1/3 (33.33%)
Farm 5	Suining	1/7 (14.29%)	1/5 (20%)	0/2 (0%)	2/7 (28.57%)	1/5 (20%)	1/2 (50%)
Farm 6	Suining	1/5 (20%)	1/7 (14.29%)	0/2 (0%)	1/5 (20%)	2/7 (28.57%)	0/2 (0%)
Farm 7	Suining	2/9 (22.22%)	3/11 (27.27%)	1/3 (33.33%)	1/9 (11.11%)	3/11 (27.27%)	2/3 (66.67%)
Farm 8	Suining	1/6 (16.67%)	2/6 (33.33%)	1/2 (50%)	2/6 (33.33%)	2/6 (33.33%)	1/2 (50%)
Farm 9	Jianyang	1/3 (33.33%)	0/2 (0%)	0/1 (0%)	0/3 (0%)	1/1 (100%)	0/1 (0%)
Farm 10	Jianyang	0/1 (0%)	-	0/1 (0%)	0/1 (0%)	0/1 (0%)	1/1 (100%)
Farm 11	Deyang	0/1 (0%)	1/3 (33.33%)	-	1/1 (100%)	0/3 (0%)	-
Farm 12	Qionglai	2/4 (50%)	1/4 (25%)	1/3 (33.33%)	1/4 (25%)	2/4 (50%)	2/3 (66.67%)
Farm 13	Qionglai	1/3 (33.33%)	1/4 (25%)	1/4 (25%)	2/3 (66.67%)	1/4 (25%)	0/4 (0%)
Famr 14	Qionglai	0/2 (0%)	1/3 (33.33%)	1/3 (33.33%)	1/2 (50%)	1/3 (33.33%)	2/3 (66.67%)
Farm 15	Dayi	-	1/4 (25%)	-	-	1/4 (25%)	-
Farm 16	Pengzhou	1/3 (33.33%)	1/1 (100%)	0/2 (0%)	0/3 (0%)	0/1 (0%)	0/2 (0%)
Farm 17	Pengzhou	1/4 (25%)	0/2 (0%)	1/4 (25%)	2/7 (28.57%)	0/2 (0%)	0/4 (0%)
Farm 18	Dazhou	0/1 (0%)	1/3 (33.33%)	2/5 (40%)	0/1 (0%)	1/3 (33.33%)	1/5 (20%)
Farm 19	Guangyuan	0/1 (0%)	1/5 (20%)	2/6 (33.33%)	1/1 (100%)	2/5 (40%)	3/6 (50%)
Farm 20	Nanchong	1/3 (33.33%)	1/5 (20%)	3/5 (60%)	2/3 (66.67%)	2/5 (40%)	2/5 (40%)
Farm 21	Zigong	1/3 (33.33%)	1/3 (33.33%)	-	0/3 (0%)	2/3 (66.67%)	-
Farm 22	Zigong	1/5 (20%)	1/3 (33.33%)	0/2 (0%)	1/5 (20%)	1/3 (33.33%)	1/2 (50%)
Farm 23	Leshan	1/3 (33.33%)	1/4 (25%)	3/5 (60%)	0/3 (0%)	2/4 (50%)	2/5 (40%)
	Total	21/87 (24.14%)	27/103 (26.13%)	20/67 (29.85%)	26/87 (33.33%)	35/103 (35.92%)	25/67 (37.31%)

–, No sample available.

TABLE 3 Positive rates of PCV3 and PCV2 in different types of swine samples during 2020–2022.

Sample type	PCV2 positive rate positive/total (%)	PCV3 positive rate positive/total (%)	Coinfection rate positive/total (%)
Heart	0/5 (0%)	1/5 (20%)	0/5 (0%)
Lung	8/33 (24.24%)	10/33 (30.30%)	3/33 (9.09%)
Liver	1/7 (14.29%)	0/7 (0%)	0/7 (0%)
Spleen	14/37 (37.84%)	17/37 (48.65%)	4/37 (10.81%)
Kidney	5/29 (17.24%)	7/29 (24.14%)	2/29 (6.90%)
Lymph node	8/20 (40%)	9/20 (45%)	2/20 (10%)
Intestine	1/6 (16.67%)	1/6 (16.67%)	0/6 (0%)
Nose swabs	2/11 (18.18%)	4/11 (27.27%)	1/11 (9.09%)
Serum	29/109(26.61%)	37/109 (33.94%)	11/109 (10.09%)
Total	68/257 (26.46%)	86/257 (33.46%)	23/257 (8.95%)

Sequence analysis of PCV2 and PCV3 prevalent in southwest Chine during 2020–2022

Sequences to submit

From this study, a total of 17 PCV2 and 23 PCV3 sequences were obtained. Among them, the unique 13 PCV2 and 18 PCV3 whole genome sequences were generated and deposited in the NCBI GenBank with accession number as follows: OP055737-OP055748(PCV2), OP189294(PCV2), ON989005(PCV3), ON586851(PCV3), and OP066314-OP066329(PCV3).

Genetic characteristics of PCV2

A phylogenetic tree was constructed based on ORF2 of 13 unique strains and 24 genotypic reference strains (PCV2a-h) (Figure 2A). The results showed that 1 strain of PCV2 belonged to PCV2a, 5 strains belonged to PCV2b and 7 strains belonged to PCV2d.

Sequence analysis indicated that the 13 strains shared 94.7–99.9% identity of their whole genomes, 89.9–99.9% identity of ORF2 and 97.1–100% of ORF2. Compared with 24 reference strains deposited in GenBank database, the 13 strains shared 90.9–99.9% identity of their whole genomes, 80.7–99.9% identity of ORF2 and 96.5–100% identity of ORF1. Among the 13 unique PCV2 sequences, 11 unique capsid (Cap) proteins and 6 unique replicase (Rep) proteins were generated based on nucleotide mutations. At the amino acid level, the similarities between the 11 Cap proteins were 88.1–99.6%, while the similarities between them and the 24 PCV2 reference genomes were 79.3–100%. Similarly, the 6 Rep proteins shared high similarity to each other (98.7–99.7%), but low similarity to some of the 24 reference genomes (87.3–100%). Compared with 24 unique reference amino acid sequences, the diversity of amino acid sequences by PCV2 ORF2 in this study was shown in Figure 3. In this study, 15 mutation sites (A47S, M72L, N77D, S86T, P88K, L89I, V130F, T131P, A133S, T151P, L185M, L187I, T190S, G191K and T206K) were identified in PCV2a ORF2 that were absent in PCV2b and PCV2d, ten mutation sites (V57I, A59R, S63K, L89R, T90S, T190A, H200I, A210E, K227R and K234*) were identified in PCV2b ORF2 that were absent in PCV2a and PCV2d and 11 substitution sites (Y8F, V30L, F53I, A68N, E104D, F129S, A133T, T134N, S169G/R, V215I and M217L) were identified in PCV2d ORF2 that were absent in PCV2a and PCV2b. Furthermore, there were 69 amino acid mutations finding in the Cap protein of these 35 PCV2 strains, 28 of which occurred in the epitope region reported in previous studies (29).

Genetic characteristics of PCV3

In this study, sequence analysis and phylogenetic study of 18 PCV3 strains were performed. The phylogenetic tree was established based on the combined coding sequences (ORF1 + ORF2) of the 18 strains and 25 reference sequences (28). The 43 PCV3 strains contained two major genotypes, PCV3a and PCV3b, among which PCV3a was further divided into PCV3a-1, PCV3a-2 and PCV3a-IM (Figure 2B). In this study, 14 strains of 19 PCV3 were clustered as PCV3a and 4 strains clustered as PCV3b.

The sequence analysis showed that the 18 stains shared 98.7–99.9% identity of their whole genomes, 97.2–100% identity of PRF2 and 97.9–99.9% of ORF1. Then, compared with 25 unique PCV3 whole genomes deposited in the GenBank database, the 18 PCV3 strains shared 99.8–99.9% identity of their whole genomes, 97.1-100% identity of ORF2 and 98.7–99.9% of OFR1. Among the 18 unique PCV3 sequences, 7 unique capsid (Cap) proteins and 8 unique replicase (Rep) proteins were generated based on nucleotide mutations. At the amino acid level, the similarities between the 7 Cap proteins were 97.7–99.5%, while the similarities between them and the 25 PCV3 reference genomes were 95.4–100%. Likewise, the similarity between the 8 Rep proteins was high (98.0–99.7%), while the similarity with the 25 published sequences was low (96.3–100%). The amino acid mutations of the Cap protein of the 18 PCV3 strains sequenced in this study was shown in Supplementary Table S2, which was also compared with 14 unique reference amino acid sequences. Overall, mutations were found in 11 amino acid positions in the Cap protein and in 14 positions in the Rep protein. Among them, there were 3 amino acids (A24V, R27K and E128D) of the Cap protein mutation falling into the antibody recognition domains (23–35aa and 119–131aa within PCV3 Cap protein)

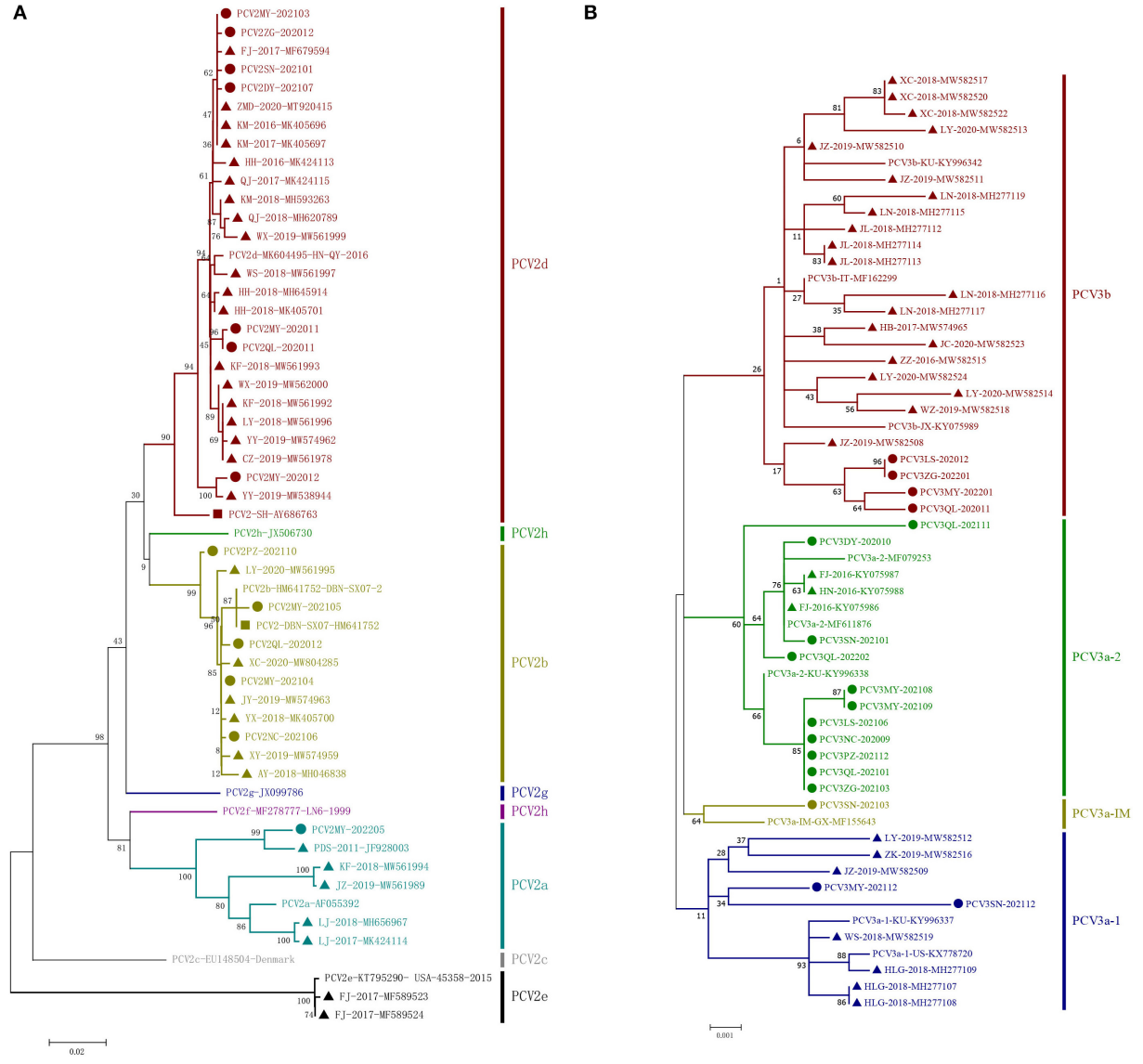

FIGURE 2
Phylogenetic trees based on the ORF2 gene of PCV2 and the complete coding sequences (ORF1 + ORF2) of PCV3. The ML tree was constructed with a p-distance model and bootstrapping at 1,000 replicates. **(A)**: PCV2. **(B)**: PCV3. The PCV3 subtypes were proposed by Li et al. (28). The strains sequenced in this study are marked with circles; the Chinese reference sequences are marked with triangle; the vaccine strains are marked with square. The different genotypes are represented by different colors as indicated in the figures.

as previously reported (30). And there were 7 Cap amino acid mutations (A5P, A24V, T77S, F104Y, E128D, L150I, and T175K) finding in the predicted B-cell epitopes in 18 PCV3 strains sequenced (28).

Discussion

A total of 257 clinical samples collected from southwest China during 2020–2022 were screened for the prevalence of PCV2 and PCV3. The positive rates of PCV2 in this study was 26.46%, which was higher than previously reported in the Midwest United States and European countries (30, 31). Meanwhile, 43.48% (10/23) and 56.52% (13/23) of the farms were positive for PCV2 and PCV3 respectively, indicating that PCV3 had a higher prevalence found that among the 23 pig farms, and 26.09% (6/23) of the farms were diagnosed as PCV2 and PCV3 coinfection. Among them, 84.62% (11/13) of farms negative for PCV2 were vaccinated against PCV2, while 30% (3/10) of the farms positive for PCV2 were vaccinated. These results showed that routine vaccination helps to prevent the prevalence and the spread of PCV2. Those infected despite

FIGURE 3
The unique amino acid sequences encoded by ORF2 of the PCV2 strains. The red open boxes show the typical motifs of ORF2 gene. The gray areas represent the epitope region reported in previous studies, including A (65–87), B (113–139), C (193–207) and D (227–233). The blue area represents the vaccine strains and the green area represents the Chinese reference sequences.

vaccination might be caused by immunization failure or by rapid genetic mutation of PCV2. The three farms that failed immunization were inoculated with inactivated PCV2 vaccine, of which 2 farms were inoculated with vaccine (SH) purchased from PULIKE BIO-ENGINEERING Co., Ltd (Henan, China), and the other farm was inoculated with vaccine (DBN-SX07) purchased from HAILINGE BIO-PHARMA CO., Ltd (Chengdu, China). PCV2QL-202012 and PCV2MY-202105 were obtained by sequencing in pig farms inoculated with SH strain. Based on SH strain, amino acid alignment analysis showed that L89R, T90S, and D210E were mutated in the typical motifs, and T200I was mutated in the epitope region. PCV2SN-202101 was detected in pig farms inoculated with DBN, and the A68N and F129S mutations were found at epitope region after comparison. These unique amino acid mutations might be responsible for its immune failure. From 2020 to 2022, PCV2 and PCV3 were detected in 12 cities in Sichuan Province, and the prevalence of both PCV2 and PCV3 is gradually increasing, which indicated that PCV2 and PCV3 are widely distributed in pig farms in the Southwest of China.

In recent years, it has been found that viremia of PCV2 and PCV3 and the manifestation of PCVAD symptoms are often accompanied by mixed infections of the two (32). In previous reports, the coinfection rate of the two in pig farms is generally 27.6-39.39% (33–35). In a research found in the last 2 years, the coinfection rate of PCV2/PCV3 has reached 69.74% in a pig farm in Henan, China, and the main symptoms has been severe watery diarrhea with poor healing (20). Compared with previous

data, the overall coinfection rates in Sichuan province (8.95%) in this study were lower than those in central China but higher than those in the Midwest of the USA (19, 30). Thus, necessity is needed to detect the coinfection of PCV2 and PCV3 in China. In the Southwest of China for last 3 years, the coinfection rate has been rising rapidly, and has even doubled from 2020 (5.75%) to 2022 (10.45%). The reason of the lower growth rate for 2021–2022 might be attributed to the lower sample size in 2022 as only the first half of the year was tested. Also, since PCVs prevalence is the highest mainly in winter after weaning (36), the incidence rate in spring 2022 cannot fully reflect the infection rate in that region. In addition, some studies have reported higher rates of infection and more pronounced clinical symptoms of PCV3 when other viruses are present, including PCV2, porcine parvovirus (PPV), and PRRSV (37, 38). In this study, PCV2 and PCV3 were more likely to co-infect with respiratory and enteroviruses, which is generally consistent with the findings in this study (39). However, in another study, PDNS-like clinical cases were replicated in piglets by attacking PCV3 alone (40), which suggests that PCV3, like PCV2, can pose a threat when infected alone.

Recent reports indicate that PCV2 and PCV3 can be detected from various tissues and serum (30). The data in this study showed that PCV2 and PCV3 are more prone to be detected in the spleen and lymph nodes than in other tissues, suggesting that PCV2 mainly colonized in the immune organs and subsequently caused significant depletion of lymphocyte, which was consistent with previous reports (19). The detection rate of circovirus in serum was higher than other tissues but lower than lymph node and spleen, illustrating that the viremia of circovirus was very obvious. Therefore, lymph node, spleen and serum should be considered as important sample types in exploring the prevalence and epidemiology studies of PCVs.

Since PCV2 was detected in 2000 in China, PCV2a has been the most predominant genotype in pig herds until a shift to PCV2b occurred around 2003 (41, 42). Since then, PCV2b has been the most prevalent genotype, and most vaccines has been genotyped PCV2a/2b to date (42). For the past few years, PCV2d has become the main prevalent genotype at home and abroad. In this study, 13 unique PCV2 whole genomes were sequenced. Most of the isolates (53.85%; 7/13) belong to the PCV2d genotype, indicating that it is the main genotype prevalent in southwest China, which is consistent with previous reports (19). Besides, the rates of PCV2a and PCV2b in PCV2-positive samples in this study were 7.69% (1/13) and 38.46% (5/13), respectively.

In phylogenetic genotyping analysis, PCV2 strains showed obvious differences. Among the 13 strains, the genome size of them was 1,767 nucleotide (nt), same as the usual sequence reported earlier. And the length of ORF1 of 13 strains was 945 nt, ORF2 of 4 strains was 702 nt, while ORF2 of the other 9 strains was 705 nt. In previous studies, the PCV2d strain had an extra acid in the C-terminus of it capsid protein compared with PCV2a and PCV2b strains, resulting in a length of 705 nt instead of 702 nt. Interestingly, PCV2MY-202103 in this study belonged to PCV2d, but its capsid protein had no additional amino acids, whilst PCV2QL-202012, PCV2MY-202104, and PCV2MY-202105 (PCV2b) had an extra amino acid, which had also been found in previous studies (19). The amino acid mutation results showed a large number of mutation sites in PCV2. The representative amino acid mutation sites which located in the epitope region were M72L, N77D, S86T, V130F, T131P, A133S, and T206K for PCV2a; H200I and K227R for PCV2b; A68N, S121T and T134N for PCV2d. The immunosuppression of PCV2 might be related to its high amino acid site variability. Nevertheless, the specific mechanisms of PCV2 pathogenicity and immune evasion are not fully understood, so further investigation are highly required.

PCV3 was first detected in 2015 in sows with PDNS and aborted fetuses, and has subsequently been identified in pigs in Asia, Europe, and the Americas (4). The construction of a phylogenetic tree was based on the whole genome sequence of PCV3 and PCV3 can be classified into three genotypes, PCV3a, PCV3b, and PCV3c, of which PCV3a can be subdivided into three genotypes, PCV3a-1, PCV3a-2, and PCV3a-IM (43). In 2019, researches based on 51 PCV3 strains from 21 provinces in China found that the proportion of PCV3a, PCV3b and PCV3c were 29.4, 41.2, and 29.4%, respectively, which showed that PCV3b accounted for the highest proportion and was presumed to be the most prevalent strain in China; PCV3a was mainly prevalent in the Central Plains, PCV3b in the Northeast, and PCV3c was widely distributed in six regions in China, including the North, Northeast, Central Plains, East, Southwest and South (39). In this study, PCV3a accounted for the majority but PCV3b was less prevalent, which was similar to the results reported from Henan Province last year (19), but was inconsistent with the findings from previous years (39), so it can been shown that the prevalent PCV3 strains in China might have shifted in recent years. In this study, homological analysis indicated that the PCV3 strains had a high identity (98.7∼99.9%) among genomes, which was agree with many previous studies (44). Therefore, it was difficult to establish a potential genotypic classification of PCV3 which might be related to this.

Based on the phylogenetic analysis and sequence alignment of Rep + Cap gene sequences, all the isolates could be classified into PCV3a and PCV3b. Interestingly, in PCV3b cluster, the 4 strains sequenced in this study with the same capsid protein were detected, and two amino acids (A24V and R27K) were conserved in this group of strains, which were different from other strains. And the two mutations might be related to the mechanism of viral immune escape (16). Moreover, 7 mutations fell within the predicted B-cell epitopes (28), suggesting that this cluster of strains might have different immunogenicity conferred by the Cap protein. The exact mechanism of PCV3 immunogenicity

and immune evasion remains unclear, which warrants further study.

In conclusion, PCV2 and PCV3 in Sichuan China from 2020 to 2022 were investigated and the results showed that PCV2 and PCV3 were ubiquitous in the Southwest of China. Furthermore, PCV2d and PCV3a were the most predominant genotype at present. As a common mixed infection, PCV2 and PCV3 are prone to cause serious PCVAD symptoms such as PDNS, PMWS and PRDC, which may bring significant economic losses to the farms. Therefore, it is necessary to take some measures to prevention and control, such as biosafety management and vaccines. Meanwhile, further studies on the invasion mechanism, immune response pathway and interaction between PCV2 and PCV3 should be conducted in the future, which may require more support from epidemiological and pathogenesis studies.

Data availability statement

The datasets presented in this study can be found in online repositories. The names of the repository/repositories and accession number(s) can be found in the article/Supplementary material.

Ethics statement

Written informed consent was obtained from animal owners for this study. All experimental procedures were reviewed and approved by the Sichuan Provincial Laboratory Management Committee [License No: SYXK (chuan) 2019–187].

Author contributions

YY and JW conceived, designed, and performed the experiments. TX, LY, SL, XS, ZX, and LZ contributed to data analysis. YY wrote the manuscript. All authors have read and approved the final version of manuscript.

Funding

This work was supported by the Porcine Major Science and Technology Project of Sichuan Science and Technology Plan (Project No. 2021ZDZX0010-3), the Sichuan Provincial Department of Science and Technology Rural Area Key R&D Program (Project No. 2020YFN0147), the Key R&D Program of Sichuan Science and Technology Plan (Project No. 2022YFN0007), and the Agricultural Industry Technology System of Sichuan Provincial Department of Agriculture (Project No. CARS-SVDIP).

Acknowledgments

The authors appreciate all the helps from our colleagues and collaborators.

Conflict of interest

The authors declare that the research was conducted in the absence of any commercial or financial relationships that could be construed as a potential conflict of interest.

Publisher's note

Supplementary material

The Supplementary Material for this article can be found online at: https://www.frontiersin.org/articles/10.3389/fvets.2022.1042792/full#supplementary-material

References

1. Ouyang T, Zhang X, Liu X, Ren L. Co-infection of swine with porcine circovirus type 2 and other swine viruses. *Viruses.* (2019) 11:185. doi: 10.3390/v11020185

2. Tischer I, Rasch R, Tochtermann G. Characterization of papovavirus-and picornavirus-like particles in permanent pig kidney cell lines. *Zentralbl Bakteriol Orig A.* (1974) 226:153–67.

3. Meehan BM, McNeilly F, Todd D, Kennedy S, Jewhurst VA, Ellis JA, et al. Characterization of novel circovirus DNAs associated with wasting syndromes in pigs. *J Gen Virol.* (1998) 79:2171–9. doi: 10.1099/0022-1317-79-9-2171

4. Phan TG, Giannitti F, Rossow S, Marthaler D, Knutson TP Li L, et al. Detection of a novel circovirus PCV3 in pigs with cardiac and multi-systemic inflammation. *Virol J.* (2016) 13:184. doi: 10.1186/s12985-016-0642-z

5. Xu T, Hou CY, Zhang YH Li HX, Chen XM, Pan JJ, et al. Simultaneous detection and genetic characterization of porcine circovirus 2 and 4 in Henan province of China. *Gene.* (2022) 808:145991. doi: 10.1016/j.gene.2021.145991

6. Tischer I, Gelderblom H, Vettermann W, Koch MA, A. very small porcine virus with circular single-stranded DNA. *Nature.* (1982) 295:64–6. doi: 10.1038/295064a0

7. Gillespie J, Opriessnig T, Meng XJ, Pelzer K, Buechner-Maxwell V. Porcine circovirus type 2 and porcine circovirus-associated disease. *J Vet Intern Med*. (2009) 23:63. doi: 10.1111/j.1939-1676.2009.0389.x

8. Segales J. Porcine circovirus type 2 (PCV2) infections: clinical signs, pathology and laboratory diagnosis. *Virus Res*. (2012) 164:10–9. doi: 10.1016/j.virusres.2011.10.007

9. Palinski R, Piñeyro P, Shang P, Yuan F, Guo R, Fang Y, et al. A novel porcine circovirus distantly related to known circoviruses is associated with porcine dermatitis and nephropathy syndrome and reproductive failure. *J Virol*. (2017) 91:e01879-16. doi: 10.1128/JVI.01879-16

10. Zhang HH, Hu WQ Li JY, Liu TN, Zhou JY, Opriessnig T, et al. Novel circovirus species identified in farmed pigs designated as Porcine circovirus 4, Hunan province, China. *Transbound Emerg Dis*. (2020) 67:1057–61. doi: 10.1111/tbed.13446

11. Li W, Liu S, Wang Y, Deng F, Yan W, Yang K, et al. Transcription analysis of the porcine alveolar macrophage response to porcine circovirus type 2. *BMC Genomics*. (2013) 14:353. doi: 10.1186/1471-2164-14-353

12. Karuppannan AK, Opriessnig T. Porcine circovirus type 2 (PCV2) vaccines in the context of current molecular epidemiology. *Viruses*. (2017) 9:99. doi: 10.3390/v9050099

13. Franzo G, Segalés J. Porcine circovirus 2 (PCV-2) genotype update and proposal of a new genotyping methodology. *PLoS ONE*. (2018) 13:e0208585. doi: 10.1371/journal.pone.0208585

14. Ouyang T, Niu G, Liu X, Zhang X, Zhang Y, Ren L. Recent progress on porcine circovirus type 3. *Infect Genet Evol*. (2019) 73:227–33. doi: 10.1016/j.meegid.2019.05.009

15. Tan CY, Opaskornkul K, Thanawongnuwech R, Arshad SS, Hassan L, Ooi PT. First molecular detection and complete sequence analysis of porcine circovirus type 3 (PCV3) in Peninsular Malaysia. *PLoS ONE*. (2020) 15:e0235832. doi: 10.1371/journal.pone.0235832

16. Fu X, Fang B, Ma J, Liu Y, Bu D, Zhou P, et al. Insights into the epidemic characteristics and evolutionary history of the novel porcine circovirus type 3 in southern China. *Transbound Emerg Dis*. (2018) 65:e296–303. doi: 10.1111/tbed.12752

17. Franzo G, He W, Correa-Fiz F, Li G, Legnardi M, Su S, et al. A shift in porcine circovirus 3 (PCV-3) history paradigm: phylodynamic analyses reveal an ancient origin and prolonged undetected circulation in the worldwide swine population. *Adv Sci*. (2019) 6:1901004. doi: 10.1002/advs.201901004

18. Chen N, Huang Y, Ye M, Li S, Xiao Y, Cui B, et al. Co-infection status of classical swine fever virus (CSFV), porcine reproductive and respiratory syndrome virus (PRRSV) and porcine circoviruses (PCV2 and PCV3) in eight regions of China from 2016 to 2018. *Infect Genet Evol*. (2019) 68:127–35. doi: 10.1016/j.meegid.2018.12.011

19. Xu T, Zhang YH, Tian RB, Hou CY Li XS, Zheng LL, et al. Prevalence and genetic analysis of porcine circovirus type 2 (PCV2) and type 3 (PCV3) between 2018 and 2020 in central China. *Infect Genet Evol*. (2021) 94:105016. doi: 10.1016/j.meegid.2021.105016

20. Guo Z, Ruan H, Qiao S, Deng R, Zhang G. Co-infection status of porcine circoviruses (PCV2 and PCV3) and porcine epidemic diarrhea virus (PEDV) in pigs with watery diarrhea in Henan province, central China. *Microb Pathog*. (2020) 142:104047. doi: 10.1016/j.micpath.2020.104047

21. Lv Q, Wang T, Deng J, Chen Y, Yan Q, Wang D, et al. Genomic analysis of porcine circovirus type 2 from southern China. *Vet Med Sci*. (2020) 6:875–89. doi: 10.1002/vms3.288

22. Zhao Y, Han HY, Fan L, Tian RB, Cui JT Li JY, et al. Development of a TB green II-based duplex real-time fluorescence quantitative PCR assay for the simultaneous detection of porcine circovirus 2 and 3. *Mol Cell Probes*. (2019) 45:31–6. doi: 10.1016/j.mcp.2019.04.001

23. Ding G, Fu Y, Li B, Chen J, Wang J, Yin B, et al. Development of a multiplex RT-PCR for the detection of major diarrhoeal viruses in pig herds in China. *Transbound Emerg Dis*. (2020) 67:678–85. doi: 10.1111/tbed.13385

24. Zheng LL, Chai LY, Tian RB, Zhao Y, Chen HY, Wang ZY. Simultaneous detection of porcine reproductive and respiratory syndrome virus and porcine circovirus 3 by SYBR Green I-based duplex real-time PCR. *Mol Cell Probes*. (2020) 49:101474. doi: 10.1016/j.mcp.2019.101474

25. Bliss N, Nelson SW, Nolting JM, Bowman AS. Prevalence of influenza a virus in exhibition swine during arrival at agricultural fairs. *Zoonoses Public Health*. (2016) 63:477–85. doi: 10.1111/zph.12252

26. Moiso N, Pieters M, Degano F, Vissio C, Camacho P, Estanguet A, et al. Detection of Mycoplasma hyopneumoniae in nasal and laryngeal swab specimens in endemically infected pig herds. *Vet Rec*. (2020) 186:27. doi: 10.1136/vr.105525

27. Gagnon CA, Tremblay D, Tijssen P, Venne MH, Houde A, Elahi SM. The emergence of porcine circovirus 2b genotype (PCV-2b) in swine in Canada. *Can Vet J*. (2007) 48:811-9.

28. Li G, He W, Zhu H, Bi Y, Wang R, Xing G, et al. Origin, genetic diversity, and evolutionary dynamics of novel porcine circovirus 3. *Adv Sci*. (2018) 5:1800275. doi: 10.1002/advs.201800275

29. Kweon CH, Nguyen LT, Yoo MS, Kang SW. Differential recognition of the ORF2 region in a complete genome sequence of porcine circovirus type 2 (PCV2) isolated from boar bone marrow in Korea. *Gene*. (2015) 569:308–12. doi: 10.1016/j.gene.2015.04.055

30. Wang Y, Noll L, Lu N, Porter E, Stoy C, Zheng W, et al. Genetic diversity and prevalence of porcine circovirus type 3 (PCV3) and type 2 (PCV2) in the Midwest of the USA during 2016-2018. *Transbound Emerg Dis*. (2020) 67:1284–94. doi: 10.1111/tbed.13467

31. Saporiti V, Huerta E, Correa-Fiz F, Grosse Liesner B, Duran O, Segalés J, et al. Detection and genotyping of Porcine circovirus 2 (PCV-2) and detection of Porcine circovirus 3 (PCV-3) in sera from fattening pigs of different European countries. *Transbound Emerg Dis*. (2020) 67:2521–31. doi: 10.1111/tbed.13596

32. Opriessnig T, Halbur PG. Concurrent infections are important for expression of porcine circovirus associated disease. *Virus Res*. (2012) 164:20–32. doi: 10.1016/j.virusres.2011.09.014

33. Li X, Qiao M, Sun M, Tian K. A duplex real-time PCR assay for the simultaneous detection of porcine circovirus 2 and circovirus 3. *Virol Sin*. (2018) 33:181–6. doi: 10.1007/s12250-018-0025-2

34. Kim HR, Park YR, Lim DR, Park MJ, Park JY, Kim SH, et al. Multiplex real-time polymerase chain reaction for the differential detection of porcine circovirus 2 and 3. *J Virol Methods*. (2017) 250:11–6. doi: 10.1016/j.jviromet.2017.09.021

35. Zheng S, Wu X, Zhang L, Xin C, Liu Y, Shi J, et al. The occurrence of porcine circovirus 3 without clinical infection signs in Shandong Province. *Transbound Emerg Dis*. (2017) 64:1337–41. doi: 10.1111/tbed.12667

36. Vangroenweghe F, Thas O. Seasonal variation in prevalence of mycoplasma hyopneumoniae and other respiratory pathogens in peri-weaned, post-weaned, and fattening pigs with clinical signs of respiratory diseases in Belgian and Dutch pig herds, using a tracheobronchial swab sampling technique, and their associations with local weather conditions. *Pathogens*. (2021) 10:1202. doi: 10.3390/pathogens10091202

37. Sukmak M, Thanantong N, Poolperm P, Boonsoongnern A, Ratanavanichrojn N, Jirawattanapong P, et al. The retrospective identification and molecular epidemiology of porcine circovirus type 3 (PCV3) in swine in Thailand from 2006 to 2017. *Transbound Emerg Dis*. (2019) 66:611–6. doi: 10.1111/tbed.13057

38. Ha Z, Xie CZ Li JF, Wen SB, Zhang KL, Nan FL, et al. Molecular detection and genomic characterization of porcine circovirus 3 in pigs from Northeast China. *BMC Vet Res*. (2018) 14:321. doi: 10.1186/s12917-018-1634-6

39. Qi S, Su M, Guo D, Li C, Wei S, Feng L, et al. Molecular detection and phylogenetic analysis of porcine circovirus type 3 in 21 Provinces of China during 2015-2017. *Transbound Emerg Dis*. (2019) 66:1004–15. doi: 10.1111/tbed.13125

40. Jiang H, Wang D, Wang J, Zhu S, She R, Ren X, et al. Induction of porcine dermatitis and nephropathy syndrome in piglets by infection with porcine circovirus type 3. *J Virol*. (2019) 93:e02045-18. doi: 10.1128/JVI.02045-18

41. Lang H, Zhang G, Wu F, Zhang C. Detection of serum antibody against postweaning multisystemic wasting syndrome in pigs. *Chin J Vet Technol*. (2000) 3:3–5. doi: 10.16656/j.issn.1673-4696.2000.03.001

42. Xu PL, Zhao Y, Zheng HH, Tian RB, Han HY, Chen HY, et al. Analysis of genetic variation of porcine circovirus type 2 within pig populations in central China. *Arch Virol*. (2019) 164:1445–51. doi: 10.1007/s00705-019-04205-0

43. Franzo G, Delwart E, Fux R, Hause B, Su S, Zhou J, et al. Genotyping porcine circovirus 3 (PCV-3) nowadays: does it make sense? *Viruses*. (2020) 12:265. doi: 10.3390/v12030265

44. Klaumann F, Correa-Fiz F, Franzo G, Sibila M, Núñez JI, Segalés J. Current knowledge on porcine circovirus 3 (PCV-3): a novel virus with a yet unknown impact on the swine industry. *Front Vet Sci*. (2018) 5:315. doi: 10.3389/fvets.2018.00315

frontiers | Frontiers in Veterinary Science

TYPE Review
PUBLISHED 22 December 2022
DOI 10.3389/fvets.2022.1083605

OPEN ACCESS

EDITED BY
Zhou Mo,
Heilongjiang University, China

REVIEWED BY
Huapeng Feng,
Zhejiang Sci-Tech University, China
Xinsheng Liu,
Lanzhou Veterinary Research Institute (CAAS), China

*CORRESPONDENCE
Longjun Guo
guolongjun@caas.cn
Li Feng
fengli@caas.cn

SPECIALTY SECTION
This article was submitted to Veterinary Infectious Diseases, a section of the journal Frontiers in Veterinary Science

RECEIVED 29 October 2022
ACCEPTED 06 December 2022
PUBLISHED 22 December 2022

CITATION
Li M, Guo L and Feng L (2022) Interplay between swine enteric coronaviruses and host innate immune. *Front. Vet. Sci.* 9:1083605. doi: 10.3389/fvets.2022.1083605

Interplay between swine enteric coronaviruses and host innate immune

Mingwei Li, Longjun Guo* and Li Feng*

State Key Laboratory of Veterinary Biotechnology, Harbin Veterinary Research Institute, Chinese Academy of Agricultural Sciences, Harbin, China

Swine enteric coronavirus (SeCoV) causes acute diarrhea, vomiting, dehydration, and high mortality in neonatal piglets, causing severe losses worldwide. SeCoV includes the following four members: transmissible gastroenteritis virus (TGEV), porcine epidemic diarrhea virus (PEDV), porcine delta coronavirus (PDCoV), and swine acute diarrhea syndrome coronavirus (SADS-CoV). Clinically, mixed infections with several SeCoVs, which are more common in global farms, cause widespread infections. It is worth noting that PDCoV has a broader host range, suggesting the risk of PDCoV transmission across species, posing a serious threat to public health and global security. Studies have begun to focus on investigating the interaction between SeCoV and its host. Here, we summarize the effects of viral proteins on apoptosis, autophagy, and innate immunity induced by SeCoV, providing a theoretical basis for an in-depth understanding of the pathogenic mechanism of coronavirus.

KEYWORDS

SeCoV, apoptosis, autophagy, innate immunity, across species transmission

1. Introduction

1.1. Swine enteric coronavirus

Coronaviruses are one of the most devastating pathogens. The sudden outbreak of COVID-19 in 2019 has had a major impact on global public health and economic development, while the devastating effects of CoVs are not only limited to humans but also occur in livestock populations. Swine enteric coronaviruses (SeCoV) pose a huge threat to the global farm industry. Four SeCoVs were identified: porcine epidemic diarrhea virus (PEDV), porcine transmissible gastroenteritis virus (TGEV), porcine delta coronavirus (PDCoV), and swine acute diarrhea syndrome coronavirus (SADS-CoV). In the last century, PEDV and TGEV were first reported (1–3), and then widely spread to many swine-producing countries in Europe and Asia (4, 5). Recently, PDCoV and SADS-CoV have emerged as SeCoVs (6, 7), Compared with PEDV and TGEV, the clinical signs caused by PDCoV and SADS-CoV infection are less severe, and the mortality rate of newborn piglets is 30–40%. It is worth mentioning that in 2021, US scientists discovered that the plasma samples of three Haitian children with unexplained fever tested positive for PDCoV, in which suggesting the risk of PDCoV across species transmission (8).

SeCoV is a single-stranded, positive-sense RNA virus, and its viral genome consists of structural proteins, non-structural proteins, and accessory proteins. Four structural proteins, spike (S), envelope (E), membrane (M), and nucleocapsid (N) proteins were identified. The S protein mediates attachment to the host receptor and is a trimer with an S1 subunit that contains the large receptor-binding domain (RBD) and an S2 subunit that contains peptides mediating cell fusion (9). E and M proteins are responsible for maintaining the structure and size of the viral envelope (10). The N protein constitutes the only protein present in the nucleocapsid and wraps the virus genome to form a nucleoprotein complex (11). ORF1ab encodes non-structural proteins *via* nsp3 and nsp5 cleavage, there are 15–16 functional non-structural proteins (nsps), These nsps are involved in the replication and transcription of viral RNA and some nsps also inhibit the host immune response (10, 12), ORF3, NS6, and NS7 encode accessory proteins to modulate viral pathogenicity (13) (Figure 1). SeCoV has become a major cause of lethal watery diarrhea in newborn piglets, imposing enormous economic losses and a public health burden on the swine industry worldwide.

1.2. Autophagy induce by SeCoV infection

Autophagy is a process in which cells use lysosomes to degrade damaged organelles and macromolecular substances under the regulation of autophagy-related genes (Atg). Previous studies have reported that autophagy is an intrinsic host defense mechanism that mediates the autophagic elimination of viral constituents or virions by targeting virus particles or virus component degradation to facilitate host innate and adaptive immunity. Increasing evidence indicates that viruses have evolved various complex strategies to escape or subvert the antiviral effects of autophagy (Figure 2). For example, SARS-CoV-2 ORF3a promotes the induction of autophagy *via* the classic ATF6 and IRE1-XBP1 UPR pathways to protect the virus from hydrolysis (14). Furthermore, ORF10 and M of SARS-CoV-2 promote the accumulation of LC3 in mitochondria and induce mitophagy, which inhibits RIG-MAVS-triggered IFN signaling (15, 16). PEDV-triggered autophagy in Vero cells *via* both the PERK and IER1 pathways promotes viral replication (17–19). Additionally, nsp6 and ORF3 of PEDV were able to induce significant autophagy in IPEC-J2 cells, and nsp6 of PEDV induced autophagy by inhibiting the PI3K/Akt/mTOR signaling pathway, which promotes cell damage and enhances the virulence of PEDV (20). Moreover, PEDV ORF3 protein triggers the endoplasmic reticulum (ER) stress response by upregulating the expression of GRP78 protein and activating the PERK-eIF2α signaling pathway to induce autophagy (21). In addition, SADS-CoV and PDCoV induce autophagy to facilitate viral replication *via* the PI3K/Akt/mTOR signaling pathway *in vitro* (22–24).

TGEV infection induces mitophagy to suppress oxidative stress and apoptosis in porcine epithelial cells (IPEC-J2 cells) to promote cell survival and, possibly, viral infection. Furthermore, N of TGEV may be involved in mitochondrial damage and mitophagy induction during TGEV infection (25). Interestingly, TGEV infection activates autophagy, whereas autophagy inhibits TGEV replication (26). Upon PDCoV infection, the upregulation of the LC3-II/LC3-I ratio and the downregulation of p62 protein levels indicate that PDCoV infection may induce autophagy, similar to other CoVs (22, 27). Additionally, PDCoV-induced autophagy enhances viral replication through the p38 signaling pathway (28).

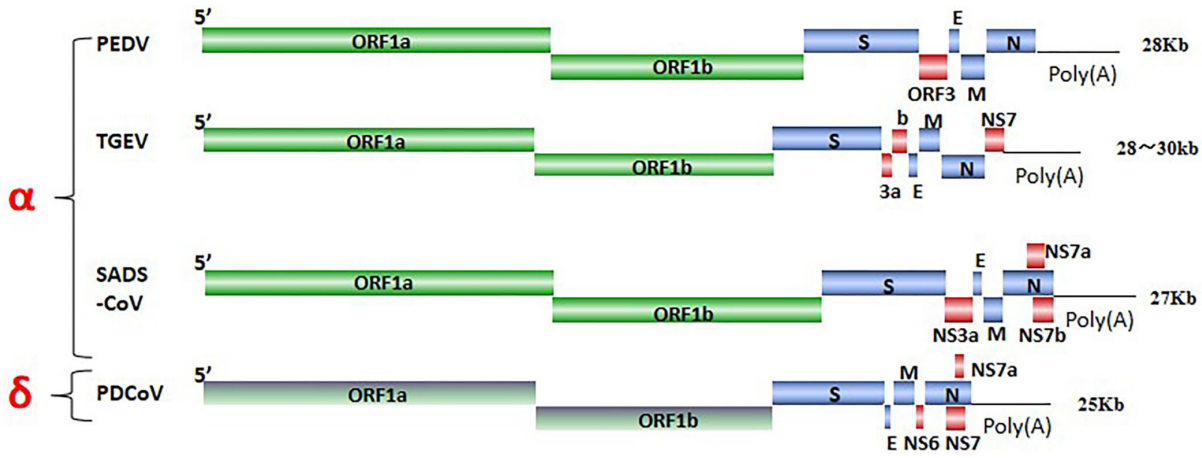

FIGURE 1
The genome structures of SeCoV.

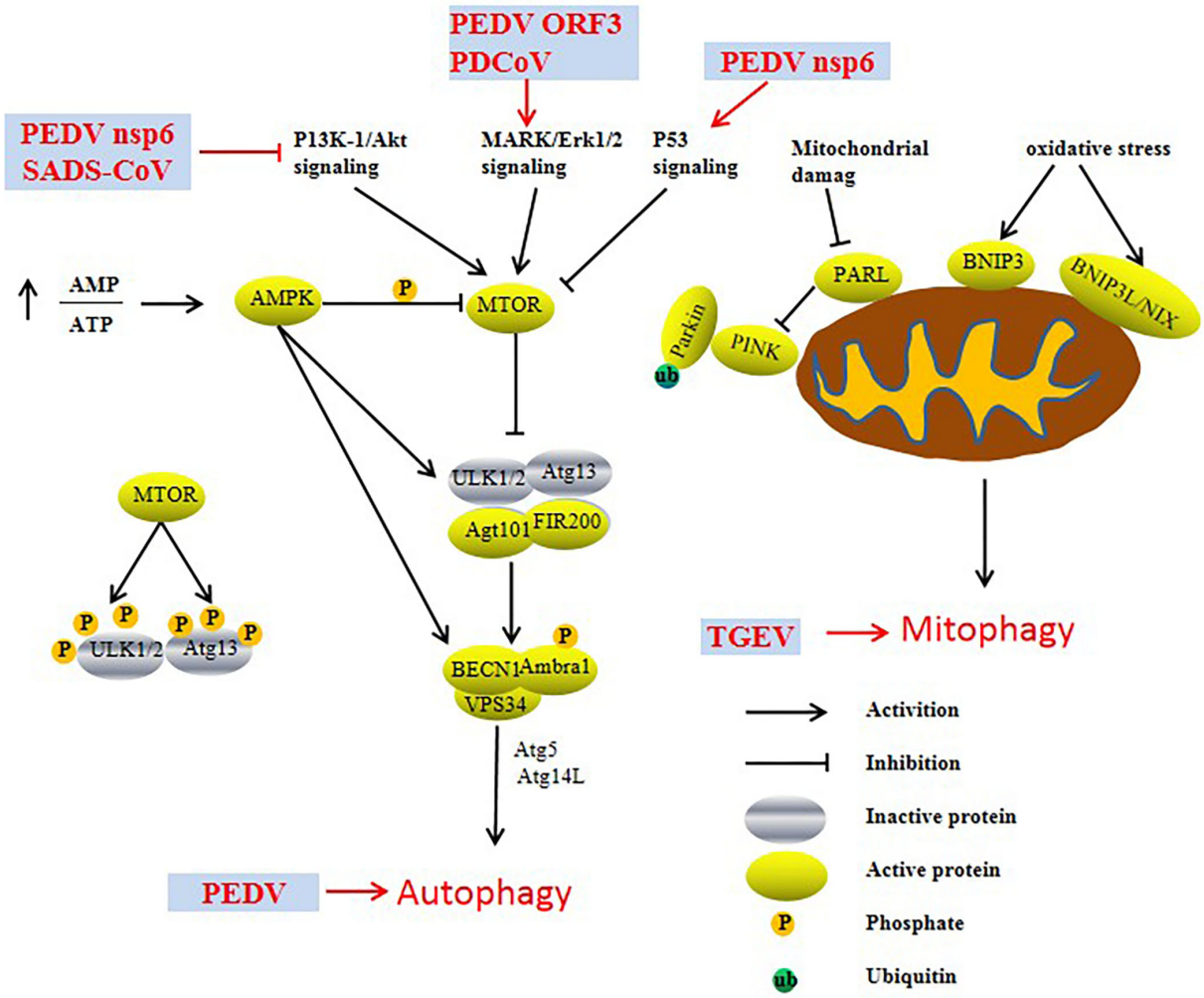

FIGURE 2
Induction and modulation of host autophagy by SeCoV infection.

1.3. Apoptosis induce by SeCoV infection

Apoptosis refers to the autonomous and orderly death of cells that is controlled by genes to maintain the stability of the internal environment. It is involved in the activation, expression, and regulation of a series of genes. There are two pathways of apoptosis, extrinsic and intrinsic. The extrinsic apoptotic pathway is mediated by death receptors (DRs) on the cell membrane, thereby activating the cascade of apoptosis signaling pathways. The intrinsic apoptosis pathway is mainly activated by apoptosis inducers in the cytoplasm to activate mitochondrial pro-apoptotic factors and destroy the integrity of the mitochondrial outer membrane. Subsequently, the increase in mitochondrial outer membrane permeability (MOMP) promotes the release of cytochrome c (Cyt c) and apoptosis-inducing factor (AIF), thereby inducing apoptosis (29).

Apoptosis is considered a host innate defense mechanism that disrupts viral replication by eliminating virus-infected cells, but some viruses utilize apoptosis as a mechanism for cell killing and viral spread (30) (Figure 3). PEDV infection induces apoptosis *via* a caspase-independent mitochondrial AIF-mediated pathway to facilitate viral replication (31–33). It has been demonstrated that the activation of p38 MAPK and JNK cascades also contributes to PEDV replication, but they are not linked to PEDV-mediated apoptosis (34, 35). P53 plays an essential role in viral infection-induced apoptosis. PEDV and TGEV induce apoptosis *via* a P53-dependent pathway (35, 36). PEDV infection activated P53-puma and reactive oxygen species (ROS)/p53 signaling pathways to induce apoptosis in Vero cells and cause cell cycle arrest at the G0/G1 phase (35, 37). The S1 protein of many coronaviruses can induce cell apoptosis; the PEDV S1 protein is the main inducer of cell apoptosis during PEDV infection, and PEDV M and nsp1, 2, 5, 6, 7, 9, and 13

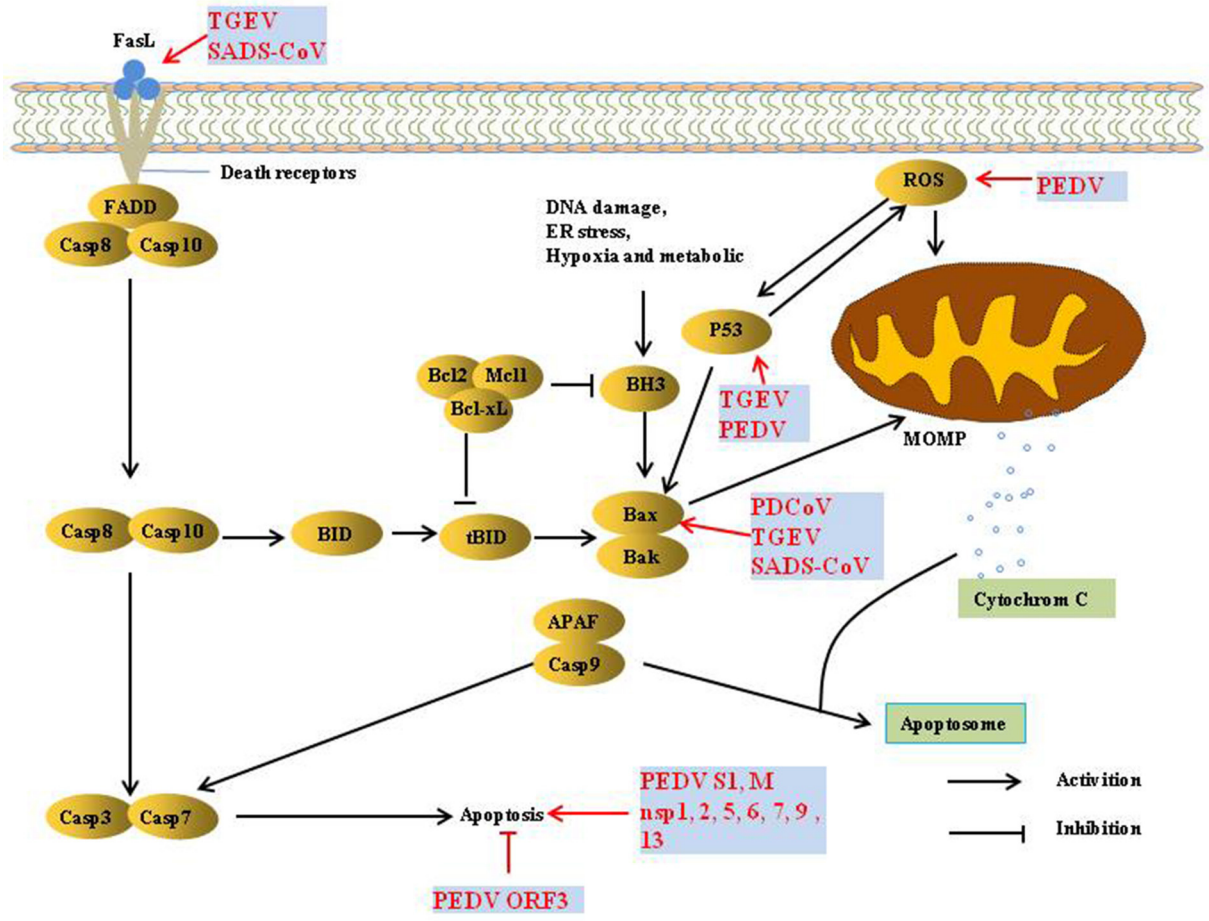

FIGURE 3
Induction and modulation of host apoptosis by SeCoV infection.

also induce cell apoptosis, but to a lesser extent. Similarly, the S protein of TGEV can strongly induce apoptosis in Vero-E6 cells, suggesting that S1 is a promising strategy to inhibit coronavirus infection (38, 39). In contrast, reverse genetics technology has been used to prove that the PEDV ORF3 protein promotes virus proliferation by inhibiting cell apoptosis (40).

TGEV induced apoptosis in PK-15 and ST cells but not in intestinal epithelial cells (41, 42), p53- and ROS-mediated AIF pathways, and caspase-dependent pathways both played a dominant role in triggering apoptosis. However, p38 MAPK signaling was only partially responsible for the activation of p53 and contributed less to TGEV-induced apoptosis (36, 42–45). Interestingly, the TGEV N protein is cleaved by caspase-6 and−7 during TGEV-induced apoptosis (46). However, TGEV N upregulated p53 and p21 and arrested the cell cycle at the S and G2/M phases, finally resulting in apoptosis of PK-15 cells (47).

PDCoV induces apoptosis to promote viral replication in both LLC-PK and ST cells but not in infected intestinal enterocytes *in vivo* (48). In addition, PDCoV and SADS-CoV infection induces apoptosis by recruiting Bax or opening the mitochondrial permeability transition pore (MPTP) and then releasing Cyt c, sequentially activating initiator caspase-9 and downstream effector caspase-3, thereby orchestrating the final apoptotic response to facilitate viral replication *in vitro*, Intrinsic caspase-9 dependent apoptosis pathway plays an important role in the successful replication of PDCoV and SADS-CoV (49, 50). Further studies showed that caspase-dependent FASL-mediated apoptotic pathways are also involved in SADS-CoV infection (50).

1.4. Innate immunity recognition of SeCoV

1.4.1. Pattern recognition receptors

The innate immune response is the host's first line of defense against pathogens. Innate immune cells recognize

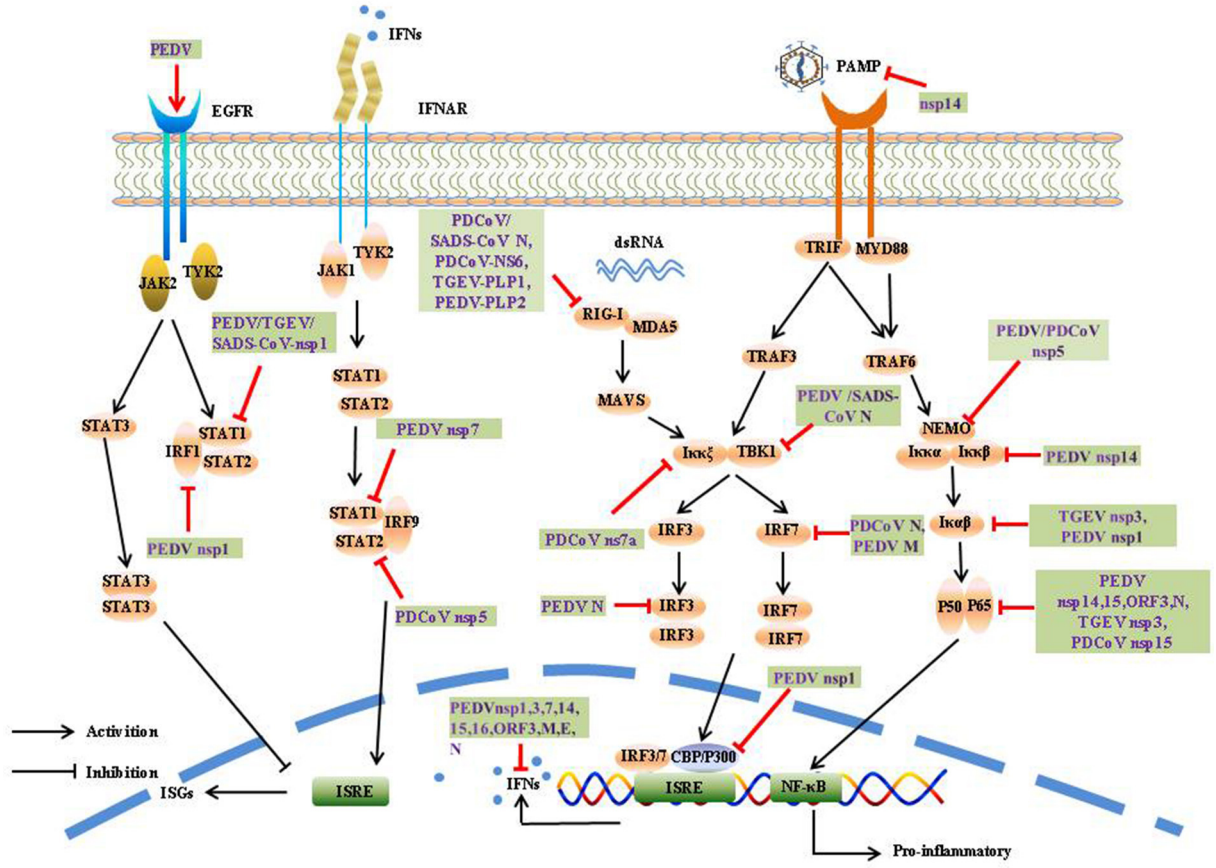

FIGURE 4
Innate immunity and modulatory mechanisms during SeCoV infection.

pathogen-associated molecular patterns (PAMP) by expressing pattern-recognition receptors (PRRs), including Toll-like receptors (TLRs), RIG-I-like receptors (RLRs), NOD-like receptors (NLRs), AIM2-like receptors (ALRs), C-type lectin receptors (CLRs), and intracellular DNA sensors, such as cyclic GMP-AMP synthase (cGAS), which are key innate immune components that recognize viral components such as viral nucleic acids and proteins (51). Among these receptors, TLRs and RLRs are the two major receptors responsible for sensing RNA virus infections and triggering antiviral IFN programs. The TLR family comprises 10 members (TLR1–TLR10) in humans and 12 (TLR1–TLR9 and TLR11–TLR13) in mice (52). TLR1, TLR2, TLR4, TLR5, and TLR6 play pivotal roles in viral protein recognition (53). The membrane proteins TLR3, TLR7/8, and TLR9 are used, respectively (54–56). The RLR family includes three members: retinoic acid-inducible gene I (RIG-I), melanoma differentiation-associated protein 5 (MDA5), and laboratory of genetics and physiology 2 (LGP2). RIG-I and MDA5 are activated by immunostimulatory RNA, which leads to the activation of cytoplasmic kinases that promote the activation of interferon regulatory factor 3 (IRF3), IRF7, and nuclear factor-kappa B (NF-κB). Activated IRF3/IRF7 binds to PRD I/III sequences and induces the expression of type I IFN genes (57). The activated form of NF-κB translocates to the nucleus and triggers IFN-β expression by binding to PRD II elements (58). IFN is then secreted, which binds to receptors on virus-infected cells, as well as uninfected neighboring cells, and activates the JAK/STAT pathway to generate hundreds of ISGs to establish an antiviral state (59).

1.4.2. Immune evasion mechanisms of SeCoV

The induction of IFN-α/β is the most rapid and effective mechanism by which the host initiates innate immune responses. To counter innate immune signaling, many coronaviruses have evolved different strategies to develop multiple strategies to evade the innate immune response and efficiently promote their replication and infective capacity, particularly by minimizing IFN production and inhibiting IFN signaling (Figure 4).

1.4.2.1. Ubiquitination and deubiquitination induced by SeCoV

Ubiquitination is a critical biological process in the post-translational modification of proteins and involves multiple signaling pathways such as protein metabolism, apoptosis, DNA damage, cell-cycle progression, and cancer development. Ubiquitin is mainly connected in eight ways (M1, K6, K11, K27, K29, K33, K48, and K63), and can regulate different functions of substrate proteins. For example, K48 polyubiquitination mainly plays the role of the ubiquitin-proteasome system to degrade substrates and proteins, whereas K63 polyubiquitination mainly regulates endocytosis, protein interaction, and signal transduction (60).

The CoV N protein, the most abundant viral protein, plays a key role in IFN interruption. The SADS-CoV N protein mediates K27-, K48-, and K63-linked ubiquitination of RIG-I and its subsequent proteasome-dependent degradation to inhibit the host IFN response (61). The PDCoV N protein could directly target porcine RIG-I to interfere with its binding to dsRNA and block its early activation by blocking porcine Riplet (pRiplet)-mediated K63-linked polyubiquitination, thus suppressing IFN-β Production (62). In addition, PDCoV N protein promotes poIRF7 degradation through the K6, K11, and K29 polyubiquitination-proteasome pathways to reduce type-I IFN production (63).

The deubiquitinase (DUB) family is responsible for the specific hydrolysis of ubiquitin molecules from ubiquitin-linked proteins or precursor proteolysis, which affects the localization, stability, and function of target proteins in cells, DUB are widely present in various viruses, and significantly influences viral activity. Interestingly, all CoV DUB activities are mediated by PLPs, and the PLPs of human coronavirus NL63 (HCoV-NL63), SARS-CoV, MHV, and MERS-CoV significantly reduced the levels of ubiquitinated STING, RIG-I, TBK1, and IRF-3, thereby negatively affecting the regulation of host antiviral innate immunity (64). Likewise, PEDV PLP2 and TGEV PL1 strongly inhibit RIG-I- and STING-activated IFN expression *via* deubiquitination (65, 66). A recent study showed that SADS-CoV PLP2 could also function as a DUB, such as PEDV PLP2, SARS-CoV PLpro, and TGEV PLP1 (67).

1.4.2.2. Protein cleavage

SeCoV encodes non-structural protein 5, also called the 3C-like protease, and is responsible for coronavirus polyprotein processing. It cleaves the polyprotein at more than 11 sites to yield the essential proteins required for virus replication and pathogenesis. At the same time, the protease can also use its cleavage activity to cleave host proteins, especially the key molecules of IFN production and signal transduction, and play an immunomodulatory role. 3CLpro is an attractive drug target because it is highly conserved among known coronavirus species. Many viruses antagonize innate immune signaling by cleaving 3C-like proteases; for example, porcine sapelovirus (PSV) 3Cpro inhibits the production of IFN-β by cleaving MAVS and degrading MDA5 and TBK1 (68). Enterovirus 71 (EV71) 3C interacts with and cleaves TAB2 and TAK1 to interfere with the inflammatory responses (69). Norovirus (NoV) encoding a 3C-like protease was found to effectively suppress Sendai virus (SEV)-mediated IFN-β production by cleaving the NF-κB essential modulator (NEMO) (70). Similar to NoV and EV71 3Cpro, PEDV and PDCoV encode a 3C-like protease, nsp5, which is an IFN antagonist that cleaves NEMO at Q231, suggesting that NEMO may be a common target for coronaviruses (71, 72). In addition, PDCoV nsp5 also suppressed IFN signaling by cleaving STAT2, a key molecule in the JAK-STAT pathway, nsp5 cleaved STAT2 at both Q685 and Q758 (73).

1.4.2.3. Competitive binding

It has been demonstrated PEDV N protein directly interacts with TBK1, thereby sequestering the association between TBK1 and IRF3, which in turn inhibits both IRF3 activation and type I IFN production (74). Moreover, the PDCoV N protein antagonizes IFN-β production by interfering with the binding of dsRNA and protein activator of protein kinase R (PACT) to RIG-I (75). The SADS-CoV N protein suppresses the RLRs Signaling pathway. Moreover, the SADS-CoV N Protein not only blocked the IPS-1–TBK1 interaction but also disrupted the formation of the TNF receptor-associated factor 3(TRAF3)–TBK1 complex, which led to reduced TBK1 activation and IFN-β production (76). It has been demonstrated PEDV nsp7 antagonizes type I IFN production, PEDV nsp7 also antagonized IFN-α-induced JAK-STAT signaling by sequestering the interaction between karyopherin α1 (KPNA1) and STAT1 (77). Cytoplasmic stress granules (SGs) can effectively exert antiviral functions; however, nsp15s of PEDV, TGEV, SARS-CoV, and SARS-CoV-2 have conserved functions that interfere with chemically induced SGs formation (78). Coronavirus accessory proteins are species specific and have low homology with other known proteins. Although current research has shown that coronavirus accessory proteins are not necessary for virus replication (79), extensive reports have indicated that many accessory proteins are involved in immune regulation and virus virulence. For example, PDCoV NS6 interacts with the CTD of RIG-I and the Hel and CTD of MDA5, and this interaction attenuates the binding of RIG-I/MDA5-dsRNA, resulting in a reduction in IFN-β production (80). PDCoV NS7a interacts with IKKε, which significantly disrupts the interaction between IKKε and TRAF3 or IRF3, thereby inhibiting IFN-β production (81).

1.4.2.4. Impair phosphorylation or suppressed the nuclear translocation

Post-translational modification of proteins is a critical way to regulate protein function. Phosphorylation is one of the most extensively investigated post-translational modifications involved in the regulation of signal transduction, but

viral encoded proteins can regulate phosphorylation and dephosphorylation to promote proliferation. The PEDV E protein has been found to block the production of IFN, but little is known about the process by which the E protein subverts host innate immunity. A previous study showed that PEDV E protein is responsible for inducing ER stress through activation of the PERK/eIF2α branch and activation of NF-κB (82). Further studies showed that PEDV E protein remarkably suppressed IFN-β production by interfering with the translocation of IRF3 from the cytoplasm to the nucleus through direct interaction with IRF3 (83, 84). PEDV N protein blocks NF-κB nuclear translocation to antagonize IFN-λ production (85). The PEDV M protein plays an important role in viral assembly, viral budding, and host immune mediation. PEDV M protein interacts with IRF7 and significantly suppresses its phosphorylation and dimerization of IRF7, leading to decreased expression of type I IFN (86). Existing study has been identified the sole accessory protein ORF3 of PEDV as NF-κB antagonist, it inhibits the phosphorylation of IκBα, in addition, PEDV ORF3 inhibits NF-κB activation by interfering the phosphorylation and expression of p65, as well as interfering nuclear translocation of p65, which ultimately leaded to the inhibition of IL-6 and IL-8 production (87). As a key virulence factor for coronaviruses, nsp1 impedes host protein expression *via* multiple mechanisms. Of the 21 PEDV proteins, nsp1, nsp3, nsp5, nsp7, nsp14, nsp15, nsp16, ORF3, and E inhibited NF-κB activity, and nsp1 appeared to be the most potent inhibitor. Nsp1 interfered with the phosphorylation and degradation of IκBα, and thus blocked p65 nuclear transport; however, PEDV nsp1 did not interfere with IRF3 phosphorylation and nuclear translocation, which interrupted the enhanceosome assembly of IRF3 and CREB-binding protein (CBP) by degrading CBP, resulting in the inhibition of ISGs expression (88, 89). Furthermore, nsp1 was found to suppress type III IFN activity by blocking the nuclear translocation of interferon regulatory factor 1 (IRF1) and reducing the number of peroxisomes (90). PEDV, TGEV, and SARS-CoV nsp1 significantly inhibited the phosphorylation of STAT1 at S727, interfering with the effect of IFN-I, and nsp1 also arrested host cells to stay in the G0/G1 phase (91, 92). In contrast, PEDV nsp1 inhibited CCAAT/enhancer-binding protein β (C/EBP-β) phosphorylation to reduce complement component 3 (C3) expression, which is considered to play a crucial role in preventing viral infection (93). Nsp14 of CoV has ExoN and guanine-N7-methyltransferase (N7-MTase) activities (94, 95), playing a key role in viral mRNA cap synthesis, CoV replication and transcription, Howerver, the function and mechanism by which nsp14 modulates and manipulates host immune responses remain largely unknown, Recently study showed PEDV nsp14 remarkably decreased NF-κB activation and proinflammatory cytokines expression, it interacted with Iκκs and p65 to inhibite the phosphorylation of Iκκs. Furthermore, nsp14 suppresses TNF-α-induced phosphorylation and nuclear import of p65 (96). TGEV nsp3 has been shown to strongly inhibits NF-κB signaling by suppressing Iκβα degradation and inhibiting p65 phosphorylation and nuclear translocation (97). Nsp15 encodes an endoribonuclease that conserves all coronaviruses. The nuclease activity of nsp15 plays a critical role in viral evasion by triggering an innate immune response. PDCoV nsp15 significantly inhibits IFN-β production by disrupting the phosphorylation and nuclear translocation of p65, independent of its endoribonuclease (98). TGEV ORF7 binds to the catalytic subunit of protein phosphatase 1 (PP1c) and regulated the dephosphorylation of eIF2α to counteract host cellular defenses (99). In addition, deletion of ORF7 increased innate immune responses and acute tissue damage, demonstrating antagonism from the opposite perspective (100).

1.4.2.5. Degradation and inactivation induced by SeCoV

In addition, SeCoV can antagonize the host innate immune response through degradation and inactivation. PEDV suppresses type I interferon response by stimulating epidermal growth factor receptor (EGFR) activation, which is responsible for STAT3 expression (101). PEDV nsp15 directly degrades the mRNA of TBK1 and IRF3 depending on its EndoU activity to inhibit the production of IFN and ISG and antagonize the host innate response to promote replication (102). CoV nsp14 can degrade dsRNA PAMPs to prevent IFN induction during CoV infection (103). Of the 21 PEDV proteins, nsp1, nsp3, nsp7, nsp14, nsp15, and nsp16 were found to inhibit IFN-β and IRF3 promoter activity (89). Further studies showed that nsp1, nsp3, nsp5, nsp8, nsp14, nsp15, nsp16, ORF3, E, M, and N suppressed type III IFN activity (90).

2. Discussion

SeCoV is a pathogenic microorganism that seriously threatens the pig industry and causes massive economic loss. The above evidence reveals the viral immune evasion mechanisms of SeCoV, where the origin of SeCoV and the interaction between the virus and host need to be further elucidated. Furthermore, the rapid global spread of highly pathogenic of SARS-CoV, MERS-CoV, and SADS-CoV-2 pose a concern about cross-species transmission, such as the discovery of PDCoV in Haitian children. It is evident that proper surveillance of viral biodiversity can be used to prevent animals becoming mixers and intermediate hosts of various coronaviruses in the future. Morever, an important feature of the epidemiology of SECoV is the emergence of several different variants, which vary in their transmissibility, virulence, clinical disease presentation, and vaccines response, resulting in unforeseeable epidemic scope and pathogenicity. Up to now, porcine aminopeptidase N (pAPN) has been identified as a receptor for TGEV, but the receptors of PEDV, PDCoV, and

SASD-CoV remain unknown, hindering the development of vaccines and drugs.

Exploration of these programs will help us further understand how SeCoV exists to ensure their survival, and also provide us with new ideas for developing drug targets for the prevention and treatment of SeCoV.

Author contributions

ML wrote the first draft of the manuscript. LG and LF contributed to conception and design of the review. All authors contributed to manuscript revision, read, and approved the submitted version.

Funding

The manuscript was supported by the National Key R&D Program of China (2021YFD1801105), Natural Science Foundation of Heilongjiang Province of China (YQ2020C023), and National Natural Science Foundation of China (31872474).

Conflict of interest

The authors declare that the research was conducted in the absence of any commercial or financial relationships that could be construed as a potential conflict of interest.

Publisher's note

References

1. Wood EN. An apparently new syndrome of porcine epidemic diarrhoea. *Vet Rec.* (1977) 100:243–4. doi: 10.1136/vr.100.12.243

2. Doyle LP, Hutchings LM. A Transmissible gastroenteritis in pigs. *J Am Vet Med Assoc.* (1946) 108:257–9.

3. Pensaert MB, Bouck PD. A new coronavirus-like particle associated with diarrhea in swine. *Arch Virol.* (1978) 58:243–7. doi: 10.1007/BF01317606

4. Hou Y, Yue X, Cai X, Wang S, Liu Y, Yuan C, et al. Complete genome of transmissible gastroenteritis virus ayu strain isolated in Shanghai, China. *J Virol.* (2012) 86:11935. doi: 10.1128/JVI.01839-12

5. Weiwei H, Qinghua Y, Liqi Z, Haofei L, Shanshan Z, Qi G, et al. Complete genomic sequence of the coronavirus transmissible gastroenteritis virus shxb isolated in China. *Arch Virol.* (2014) 159:2295–302. doi: 10.1007/s00705-014-2080-9

6. Woo PCY, Lau SKP, Lam CSF, Lau CCY, Tsang AKL, Lau JHN, et al. Discovery of seven novel mammalian and avian coronaviruses in the genus deltacoronavirus supports bat coronaviruses as the gene source of alphacoronavirus and betacoronavirus and avian coronaviruses as the gene source of gammacoronavirus and deltacoronavirus. *J Virol.* (2012) 86:3995–4008. doi: 10.1128/JVI.06540-11

7. Pan Y, Tian X, Qin P, Wang B, Zhao P, Yang YL, et al. Discovery of a novel swine enteric alphacoronavirus (Seacov) in Southern China. *Vet Microbiol.* (2017) 211:15–21. doi: 10.1016/j.vetmic.2017.09.020

8. Lednicky JA, Tagliamonte MS, White SK, Elbadry MA, Alam MM, Stephenson CJ, et al. Independent infections of porcine deltacoronavirus among Haitian children. *Nature.* (2021) 600:133–7. doi: 10.1038/s41586-021-04111-z

9. de Groot RJ, Luytjes W, Horzinek MC, van der Zeijst BA, Spaan WJ, Lenstra JA. Evidence for a coiled-coil structure in the spike proteins of coronaviruses. *J Mol Biol.* (1987) 196:963–6. doi: 10.1016/0022-2836(87)90422-0

10. Fehr AR, Perlman S. Coronaviruses: an overview of their replication and pathogenesis. *Methods Mol Biol.* (2015) 1282:1–23. doi: 10.1007/978-1-4939-2438-7_1

11. Masters PS. The molecular biology of coronaviruses. *Adv Virus Res.* (2006) 66:193–292. doi: 10.1016/S0065-3527(06)66005-3

12. Zhang J. Porcine deltacoronavirus: overview of infection dynamics, diagnostic methods, prevalence and genetic evolution. *Virus Res.* (2016) 226:71–84. doi: 10.1016/j.virusres.2016.05.028

13. Koonpaew S, Teeravechyan S, Frantz PN, Chailangkarn T, Jongkaewwattana A. Pedv and Pdcov pathogenesis: the interplay between host innate immune responses and porcine enteric coronaviruses. *Front Vet Sci.* (2019) 6:34. doi: 10.3389/fvets.2019.00034

14. Su WQ, Yu XJ, Zhou CM. SARS-CoV-2 ORF3a induces incomplete autophagy via the unfolded protein response. *Viruses.* (2021) 13:2467. doi: 10.3390/v13122467

15. Hui X, Zhang L, Cao L, Huang K, Zhao Y, Zhang Y, et al. SARS-CoV-2 promote autophagy to suppress type i interferon response. *Signal Transd Targeted Ther.* (2021) 6:180. doi: 10.1038/s41392-021-00574-8

16. Li X, Hou P, Ma W, Wang X, Wang H, Yu Z, et al. SARS-CoV-2 ORF10 suppresses the antiviral innate immune response by degrading mavs through mitophagy. *Cell Mol Immunol.* (2022) 19:67–78. doi: 10.1038/s41423-021-00807-4

17. Guo X, Zhang M, Zhang X, Tan X, Guo H, Zeng W, et al. Porcine epidemic diarrhea virus induces autophagy to benefit its replication. *Viruses.* (2017) 9:53. doi: 10.3390/v9030053

18. Sun P, Jin J, Wang L, Wang J, Zhou H, Zhang Q, et al. Porcine epidemic diarrhea virus infections induce autophagy in vero cells via ros-dependent endoplasmic reticulum stress through Perk and Ire1 Pathways. *Vet Microbiol.* (2021) 253:108959. doi: 10.1016/j.vetmic.2020.108959

19. Park JY, Ryu J, Hong EJ, Shin HJ. Porcine epidemic diarrhea virus infection induces autophagosome formation but inhibits autolysosome formation during replication. *Viruses.* (2022) 14:1050. doi: 10.3390/v14051050

20. Lin H, Li B, Liu M, Zhou H, He K, Fan H. Nonstructural protein 6 of porcine epidemic diarrhea virus induces autophagy to promote viral replication via the Pi3k/Akt/Mtor axis. *Vet Microbiol.* (2020) 244:108684. doi: 10.1016/j.vetmic.2020.108684

21. Zou D, Xu J, Duan X, Xu X, Li P, Cheng L, et al. Porcine epidemic diarrhea virus Orf3 protein causes endoplasmic reticulum stress to facilitate autophagy. *Vet Microbiol.* (2019) 235:209–19. doi: 10.1016/j.vetmic.2019.07.005

22. Qin P, Du EZ, Luo WT, Yang YL, Zhang YQ, Wang B, et al. Characteristics of the life cycle of porcine deltacoronavirus (Pdcov) *in vitro*: replication kinetics, cellular ultrastructure and virion morphology, and evidence of inducing autophagy. *Viruses.* (2019) 11:455. doi: 10.3390/v11050455

23. Zeng S, Peng O, Sun R, Xu Q, Hu F, Zhao Y, et al. Transcriptional landscape of Vero E6 cells during early swine acute diarrhea syndrome coronavirus infection. *Viruses.* (2021) 13:674. doi: 10.3390/v13040674

24. Zhou X, Zhou L, Ge X, Guo X, Han J, Zhang Y, et al. Quantitative proteomic analysis of porcine intestinal epithelial cells infected with porcine deltacoronavirus using itraq-coupled Lc-Ms/Ms. *J Proteome Res.* (2020) 19:4470–85. doi: 10.1021/acs.jproteome.0c00592

25. Zhu L, Mou C, Yang X, Lin J, Yang Q. Mitophagy in Tgev infection counteracts oxidative stress and apoptosis. *Oncotarget.* (2016) 7:27122–41. doi: 10.18632/oncotarget.8345

26. Guo L, Yu H, Gu W, Luo X, Li R, Zhang J, et al. Autophagy negatively regulates transmissible gastroenteritis virus replication. *Sci Rep.* (2016) 6:23864. doi: 10.1038/srep23864

27. Prentice E, Jerome WG, Yoshimori T, Mizushima N, Denison MR. Coronavirus replication complex formation utilizes components of cellular autophagy. *J Biol Chem.* (2004) 279:10136–41. doi: 10.1074/jbc.M306124200

28. Duan C, Liu Y, Hao Z, Wang J. Ergosterol peroxide suppresses porcine deltacoronavirus (Pdcov)-induced autophagy to inhibit virus replication via P38 signaling pathway. *Vet Microbiol.* (2021) 257:109068. doi: 10.1016/j.vetmic.2021.109068

29. Willis S, Day CL, Hinds MG, Huang DC. The Bcl-2-regulated apoptotic pathway. *J Cell Sci.* (2003) 116(Pt 20):4053–6. doi: 10.1242/jcs.00754

30. Shen Y, Shenk TE. Viruses and apoptosis. *Curr Opin Genet Dev.* (1995) 5:105–11. doi: 10.1016/S0959-437X(95)90061-6

31. Sun P, Wu H, Huang J, Xu Y, Yang F, Zhang Q, et al. Porcine epidemic diarrhea virus through P53-dependent pathway causes cell cycle arrest in the G0/G1 phase. *Virus Res.* (2018) 253:1–11. doi: 10.1016/j.virusres.2018.05.019

32. Kim Y, Lee C. Porcine epidemic diarrhea virus induces caspase-independent apoptosis through activation of mitochondrial apoptosis-inducing factor. *Virology.* (2014) 460–1:180–93. doi: 10.1016/j.virol.2014.04.040

33. Shen X, Yin L, Pan X, Zhao R, Zhang D. Porcine epidemic diarrhea virus infection blocks cell cycle and induces apoptosis in pig intestinal epithelial cells. *Microbial Pathog.* (2020) 147:104378. doi: 10.1016/j.micpath.2020.104378

34. Lee C, Kim Y, Jeon JH. Jnk and P38 mitogen-activated protein kinase pathways contribute to porcine epidemic diarrhea virus infection. *Virus Res.* (2016) 222:1–12. doi: 10.1016/j.virusres.2016.05.018

35. Xu X, Xu Y, Zhang Q, Yang F, Yin Z, Wang L, et al. Porcine epidemic diarrhea virus infections induce apoptosis in vero cells via a reactive oxygen species (Ros)/P53, but Not P38 Mapk and Sapk/Jnk signalling pathways. *Vet Microbiol.* (2019) 232:1–12. doi: 10.1016/j.vetmic.2019.03.028

36. Ding L, Li J, Li W, Fang Z, Li N, Wu S, et al. P53- and ros-mediated aif pathway involved in Tgev-induced apoptosis. *J Vet Med Sci.* (2018) 80:1775–81. doi: 10.1292/jvms.18-0104

37. Yang L, Wang C, Shu J, Feng H, He Y, Chen J, et al. Porcine epidemic diarrhea virus induces vero cell apoptosis via the P53-puma signaling pathway. *Viruses.* (2021) 13:1218. doi: 10.3390/v13071218

38. Chen Y, Zhang Z, Li J, Gao Y, Zhou L, Ge X, et al. Porcine epidemic diarrhea virus S1 protein is the critical inducer of apoptosis. *Virol J.* (2018) 15:170. doi: 10.1186/s12985-018-1078-4

39. Sun M, Ma J, Yu Z, Pan Z, Lu C, Yao H. Identification of two mutation sites in spike and envelope proteins mediating optimal cellular infection of porcine epidemic diarrhea virus from different pathways. *Vet Res.* (2017) 48:44. doi: 10.1186/s13567-017-0449-y

40. Si F, Hu X, Wang C, Chen B, Wang R, Dong S, et al. Porcine epidemic diarrhea virus (Pedv) Orf3 enhances viral proliferation by inhibiting apoptosis of infected cells. *Viruses.* (2020) 12:214. doi: 10.3390/v12020214

41. Kim B, Kim O, Tai JH, Chae C. Transmissible gastroenteritis virus induces apoptosis in swine testicular cell lines but not in intestinal enterocytes. *J Comp Pathol.* (2000) 123:64–6. doi: 10.1053/jcpa.2000.0386

42. Ding L, Zhao X, Huang Y, Du Q, Dong F, Zhang H, et al. Regulation of Ros in transmissible gastroenteritis virus-activated apoptotic signaling. *Biochem Biophys Res Commun.* (2013) 442:33–7. doi: 10.1016/j.bbrc.2013.10.164

43. Eleouet JF, Chilmonczyk S, Besnardeau L, Laude H. Transmissible gastroenteritis coronavirus induces programmed cell death in infected cells through a caspase-dependent pathway. *J Virol.* (1998) 72:4918–24. doi: 10.1128/JVI.72.6.4918-4924.1998

44. Ding L, Xu X, Huang Y, Li Z, Zhang K, Chen G, et al. Transmissible gastroenteritis virus infection induces apoptosis through fasl- and mitochondria-mediated pathways. *Vet Microbiol.* (2012) 158:12–22. doi: 10.1016/j.vetmic.2012.01.017

45. Huang Y, Ding L, Li Z, Dai M, Zhao X, Li W, et al. Transmissible gastroenteritis virus infection induces cell apoptosis via activation of P53 signalling. *J Gen Virol.* (2013) 94(Pt 8):1807–17. doi: 10.1099/vir.0.051557-0

46. Eléouët JF, Slee EA, Saurini F, Castagné N, Poncet D, Garrido C, et al. The viral nucleocapsid protein of transmissible gastroenteritis coronavirus (Tgev) is cleaved by caspase-6 and−7 during tgev-induced apoptosis. *J Virol.* (2000) 74:3975–83. doi: 10.1128/JVI.74.9.3975-3983.2000

47. Ding L, Huang Y, Du Q, Dong F, Zhao X, Zhang W, et al. Tgev nucleocapsid protein induces cell cycle arrest and apoptosis through activation of P53 signaling. *Biochem Biophys Res Commun.* (2014) 445:497–503. doi: 10.1016/j.bbrc.2014.02.039

48. Jung K, Hu H, Saif LJ. Porcine deltacoronavirus induces apoptosis in swine testicular and Llc porcine kidney cell lines *in vitro* but not in infected intestinal enterocytes *in vivo*. *Vet Microbiol.* (2016) 182:57–63. doi: 10.1016/j.vetmic.2015.10.022

49. Lee YJ, Lee C. Porcine deltacoronavirus induces caspase-dependent apoptosis through activation of the cytochrome C-mediated intrinsic mitochondrial pathway. *Virus Res.* (2018) 253:112–23. doi: 10.1016/j.virusres.2018.06.008

50. Zhang J, Han Y, Shi H, Chen J, Zhang X, Wang X, et al. Swine acute diarrhea syndrome coronavirus-induced apoptosis is caspase- and cyclophilin D- dependent. *Emerg Microbes Infect.* (2020) 9:439–56. doi: 10.1080/22221751.2020.1722758

51. Akira S, Uematsu S, Takeuchi O. Pathogen recognition and innate immunity. *Cell.* (2006) 124:783–801. doi: 10.1016/j.cell.2006.02.015

52. Kawasaki T, Kawai T. Toll-like receptor signaling pathways. *Front Immunol.* (2014) 5:461. doi: 10.3389/fimmu.2014.00461

53. Prinz M, Heikenwalder M, Schwarz P, Takeda K, Akira S, Aguzzi A. Prion pathogenesis in the absence of toll-like receptor signalling. *EMBO Rep.* (2003) 4:195–9. doi: 10.1038/sj.embor.embor731

54. Diebold SS, Kaisho T, Hemmi H, Akira S, Reis e Sousa C. Innate antiviral responses by means of Tlr7-mediated recognition of single-stranded RNA. *Science.* (2004) 303:1529–31. doi: 10.1126/science.1093616

55. Heil F, Hemmi H, Hochrein H, Ampenberger F, Kirschning C, Akira S, et al. Species-specific recognition of single-stranded Rna via toll-like receptor 7 and 8. *Science.* (2004) 303:1526–9. doi: 10.1126/science.1093620

56. Okahira S, Nishikawa F, Nishikawa S, Akazawa T, Seya T, Matsumoto M. Interferon-beta induction through toll-like receptor 3 depends on double-stranded RNA structure. *DNA Cell Biol.* (2005) 24:614–23. doi: 10.1089/dna.2005.24.614

57. Hermant P, Michiels T. Interferon-Λ in the context of viral infections: production, response and therapeutic implications. *J Innate Immunity.* (2014) 6:563–74. doi: 10.1159/000360084

58. Escalante CR, Shen L, Thanos D, Aggarwal AK. Structure of Nf-Kappab P50/P65 heterodimer bound to the Prdii DNA element from the interferon-beta promoter. *Structure.* (2002) 10:383–91. doi: 10.1016/S0969-2126(02)00723-2

59. Stark GR, Darnell JE Jr. The Jak-Stat pathway at twenty. *Immunity.* (2012) 36:503–14. doi: 10.1016/j.immuni.2012.03.013

60. Tracz M, Bialek W. Beyond K48 and K63: non-canonical protein ubiquitination. *Cell Mol Biol Lett.* (2021) 26:1. doi: 10.1186/s11658-020-00245-6

61. Liu Y, Liang QZ, Lu W, Yang YL, Chen R, Huang YW, et al. A comparative analysis of coronavirus nucleocapsid (N) proteins reveals the Sads-Cov N protein antagonizes Ifn-β production by inducing ubiquitination of Rig-I. *Front Immunol.* (2021) 12:688758. doi: 10.3389/fimmu.2021.688758

62. Likai J, Shasha L, Wenxian Z, Jingjiao M, Jianhe S, Hengan W, et al. Porcine deltacoronavirus nucleocapsid protein suppressed ifn-β production by interfering porcine Rig-I Dsrna-binding and K63-linked polyubiquitination. *Front Immunol.* (2019) 10:1024. doi: 10.3389/fimmu.2019.01024

63. Ji L, Wang N, Ma J, Cheng Y, Wang H, Sun J, et al. Porcine deltacoronavirus nucleocapsid protein species-specifically suppressed Irf7-induced type I interferon production via ubiquitin-proteasomal degradation pathway. *Vet Microbiol.* (2020) 250:108853. doi: 10.1016/j.vetmic.2020.108853

64. Sun L, Xing Y, Chen X, Zheng Y, Yang Y, Nichols DB, et al. Coronavirus papain-like proteases negatively regulate antiviral innate immune response through disruption of sting-mediated signaling. *PLoS ONE.* (2012) 7:e30802. doi: 10.1371/journal.pone.0030802

65. Xing Y, Chen J, Tu J, Zhang B, Chen X, Shi H, et al. The papain-like protease of porcine epidemic diarrhea virus negatively regulates type I interferon pathway by acting as a viral deubiquitinase. *J Gen Virol.* (2013) 94(Pt 7):1554–67. doi: 10.1099/vir.0.051169-0

66. Hu X, Tian J, Kang H, Guo D, Liu J, Liu D, et al. Transmissible gastroenteritis virus papain-like protease 1 antagonizes production of interferon-β through its deubiquitinase activity. *Biomed Res Int.* (2017) 2017:7089091. doi: 10.1155/2017/7089091

67. Wang L, Hu W, Fan C. Structural and biochemical characterization of sads-cov papain-like protease 2. *Protein Sci.* (2020) 29:1228–41. doi: 10.1002/pro.3857

68. Yin M, Wen W, Wang H, Zhao Q, Zhu H, Chen H, et al. Porcine sapelovirus 3c(Pro) inhibits the production of type I interferon. *Front Cell Infect Microbiol.* (2022) 12:852473. doi: 10.3389/fcimb.2022.852473

69. Lei X, Han N, Xiao X, Jin Q, He B, Wang J. Enterovirus 71 3c inhibits cytokine expression through cleavage of the Tak1/Tab1/Tab2/Tab3 complex. *J Virol.* (2014) 88:9830–41. doi: 10.1128/JVI.01425-14

70. Zhang H, Jiang P, Chen Z, Wang D, Zhou Y, Zhu X, et al. Norovirus 3c-like protease antagonizes interferon-β production by cleaving nemo. *Virology.* (2022) 571:12–20. doi: 10.1016/j.virol.2022.04.004

71. Zhu X, Fang L, Wang D, Yang Y, Chen J, Ye X, et al. Porcine deltacoronavirus Nsp5 inhibits interferon-β production through the cleavage of nemo. *Virology.* (2017) 502:33–8. doi: 10.1016/j.virol.2016.12.005

72. Wang D, Fang L, Shi Y, Zhang H, Gao L, Peng G, et al. Porcine epidemic diarrhea virus 3c-like protease regulates its interferon antagonism by cleaving nemo. *J Virol.* (2016) 90:2090–101. doi: 10.1128/JVI.02514-15

73. Zhu X, Wang D, Zhou J, Pan T, Chen J, Yang Y, et al. Porcine deltacoronavirus Nsp5 antagonizes type I interferon signaling by cleaving Stat2. *J Virol.* (2017) 91(10). doi: 10.1128/JVI.00003-17

74. Ding Z, Fang L, Jing H, Zeng S, Wang D, Liu L, et al. Porcine epidemic diarrhea virus nucleocapsid protein antagonizes beta interferon production by sequestering the interaction between Irf3 and Tbk1. *J Virol.* (2014) 88:8936–45. doi: 10.1128/JVI.00700-14

75. Chen J, Fang P, Wang M, Peng Q, Ren J, Wang D, et al. Porcine deltacoronavirus nucleocapsid protein antagonizes Ifn-β production by impairing Dsrna and pact binding to Rig-I. *Virus Genes.* (2019) 55:520–31. doi: 10.1007/s11262-019-01673-z

76. Zhou Z, Sun Y, Xu J, Tang X, Zhou L, Li Q, et al. Swine acute diarrhea syndrome coronavirus nucleocapsid protein antagonizes interferon-β production via blocking the interaction between Traf3 and Tbk1. *Front Immunol.* (2021) 12:573078. doi: 10.3389/fimmu.2021.573078

77. Zhang J, Yuan S, Peng Q, Ding Z, Hao W, Peng G, et al. Porcine epidemic diarrhea virus Nsp7 inhibits interferon-induced jak-stat signaling through sequestering the interaction between Kpna1 and Stat1. *J Virol.* (2022) 96:e0040022. doi: 10.1128/jvi.00400-22

78. Gao B, Gong X, Fang S, Weng W, Wang H, Chu H, et al. Inhibition of anti-viral stress granule formation by coronavirus endoribonuclease Nsp15 ensures efficient virus replication. *PLoS Pathog.* (2021) 17:e1008690. doi: 10.1371/journal.ppat.1008690

79. Yount B, Roberts RS, Sims AC, Deming D, Frieman MB, Sparks J, et al. severe acute respiratory syndrome coronavirus group-specific open reading frames encode nonessential functions for replication in cell cultures and mice. *J Virol.* (2005) 79:14909–22. doi: 10.1128/JVI.79.23.14909-14922.2005

80. Fang P, Fang L, Ren J, Hong Y, Liu X, Zhao Y, et al. Porcine deltacoronavirus accessory protein Ns6 antagonizes interferon beta production by interfering with the binding of Rig-I/Mda5 to double-stranded Rna. *J Virol.* (2018) 92:e00712-18. doi: 10.1128/JVI.00712-18

81. Fang P, Fang L, Xia S, Ren J, Zhang J, Bai D, et al. Porcine deltacoronavirus accessory protein Ns7a antagonizes Ifn-β production by competing with Traf3 and Irf3 for binding to Ikkε. *Front Cell Infect Microbiol.* (2020) 10:257. doi: 10.3389/fcimb.2020.00257

82. Xu X, Zhang H, Zhang Q, Dong J, Liang Y, Huang Y, et al. Porcine epidemic diarrhea virus E protein causes endoplasmic reticulum stress and up-regulates interleukin-8 expression. *Virol J.* (2013) 10:26. doi: 10.1186/1743-422X-10-26

83. Zheng L, Wang X, Guo D, Cao J, Cheng L, Li X, et al. Porcine epidemic diarrhea virus e protein suppresses Rig-I signaling-mediated interferon-β production. *Vet Microbiol.* (2021) 254:108994. doi: 10.1016/j.vetmic.2021.108994

84. Zheng L, Liu H, Tian Z, Kay M, Wang H, Wang X, et al. Porcine epidemic diarrhea virus E protein inhibits type I interferon production through endoplasmic reticulum stress response (Ers)-mediated suppression of antiviral proteins translation. *Res Vet Sci.* (2022) 152:236–44. doi: 10.1016/j.rvsc.2022.07.019

85. Shan Y, Liu ZQ, Li GW, Chen C, Luo H, Liu YJ, et al. Nucleocapsid protein from porcine epidemic diarrhea virus isolates can antagonize interferon-Λ production by blocking the nuclear factor-κb nuclear translocation. *J Zhejiang Univ Sci B.* (2018) 19:570–80. doi: 10.1631/jzus.B1700283

86. Li S, Zhu Z, Yang F, Cao W, Yang J, Ma C, et al. Porcine epidemic diarrhea virus membrane protein interacted with Irf7 to inhibit type I Ifn production during viral infection. *J Immunol.* (2021) 206:2909–23. doi: 10.4049/jimmunol.2001186

87. Wu Z, Cheng L, Xu J, Li P, Li X, Zou D, et al. The accessory protein Orf3 of porcine epidemic diarrhea virus inhibits cellular interleukin-6 and interleukin-8 productions by blocking the nuclear factor-Kb P65 activation. *Vet Microbiol.* (2020) 251:108892. doi: 10.1016/j.vetmic.2020.108892

88. Zhang Q, Ma J, Yoo D. Inhibition of Nf-Kb Activity by the porcine epidemic diarrhea virus nonstructural protein 1 for innate immune evasion. *Virology.* (2017) 510:111–26. doi: 10.1016/j.virol.2017.07.009

89. Zhang Q, Shi K, Yoo D. Suppression of type I interferon production by porcine epidemic diarrhea virus and degradation of Creb-binding protein by Nsp1. *Virology.* (2016) 489:252–68. doi: 10.1016/j.virol.2015.12.010

90. Zhang Q, Ke H, Blikslager A, Fujita T, Yoo D. Type III interferon restriction by porcine epidemic diarrhea virus and the role of viral protein Nsp1 in Irf1 signaling. *J Virol.* (2018) 92:e01677-17. doi: 10.1128/JVI.01677-17

91. Shen Z, Yang Y, Yang S, Zhang G, Xiao S, Fu ZF, et al. Structural and biological basis of alphacoronavirus Nsp1 associated with host proliferation and immune evasion. *Viruses.* (2020) 12:812. doi: 10.3390/v12080812

92. Wang X, Li H, Li Y, Gao D, Chen L, Chang H, et al. [Effect of porcine epidemic diarrhea virus Nsp1 on type I interferon response]. *Sheng Wu Gong Cheng Xue Bao.* (2017) 33:1325–34. doi: 10.13345/j.cjb.170068

93. Fan B, Peng Q, Song S, Shi D, Zhang X, Guo W, et al. Nonstructural protein 1 of variant Pedv plays a key role in escaping replication restriction by complement C3. *J Virol.* (2022) 2022:e0102422. doi: 10.1128/jvi.01024-22

94. Chen Y, Cai H, Pan J, Xiang N, Tien P, Ahola T, et al. Functional screen reveals sars coronavirus nonstructural protein Nsp14 as a novel cap N7 methyltransferase. *Proc Natl Acad Sci USA.* (2009) 106:3484–9. doi: 10.1073/pnas.0808790106

95. Minskaia E, Hertzig T, Gorbalenya AE, Campanacci V, Cambillau C, Canard B, et al. Discovery of an Rna virus 3′->5′ exoribonuclease that is critically involved in coronavirus Rna synthesis. *Proc Natl Acad Sci USA.* (2006) 103:5108–13. doi: 10.1073/pnas.0508200103

96. Li S, Yang F, Ma C, Cao W, Yang J, Zhao Z, et al. Porcine epidemic diarrhea virus Nsp14 inhibits Nf-Kb pathway activation by targeting the Ikk complex and P65. *Anim Dis.* (2021) 1:24. doi: 10.1186/s44149-021-00025-5

97. Wang Y, Sun A, Sun Y, Zhang S, Xia T, Guo T, et al. Porcine transmissible gastroenteritis virus inhibits Nf-Kb activity via nonstructural protein 3 to evade host immune system. *Virol J.* (2019) 16:97. doi: 10.1186/s12985-019-1206-9

98. Liu X, Fang P, Fang L, Hong Y, Zhu X, Wang D, et al. Porcine deltacoronavirus Nsp15 antagonizes interferon-β production independently of its endoribonuclease activity. *Mol Immunol.* (2019) 114:100–7. doi: 10.1016/j.molimm.2019.07.003

99. Cruz JL, Sola I, Becares M, Alberca B, Plana J, Enjuanes L, et al. Coronavirus gene 7 counteracts host defenses and modulates virus virulence. *PLoS Pathog.* (2011) 7:e1002090. doi: 10.1371/journal.ppat.1002090

100. Cruz JL, Becares M, Sola I, Oliveros JC, Enjuanes L, Zúñiga S. Alphacoronavirus protein 7 modulates host innate immune response. *J Virol.* (2013) 87:9754–67. doi: 10.1128/JVI.01032-13

101. Yang L, Xu J, Guo L, Guo T, Zhang L, Feng L, et al. Porcine epidemic diarrhea virus-induced epidermal growth factor receptor activation impairs the antiviral activity of type I interferon. *J Virol.* (2018) 92:e02095-17. doi: 10.1128/JVI.02095-17

102. Wu Y, Zhang H, Shi Z, Chen J, Li M, Shi H, et al. Porcine epidemic diarrhea virus Nsp15 antagonizes interferon signaling by Rna degradation of Tbk1 and Irf3. *Viruses.* (2020) 12:599. doi: 10.3390/v12060599

103. Kindler E, Thiel V. To sense or not to sense viral RNA–essentials of coronavirus innate immune evasion. *Curr Opin Microbiol.* (2014) 20:69–75. doi: 10.1016/j.mib.2014.05.005

frontiers | Frontiers in Veterinary Science

TYPE Original Research
PUBLISHED 29 December 2022
DOI 10.3389/fvets.2022.1053198

OPEN ACCESS

EDITED BY
Lian-Feng Li,
Harbin Veterinary Research Institute (CAAS), China

REVIEWED BY
Yuexiu Zhang,
The Ohio State University, United States
Francesco Ria,
Catholic University of the Sacred Heart, Italy

*CORRESPONDENCE
Yin Wang
10334@sicau.edu.cn

†These authors have contributed equally to this work and share first authorship

SPECIALTY SECTION
This article was submitted to Veterinary Infectious Diseases, a section of the journal Frontiers in Veterinary Science

RECEIVED 25 September 2022
ACCEPTED 30 November 2022
PUBLISHED 29 December 2022

CITATION
Pang M, Tu T, Wang Y, Zhang P, Ren M, Yao X, Luo Y and Yang Z (2022) Design of a multi-epitope vaccine against *Haemophilus parasuis* based on pan-genome and immunoinformatics approaches. *Front. Vet. Sci.* 9:1053198. doi: 10.3389/fvets.2022.1053198

Design of a multi-epitope vaccine against *Haemophilus parasuis* based on pan-genome and immunoinformatics approaches

Maonan Pang[1,2†], Teng Tu[1,2†], Yin Wang[1,2*], Pengfei Zhang[1,2], Meishen Ren[1,2], Xueping Yao[1,2], Yan Luo[1,2] and Zexiao Yang[1,2]

[1]College of Veterinary Medicine, Sichuan Agricultural University, Chengdu, China, [2]Key Laboratory of Animal Diseases and Human Health of Sichuan Province, Chengdu, Sichuan, China

Background: Glässer's disease, caused by *Haemophilus parasuis* (HPS), is responsible for economic losses in the pig industry worldwide. However, the existing commercial vaccines offer poor protection and there are significant barriers to the development of effective vaccines.

Methods: In the current study, we aimed to identify potential vaccine candidates and design a multi-epitope vaccine against HPS by performing pan-genomic analysis of 121 strains and using a reverse vaccinology approach.

Results: The designed vaccine constructs consist of predicted epitopes of B and T cells derived from the outer membrane proteins of the HPS core genome. The vaccine was found to be highly immunogenic, non-toxic, and non-allergenic as well as have stable physicochemical properties. It has a high binding affinity to Toll-like receptor 2. In addition, *in silico* immune simulation results showed that the vaccine elicited an effective immune response. Moreover, the mouse polyclonal antibody obtained by immunizing the vaccine protein can be combined with different serotypes and non-typable *Haemophilus parasuis in vitro*.

Conclusion: The overall results of the study suggest that the designed multi-epitope vaccine is a promising candidate for pan-prophylaxis against different strains of HPS.

KEYWORDS

***Haemophilus parasuis*, reverse vaccinology, pan-genome analysis, multi-epitope vaccine, immunoinformatics**

Introduction

The disease caused by *Haemophilus parasuis* (HPS), known as Glässer's disease, is characterized by fibrinous polyserositis and arthritis (Figures 1, 2). It is one of the main infectious diseases in the day-old isolated farming model of the global pig industry and causes significant economic losses (1). *H. parasuis* strains are heterogeneous in

terms of phenotypic and genotypic traits. Strains have been classified into 15 serotypes, but a large proportion of isolates remain non-typable (2). Currently, vaccination is the main measure for preventing HPS infection. Commercially available inactivated bacterin vaccines are based on serovar 5, a combination of serovars 4 and 5, or a combination of serovars 1 and 6. However, all these vaccine products showed limited cross-protection against heterologous strains. There is often even failure to achieve the desired effect in protection against different isolates of the same serotype (3). Moreover, the protection against non-typable strains remains elusive. In addition, more than one strain of HPS is often present in a pig farm. For example, 4–5 strains can be isolated from a herd at a given time, and up to 16 different strains can be isolated in a single pig farm during one production cycle (4–6). This epidemiological feature also poses a great challenge for the selection of HPS vaccines in the breeding process.

Given the challenges faced by inactivated bacterial vaccines for treatment of HPS described above, the use of reverse vaccinology to develop protein vaccines against protective epitopes of the pathogen is a viable strategy. Reverse vaccinology involves computer programs to identify antigenic epitopes based on bacterial genome sequence information for vaccine development and design, avoiding the disadvantages of traditional vaccine design which is expensive and time consuming (7, 8). Moreover, with the constant updating of sequencing technologies, sequence information of bacterial genomes can be obtained at a low cost and in a short time, which also reduces the time required for vaccine design.

Hence, in this study, we used pan genome analysis to identify the core genome of HPS. Then, *in silico* prediction of B and T cell epitopes of outer membrane proteins in the core genome were performed to design a multi-epitope vaccine. An adjuvant was also ligated with to the vaccine to enhance the immunogenicity of the vaccine to obtain the final multi-epitope vaccine construct. Subsequently, the antigenicity and physicochemical properties of the vaccine construct were estimated. In addition, the secondary and tertiary structures of the construct were predicted and the interaction of the vaccine with Toll-like receptor 2 was assessed by molecular docking simulations. Finally, immune simulations were performed to confirm the immune potential of the vaccine construct and a vector was constructed for its expression in *E. coli*. The application potential of multi-epitope vaccine was preliminarily tested in mouse immunization test. Thus, in this work, a multi-epitope vaccine candidate was created using a novel vaccine design strategy based on pan-genomic analysis and reverse vaccinology techniques that will also help to accelerate the development of vaccines against other pathogens.

Materials and methods

Bacterial strains

In this study, we retrieved the complete genome of 105 HPS strains with rich geographical, virulent and serological diversity, which were available in March 2020 from NCBI (ftp://ftp.ncbi.nih.gov/genomes/all/). Information about the 105 strains is summarized in Supplementary Table 1.

In addition, 16 clinical strains isolated in Sichuan between 2015 and 2020 were sequenced. DNA was extracted from overnight culture using an E.Z.N.A Bacterial DNA Kit (OMEGA) following the manufacturer's guidelines and sequenced using the Min-ION MK1B platform. Raw ONT reads were corrected using Canu (9) (v1.5 https://github.com/marbl/canu, accessed on 15 October 2020) and SMARTdenovo (https://github.com/ruanjue/smartdenovo, accessed on 15 October 2020) was then used to assemble the error-corrected reads to obtain the assembled genome sequence. Lastly, Medaka (v1.0.1https://github.com/nanoporetech/medaka, accessed on 15 October 2020) and Homopolish (10) (v0.2.1 https://github.com/ythuang0522/homopolish, accessed on 15 May 2021) was used to perform multiple rounds of polishing for draft assemblies. One hundred and fifteen HPS strains were isolated from clinical cases with Glässer disease, and six strains were from the upper respiratory tract of healthy pigs.

Pan-genomic and phylogenetic analysis

To maintain the consistency and reliability of gene prediction and annotation, a standard software tool the Prokaryotic Genome Annotation System (Prokka) pipeline (11) (v1.14.5 https://github.com/tseemann/prokka, accessed on 5 September 2021) was uniformly applied to all the 121 HPS genomes. Based on the GFF3 files produced by Prokka, the Roary program (12) (https://github.com/sanger-pathogens/Roary, accessed on 6 October 2021) was used to carry out the pan-genomic analysis to identify core and accessory genes with a minimum percentage identity of 95% between each predicted protein homolog. Then, a NJ (neighbor-joining) tree was constructed according to the core genes of HPS strains using MEGA (13) with 1,000 bootstrap replications.

Selection of protein sequences for vaccine designing

The protein sequences of core genes and soft-core genes were extracted based on the results of the pan-genomic analysis. Then, the SignalP 5.0 server (14) was used to

FIGURE 1
Group of nursery pigs diagnosed with Glässer's disease. **(A,B)** Pigs gather in the corner of the pen to protect themselves from the cold, their bodies are dirty, and their coats are ragged. Photographs taken by the author.

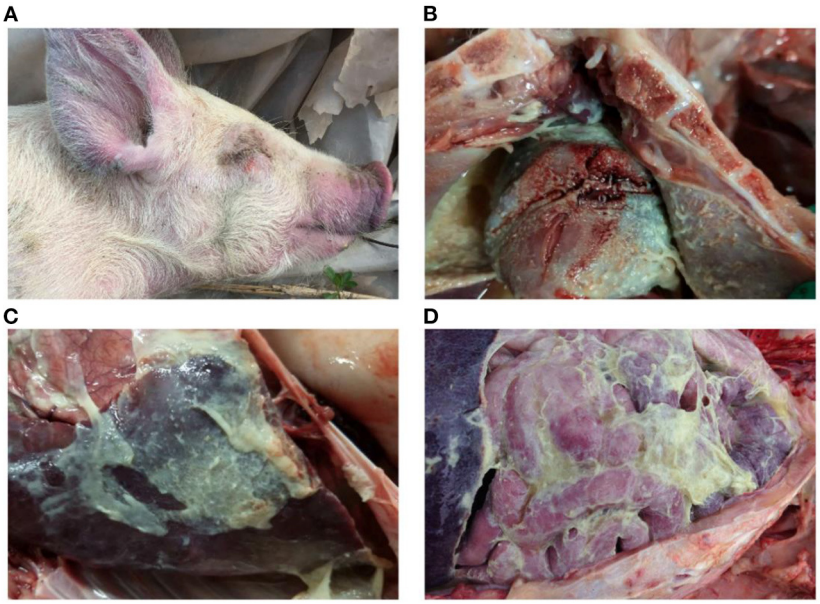

FIGURE 2
Gross lesions of Glässer's disease: **(A)** purple marks on the ears, skin around the eyes and tip of the nose of a pig that died of *H. parasuis* infection; **(B)** fibrinopurulent exudate on pericardial surface; and **(C,D)** fibrinopurulent exudate on serosal membranes in peritoneal and thoracic cavities. Photographs taken by the author.

analyze for the presence of signal peptides (https://services.healthtech.dtu.dk/service.php?SignalP-5.0, accessed on 3 November 2021) and differentiate between secretory and non-secretory proteins. The subcellular localization of secreted proteins was further checked on Vaxign (http://www.violinet.org/vaxign/, accessed on 3 November 2021) to select outer membrane proteins as candidates for vaccine construction (15).

Prediction of B-cell epitopes

B cells are a central component of the adaptive immune system, and they provide long-term protection against infectious pathogens by producing antibodies. In this study, linear B-cell epitopes of the candidate proteins were predicted by BepiPred-2.0 web server (16) (https://services.healthtech.dtu.dk/service.php?BepiPred-2.0, accessed on 4 November 2021).

Prediction of cytotoxic T-lymphocyte (CTL) and helper T-lymphocyte (HTL) epitopes

The cytotoxic T-lymphocyte (CTL) epitopes from candidate protein sequences were predicted using the NetCTL 1.2 server (https://services.healthtech.dtu.dk/service.php?NetCTL-1.2, accessed on 4 November 2021). Default settings were used (threshold, 0.75) for the estimation of CTL epitopes (17). Then, the helper T cells 15-mer epitopes for candidate protein sequences were predicted by using the NetMHCII 2.3 server (https://services.healthtech.dtu.dk/service.php?NetMHCII-2.3, accessed on 4 November 2021). Seven mouse H2 class II alleles were evaluated. According to standards, the lowest consensus scores of the peptides were chosen to be the best binders and a lower percentile rank indicates higher affinity. The selection criterion was a cut-off of IC50 $\leq$ 50 and percentile rank $<$ 1 (18).

Vaccine construction

A putative vaccine candidate sequence was designed by combining B-cell epitopes with high-scoring CTL epitopes and high binding affinity HTL epitopes. TLR-2 agonist, phenol soluble modulin α4 (accession no. A9JX08) protein, was preferred as an adjuvant to enhance the immunogenicity of the vaccine (19). The adjuvant was linked to the first B-cell epitope through an EAAAK linker at the N terminal of the sequence, whereas the remaining B-cell and HTL epitopes were interlinked *via* GPGPG linkers. AAY linkers were used for joining the CTLs epitopes.

Evaluation of antigenicity, allergenicity, and physicochemical properties of the protein

In order to predict the antigenicity and allergenicity of the vaccine, VaxiJen v2.0 server (http://www.ddg-pharmfac.net/vaxijen/VaxiJen/VaxiJen.html, accessed on 5 November 2021) and AllerTOP v2.0 server (http://www.ddg-pharmfac.net/AllerTOP, accessed on 5 November 2021) were utilized, respectively (20, 21). The solubility of the designed vaccine was evaluated using the SOLpro server (22) (https://scratch.proteomics.ics.uci.edu, accessed on 5 November 2021). Furthermore, the designed vaccine was assessed for several physicochemical properties by using the ProtParam server (http://web.expasy.org/protparam/, accessed on 5 November 2021).

Extrapolation of secondary structure of the protein

The secondary structure of the multi-epitope vaccine was predicted using PSIPRED (http://bioinf.cs.ucl.ac.uk/psipred/, accessed on 6 November 2021) server and RaptorX (http://raptorx.uchicago.edu/StructurePropertyPred/predict/, accessed on 6 November 2021) with default parameters (23, 24).

Three-dimensional modeling and validation of the protein

Homology modeling of the final vaccine construct was performed using the Robetta server (25) (https://robetta.bakerlab.org/, accessed on 7 November 2021). Non-bond interactions between different types of atoms were analyzed using the ERRAT server (26) (http://services.mbi.ucla.edu/ERRAT/, accessed on 7 November 2021) to verify the tertiary structure. The Ramachandran plot was generated using the PROCHECK server (27) (https://servicesn.mbi.ucla.edu/PROCHECK/, accessed on 7 November 2021) to determine the relative proportion of amino acids in favored regions.

Prediction of discontinuous B-cell Epitopes

ElliPro (http://tools.iedb.org/ellipro/, accessed on 7 November 2021) was used for prediction of B-cell discontinuous epitopes in the protein model (28).

Molecular docking of the protein with TLR2

Toll-like receptors are sensors of the innate immune response, with TLR-2 recognizing the broadest range of PAMPs molecules and inducing significant antibacterial and antiviral responses. We used the ClusPro server (https://cluspro.bu.edu/login.php, accessed on 8 November 2021) to determine the docking of TLR-2 with the vaccine protein (29). The structural coordinates of the TLR-2 (PDB ID: 3A7C) were retrieved from the Protein Data Bank (30) (https://www.rcsb.org/, accessed on 8 November 2021). The docked structures were visualized *via* PyMOL (http://www.pymol.org, accessed on 8 November 2021) to analyze the interaction between the vaccine protein and TLR-2.

Characterization of the construct immune profile

For analyses of the immune responses of the vaccine construct in the mouse model, the online dynamic immune simulation C-lmmSim server (https://www.iac.cnr.it/$\sim$filippo/c-immsim/index.html, accessed on 9 November 2021) was employed (31). This online server functions based on a position specific scoring matrix (PSSM) for the prediction of immunogenic epitopes and immune interactions. All default simulation parameters were used with time steps specified at 1, 90, and 180.

In silico optimization and cloning of the protein

To ensure the efficient expression of the vaccine construct in *Escherichia coli* cells, we performed the reverse translation and codon optimization of the vaccine protein sequence using the Java Codon Adaptation Tool (32) (http://www.jcat.de/, accessed on 9 November 2021). *E. coli* strain K12 was selected as the expression host. During the run, the options were chosen to avoid rho-independent transcription terminators, bacterial ribosome binding sites, and restriction enzyme cleavage sites. Finally, the vaccine protein sequence was designed for cloning into a suitable host vector pET-28a(+)-MEV by employing the SnapGene software (https://www.snapgene.com/, accessed on 9 November 2021).

Inducible expression and purification of vaccine proteins

The synthetic expression vector named pET-28a(+)-MEV is available from Chengdu YouKang Jianxing Biotechnology Co. The pET-28a(+)-MEV was transformed into *E. coli* BL21 (DE3), and positive colonies were inoculated in LB liquid medium containing kanamycin and incubated overnight in a water bath shaker at 37°C. A 10 mL aliquot of overnight culture was inoculated into 1 L of LB medium containing kanamycin, and the culture was expanded to mid-log growth (OD600 $\approx$ 0.6) at 37°C in a water bath shaker. IPTG was added to the culture and incubated at 37°C for 5 h. The bacteria were collected by centrifugation and ultrasonically fragmented. After sonication, the vaccine protein was purified using a Ni^{2+}-NTA resin column and concentrated by desalting using an Amicon® Ultra-4 10K centrifuge filter.

Mouse immunoassay and ELISA assay

Ten 6-week-old SPFKM grade Kunming mice were randomly divided into test and control groups of five mice each. The vaccine protein was diluted to 1 μg/μL and 50 μL was mixed with an equal volume of Quick Antibody immunoadjuvant. A 100 μL aliquot of the vaccine solution was intramuscularly injected into the hind legs of mice, which were immunized again with the same dose on day 14. The control group was injected with a mixture of saline and immune adjuvant. Blood was collected from the tail vein of the mice at 21 days post-immunization and the serum was isolated and preserved. Sixteen clinical isolates of HPS were coated onto ELISA plates and the absorbance was measured at OD450 and the data recorded. Statistical analysis and visualization of the data were carried out using R 4.1.

Results

Nanopore sequencing and genome assembly of 16 clinical isolates of HPS

To construct a more complete pan-genome of HPS, 16 clinical isolates of HPS (HPS-1–HPS-15) were sequenced using the ONT MinION MK1B platform. Reads of each strain with a depth of about 100× were obtained. The raw ONT reads were corrected using Canu, and SMARTdenovo was then used to assemble the error-corrected reads to obtain the assembled genome sequence. Then, the raw reads were subjected to for multiple rounds of polishing using Medaka and Homopolish to improve the quality of the draft assemblies. The data that support the findings of this study have been deposited into the CNGB Sequence Archive (CNSA) of China National GeneBank DataBase (CNGBdb) with accession number CNP0002150 (33, 34). Information about the 16 strains is summarized in Supplementary Table 2.

Results of the pan-genomic and phylogenetic analysis

The observed pan-genome shared by the 121 HPS strains consists of 8,885 genes including 390 core genes and 8,495 accessory genes (Figure 3A). The non-linear regression analysis showed an obvious open pan-genome, and the size of core genes approached a constant value (Figure 3B). Based on concatenated core genes, we constructed a phylogenetic tree of the HPS, which showed the rich phylogenetic diversity of HPS (Figure 3C). These results indicate that the genome of HPS is highly variable and that it can continuously obtain foreign genes to adapt to different environments. This is the main reason why conventional vaccines are less protective.

Protein sequences for vaccine designing

Eight proteins with secreted signal peptides localized to the outer membrane were screened from the core and soft-core genes using Signal 5.0 and Vaxign (Table 1). These protein sequences were then further subjected to epitope prediction in B, T, and helper cells.

Prediction of B-cell, cytotoxic T-lymphocyte (CTL), and helper T-lymphocyte (HTL) epitopes

BepiPred 2.0 server was used to select B cell epitopes with the default threshold > 0.6. Epitopes that are exposed and have a coiled structure were further selected for vaccine design (Table 2). The protein sequences were analyzed by NetCTL 1.2 server to identify the most immunodominant regions. Peptides with the highest binding affinity scores in each protein were identified as high-potential CTL epitope candidates and a total of three epitopes were screened (Table 2). The NetMHCII 2.3 web server predicted the MHC-II epitopes with the highest binding corresponding to the alleles based on the IC50 score. A total of 6 HTL epitopes were chosen for the final chimeric construct (Table 2).

Vaccine construction

A total of 5 B cell epitopes, six HTL epitopes and three HTL epitopes were used to construct multi-epitope vaccine chimeras. The B cell and HTL epitopes were linked together by GPGPG linkers, while AY linkers were used to link the CTL epitopes. Phenolic soluble modulin α4 (UniProt Id: A9JX08), a TLR-2 agonist, was added as an adjuvant at the N-terminal end with an EAAAK linker to enhance the immunogenicity of the vaccine. The final chimeric construct constituted 280 amino acids (Figure 4).

Antigenicity, allergenicity, and physicochemical properties of the vaccine protein

VaxiJen 2.0 web server was used to predict the antigenicity of the vaccine design attached with an adjuvant, as 0.7756 with the bacterial model by opting for a threshold of 0.4. The antigenicity of the vaccine candidate was also checked without including the adjuvant part for which VaxiJen gave scores of 0.7114 in a model of bacteria. AllerTOP v.2 and AllergenFP online servers predicted the vaccine sequence to be non-allergenic in nature in the presence and absence of the adjuvant.

Solubility and physicochemical properties of the vaccine protein

The SOLpro server of the Scratch protein prediction tool predicted a solubility probability of 0.887834 for this vaccine protein. ExPASy ProtParam was used to predict the molecular weight (MW) of the vaccine protein as 29.4 kDa. The pI (theoretical isoelectric point value) of the protein was calculated as 9.65. The estimated half-life of the protein in mammals, yeast, and E. coli was estimated as 30 h, >20 h, and >10 h, respectively. In addition, the protein was predicted to have an instability index (II) of 24.99 by ProtParam, classifying it as stable since a value of >40 indicates instability. The values of 70.03 and −0.438 for the aliphatic index and GRAVY (grand average of hydropathicity) reflect the high thermostability and hydrophilic nature, respectively.

Secondary structure of the vaccine protein

Based on PSIPRED and RaptorX server results, the protein vaccine consists of 22% helix (H), 3% beta strand (E), and 73% coil (C) secondary structural elements (Figure 5A). Based on the accessibility of amino acid residues, 62% residues were predicted to be exposed, 18% medium exposed, and 18% were predicted to be buried (Figure 5B). In total, only 2% of residues were found to be localized in disordered structural domains.

Three-dimensional modeling and validation of the vaccine protein

The 3D model of the vaccine protein was generated by Robetta server (Figure 6) and was visualized using PyMOL software. Ramachandran plot analysis showed that 100% of the residues were in the allowed regions and 91.1% of the residues were in the most favored regions. The overall quality factor score generated by the ERRAT2 was 92.647%. The above results for the 3D model demonstrate that the vaccine construct has a stable chemical structure.

Prediction of discontinuous B-cell epitopes

ElliPro server was used to predict discontinuous B-cell epitopes for the vaccine constructs. The results showed that the vaccine constructs had five discontinuous B-cell epitopes that ranged in size from 7 to 38 residues, with scores ranging from 0.588 to 0.822 (Figure 7 and Table 3).

10.3389/fvets.2022.1053198

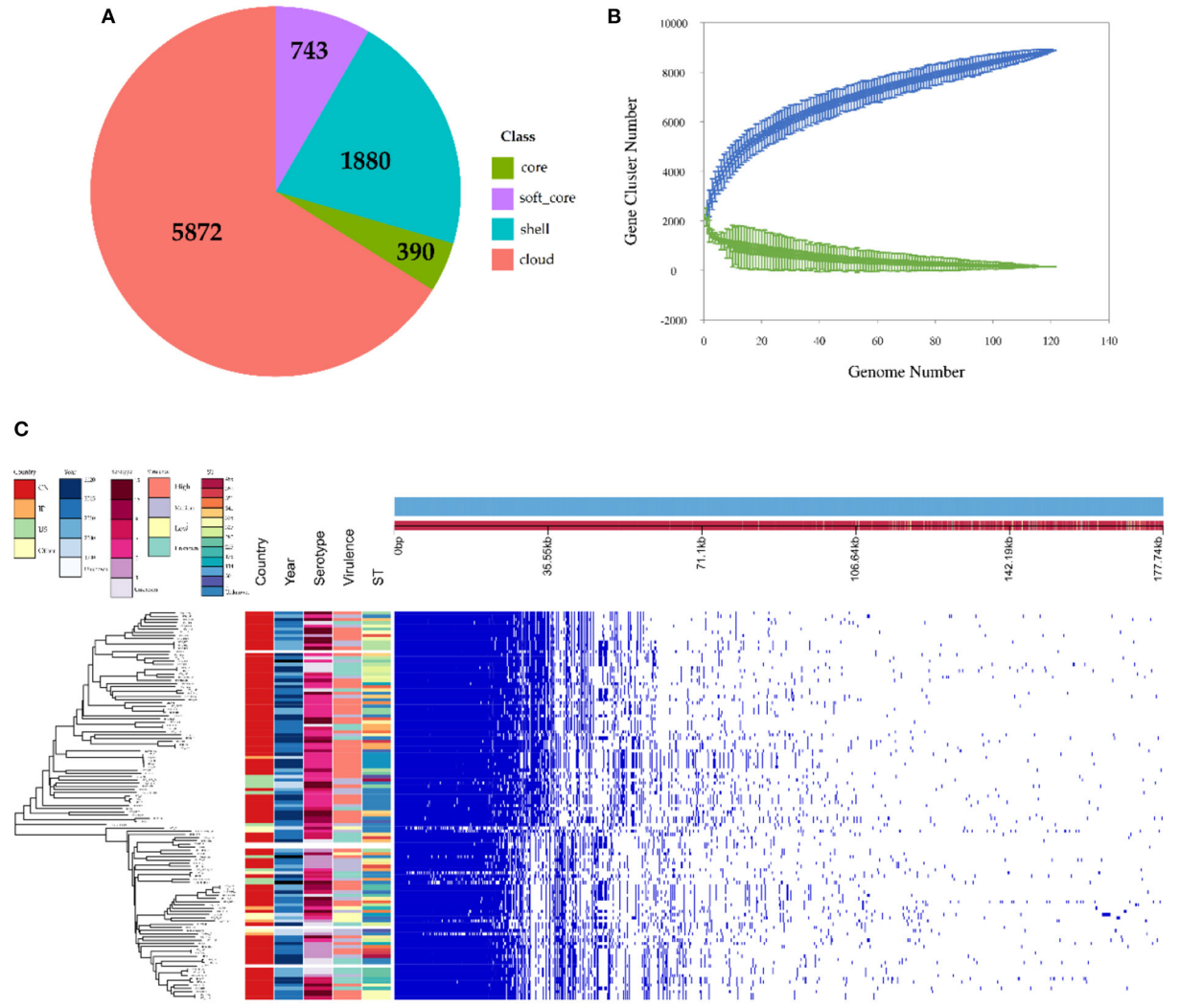

FIGURE 3
Pan-genomic and phylogenetic analysis of HPS based on 121 strains. **(A)** Core and accessory genes of HPS. Core: 119 ≤ strains ≤ 121; soft-core: 114≤ strains < 119; shell: 18 ≤ strains < 114; cloud: strains < 18. **(B)** Core and pan-genome curves for HPS. The blue dots and lines indicate the size of the pan-genome for each strain combination, and the relationship between pan-genome size and genome number, respectively. The green dots and lines indicate corresponding information for the core genome. **(C)** The left tree is a neighbor-joining phylogenetic tree constructed based on the core genes and annotated with the location of isolation, time of isolation, serotype, ST type, and virulence of each strain. The right matrix plot denotes the presence and absence of every gene over all strains by blue and white, respectively.

Molecular docking of the vaccine protein with TLR2

Immune cells recognize evolutionarily conserved pathogen patterns in a targeted manner and respond by expressing Toll-like receptors. Within the TLR family, TLR2 has a broad recognition spectrum, recognizing lipoproteins, lipopolysaccharides, peptidoglycans and other signals indicating danger (35). Therefore, we used the ClusPro server to determine the docking of TLR 2 with the vaccine protein. The central energy between ligand receptor is −820.2, and the lowest energy of the docking complex is −857.6. The vaccine protein has multiple hydrogen-bonded interactions with TLR2 and exhibits a high binding affinity. The residues of the vaccine-TLR2 complex showing H-bond interactions are LYS25–ASP294, ARG28–GLY293, ARG28–PHE295, ARG271–LEU350, SER274–ASN379, ALA278–ASN379, LYS259–ARG400, LYS259–GLU374, and LYS259–GLU375 with a distance of 2.1, 1.8, 1.8, 2.2, 2.4, 1.6, 2.1, 1.9, and 1.9Å, respectively (Figure 8).

TABLE 1 Selected proteins in the core and soft-core genes of HPS.

Protein	Product
kpsD	Polysaccharide export protein
bamA	Outer membrane protein assembly factor
lptD	LPS-assembly protein
Pal	Peptidoglycan-associated lipoprotein Pal
mlaA	MlaA family lipoprotein
tama	Autotransporter assembly complex protein TamA
nlpD	Murein hydrolase activator NlpD
Gbp	Porin family protein

TABLE 2 Predicted B-cell, CTL, and HTL epitopes for the design of the vaccine protein.

	Protein	Epitope sequence
B-cell epitopes	KpsD	APRAVKASDNIGLEQQIKR
	bamA	AQREFNRELYVQSMKFPIDNDLNVYKKI
	LptD	QGNIGVRNPKYLGL
	pal	NAGQTFGGMSAQDL
	gbp	NINNAPKAGTTYGNWHAPKRES
HTL epitopes	tama	YLADWRLGY
	LptD	ETKLYTTYY
	LptD	YVENDSTTY
	bamA	TTPGSDNKY
	mlaA	ATPWSITKY
	nlpD	TAANNTPNY
CTL epitopes	gbp	DPILTKWASAIVAKK
	gbp	ILTKWASAIVAKKNQ
	tama	AGIGVRWASPIGAVK

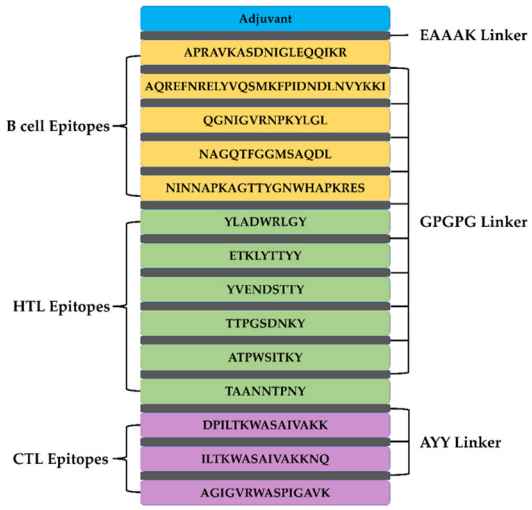

FIGURE 4
The structural arrangement of B- and T-cell epitopes along with linkers and adjuvant for the final multi-epitope vaccine construct.

Immune simulation of the vaccine construct

Immunological characterization of the designed vaccine construct was analyzed using the C-ImmSim server. The C-ImmSim server immune simulation outcomes confirmed consistency with real immune reactions. As shown in Figure 9A, IgM production was recorded in the first injection of the vaccine construct and increased levels of IgM+IgG and IgG1+IgG2 were observed after the second and third immunizations. High levels of B-cell populations were observed after multiple injections of the vaccine constructs, indicating the formation of immune memory (Figure 9C). In addition, an increase in cytotoxicity and helper T-lymphocytes was observed following vaccination, thus indicating activation of cell-mediated immune responses (Figures 9B,D). The above results demonstrate the ability of the vaccine construct to induce an effective immune response to clear the antigen.

Codon optimization and *in silico* cloning

The Java Codon Adaptation Tool was used for codon optimization. The vaccine protein sequence was reverse translated for optimal expression in E. coli (strain K12). The optimized DNA sequence had a codon adaptation index (CAI) value of 1 and a GC content of 54.05%, indicating that the designed vaccine is theoretically stably expressed in the selected microbial hosts. In addition, the DNA sequence for cloning into the E. coli vector pET-28a(+) was designed using the SnapGene software for recombinant plasmid construction (Figure 10).

Inducible expression and purification of vaccine proteins

IPTG was added to E. coli BL21 (DE3) to induce the expression of pET-28a(+)-MEV, and the product was examined by SDS-PAGE gel electrophoresis. The results showed that the induced pET-28a(+)-MEV recombinant produced a specific protein band around 33 kD as expected (Figure 11), whereas the uninduced sample did not show such a band. The sonicated lysates were purified using a Ni^{2+}-NTA resin column, the eluate was collected and concentrated using an Amicon® Ultra-4 10K centrifuge filter, and the final vaccine protein was stored in 10% glycerol at −80°C.

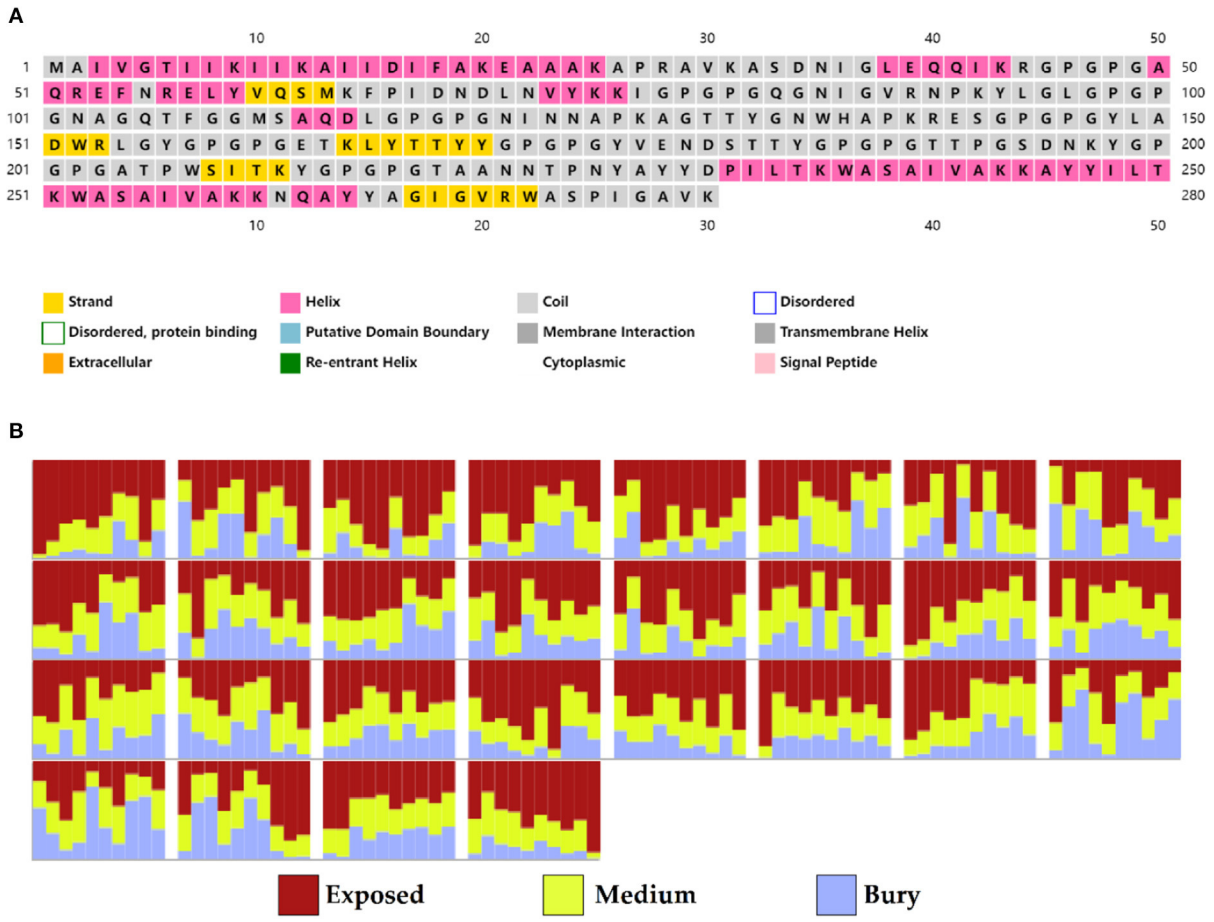

FIGURE 5
Secondary structure prediction of the vaccine protein sequence by using PSIPRED and RaptorX server showing **(A)** secondary structural elements and **(B)** solvent accessibility according to three states.

ELISA of 16 HPS clinical isolates

Pure cultures of each of the 16 HPS clinical isolates were used to coat enzyme-labeled plates at the same concentration and volume, and ELISA assays were performed using mouse polyclonal antibodies obtained by immunization with a multi-epitope vaccine, with a negative serum control. The results are shown in Table 4 and Figure 12: the mouse polyclonal antibodies obtained were able to bind to all 16 HPS clinical isolates, including seven serotype 5, two serotype 10, one serotype 1, two serotype 7, and four non-typable strains, and a one-tailed heteroscedasticity t-test was performed on the OD450 values of each isolate against the corresponding negative serum OD450 values, with all the p-values being less than the test level ($\alpha = 0.05$), indicating the differences were significant. These results indicate that the antibodies obtained from mice immunized with the multi-epitope vaccine designed in this study were able to bind to different serotyped or non-typable HPS isolates.

Discussion

Haemophilus parasuis mainly causes Glässer's disease, characterized by fibrinous polyserositis and arthritis in nursery pigs and affecting growing pigs and sows. Vaccination is an effective measure to prevent mortality (36, 37). However, the available commercial vaccines only provide protection against a limited number of serotypes. Although autogenous vaccines are highly effective in protecting susceptible pigs, the strains used to prepare the vaccines are not isolated until after a disease outbreak (38). Furthermore, for the treatment of HPS infection, the timing of antibiotic administration is critical, and effective treatment should be administered before fibrinous inflammation develops. However, due to the difficulty of early diagnosis, the sick pigs have usually developed severe fibrinous inflammation by the time of diagnosis. Even if the pathogen has been killed by antibiotics, the pigs may still die due to the inflammation-induced cytokine storm and irreversible

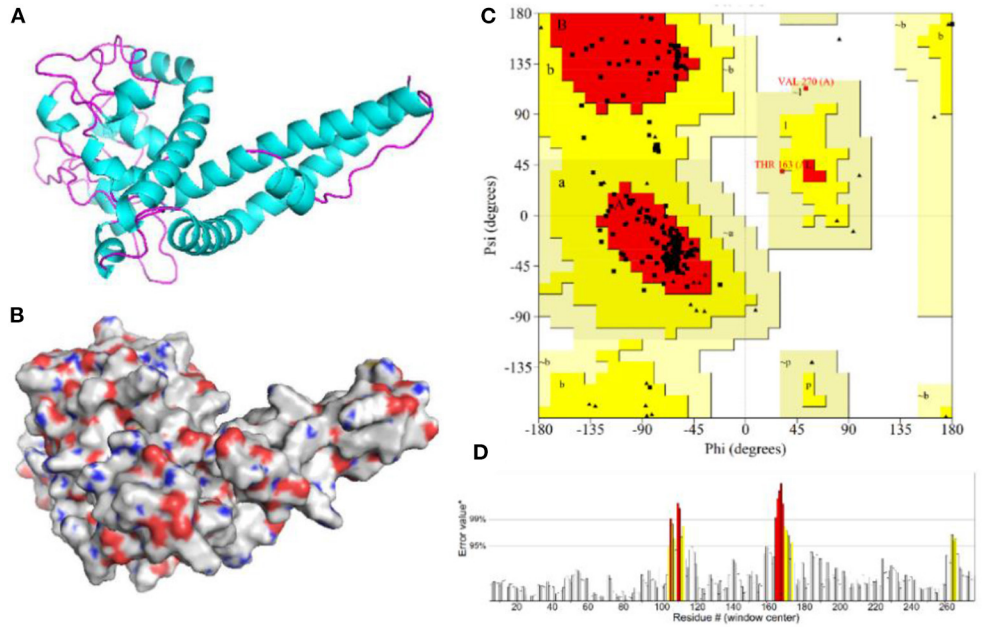

FIGURE 6
Homology modeling and validation of the three-dimensional structure of vaccine constructs. **(A,B)** 3D models of vaccine constructs generated by homology modeling on Robetta and visualized by PyMOL software. **(C)** Ramachandran plot analysis shows 100% of residues in the allowed region. **(D)** The overall quality factor score for the model was 92.647%.

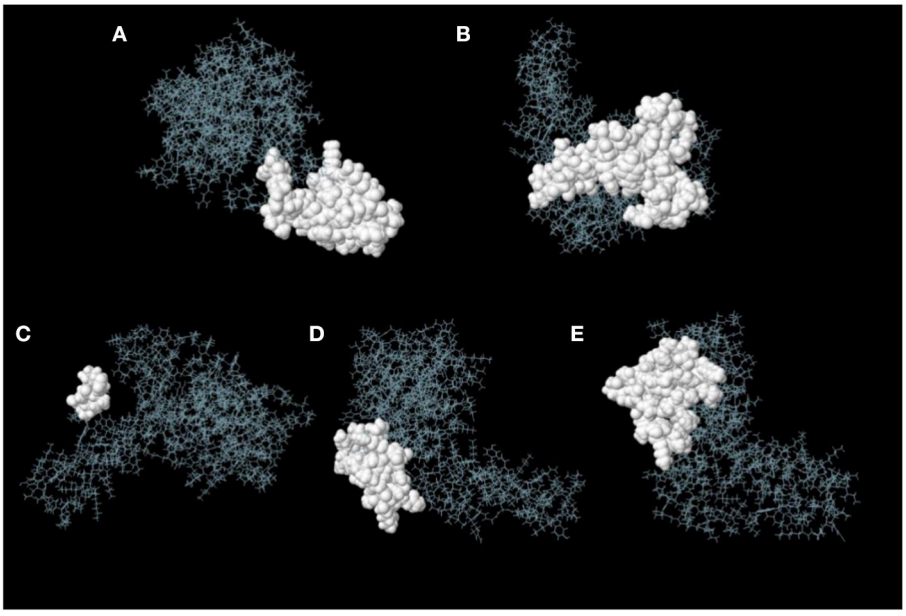

FIGURE 7
Discontinuous B-cell epitopes of vaccine constructs predicted by ElliPro. **(A–E)** The epitopes are represented by a white surface. The gray sticks correspond to the remainder of the protein.

histopathological damage (39), and conventional antibiotic treatment is often ineffective. Therefore, this study aims to design a multi-epitope vaccine that is expected to provide broad protection against HPS infection in pig farms (all serotypes and

10.3389/fvets.2022.1053198

TABLE 3 Discontinuous B-cell epitopes of vaccine constructs predicted by ElliPro.

No.	Residues	Number of residues	Score
A	A:M1, A:A2, A:I3, A:V4, A:G5, A:T6, A:I7, A:I8, A:K9, A:I10, A:I11, A:K12, A:A13, A:I14, A:D16, A:I17, A:T250, A:K251, A:A253, A:S254, A:A255, A:I256, A:V257, A:A258, A:K259, A:K260, A:N261, A:Q262, A:A263, A:Y264, A:Y265, A:A266, A:G267, A:I268, A:G269, A:V270, A:R271, A:W272	38	0.822
B	A:P138, A:K139, A:R140, A:E141, A:S142, A:G143, A:P144, A:G145, A:P146, A:G147, A:Y156, A:G157, A:P158, A:G159, A:P160, A:G161, A:E162, A:T163, A:K164, A:Y166, A:Y169, A:Y170, A:G171, A:P172, A:G173, A:P174, A:G175, A:Y176, A:V177, A:E178, A:N179, A:D180, A:S181, A:T182, A:T183, A:Y184, A:G185, A:P186, A:G187, A:P188, A:G189, A:T190, A:T191, A:P192, A:G193, A:S194, A:D195, A:Y198	48	0.678
C	A:A273, A:S274, A:P275, A:G277, A:A278, A:V279, A:K280	7	0.664
D	A:N35, A:I36, A:L38, A:E39, A:Q40, A:Q41, A:I42, A:K43, A:R44, A:G45, A:P46, A:G47, A:P48, A:G49, A:A50, A:Q51, A:R52, A:E53, A:G116, A:I122, A:N123, A:N124, A:A125, A:P126, A:K127, A:G129, A:T130, A:T131, A:Y132	29	0.664
E	A:L71, A:Y74, A:K75, A:I77, A:G78, A:P79, A:G80, A:P81, A:G82, A:Q83, A:G84, A:N85, A:I86, A:G87, A:V88, A:R89, A:N90, A:P91, A:K92, A:Y93, A:L96, A:G97, A:P98, A:G99, A:P100, A:G101, A:N102, A:A103, A:G104, A:Q105, A:G109, A:G215, A:P216, A:G217, A:T218	35	0.588

non-typable strains). Pan-genomic analysis was used to identify the core genome of HPS, software programs and databases were used to predict the antigenic epitopes of outer membrane proteins in the core genome, and reverse vaccinology techniques were used to design the final multi-epitope vaccine, reducing traditional laboratory-based experimental practices.

Herein, we first sequenced the genomes of 16 HPS strains using Oxford nanopore sequencing technology (ONT) and obtained complete assemblies of high quality. Compared with second-generation sequencing platforms, the ONT platform has the advantages of lower cost, faster sequencing speed, longer read length, and greater ease of operation (40). Subsequently, the 16 HPS genomes obtained together with the 105 NCBI-indexed genomes were used to construct the HPS pangenome using Roary software. The analysis results showed that HPS has an open pan-genome. The number of core genes represents only 14% of the CDS of an individual genome, and the rest is highly variable. The large variation in the genomes of different isolates of HPS is the main reason for the lack of cross-protection of existing vaccines. It is also worth clarifying that not only virulent strains but also non-virulent strains were used to construct the pan-genome. The reason for this is that non-virulent strains have the potential to be converted into virulent strains. For example, serovar 7 strains were considered to all be non-virulent, but some serovar 7 strains have been isolated from systemic lesions of Glässer's disease, and disease has been reproduced with one of them (41, 42).

The following eight outer membrane proteins were identified from core and soft core genes by signal peptide prediction and subcellular localization: (1) Podoconjugate export protein kpsD—this protein is mainly involved in translocation of podoconjugates from the site of synthesis to the cell surface (43). (2) Outer membrane protein assembler bamA—bamA is mainly involved in catalyzing the assembly of bacterial transmembrane proteins and could be a potential vaccine candidate for the prevention of Escherichia coli and Salmonella infections (44, 45). (3) Lipopolysaccharide assembly protein lptD—this protein mediates lipopolysaccharide transport and lptD of Vibrio Parahemolyticus is highly immunogenic, providing 100% protection against Vibrio infection in mice and is a potential vaccine antigen (46). (4) Peptidoglycan-associated lipoprotein Pal—this protein interacts with Tol Pal is a natural TLR2 agonist and binds tightly to LPS, which is released into the bloodstream during infection causing sepsis (47, 48). In addition, Pal from Legionella pneumophila, Haemophilus influenzae, and Campylobacter jejuni was shown to be highly immunogenic and capable of inducing early innate and adaptive immune responses (49–51). (5) Lipoprotein mlaA—this protein, which belongs to the same class of lipoproteins as Pal, is also involved in maintaining the lipid asymmetry of the outer membrane of Gram-negative bacteria, forming an osmotic barrier to prevent the entry of toxic molecules (e.g., antibiotics, disinfectants, etc.). (6) The autotransport assembly complex protein TamA—studies suggest that this protein may be involved as a substrate for secretion to facilitate the secretion of autotransport proteins rather than in an autotransport system for pathogen colonization in the host (52). (7) Urea hydrolase-activating protein nlpD—this protein is also a lipoprotein, and in Cronobacter sakazakii, nlpD responds to acid stress to resist phagocytosis by maintaining membrane integrity. In addition, nlpD may also be involved in the regulation of iron uptake and the activity of the bis-arginine system (53, 54). (8) Pore protein gbp—pore proteins are abundantly present on the surface of bacteria as a sieving barrier and

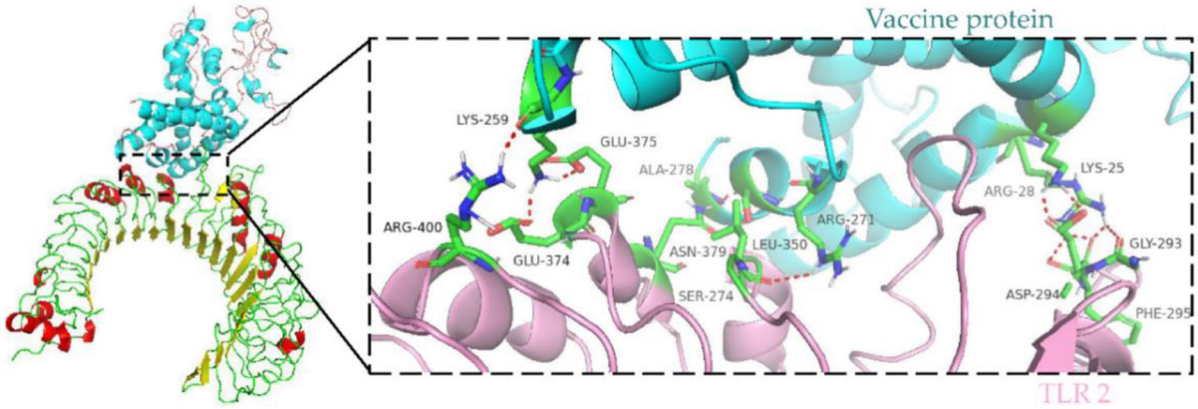

FIGURE 8
Molecular docking of subunit vaccine with TLR2. Docking complex of vaccine protein and TLR2, with the vaccine protein colored sky blue and the A chain of TLR2 colored light pink. Residues with H-bond interactions are represented in the sticks model and the remaining residues are represented in the cartoon model. Hydrogen bonds are represented as red dashed lines.

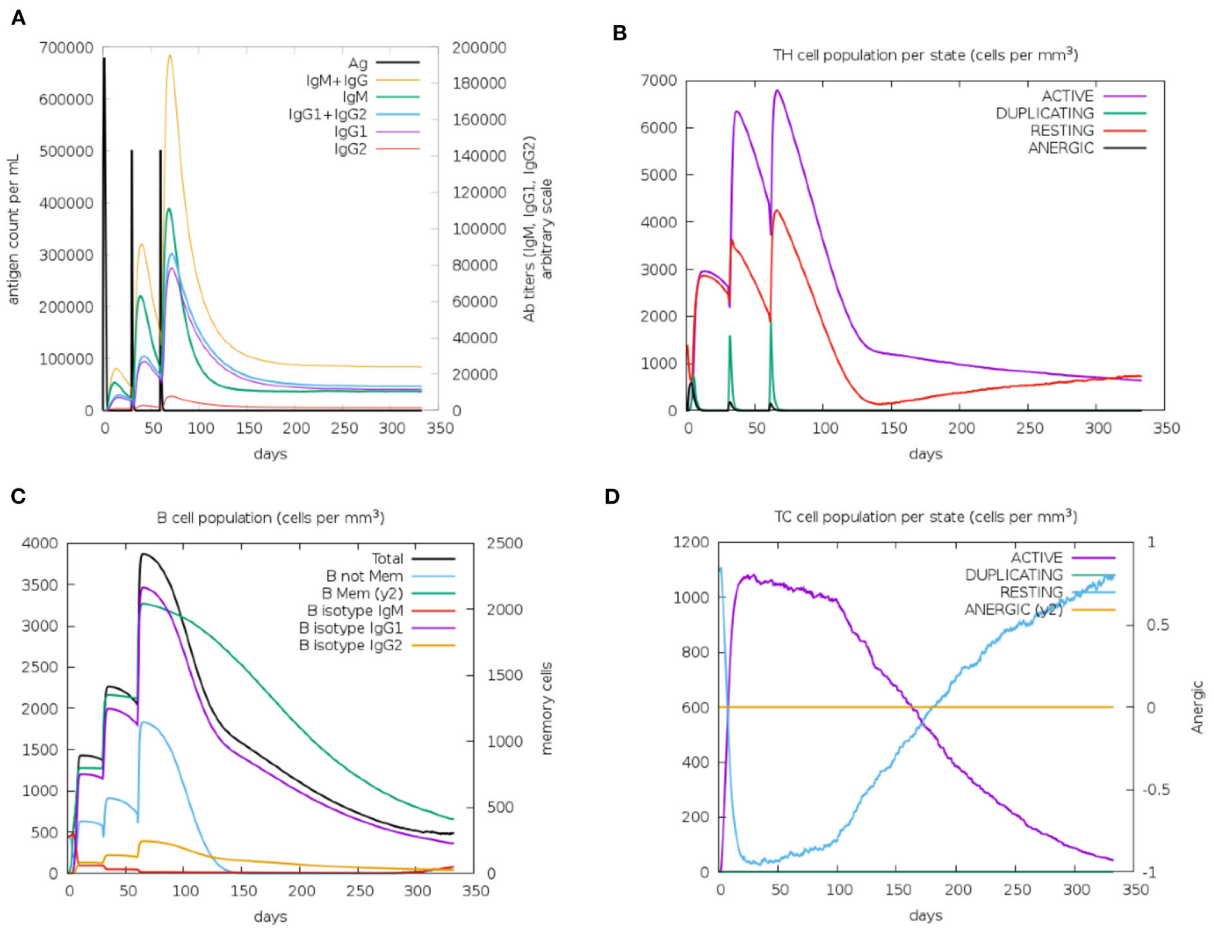

FIGURE 9
Simulated immunity of vaccine constructs using C-ImmSim server showing **(A)** an increase in immunoglobulins following vaccination **(B,D)**, that the population of cytotoxic T-lymphocytes and helper T-lymphocytes increases after vaccination and remains higher during the entire exposure time, and **(C)** an increase in B-cell populations after vaccination, producing high levels of memory immunoglobulins.

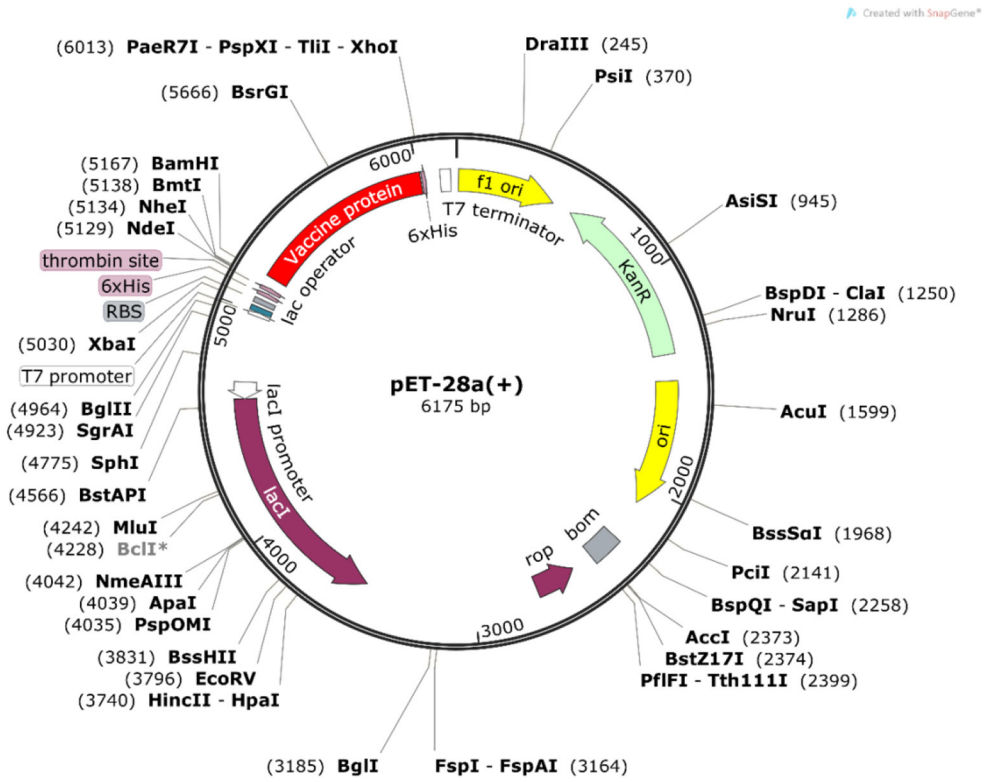

FIGURE 10
In silico cloning of the vaccine construct. The codon-optimized DNA sequence of the vaccine construct (in red) was cloned between the BamH I and Xho I restriction sites of the pET-28a(+) expression vector (shown in black circles).

play an important role in host-bacteria interactions, making them potential vaccine candidate antigens and therapeutic targets (55). Then, B cell epitopes (n = 5), CTL epitopes (n = 3), and HTL epitopes (n = 6) were identified from these outer membrane proteins for use in the construction of the vaccine. To improve the stability of the vaccine structure, epitopes were linked together using the EAAAK linker and the GPGPG linker (56, 57). The multi-epitope vaccine was then linked to the phenol-soluble modulin α4 protein (a TLR 2 agonist) selected as an adjuvant using an AYY linker to enhance the immunogenicity of the vaccine (19). The vaccine construct was subsequently tested for antigenicity and allergenicity and was shown to be antigenic and non-allergenic with or without linking to the adjuvant; a higher antigenicity score was predicted for coupling with the adjuvant.

The final vaccine construct containing B-cell epitopes, CTL epitopes, and HTL epitopes as well as linkers and adjuvant is 280 amino acid residues and has a molecular weight of 29.38 kD. The theoretical pI of this vaccine protein was 9.65, indicating the basic nature of the protein. The instability index of the protein is 24.99, whereby a value of <40 indicates that the vaccine construct will be stable whenever expressed (58). In addition, other indicators demonstrated the high thermostability, hydrophilic nature and solubility of the vaccine construct.

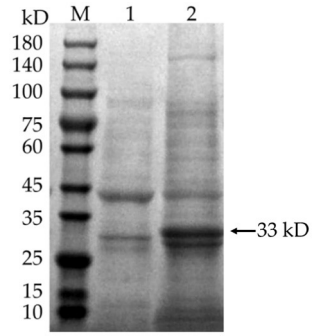

FIGURE 11
Induced expression of the vaccine protein. M: protein molecular quality standard (10–180 kD); 1: pET-28a(+)-MEV recombinant bacteria, uninduced; 2: pET-28a(+)-MEV recombinant bacteria, induced. Full-length gels are presented in Supplementary Image 1.

The secondary structure prediction of the vaccine constructs showed that only 2% of the amino acid residues were disordered,

TABLE 4 ELISA results for each isolate.

Isolates	Isolate	Mean ± SD	Negative serum OD450	Mean ± SD	*p*-value
	OD450				
HPS 01	0.563	0.57 ± 0.0158	0.214	0.202 ± 0.009	1.53E-07
	0.591		0.202		
	0.57		0.196		
	0.554		0.194		
HPS 02	0.847	0.835 ± 0.0243	0.213	0.211 ± 0.0129	1.49E-07
	0.802		0.192		
	0.858		0.222		
	0.833		0.215		
HPS 03	0.517	0.556 ± 0.0295	0.234	0.207 ± 0.0213	1.60E-06
	0.571		0.193		
	0.585		0.213		
	0.551		0.187		
HPS 04	0.79	0.757 ± 0.037	0.237	0.219 ± 0.0278	4.56E-07
	0.709		0.182		
	0.782		0.243		
	0.748		0.212		
HPS 05	0.535	0.501 ± 0.0419	0.216	0.209 ± 0.0118	0.000203
	0.497		0.208		
	0.443		0.192		
	0.528		0.218		
HPS 06	0.673	0.635 ± 0.0416	0.281	0.268 ± 0.0189	3.16E-05
	0.657		0.285		
	0.633		0.245		
	0.578		0.259		
HPS 07	0.485	0.469 ± 0.0389	0.194	0.217 ± 0.018	0.000109
	0.411		0.218		
	0.491		0.218		
	0.49		0.238		
HPS 08	0.626	0.575 ± 0.0516	0.192	0.197 ± 0.0053	0.000312
	0.547		0.197		
	0.61		0.194		
	0.517		0.204		
HPS 09	0.646	0.627 ± 0.0507	0.199	0.194 ± 0.0129	0.000116
	0.675		0.208		
	0.63		0.178		
	0.556		0.189		
HPS 10	0.432	0.447 ± 0.018	0.206	0.2 ± 0.0066	1.06E-05
	0.436		0.192		
	0.472		0.196		
	0.449		0.204		
HPS 11	0.784	0.768 ± 0.021	0.224	0.213 ± 0.0103	2.18E-07
	0.74		0.201		
	0.763		0.209		
	0.784		0.219		
HPS 12	0.79	0.784 ± 0.0279	0.18	0.185 ± 0.0076	4.49E-06
	0.746		0.195		
	0.788		0.178		
	0.813		0.186		
HPS 13	0.606	0.59 ± 0.0202	0.203	0.198 ± 0.0041	1.04E-05
	0.597		0.198		
	0.595		0.193		
	0.56		0.198		
HPS 14	0.595	0.571 ± 0.0422	0.221	0.22 ± 0.0089	0.000153
	0.605		0.207		
	0.573		0.222		
	0.511		0.228		
HPS 15	0.53	0.481 ± 0.0538	0.176	0.175 ± 0.0126	0.000482
	0.485		0.187		
	0.503		0.157		
	0.405		0.178		
HPS 16	0.64	0.634 ± 0.0192	0.206	0.209 ± 0.0168	3.04E-08
	0.606		0.232		
	0.642		0.204		
	0.649		0.192		

confirming the stability of the constructs. The construct is mainly composed of coils (73%), which will facilitate antibody production. Moreover, the vaccine construct was modeled and validated, and the interaction of the vaccine construct with TLR2 was investigated using molecular docking simulations to elucidate an effective immune response. The validation of the 3D structure showed that all the residues were in the allowed regions, and over 90% were present in favorable regions, confirming that we obtained a high-quality structural model. Furthermore, the construct had a high binding affinity to TLR2, indicating that it has the potential to stimulate the generation of an immune response. According to the immune simulation results of the C-ImmSim server, a high level of memory B cell formation and antibody production, as well as an increased and prolonged maintenance of cytotoxic and helper T-lymphocytes could be observed after multiple immunizations, thus creating a humoral and cellular immune response that will help prevent infections. In addition, codon optimization was performed after reverse translation of the vaccine protein. The GC and CAI values predicted for the vaccine protein were 54.05% and 1 respectively, indicating that the protein can be expressed in large quantities in E. coli.

The vaccine protein was reverse-translated and codon-optimized, and the E. coli expression vector pET-28a(+)-MEV was constructed and transferred to E. coli BL21 (DE3) for induction of expression, and the target vaccine protein was

10.3389/fvets.2022.1053198

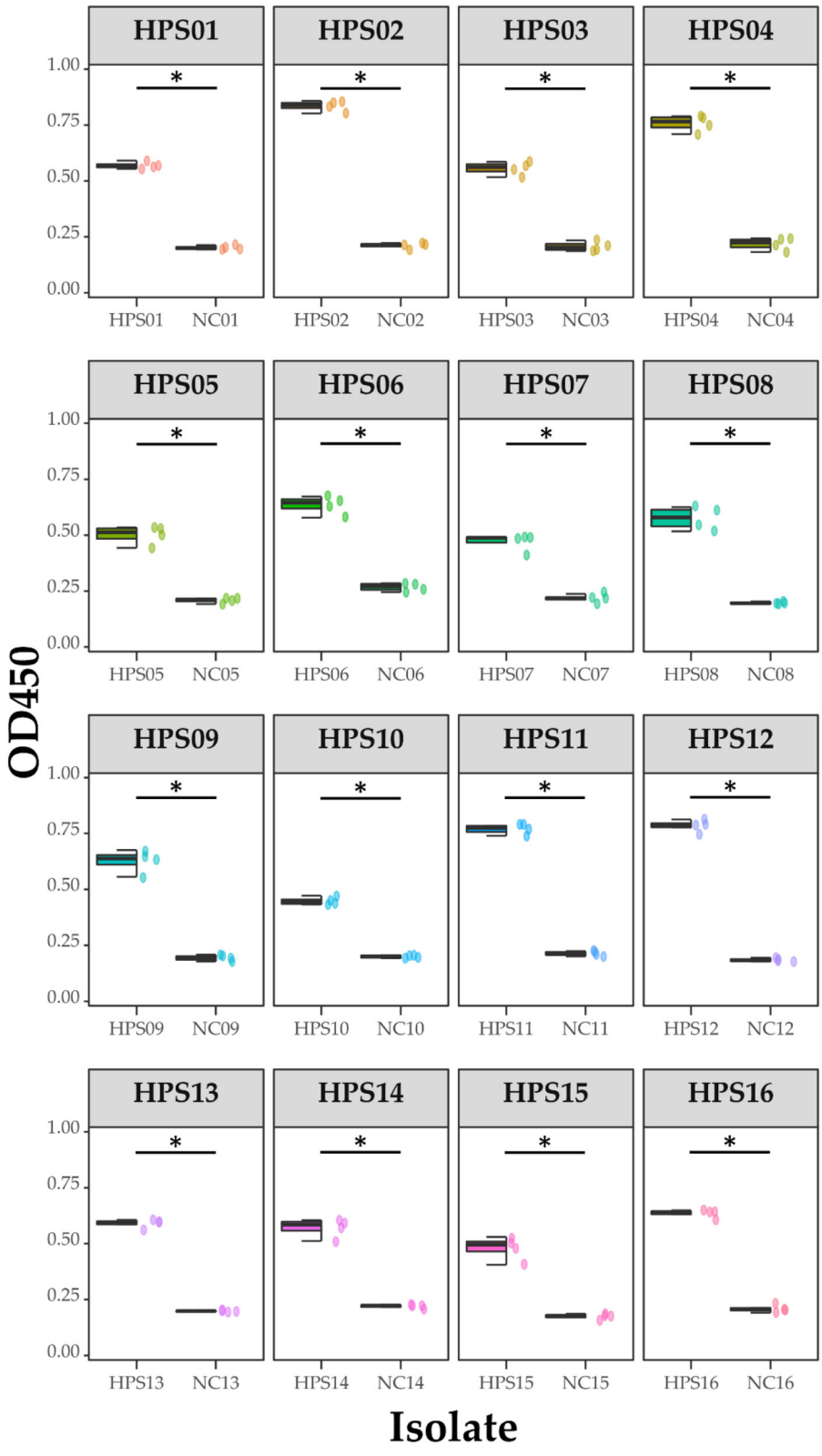

FIGURE 12
ELISA results for each isolate. Data are presented using box and scatter plots; NC is negative serum control; * indicates statistically significant difference.

purified. Polyclonal antibodies obtained from mice immunized with the vaccine protein were able to bind to different serotypes or non-typable HPS isolates, preliminary indicating that the vaccine protein is a promising vaccine candidate. The multi-epitope vaccine designed in this study also has multiple clinical use strategies based on the infection and epidemiological characteristics of HPS—For example, in the direct immunization of piglets against HPS infection. In addition, because the virulent strain of HPS can colonize the respiratory tract of piglets under the protection of maternal antibodies and thus stimulate the piglet organism to produce an immune response to prevent morbidity and mortality, this process is limited to the strain to which the sow has been exposed. Therefore, an alternative immunization strategy that may be more effective is the use of multi-epitope vaccines to immunize reserve or pregnant sows to stimulate the production of antibodies against various serotypes or non-typable HPS, with the piglets being protected by maternal antibodies exhibiting a wide range of reactivities and colonized by different strains of HPS virulence, thus producing an immune response to prevent infection.

Conclusion

The development of a new vaccine is necessary to address the complex epidemiological situation of Haemophilus parasuis and to solve the problems associated with existing vaccines. In this study, we utilized pan-genomic analysis with reverse vaccine technology to construct a vaccine with the potential to prevent infection by all serotypes as well as non-typable of Haemophilus parasuis, and this process that avoids the high cost and time-consuming drawbacks of traditional vaccine development. The vaccine construct had multiple B and T cell epitopes and exhibited high antigenicity, non-toxicity and non-allergenicity. In addition, immune simulation results showed that the vaccine activated high levels of humoral and cellular immune responses. The antibodies obtained from mice immunized with the multi-epitope vaccine were able to bind to different serotyped or untypable HPS isolates. In conclusion, the vaccine designed in this study is a promising candidate for the control of Haemophilus parasuis.

Data availability statement

The original contributions presented in the study are included in the article/Supplementary material, further inquiries can be directed to the corresponding author.

Ethics statement

The animal study was reviewed and approved by the Sichuan Provincial Laboratory Animal Management Committee.

Author contributions

MP and TT: methodology. MP and MR: software. PZ and TT: validation. PZ and YL: data curation. MP: writing-original draft preparation. TT and YW: writing-review and editing. XY and ZY: project administration. All authors have read and agreed to the published version of the manuscript.

Funding

This work was funded by the Sichuan Province Science and Technology Planning Project (Project Number: 2020YJ0345; Title: Molecular Regulation Mechanism of *Haemophilus Parasuis* Type II Toxin Antitoxin System in Bacterial Biofilm Formation); Sichuan Province Science and Technology Planning Project (Project Number: 2021YFSY0005; Title: Development of Synergist for Swine Disease Vaccine Based on Plant Polysaccharides and Cytokines); Sichuan Province Science and Technology Planning Project (Project Number: 2021YJ0270; Title: Establishment of Detection Method for Identification of African Swine Fever Virus Infection and Its Application in Biosafety Control System).

Acknowledgments

We thank YW for his insightful comments on the design of the study.

Conflict of interest

The authors declare that the research was conducted in the absence of any commercial or financial relationships that could be construed as a potential conflict of interest.

Publisher's note

Supplementary material

The Supplementary Material for this article can be found online at: https://www.frontiersin.org/articles/10.3389/fvets.2022.1053198/full#supplementary-material

References

1. Brockmeier SL, Register KB, Kuehn JS, Nicholson TL, Loving CL, Bayles DO, et al. Virulence and draft genome sequence overview of multiple strains of the swine pathogen *Haemophilus parasuis*. *PLoS ONE.* (2014) 9:e103787. doi: 10.1371/journal.pone.0103787

2. Kielstein P, Rapp-Gabrielson VJ. Designation of 15 serovars of *Haemophilus parasuis* on the basis of immunodiffusion using heat-stable antigen extracts. *J Clin Microbiol.* (1992) 30:862–5. doi: 10.1128/jcm.30.4.862-865.1992

3. Blackall PJ, Trott DJ, Rapp-Gabrielson V, Hampson DJ. Analysis of *Haemophilus parasuis* by multilocus enzyme electrophoresis. *Vet Microbiol.* (1997) 56:125–34. doi: 10.1016/S0378-1135(96)01342-9

4. Cerdà-Cuéllar M, Naranjo JF, Verge A, Nofrarías M, Cortey M, Olvera A, et al. Sow vaccination modulates the colonization of piglets by *Haemophilus parasuis*. *Vet Microbiol.* (2010) 145:315–20. doi: 10.1016/j.vetmic.2010.04.002

5. Olvera A, Cerdà-Cuéllar M, Aragon V. Study of the population structure of *Haemophilus parasuis* by multilocus sequence typing. *Microbiology.* (2006) 152:3683–90. doi: 10.1099/mic.0.29254-0

6. Olvera A, Cerdà-Cuéllar M, Nofrarías M, Revilla E, Segalés J, Aragon V. Dynamics of *Haemophilus parasuis* genotypes in a farm recovered from an outbreak of Glässer's disease. *Vet Microbiol.* (2007) 123:230–7. doi: 10.1016/j.vetmic.2007.03.004

7. Jalal K, Khan K, Ahmad D, Hayat A, Basharat Z, Abbas MN, et al. Pan-genome reverse vaccinology approach for the design of multi-epitope vaccine construct against *Escherichia albertii*. *Int J Mol Sci.* (2021) 22:12814. doi: 10.3390/ijms222312814

8. D'Mello A, Ahearn CP, Murphy TF, Tettelin H. ReVac: a reverse vaccinology computational pipeline for prioritization of prokaryotic protein vaccine candidates. *BMC Genomics.* (2019) 20:981. doi: 10.1186/s12864-019-6195-y

9. Koren S, Walenz BP, Berlin K, Miller JR, Bergman NH, Phillippy AM. Canu: scalable and accurate long-read assembly *via* adaptive k-mer weighting and repeat separation. *Genome Res.* (2017) 27:722–36. doi: 10.1101/gr.215087.116

10. Huang Y, Liu P, Shih P. Homopolish: a method for the removal of systematic errors in nanopore sequencing by homologous polishing. *Genome Biol.* (2021) 22:95. doi: 10.1186/s13059-021-02282-6

11. Seemann T. Prokka: rapid prokaryotic genome annotation. *Bioinformatics.* (2014) 30:2068–9. doi: 10.1093/bioinformatics/btu153

12. Page AJ, Cummins CA, Hunt M, Wong VK, Reuter S, Holden MTG, et al. Roary: rapid large-scale prokaryote pan genome analysis. *Bioinformatics.* (2015) 31:3691–3. doi: 10.1093/bioinformatics/btv421

13. Kumar S, Stecher G, Li M, Knyaz C, Tamura K. MEGA X: molecular evolutionary genetics analysis across computing platforms. *Mol Biol Evol.* (2018) 35:1547–9. doi: 10.1093/molbev/msy096

14. Almagro Armenteros JJ, Tsirigos KD, Sønderby CK, Petersen TN, Winther O, Brunak S, et al. SignalP 50 improves signal peptide predictions using deep neural networks. *Nat Biotechnol.* (2019) 37:420–3. doi: 10.1038/s41587-019-0036-z

15. Ong E, Wang H, Wong MU, Seetharaman M, Valdez N, He Y. Vaxign-ML: supervised machine learning reverse vaccinology model for improved prediction of bacterial protective antigens. *Bioinformatics.* (2020) 36:3185–91. doi: 10.1093/bioinformatics/btaa119

16. Jespersen MC, Peters B, Nielsen M, Marcatili P. BepiPred-2.0: improving sequence-based B-cell epitope prediction using conformational epitopes. *Nucleic Acids Res.* (2017) 45:W24–9. doi: 10.1093/nar/gkx346

17. Peters B, Bulik S, Tampe R, Van Endert PM, Holzhütter H. Identifying MHC class I epitopes by predicting the TAP transport efficiency of epitope precursors. *J Immunol.* (2003) 171:1741–9. doi: 10.4049/jimmunol.171.4.1741

18. Nielsen M, Lund O. NN-align: an artificial neural network-based alignment algorithm for MHC class II peptide binding prediction. *BMC Bioinformat.* (2009) 10:296. doi: 10.1186/1471-2105-10-296

19. Chatterjee R, Sahoo P, Mahapatra SR, Dey J, Ghosh M, Kushwaha GS, et al. Development of a conserved chimeric vaccine for induction of strong immune response against *Staphylococcus aureus* using immunoinformatics approaches. *Vaccines.* (2021) 9:1038. doi: 10.3390/vaccines9091038

20. Doytchinova IA, Flower DR. VaxiJen: a server for prediction of protective antigens, tumour antigens and subunit vaccines. *BMC Bioinformat.* (2007) 8:4. doi: 10.1186/1471-2105-8-4

21. Dimitrov I, Bangov I, Flower DR, Doytchinova I. AllerTOP v.2–a server for *in silico* prediction of allergens. *J Mol Model.* (2014) 20:2278. doi: 10.1007/s00894-014-2278-5

22. Magnan CN, Randall A, Baldi P. SOLpro: accurate sequence-based prediction of protein solubility. *Bioinformatics.* (2009) 25:2200–7. doi: 10.1093/bioinformatics/btp386

23. McGuffin LJ, Bryson K, Jones DT. The PSIPRED protein structure prediction server. *Bioinformatics.* (2000) 16:404–5. doi: 10.1093/bioinformatics/16.4.404

24. Wang S, Li W, Liu S, Xu J. RaptorX-Property: a web server for protein structure property prediction. *Nucleic Acids Res.* (2016) 44:W430–5. doi: 10.1093/nar/gkw306

25. Kim DE, Chivian D, Baker D. Protein structure prediction and analysis using the Robetta server. *Nucleic Acids Res.* (2004) 32:W526–31. doi: 10.1093/nar/gkh468

26. Colovos C, Yeates TO. Verification of protein structures: patterns of nonbonded atomic interactions. *Protein Sci.* (1993) 2:1511–9. doi: 10.1002/pro.5560020916

27. Laskowski RA, MacArthur MW, Moss DS, Thornton JM. PROCHECK: a program to check the stereochemical quality of protein structures. *J Appl Crystallogr.* (1993) 26:283–91. doi: 10.1107/S0021889892009944

28. Ponomarenko J, Bui H, Li W, Fusseder N, Bourne PE, Sette A, et al. ElliPro: a new structure-based tool for the prediction of antibody epitopes. *BMC Bioinformat.* (2008) 9:514. doi: 10.1186/1471-2105-9-514

29. Kozakov D, Hall DR, Xia B, Porter KA, Padhorny D, Yueh C, et al. The ClusPro web server for protein-protein docking. *Nat Protoc.* (2017) 12:255–78. doi: 10.1038/nprot.2016.169

30. Berman HM, Westbrook J, Feng Z, Gilliland G, Bhat TN, Weissig H, et al. The protein data bank. *Nucleic Acids Res.* (2000) 28:235–42. doi: 10.1093/nar/28.1.235

31. Rapin N, Lund O, Bernaschi M, Castiglione F. Computational immunology meets bioinformatics: the use of prediction tools for molecular binding in the simulation of the immune system. *PLoS ONE.* (2010) 5:e9862. doi: 10.1371/journal.pone.0009862

32. Grote A, Hiller K, Scheer M, Münch R, Nörtemann B, Hempel DC, et al. JCat: a novel tool to adapt codon usage of a target gene to its potential expression host. *Nucleic Acids Res.* (2005) 33:W526–31. doi: 10.1093/nar/gki376

33. Chen FZ, You LJ, Yang F, Wang LN, Guo XQ, Gao F, et al. CNGBdb: China National GeneBank DataBase. *Yi chuan Hereditas.* (2020) 42:799–809.

34. Guo X, Chen F, Gao F, Li L, Liu K, You L, et al. CNSA: a data repository for archiving omics data. *Database.* (2020) 2020:baaa055. doi: 10.1093/database/baaa055

35. Majid M, Andleeb S. Designing a multi-epitopic vaccine against the enterotoxigenic *Bacteroides fragilis* based on immunoinformatics approach. *Sci Rep.* (2019) 9:19780. doi: 10.1038/s41598-019-55613-w

36. Martín de la Fuente AJ, Rodríguez-Ferri EF, Frandoloso R, Martínez S, Tejerina F, Gutiérrez-Martín CB. Systemic antibody response in colostrum-deprived pigs experimentally infected with *Haemophilus parasuis*. *Res Vet Sci.* (2009) 86:248–53. doi: 10.1016/j.rvsc.2008.07.017

37. Takahashi K, Naga S, Yagihashi T, Ikehata T, Nakano Y, Senna K, et al. A cross-protection experiment in pigs vaccinated with *Haemophilus parasuis* serovars 2 and 5 bacterins, and evaluation of a bivalent vaccine under laboratory and field conditions. *J Vet Medical Sci.* (2001) 63:487–91. doi: 10.1292/jvms.63.487

38. McOrist S, Bowles R, Blackall P. Autogenous sow vaccination for Glasser's disease in weaner pigs in two large swine farm systems. *J Swine Health Prod.* (2009) 17:90–6.

39. Costa-Hurtado M, Olvera A, Martinez-Moliner V, Galofré-Milà N, Martínez P, Dominguez J, et al. Changes in macrophage phenotype after infection of pigs with *Haemophilus parasuis* strains with different levels of virulence. *Infect Immun.* (2013) 81:2327–33. doi: 10.1128/IAI.00056-13

40. Zhang P, Jiang D, Wang Y, Yao X, Luo Y, Yang Z. Comparison of *de novo* assembly strategies for bacterial genomes. *Int J Mol Sci.* (2021) 22:14. doi: 10.3390/ijms22147668

41. Aragon V, Cerdà-Cuéllar M, Fraile L, Mombarg M, Nofrarías M, Olvera A, et al. Correlation between clinico-pathological outcome and typing of *Haemophilus parasuis* field strains. *Vet Microbiol.* (2010) 142:387–93. doi: 10.1016/j.vetmic.2009.10.025

42. Dazzi CC, Guizzo JA, Prigol SR, Kreutz LC, Driemeier D, Chaudhuri S, et al. New pathological lesions developed in pigs by a "non-virulent" strain of *Glaesserella parasuis*. *Front Vet Sci.* (2020) 7:98. doi: 10.3389/fvets.2020.00098

43. Arrecubieta C, Hammarton TC, Barrett B, Chareonsudjai S, Hodson N, Rainey D, et al. The transport of group 2 capsular polysaccharides across the

periplasmic space in *Escherichia coli*. Roles for the KpsE and KpsD proteins. *J Biol Chem.* (2001) 276:4245–50. doi: 10.1074/jbc.M008183200

44. Guan Q, Wang X, Wang X, Teng D, Wang J. *In silico* analysis and recombinant expression of BamA protein as a universal vaccine against *Escherichia coli* in mice. *Appl Microbiol Biot.* (2016) 100:5089–98. doi: 10.1007/s00253-016-7467-y

45. Konovalova A, Kahne DE, Silhavy TJ. Outer membrane biogenesis. *Annu Rev Microbiol.* (2017) 71:539–56. doi: 10.1146/annurev-micro-090816-093754

46. Zha Z, Li C, Li W, Ye Z, Pan J. LptD is a promising vaccine antigen and potential immunotherapeutic target for protection against *Vibrio* species infection. *Sci Rep.* (2016) 6:38577. doi: 10.1038/srep38577

47. Godlewska R, Wiśniewska K, Pietras Z, Jagusztyn-Krynicka EK. Peptidoglycan-asso-ciated lipoprotein (Pal) of Gram-negative bacteria: function, structure, role in pathogenesis and potential application in immunoprophylaxis. *FEMS Microbiol Lett.* (2009) 298:1–11. doi: 10.1111/j.1574-6968.2009.01659.x

48. Liang MD, Bagchi A, Warren HS, Tehan MM, Trigilio JA, Beasley-Topliffe LK, et al. Bacterial peptidoglycan-associated lipoprotein: a naturally occurring toll-like receptor 2 agonist that is shed into serum and has synergy with lipopolysaccharide. *J Infect Dis.* (2005) 191:939–48. doi: 10.1086/427815

49. Mobarez AM, Rajabi RA, Salmanian AH, Khoramabadi N, Hosseini Doust SR. Induction of protective immunity by recombinant peptidoglycan associated lipoprotein (rPAL) protein of *Legionella pneumophila* in a BALB/c mouse model. *Microb Pathogenesis.* (2019) 128:100–5. doi: 10.1016/j.micpath.2018.12.014

50. Kodama S, Hirano T, Suenaga S, Abe N, Suzuki M. Eustachian tube possesses immunological characteristics as a mucosal effector site and responds to P6 outer membrane protein of nontypeable *Haemophilus influenzae*. *Vaccine.* (2006) 24:1016–27. doi: 10.1016/j.vaccine.2005.07.110

51. Cordwell SJ, Len ACL, Touma RG, Scott NE, Falconer L, Jones D, et al. Identification of membrane-associated proteins from *Campylobacter jejuni* strains using complementary proteomics technologies. *Proteomics*. (2008) 8:122–39. doi: 10.1002/pmic.200700561

52. Selkrig J, Mosbahi K, Webb CT, Belousoff MJ, Perry AJ, Wells TJ, et al. Discovery of an archetypal protein transport system in bacterial outer membranes. *Nat Struct Mol Biol.* (2012) 19:506–10. doi: 10.1038/nsmb.2261

53. Ji X, Lu P, Xue J, Zhao N, Zhang Y, Dong L, et al. The lipoprotein NlpD in *Cronobacter sakazakii* responds to acid stress and regulates macrophage resistance and virulence by maintaining membrane integrity. *Virulence.* (2021) 12:415–29. doi: 10.1080/21505594.2020.1870336

54. Tidhar A, Levy Y, Zauberman A, Vagima Y, Gur D, Aftalion M, et al. Disruption of the NlpD lipoprotein of the plague pathogen *Yersinia pestis* affects iron acquisition and the activity of the twin-arginine translocation system. *Plos Neglect Trop D.* (2019) 13:e0007449. doi: 10.1371/journal.pntd.0007449

55. Sharma A, Yadav SP, Sarma D, Mukhopadhaya A. Modulation of host cellular responses by gram-negative bacterial porins. *Adv Protein Chem STR.* (2022) 128:35–77. doi: 10.1016/bs.apcsb.2021.09.004

56. Chen X, Zaro JL, Shen W. Fusion protein linkers: property, design and functionality. *Adv Drug Deliver Rev.* (2013) 65:1357–69. doi: 10.1016/j.addr.2012.09.039

57. Arai R, Ueda H, Kitayama A, Kamiya N, Nagamune T. Design of the linkers which effectively separate domains of a bifunctional fusion protein. *Protein Eng.* (2001) 14:529–32. doi: 10.1093/protein/14.8.529

58. Guruprasad K, Reddy BV, Pandit MW. Correlation between stability of a protein and its dipeptide composition: a novel approach for predicting *in vivo* stability of a protein from its primary sequence. *Protein Eng.* (1990) 4:155–61. doi: 10.1093/protein/4.2.155

Frontiers in Veterinary Science

Transforms how we investigate and improve animal health

The third most-cited veterinary science journal, bridging animal and human health with a comparative approach to medical challenges. It explores innovative biotechnology and therapy for improved health outcomes.

Discover the latest Research Topics

See more →

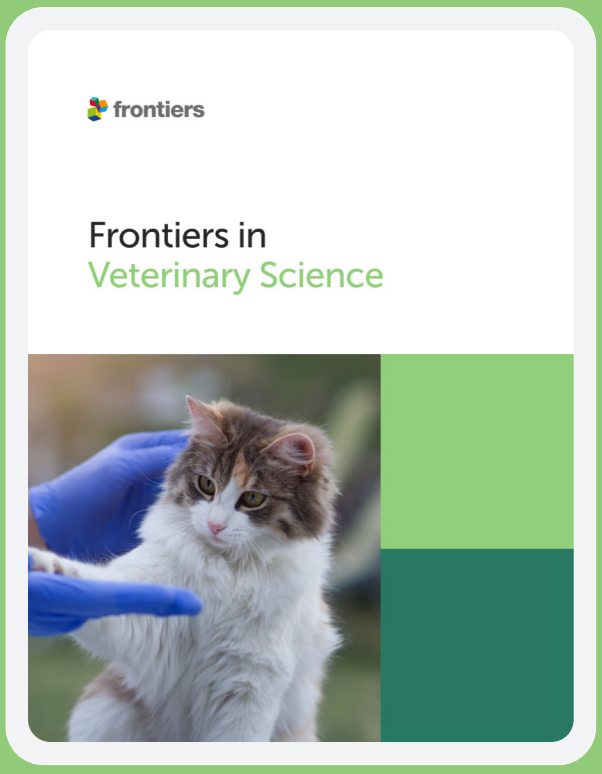

Frontiers

Avenue du Tribunal-Fédéral 34
1005 Lausanne, Switzerland
frontiersin.org

Contact us

+41 (0)21 510 17 00
frontiersin.org/about/contact